

An assessment of flow and pressure control
in experimental models
of glaucoma drainage surgery

Amir Bin Samsudin

Thesis submitted for the degree of PhD

University College London

2014

Declaration

I, Amir Bin Samsudin confirm that the work presented in this thesis is my own. Where information has been derived from other sources, I confirm that this has been indicated in the thesis.

Amir Bin Samsudin

List of presentations arising from this thesis

The influence of scleral flap geometry and sutures on pressure change and aqueous humour flow direction in a trabeculectomy model – Poster presented at the Meeting of the Association for Research in Vision and Ophthalmology (ARVO), 10 May 2012.

Fluid-structure characteristics of the scleral flap in the trabeculectomy procedure – Paper presented at the Institute of Mathematics and its Applications (IMA) Conference on Mathematics of Medical Devices and Surgical Procedures, 18 September 2012.

The effect of aqueous humour protein content and viscosity on equilibrium pressure under the scleral flap in trabeculectomies - Poster presented at the Meeting of the Association for Research in Vision and Ophthalmology (ARVO), 8 May 2013.

Acknowledgement

I thank my supervisors Professor Sir Peng Tee Khaw, Professor Ian Eames and Professor Steve Brocchini who have all tirelessly taught, advised and inspired me about research.

This thesis would also not be possible without the love, sacrifice, comfort and support from my wife, my parents, my family and my friends.

I am thankful to my colleagues from the UCL Institute of Ophthalmology, UCL Department of Mechanical Engineering and UCL School of Pharmacy who provided guidance, assistance and companionship during my time there; and also those from the University of Malaya who provided support and encouragement during my time away.

Finally, I would like to give appreciation to the University of Malaya and the Ministry of Education in Malaysia for the financial support during this period of research.

Thesis abstract

There are a number of surgical methods for treating glaucoma, including trabeculectomy and the insertion of drainage devices. At the current time, these procedures are still associated with post-operative problems for a significant number of patients, particularly with the control of aqueous humour flow and pressure e.g. hypotony. The main aim of this work was to look at ways of improving the outcomes of the procedures.

The usual approach in assessing surgical techniques is to test them on live human or animal eyes. This is inherently complex, with a significant challenge to keep some of the major parameters e.g. aqueous humour inflow and wound healing consistent throughout a series of tests, and with this the problem of reproducibility. The approach used in this work includes a review and analysis of the different surgical methods and devices from an engineering perspective, the use of scaling analysis and a large-scale physical model coupled with image processing to study trabeculectomy scleral flap characteristics and its effect on flow and pressure, and also the use of model drainage devices in *ex vivo* settings to look at flow and pressure. For each experiment, implications for clinical practice are discussed.

Applying engineering principles to glaucoma procedures and devices provided novel insight into their functions. It was found that the trabeculectomy scleral flap acts as a valve to guard from excessive aqueous humour outflow and low pressures, and parameters such as the number and position of sutures and scleral flap geometry can be tailored to alter aqueous humour outflow. Additionally, 50 μm internal diameter tubes show promise for controlled aqueous humour flow into the subconjunctival space with avoidance of low pressures. Engineering methodology can be used in the development of new treatments and devices. However, some results may not translate exactly into the more complex living eye.

Table of contents

Title page.....	1
Declaration and list of presentations.....	2
Acknowledgment.....	3
Thesis abstract.....	4
Table of contents.....	5
List of tables.....	9
List of figures.....	10
List of abbreviations.....	18
List of symbols.....	19

Chapters

1	Introduction.....	20
2	Review and analysis of glaucoma surgery.....	25
2.1	Aqueous humour and IOP.....	25
2.2	Large trials looking at IOP reduction and control of glaucoma.....	29
2.3	Current treatment of raised IOP.....	33
2.4	Subconjunctival space drainage.....	37
2.4.1	Trabeculectomy.....	37
2.4.2	Subconjunctival space GDD.....	49

2.4.3	Other subconjunctival space GDD.....	67
2.5	Schlemm’s canal and suprachoroidal space drainage	75
2.5.1	Schlemm’s canal GDD	75
2.5.2	Suprachoroidal space GDD.....	79
2.6	Fluid mechanics of trabeculectomy and glaucoma drainage devices	84
2.6.1	Electrical circuit analogy	85
2.6.2	Pressure-flow response of GDD	95
2.7	Conclusion and Research Questions	98
3	Fluid-structure characteristics of the scleral flap and the influence of the scleral flap and sutures on intraocular pressure (IOP) and aqueous humour flow direction.....	100
3.1	Introduction	100
3.2	Methods.....	101
3.2.1	Scaling analysis.....	101
3.2.2	Physical model	105
3.3	Results	118
3.3.1	Comparison between scaling analysis and physical model	118
3.3.2	Pressure under the scleral flap	119
3.3.3	Fluid flow under the scleral flap	125
3.4	Discussion	132
3.4.1	Comparison between scaling analysis and physical model	132
3.4.2	Pressure and fluid flow under the scleral flap.....	133

3.5	Conclusion.....	140
4	The effect of scleral flap shapes, suture numbers and aqueous humour protein content and viscosity on equilibrium pressure under the trabeculectomy scleral flap in a porcine model.....	141
4.1	Introduction	141
4.2	Methods.....	144
4.3	Results	152
4.4	Discussion	156
4.5	Conclusion.....	160
5	An evaluation of fixed resistance tubes for drainage into the subconjunctival space ...	161
5.1	Introduction	161
5.2	Methods.....	166
5.2.1	Material testing	166
5.2.2	Electron microscopy	166
5.2.3	Flow studies	167
5.2.4	Porcine sclera model.....	174
5.3	Results	179
5.3.1	Material testing	179
5.3.2	Electron microscopy	179
5.3.3	Flow studies	183

5.3.4	Porcine sclera model	189
5.4	Discussion	191
5.4.1	Material testing	191
5.4.2	Electron microscopy	192
5.4.3	Flow studies	193
5.4.4	Porcine sclera model	197
5.5	Conclusion.....	199
6	General discussion, conclusion and future work	200
	References.....	206
	Appendix A Fluid-structure characteristics of a rectangular elastic flap valve.....	245
	Appendix B The effect of an air bubble in the anterior chamber on the change in intraocular pressure (IOP).....	253

List of tables

Table 2.1 Typical values for Goldmann equation variables for humans.	28
Table 2.2 IOP outcomes after trabeculectomy in recent studies.....	46
Table 2.3 List of common complications after trabeculectomy surgery in recent studies (early - < 4-6 weeks, late - > 4-6 weeks).....	47
Table 2.4 Summary of glaucoma drainage devices and trabeculectomy.....	53
Table 2.5 IOP outcomes after GDD surgery in recent studies.....	64
Table 2.6 Incidences of hypotony and bleb-related complications after GDD surgery in recent studies (early - < 4-6 weeks, late - > 6 weeks).	65
Table 2.7 Permeability (K) values for Ahmed Glaucoma Valve, Baerveldt, Krupin, Optimed and ExPress devices compared to that of normal eyes. The values in brackets are the flow rates used during testing.....	90
Table 5.1 Summary of tube and device dimensions.	180
Table 5.2 Experimental and predicted permeability of devices.....	186
Table 5.3 Pre and post insertion pressures in index of external leakage experiment.	190

List of figures

Figure 2.1 (a) Aqueous humour movement (blue arrow) from the ciliary body to the trabecular meshwork and Schlemm's canal. (b) Structure of trabecular meshwork and Schlemm's canal (from Allingham et al., 2005).....	26
Figure 2.2 Schematic diagram showing the subconjunctival (grey), Schlemm's canal (yellow) and suprachoroidal (red) spaces for alternative aqueous humour drainage.	36
Figure 2.3 a) Schematic diagram of trabeculectomy showing the direction of aqueous humour outflow (broken arrow). b) Schematic diagram of trabeculectomy scleral flap. The conjunctival layer and bleb are not shown. Black arrows show aqueous humour outflow under the conjunctival bleb. c) Intra-operative photograph of trabeculectomy scleral flap. ...	38
Figure 2.4 a) Photograph of Ahmed Glaucoma Valve (scale bar = 5 mm). b) Schematic cross-section diagram of the resistance mechanism (adapted from Lim (1998)). The valve sheets are said to separate at 8 mmHg or higher.	56
Figure 2.5 a) Photograph of Molteno 3 device (scale bar = 5 mm). b) Schematic cross-section diagram of the device (adapted from Lim (1998)). Aqueous humour flow from the primary drainage area to the secondary drainage area is limited by overlying conjunctiva to prevent continuous drainage leading to hypotony.	59
Figure 2.6 a) Photograph of Baerveldt device (scale bar = 5 mm). b) Schematic cross-section diagram of the device (adapted from Lim (1998)).....	62
Figure 2.7 Scanning electron micrograph of ExPress P200 device (scale bar = 500 μ m). The disc-like flange lies under the scleral flap in the subconjunctival space while the spur and labelled orifices lie in the anterior chamber.....	68

Figure 2.8 a) Photograph of 6 mm long AqueSys tube beside an Ahmed Glaucoma Valve. b) Cross section of AqueSys tube on scanning electron micrograph (1000 × magnification). The lumen diameter is 50 μm.....70

Figure 2.9 Plan view of MIDI-Arrow device. The lumen diameter is 70 μm.71

Figure 2.10 a) Schocket device. b) Krupin device. c) OptiMed device.....74

Figure 2.11 a) iStent GTS100 device. b) iStent Inject (GTS 400) device. c) Hydrus device..78

Figure 2.12 a) Gold Micro Shunt device. b) CyPass device. c) Aquashunt device.83

Figure 2.13 a) Electrical circuit diagram of pre-operative outflow pathway. b) Electrical circuit diagram of post-operative outflow pathway (subconjunctival and suprachoroidal drainage). c) Electrical circuit diagram of post-operative outflow pathway (Schlemm’s canal drainage).87

Figure 2.14 a) Calculated variation of post-operative pressure with ratio of permeability of a subconjunctival drainage device to that of the physiological route (from Equation 2.9). A reduction of IOP from 25-50 mmHg to 15 mmHg ($\Delta P_{post}/\Delta P_{pre}$ of 0.15-0.38) requires the permeability of the device to be about 1.5-6.0 times the permeability of the physiological route. b) The same permeability ratio correlates to around 55-85% of total flow passing through the device (from Equation 2.10).....88

Figure 2.15 Calculated variation of post-operative pressure with ratio of permeability of a Schlemm’s canal device to that of the physiological route (from Equation 2.13). The pressure drop is less than 50% and a reduction of IOP from 24 mmHg to 18 mmHg ($\Delta P_{post}/\Delta P_{pre}$ of 0.6) requires the permeability of the device to be around 8 times the permeability of the physiological route.....92

Figure 2.16 Normogram for assessing K values (in μl/min/mmHg). The black shaded area indicates the range for an ideal device while the red and blue shaded areas indicate the range

of experimental values for the ExPress P50/ R50 and ExPress P200 respectively. The values for the MIDI-Arrow (*), AqueSys (x) and CyPass (o) devices are superimposed.....94

Figure 2.17 a) Expected resistance-flow rate response curves of a fixed resistance device (dashed line) and a valved device (solid line). b) Expected pressure-flow rate response curves of a fixed resistance device (dashed line) and a valved device (solid line). (R – resistance, P – pressure, Q – flow rate).....96

Figure 3.1 Schematic diagram of scleral flap from above and a cross section view. In the physical model, the silicone sheet (scleral flap) is indicated in grey and the back plate (limbus) and ‘sutures’ in red. The inlet hole (sclerostomy) is indicated in blue and the bottom plate in white. W – width, L - length, T - sheet thickness, H - fluid height. 102

Figure 3.2 Elevated view photograph of the main assembly with a triangular sheet in position. 107

Figure 3.3 Configurations of sheets and sutures. Top row shows rectangles and squares with 2 sutures (left), 4 sutures (middle) and 5 sutures (right). Bottom row shows triangles with 1 suture (left) and 3 sutures (right). 109

Figure 3.4 Photograph of complete setup. The syringe driver pumped dyed fluid and the pressure transducer measured pressure under the transparent sheet on the main assembly. The black and white camera recorded images for analysis of the direction of flow..... 110

Figure 3.5 Calibration of pressure transducer showing linear response to change in pressure. The pressure transducer provided a ‘base’ voltage reading even with 0 mmHg pressure..... 112

Figure 3.6 Typical pressure curve showing an initial spike, before equilibration after the silicone sheet flap valve opened. 113

Figure 3.7 Calibration using dyed glycerine increments. Serial images are taken after each addition and analysed using MATLAB. 114

Figure 3.8 Calibration curve for image processing. The curve levelled out after around 4 mm thickness..... 115

Figure 3.9 Method of processing false colour image by MATLAB. The initial image is compared with the final image and the difference in intensity converted into fluid height in the processed image. Suture positions can just be visualised in the processed image..... 116

Figure 3.10 Experimental variation of H/T with $Q\mu L^4/ET^7$ (see Equations 3.6 and 3.8), showing 1/4 and 1/6 gradients corresponding to the bending and stretching states. 118

Figure 3.11 Experimental variation of P/E with $Q\mu/EL^3$ (see Equations 3.10 and 3.11), showing the wide scattering of data points. 119

Figure 3.12 Comparison between thicknesses when there were 3 sutures for triangles and 2 sutures for rectangles and squares. With all 3 shapes, pressures were higher with the thicker sheet. 121

Figure 3.13 Comparison between thicknesses when there were 3 sutures for triangles and 5 sutures for rectangles and squares. With all 3 shapes, pressures were higher with the thicker sheet. 121

Figure 3.14 Comparison between shapes when there were 3 sutures for triangles and 2 sutures for rectangles and squares. Triangles maintained higher pressures, followed by rectangles and squares..... 122

Figure 3.15 Comparison between shapes when there were 3 sutures for triangles and 5 sutures for rectangles and squares. There were no statistically significant differences between the shapes..... 123

Figure 3.16 Comparison between number of sutures in the rectangle group. Generally, higher pressures were maintained with more sutures. 124

Figure 3.17 Comparison between number of sutures in the square group. Generally, higher pressures were maintained with more sutures. 124

Figure 3.18 Comparison between number of sutures in the triangle group. Higher pressures were maintained with more sutures. 125

Figure 3.19 False colour final images showing fluid height under a) rectangle (b) square and (c) triangle sheets. Suture positions (grey boxes) are superimposed on the images. The images on the left are for 1.6 mm thickness while those on the right are for 0.8 mm thickness. Fluid heights under the thinner sheets were higher and wider for all three sheet shapes. 127

Figure 3.20 False colour final images showing fluid movement under a (a) rectangle with 4 sutures, (b) square with 4 sutures, c) rectangle with 2 sutures, d) square with 2 sutures, e) triangle with 3 sutures and (f) triangle with 1 suture. Suture positions (grey boxes) are superimposed on the images. With 4-suture rectangle and square sheets, the direction of flow was away from the limbus towards the opposite edge. With the 2-suture rectangle sheet the flow was away from the limbus and also to the sides. With the..... 128

Figure 3.21 False colour final images showing fluid movement under a rectangular sheet with (a) 5, (b) 4 and (c) 2 sutures. Suture positions (grey boxes) are superimposed on the images. With 5 sutures, fluid accumulated under the sheet as it was well constrained. With 4 sutures, the flow was directed posteriorly while with 2 sutures the flow was directed posteriorly and to the sides..... 130

Figure 3.22 False colour final images showing fluid movement under a square sheet with (a) 5, (b) 4 and (c) 2 sutures. Suture positions (grey boxes) are superimposed on the images. With 5 sutures, fluid accumulated under the sheet as it was well constrained. With 4 sutures, the flow was directed posteriorly while with 2 sutures the flow was directed to the sides. .. 131

Figure 3.23 False colour final images showing fluid movement under a triangular sheet with (a) 3 sutures and (b) 1 suture. Suture positions (grey boxes) are superimposed on the images. With 3 sutures, the flow was away from the limbus but with 1 suture it was to the sides. ... 132

Figure 4.1 Enucleated porcine eye before sectioning (left), after sectioning and removal of iris, lens, vitreous and choroid (right). 145

Figure 4.2 Barron artificial anterior chamber used to mount corneoscleral segments. 145

Figure 4.3 Experimental setup. The artificial anterior chamber was connected to the infusion pump and pressure transducer using non-expansile tubing and a 3-way tap. 146

Figure 4.4 a) Porcine eye mounted on artificial anterior chamber, b) scleral flap margin demarcated, c) scleral flap created and reflected, d) after sclerostomy, e) after resuturing (2 sutures), f) after resuturing (4 sutures). 148

Figure 4.5 Configurations of scleral flaps and sutures. Top row shows 2 sutures each in the comparison between different scleral flap shapes. Bottom row shows rectangles with 2 and 4 sutures each, used in the comparison between different fluids. 149

Figure 4.6 Typical pressure curve after resuturing the scleral flap, showing equilibrium as fluid flows out under the scleral flap. Due to compliance of the sclera and chamber space, there was no spike in the increase in pressure. 150

Figure 4.7 Comparison between different shapes, using BSS as the working fluid. There was no statistically significant difference between the shapes. 153

Figure 4.8 Comparison between fluids in the 4-suture group. There was no statistically significant difference between the fluids. 154

Figure 4.9 Comparison between fluids in the 2-suture group. There was no statistically significant difference between the fluids. 154

Figure 4.10 Comparisons between same fluids with 4 or 2 sutures. When considering the same fluid, 4 sutures always maintained higher pressures. 155

Figure 5.1 Permeability (K , in $\mu\text{l}/\text{min}/\text{mmHg}$). The black shaded area covers our desired values for an ideal device. L - length of tube, d – diameter of tube. 162

Figure 5.2 Pressure drop across a tube (in mmHg, at a flow rate of 3 μ l/min). * indicates the value for a 5 mm long, 50 μ m ID tube. If the flow rate is halved, the pressure drop is also halved.....	163
Figure 5.3 Setup for fixed flow rate method.....	168
Figure 5.4 Typical steps in pressure when flow rates were increased.	169
Figure 5.5 Setup for fixed pressure method (tubes). The manometer level was kept constant by addition from a BSS bottle and tube (not shown).....	171
Figure 5.6 Setup for fixed pressure method (ExPress devices). The manometer level was kept constant by addition from a BSS bottle and tube (not shown).	172
Figure 5.7 Setup for equilibrium pressure without a flap experiment. The scleral flap was not repositioned or sutured after device insertion.	175
Figure 5.8 Photograph of ExPress device <i>in situ</i> (arrow) and reflected scleral flap.....	175
Figure 5.9 Diagram of ExPress device under a sutured flap.....	176
Figure 5.10 Typical pressure curve in equilibrium pressure with an overlying flap experiment. The pressure levelled out after the flap opened to allow flow.	177
Figure 5.11 Setup for index of external leakage experiment. Scleral flaps were not repositioned or sutured, and no BSS was added to the manometer during the test.	178
Figure 5.12 Cross-sections of (a) 50 μ m and (b) 100 μ m tubes (500 \times magnification).	181
Figure 5.13 Profile of two ExPress P200 devices (78 \times magnification).....	181
Figure 5.14 Subconjunctival space ends of (a) P50 and (b) P200 devices (100 \times magnification). The external dimensions and lumens are similarly sized.	182
Figure 5.15 Anterior chamber ends of (a) P50 (160 \times magnification) and (b) P200 devices (200 \times magnification). The external dimensions and lumens are similarly sized.	182
Figure 5.16 AqueSys device (1000 \times magnification).	183

Figure 5.17 (a) Pressure-flow rate relationship with fixed flow rate method. Resistance is calculated from the gradient of the best-fit line. (b) Flow rate-pressure relationship with fixed pressure method. The gradient reflects the facility i.e. the inverse of resistance. 184

Figure 5.18 (a) Flow rate and (b) resistance of ExPress devices with fixed pressure method. The devices demonstrated fixed resistance characteristics. 185

Figure 5.19 Resistance of PTFE tubes with different fluids (n = 6 each). * indicates a statistically significant difference compared to BSS. In the 50 μm tubes, only albumin in BSS (3000 mg/ 100 ml) resulted in higher tube resistance than BSS. In the 100 μm tubes, there were no statistically significant differences between fluids. 187

Figure 5.20 Resistance of ExPress devices with different fluids (n = 4 each). There were no statistically significant differences between fluids in both devices. 188

Figure 5.21 There was no statistically significant difference in equilibrium pressures between the ExPress devices and a trabeculectomy. However, the standard deviation with a trabeculectomy was larger, indicating a wider variability in readings. This may be due to lumen size variations in the trabeculectomy. 190

Figure 5.22 Inner bar (in grey) in the lumen of the P50 device. This bar is located centrally in the device. 193

List of abbreviations

5FU	5-fluorouracil
AC	Anterior chamber
ACG	Angle closure glaucoma
ALT	Argon laser trabeculoplasty
ANOVA	Analysis of variance
BSS	Balanced salt solution
CFD	Computational fluid dynamics
EVP	Episcleral venous pressure
FDA	Food and Drug Administration (USA)
GDD	Glaucoma drainage device
GMS	Gold Micro Shunt
ID	Inner diameter
IOP	Intraocular pressure
LASIK	Laser-assisted <i>in situ</i> keratomileusis
MMC	Mitomycin C
MVR	Micro vitreo-retinal
OD	Outer diameter
OR	Odds ratio
(P)OAG	(Primary) open angle glaucoma
PTFE	Polytetrafluoroethylene
RCT	Randomised controlled trial
SD	Standard deviation
SE	Standard error (of the mean)
SLT	Selective laser trabeculoplasty
TVT	Tube vs Trabeculectomy (Study)

List of symbols

A	Area
ρ	Density
d	Diameter
μ	Dynamic viscosity
Q	Flow rate
H, h	Height
ν	Kinematic viscosity or Poisson's ratio (individually stated in text)
L, l	Length
C	Outflow facility
K	Permeability
P	Pressure
R	Resistance
T	Thickness
t	Time
U	Uveoscleral outflow
u	Velocity
W	Width
E	Young's modulus

Chapter 1

1 Introduction

Glaucoma can be regarded as a group of diseases that have as a common end point a characteristic optic neuropathy which is determined by both structural change and functional deficit (World Health Organisation, 2013). It is the commonest cause of irreversible blindness in the world. The estimate for 2010 is more than 60 million people worldwide are afflicted with this disease and this number will increase to nearly 80 million by 2020 (Quigley & Broman, 2006). Those blind in both eyes amount to more than 8 million people and this will increase to more than 10 million. Glaucoma is classified according to the mechanism of damage and described as either open angle or angle closure types (Foster, Buhrmann, Quigley, & Johnson, 2002). Both of these can be further subdivided into primary (unknown cause) or secondary (due to another ocular pathology) subtypes. The most common type is open angle glaucoma, which accounts for more than 75% of cases globally. Angle closure glaucoma accounts for the remainder but is more common (87% of the total) in Asians, particularly the Chinese (48% of the total). Of the two types, angle closure glaucoma has a greater morbidity, accounting for a nearly equal number of blindness as the more common open angle glaucoma.

The pathogenesis of glaucoma is not fully understood (Weinreb & Khaw, 2004; Kwon, Fingert, Kuehn, & Alward, 2009; Quigley, 2011). The biomechanical theory of glaucoma suggests that raised intraocular pressure (IOP) leads to stress and outward deformation of the weakest part of the scleral shell which is at the lamina cribrosa (Sigal & Ethier, 2009; Downs, Roberts, & Sigal, 2011). Blood flow and nutrient supply to the optic nerve head, which is made up of axons of retinal ganglion cells, become compromised. Additionally, there is also obstruction of retrograde axoplasmic flow carrying essential neurotrophic factors to the

retinal ganglion cell bodies in the retina, thus leading to apoptosis. In the long-term, neural tissue thinning and connective tissue re-modelling through activated astrocytes and lamina cribrosa cells occur, which result in the characteristic cupping appearance of the optic nerve head and functional visual field defects. Independently or in addition is the effect of altered blood flow to the eye and retinal ganglion cells (Grieshaber & Flammer, 2005). Studies which showed progression of glaucoma despite 'normal' IOP readings have challenged the pathophysiological concept of glaucoma based only on raised IOP. Low ocular perfusion pressure, defined by ocular arterial blood pressure minus IOP, is associated with an increased risk of glaucoma, and is likely to be due to disturbed autoregulation and perfusion instability (Caprioli & Coleman, 2010; Cherecheanu, Garhofer, Schmidl, Werkmeister, & Schmetterer, 2013). It may be that ischemia increases susceptibility to pressure-mediated damage. However, at the moment there is no evidence to support the value of increasing a patient's blood pressure as therapy for glaucoma, especially with the potentially serious cardiovascular side effects such as myocardial infarction and cerebrovascular accidents (Quaranta, Katsanos, Russo, & Riva, 2013).

What has been proven in large trials such as the Early Manifest Glaucoma Trial, Ocular Hypertension Treatment Study, Collaborative Normal Tension Glaucoma Study and Advanced Glaucoma Intervention Study is that reducing IOP by 20-30% reduces the potential for disease progression by at least 40% (Heijl et al., 2002; Kass et al., 2002; Collaborative Normal-Tension Glaucoma Study Group, 1998a; Advanced Glaucoma Intervention Study Investigators, 2000). There are many different strategies for reducing IOP, but in advanced cases the form of intervention is usually surgical (Quigley, 2011; Weinreb & Khaw, 2004). The general aim of this thesis is to analyse the effect of surgical intervention in terms of reducing IOP, and engineering methodology is applied to aid this understanding.

The usual approach in assessing surgical techniques and devices is to test them on living eyes. This is inherently complex; along with issues such as medical ethics and cost, there is a significant challenge from biological variability to keep some of the major parameters e.g. aqueous humour inflow and wound healing consistent throughout a series of tests, and with this the problem of reproducibility. There are a number of other research methodologies that can be applied to answer the research question, including *ex vivo* biological tissue models, physical analogue models and computational fluid dynamics (CFD). These different methodologies have distinct advantages and disadvantages. *Ex vivo* biological models such as enucleated eyes are less costly and enable the control or fixation of certain variables such as ‘aqueous humour’ composition and flow rate but they cannot completely replicate the intact *in vivo* biological conditions and reactions (Weinreb & Lindsey, 2005). Experimental outcomes with these models may also be different, due to tissue disorganisation or the variability of post-mortem tissue samples. Physical analogue and CFD experiments enable even more control of variables and more efficient testing but have less relevance than *in vivo* or *ex vivo* experiments as they lack many biological features and require more assumptions. Additionally, with these experiments there is the difficulty in ensuring the correct specification of the material properties or geometry to ensure realistic conditions. Overall, these latter techniques simplify and standardise conditions to tell us general principles to guide the evolution of surgical procedures. The experimental approach used in this thesis includes the use of a large-scale physical analogue model coupled with an image processing technique to study scleral flap characteristics and its effect on aqueous humour flow and pressure control, and also the use of actual and newly developed devices in *ex vivo* experimental settings to look at flow and pressure control which are important in determining the outcome of glaucoma surgery.

In chapter 2, the trabeculectomy and glaucoma drainage devices are described and reviewed. This is followed by a fluid mechanical analysis of the procedure and devices to provide the research questions of this thesis. The analysis using an electrical circuit analogy identifies how the optimal resistance/ permeability characteristics depend on which route the aqueous humour drains by. Another analysis shows the relationship between pressure drop and aqueous humour flow across the device depends on whether it operates in the manner of a valve or a fixed resistor. These provide the impetus for the subsequent experiments.

In chapter 3, a mathematical analysis of the trabeculectomy scleral flap is described, followed by a supporting experiment with a physical model of the trabeculectomy scleral flap. A related piece of work on rectangular flaps (applied to understand Ahmed Glaucoma Valves) is described in Appendix A. The physical model of the trabeculectomy scleral flap is then used to look at the effect of scleral flap geometry and sutures on pressure change and aqueous humour flow direction. This was to look at methods of altering surgical parameters which could help towards achieving desired outcomes.

In chapter 4, a small *ex vivo* study was performed in the process of devising and refining the porcine eye model, to provide confidence in the experimental methodology that is applied in chapter 5, which looked at using smaller diameter tubes to drain aqueous humour out of the anterior chamber. The performances of these tubes were also compared with those of the Express devices.

Another related piece of work is presented in Appendix B. This describes an experiment to look at the effect of a specific intervention (injection of air bubbles into the anterior chamber) during glaucoma surgery.

In this thesis, there is an emphasis on the fluid mechanics in glaucoma surgery but implications for surgical practice are made within each chapter. The general conclusion is stated in chapter 6, along with suggestions for future work that can be done following this one.

Chapter 2

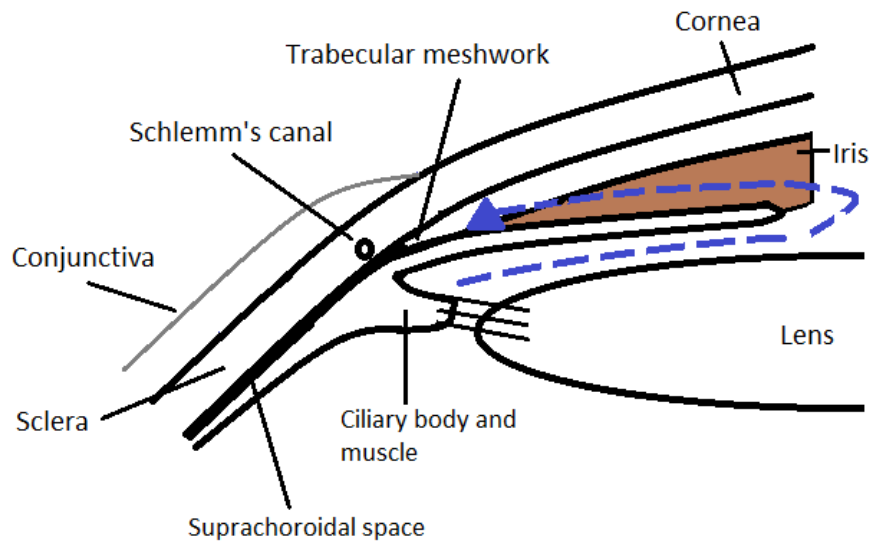
2 Review and analysis of glaucoma surgery

The aim of this review is to describe the trabeculectomy procedure and devices used in glaucoma surgery and analyse them from an engineering perspective. We start off by introducing the concept of IOP and its treatment and follow that up with a description of the technique and devices, organised according to their drainage pathways. Finally, a fluid mechanical analysis is presented that enables the techniques and devices to be classified in a useful conceptual framework, before concluding in section 2.7.

2.1 Aqueous humour and IOP

Aqueous humour provides nutrients to the cornea and surrounding tissue while also removing their metabolic products (Allingham, Damji, Freedman, Moroi, & Shafranov, 2005). In humans, it is produced by ciliary processes on the ciliary body at a secretion rate which varies with a circadian rhythm. Fluorophotometry measurements have shown the rate to be between 1.5 $\mu\text{l}/\text{min}$ at night and 3.0 $\mu\text{l}/\text{min}$ in the morning (Brubaker, 1991). From the ciliary body in the posterior chamber, aqueous humour flows anterior to the lens and through the pupil into the anterior chamber (Figure 2.1a). It then flows peripherally towards the trabecular meshwork at the anterior chamber angle. Up to 90% of outflow occurs through this trabecular or conventional outflow pathway. The trabecular meshwork consists of uveal, corneoscleral and juxtacanalicular layers (Figure 2.1b). After the juxtacanalicular layer, aqueous humour enters the Schlemm's canal through vacuoles and both intra-cellular and para-cellular pores in the inner wall endothelium of the canal, and then exits via collector channels to the aqueous and episcleral veins to rejoin the circulation (Johnson, 2006; Tamm,

a)



b)

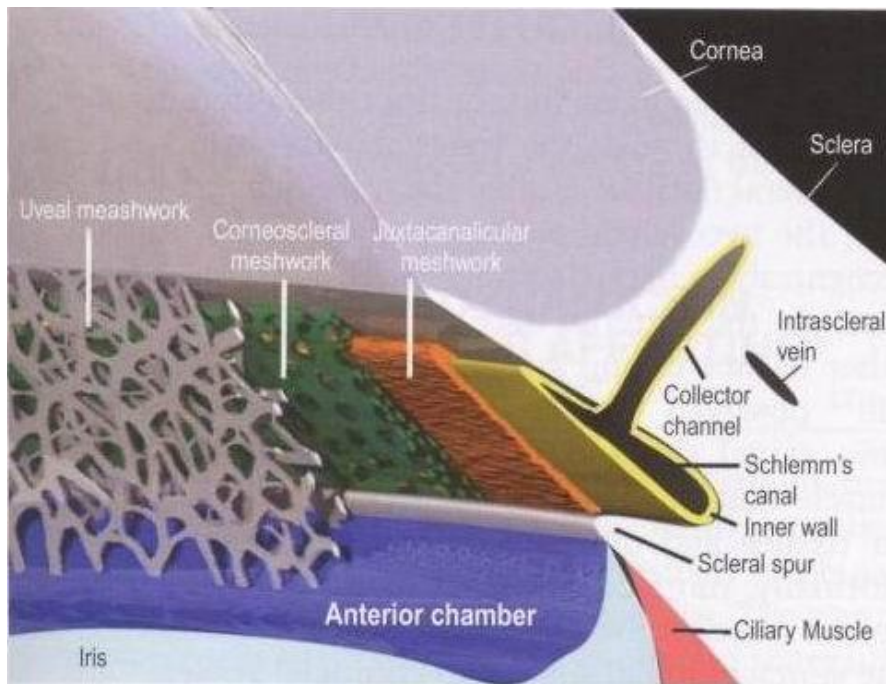


Figure 2.1 (a) Aqueous humour movement (blue arrow) from the ciliary body to the trabecular meshwork and Schlemm's canal. (b) Structure of trabecular meshwork and Schlemm's canal (from Allingham et al., 2005).

2009). The remaining aqueous humour outflow drains out of the eye via the uveoscleral pathway. This pathway starts with aqueous humour entry via the iris root and then through spaces within the ciliary muscle. From the spaces, it enters the supraciliary and suprachoroidal spaces and then finally into the choroidal, scleral and episcleral vessels (Alm & Nilsson, 2009).

IOP is generated by aqueous humour circulation in the anterior chamber of the eye and the resistance to its outflow. Regarding this outflow, the juxtacanalicular trabecular meshwork and inner wall of Schlemm's canal contribute the highest resistance (McEwen, 1958; Grant, 1963; Rosenquist, 1989; Maepea & Bill, 1989). McEwen calculated flow resistance based on dimensions of flow passages in the uveal and corneoscleral trabecular meshwork and found that both did not generate significant resistance. In Grant's study, incision of the uveal and corneoscleral trabecular meshwork in enucleated human eyes resulted in minimal change in outflow facility (or the inverse of resistance). However, when the juxtacanalicular meshwork was excised, the resistance reduced by 75%. In Maepea et al.'s study, micropipettes were inserted in the trabecular meshwork, Schlemm's canal and episcleral veins to look at pressures within them. The bulk of the pressure drop was localised to the vicinity of the juxtacanalicular trabecular meshwork and inner wall of Schlemm's canal. The relationship between IOP, P and aqueous humour flow, Q is shown by the Goldmann equation (Goldmann, 1951; Brubaker, 2004). For an intact conventional aqueous humour outflow pathway,

$$P = \frac{(Q - U)}{C} + EVP, \quad (2.1)$$

where U = uveoscleral outflow, C = outflow facility and EVP = episcleral venous pressure. Typical values for humans are shown in Table 2.1. In particular, episcleral venous pressure has been reported to be between 7 mmHg to 10 mmHg (Zeimer et al., 1983; Toris & Camras,

2008). From here, we can see that this would be the minimum for IOP as long as the conventional outflow pathway is intact.

Table 2.1 Typical values for Goldmann equation variables for humans.

	Range	References
IOP, P (mmHg)	10-21	(Leydhecker, Akiyama, & Neumann, 1958; Klein et al., 1992; Mitchell, Smith, Attebo, & Healey, 1996; Dandona et al., 2000; Czudowska et al., 2010)
Aqueous humour flow rate, Q ($\mu\text{l}/\text{min}$)	1.5-3.0	(Brubaker, 1991)
Uveoscleral outflow, U ($\mu\text{l}/\text{min}$)	0.08-0.28 (direct measurement), 1.1-1.5 (indirect calculation)	(Bill & Phillips, 1971), (Toris, Yablonski, Wang, & Camras, 1999)
Outflow facility, C ($\mu\text{l}/\text{min}/\text{mmHg}$)	0.2-0.4	(Toris & Camras, 2008; Gulati, Ghatge, Camras, & Toris, 2011; Liu et al., 2011)
Episcleral venous pressure, EVP (mmHg)	7-10	(Zeimer et al., 1983; Toris et al., 2008)

Population studies have shown that IOP lies between 10-21 mmHg in $\geq 95\%$ of the subjects examined (Table 2.1; for example, mean IOP 15.5 +/- 2.6 mmHg in the study by Leydhecker et al., 1958). This range has limited functional significance. Glaucoma can occur in patients with IOP values within this range (Collaborative Normal-Tension Glaucoma Study Group, 1998a; Collaborative Normal-Tension Glaucoma Study Group, 1998b). On the other hand, patients with ocular hypertension are able to tolerate pressures higher than 21 mmHg without developing the physical or functional changes of glaucoma (Kass et al., 2002). However, what has been shown convincingly by the large randomised controlled trials looking at IOP reduction and control of glaucoma is that IOP reduction can prevent the progression of glaucoma, and their summaries are presented below.

2.2 Large trials looking at IOP reduction and control of glaucoma

The Early Manifest Glaucoma Trial (EMGT) was a randomised controlled trial involving 255 patients with early visual field loss and median IOP of 20 mmHg, and showed that IOP reductions of 5.1 mmHg or 25% with trabeculoplasty and topical betaxolol reduced disease progression at 6 years (45% in the treated group versus 62% in the non-treated group, a 27.4% difference in disease progression) (Heijl et al., 2002; Leske et al., 2003). Disease progression in the treated group was delayed by a median of 18 months when compared to controls (median time to progression 48 months in the non-treated group and 64 months in the treated group). There was a dose-response effect to treatment, the study estimated that each 1 mmHg reduction in IOP from baseline could decrease the risk of glaucoma progression by 10%. However, it is also important to note that 45% of the treated group still showed disease progression while 38% of the control group were stable, highlighting that IOP is not the only factor involved in disease progression (Wishart, 2009).

In the randomised controlled Collaborative Normal Tension Glaucoma Study (CNTGS), the influence of IOP on normal tension glaucoma was examined (Collaborative Normal-Tension Glaucoma Study Group, 1998a). 140 patients with progressing disease were randomised to IOP reduction of 30% within 6 months by medical, laser and surgical means with subsequent maintenance for 4 years, or untreated. The mean IOP in the treatment group was 10.6 mmHg and in the untreated group was 16.0 mmHg, and disease progression occurred less in the treatment group (14% versus 35%) when examining for specifically defined end-point criteria of glaucomatous optic disc progression or visual field loss. However, the incidence of cataracts was higher with treatment (38% versus 14%), contributed mainly by filtration surgery, which could have influenced the visual field analysis. When an intention-to-treat analysis was performed, the results failed to show any beneficial effect of treatment despite the 30% reduction in IOP (Collaborative Normal-Tension Glaucoma Study Group, 1998b).

The Ocular Hypertension Treatment Study (OHTS) was a randomised controlled trial which demonstrated that medical therapy could reduce IOP by 22.5% and lowering IOP by 20% using topical medication reduced the cumulative probability of glaucomatous visual field loss and/or optic disc changes in patients with ocular hypertension (IOP between 24 mmHg and 32 mmHg) from 9.5% in the observation group to 4.4% in the treatment group at 5 years (Kass et al., 2002). In the second phase report (Kass et al., 2010), when the original observation group received treatment after 7.5 years and then followed-up for another 5.5 years, its IOP reduction was also more than 20% and the cumulative proportion developing glaucoma after the total 13 years of follow-up was 0.16 in the original treated group and 0.22 in the original observation group. One limitation of this study was that if patients who developed only glaucomatous visual field loss were considered, then the difference between

the treatment arm (8.3%) and the non-treatment arm (10.1%) was not statistically significant (Wishart, 2009).

The Advanced Glaucoma Intervention Study (AGIS) was a randomised controlled trial which analysed IOP control and visual field loss progression in patients diagnosed with open-angle glaucoma non-responsive to medical treatment (Advanced Glaucoma Intervention Study Investigators, 2000). 789 eyes in 591 patients were involved, receiving either primary ALT or primary trabeculectomy, supplemented by topical medication and followed by planned additional treatment as necessary to reduce IOP to < 18 mmHg. After 6 years, results showed that patients with average IOP > 17.5 mmHg in the first 18 months had greater visual field defects (by 1.00 units of score), as opposed to patients with IOP < 14 mmHg. The group of eyes with IOP < 18 mmHg in 100% of follow-ups (mean IOP 12.3 mmHg) had no deterioration of the mean visual field defect score compared to those with IOP > 18 mmHg in $> 50\%$ of visits who showed progression by 0.78 units. However, in one subsequent report where data from this study was reanalysed using a point-wise linear regression rather than the original scoring system, there was no relationship between mean IOP and visual field loss, although greater fluctuations in IOP and older age increased the odds of visual field progression (Nouri-Mahdavi et al., 2004).

The Collaborative Initial Glaucoma Treatment Study (CIGTS) was a prospective, randomised controlled trial that compared medical treatment with surgical trabeculectomy as initial therapy for 607 patients with early primary open angle glaucoma (POAG), pseudoexfoliative glaucoma and pigmentary glaucoma (Lichter et al., 2001; Feiner & Piltz-Seymour, 2003). Patients in the surgical group underwent trabeculectomy, with argon laser trabeculoplasty (ALT) if further treatment was needed, followed by a sequence of medications and repeat trabeculectomy. In the medical group, patients received a sequence of

medications which usually began with a topical beta-blocker followed by an alternate, single topical therapeutic agent, and alternate combination medications. Follow-up was at least 6-monthly for a minimum of 4 years. The study found that surgery reduced IOP greater and to a lower number (46% reduction, to 14-15 mmHg) compared to medical treatment (38% reduction, to 17-18 mmHg). However, at the end of the study, the visual field defect scores were similar between the groups and the trabeculectomy group also developed more cataracts (17.3% versus 3.2%). The authors concluded that the results did not support altering treatment paradigms at the time for the initial therapy of newly diagnosed glaucoma patients.

The Glaucoma Laser Trial (GLT) was a prospective, randomised controlled trial to compare Argon Laser Trabeculoplasty (ALT) with topical medication (timolol maleate, a beta-blocker) for patients with newly-diagnosed POAG (Glaucoma Laser Trial Research Group, 1990). 271 patients were enrolled, with each eye randomly assigned to ALT or topical medication and followed-up every 3 months for a period of at least 2 years with IOP, optic disc and visual field checks. The Glaucoma Laser Trial Follow-up Study followed-up 203 of the initial 271 patients in the GLT over median 7 years (Glaucoma Laser Trial Research Group, 1995). If IOP was still elevated (> 21 mmHg or $> 80\%$ of the reference) after the initial intervention, another topical medication (dipivefrin, an alpha- and beta-agonist) was added or drops were started on the laser eye. If intraocular pressure was still not successfully reduced, surgery or further laser treatment was performed according to standardised procedures. When compared with eyes initially treated with topical medication, eyes initially treated with ALT had 1.2 mmHg greater reduction in IOP and 0.6 dB greater improvement in the visual field. The ALT group optic discs also maintained better optic cup area to optic disc area ratios by -0.01 units. The authors concluded that ALT was at least as efficacious as topical medication with regard to IOP lowering in POAG.

2.3 Current treatment of raised IOP

As yet, there is no treatment to restore the visual field loss due to glaucoma. Current treatment modalities aim at the prevention of glaucoma or its progression by reducing IOP, which is still the only modifiable risk factor for this disease. The typical treatment strategy for raised IOP is largely based on the results of the studies described in the preceding section and is generally first with topical medication or laser treatment, followed by surgery (Quigley, 2011; Weinreb & Khaw, 2004).

Topical medication offers the least invasive and least risk option, and up to 30% IOP reduction as seen from the previously described studies. It functions to reduce the production of aqueous humour or increase its outflow. Drugs in the former category include beta-blockers, alpha-adrenergic agonists and carbonic anhydrase inhibitors. Prostaglandin analogues, on the other hand increase the outflow of aqueous humour by the uveoscleral pathway. Laser treatment in open angle glaucoma aims to reduce IOP by enhancing aqueous humour drainage through the trabecular meshwork. ALT and the equally effective selective laser trabeculoplasty (SLT) can reduce IOP by around 30% and have been described as alternatives to regular medication for glaucoma (Juzych et al., 2004; Damji et al., 2006; Glaucoma Laser Trial Research Group, 1990; Glaucoma Laser Trial Research Group, 1995). There are other laser applications for allowing passage of aqueous humour to the trabecular meshwork in angle closure glaucoma such as laser peripheral iridotomy and laser peripheral iridoplasty (Boey, Singhal, Perera, & Aung, 2012) which will not be discussed in this review as they are beyond the scope of this thesis.

Surgical procedures can offer the largest reductions in IOP (40-50%) and are usually reserved for more advanced cases which are not controlled by medical or laser treatment (Quigley, 2011; Weinreb & Khaw, 2004). Additionally, the cost of long-term medical therapy and lack of access to regular medical review and supplies may make surgery the most

suitable first line of treatment in some countries. In these cases, surgeons may only get one attempt at controlling IOP without the ability to follow-up patients frequently (Thomas, Sekhar, & Kumar, 2004).

Glaucoma surgery is aimed at increasing aqueous humour outflow by either shunting it into an alternative drainage location or increasing its flow through the normal pathway, and classified as either penetrating or non-penetrating. Penetrating procedures include trabeculectomy and the insertion of most glaucoma drainage devices (GDD). They involve making a direct connection between the anterior chamber and the subconjunctival space, Schlemm's canal or suprachoroidal space (Figure 2.2). Additionally, with drainage into the subconjunctival space, an overlying conjunctival bleb is formed. The non-penetrating surgical procedures include deep sclerectomy, viscocanalostomy and viscocanaloplasty. With these procedures, the Schlemm's canal is un-roofed to bypass the juxtacanalicular trabecular meshwork and inner wall of Schlemm's canal (Mendrinós & Shaarawy, 2008). There is no direct connection between the anterior chamber and the Schlemm's canal. Instead, they are separated by a thin remaining trabeculo-Descemet's membrane which provides enough outflow resistance to prevent post-operative hypotony. Additionally, no peripheral iridotomy is performed and there is no significant conjunctival bleb formation. Clinical studies have shown that, compared to trabeculectomy, these procedures are associated with lower risks of hypotony, shallow anterior chambers, hyphaema and cataract formation but the reduction in IOP is less, with IOP usually settling in the high teens (Chai & Loon, 2010; Cheng, Xi, Wei, Cai, & Li, 2010; Hondur, 2008). In the meta-analysis by Chai et al. (2010), IOP reduction was 3.6 mmHg less at 1 year and 3.4 mmHg less at 2 years than with trabeculectomies. Relative risks of hypotony, shallow anterior chambers, hyphaema and cataract formation were 0.29, 0.50, 0.19 and 0.31 respectively in relation to trabeculectomy. Additionally, the

procedures also have higher learning curves, particularly to avoid perforating the trabeculo-
Descemet's membrane.

Angle surgery is another category of procedures which is non-penetrating and includes trabeculotomy, goniotomy and the Trabectome procedure. The trabeculotomy and goniotomy procedures are less successful for adults but effective in congenital glaucoma cases (Luntz & Livingston, 1977; Mendicino et al., 2000; Alodhayb, Morales, Edward, & Abu-Amero, 2013). The IOP reduction with the Trabectome is modest, with most settling in the mid to high teens (Maeda, Watanabe, & Ichikawa, 2013; Mosaed, Dustin, & Minckler, 2009).

In this review, the emphasis is on penetrating surgery procedures due to their greater potential for IOP reductions. We classify these interventions in terms of the target site for drainage, whether into the subconjunctival space, Schlemm's canal or suprachoroidal space. This classification is used because these target sites essentially control the resistance characteristics of the operation or device, as will be discussed in section 2.6.

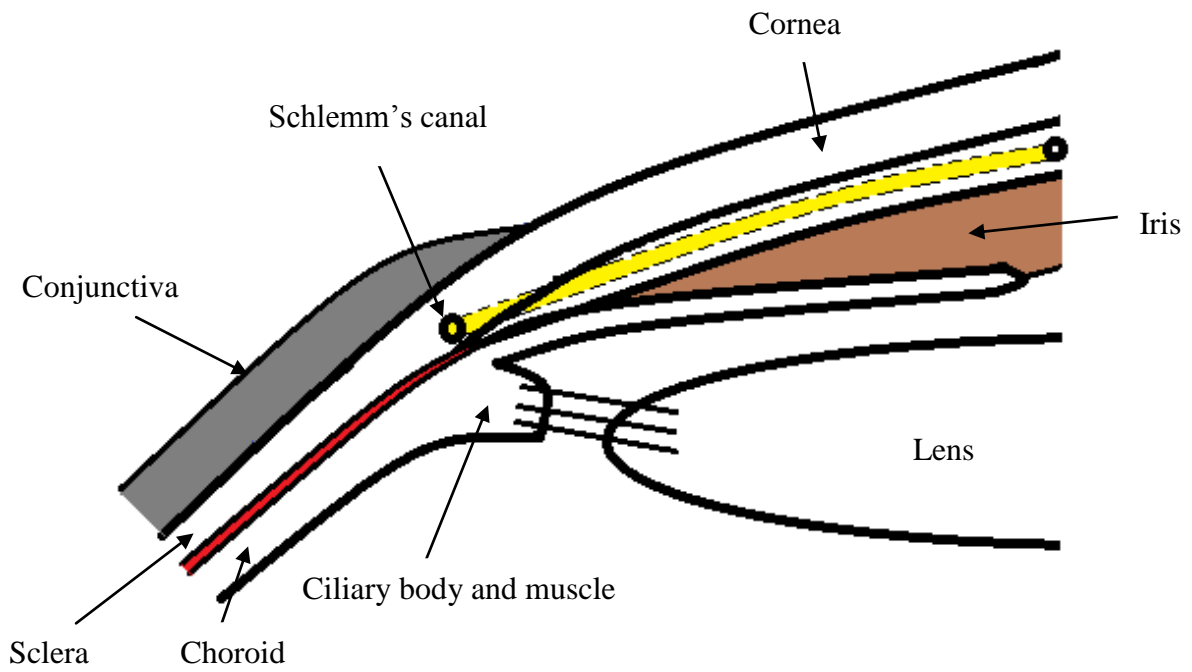


Figure 2.2 Schematic diagram showing the subconjunctival (grey), Schlemm's canal (yellow) and suprachoroidal (red) spaces for alternative aqueous humour drainage.

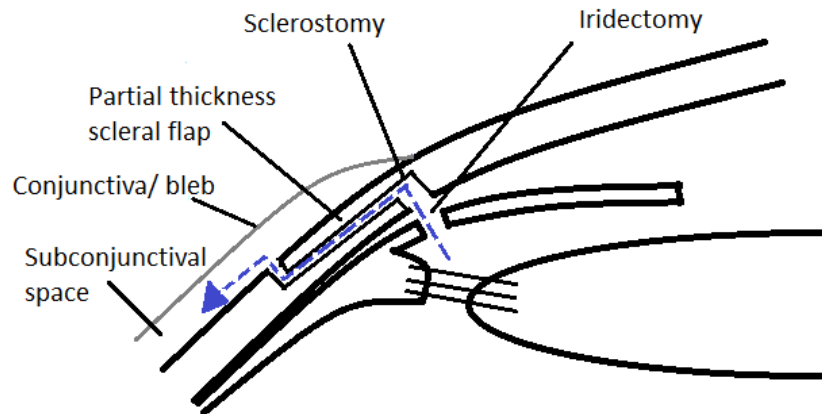
2.4 Subconjunctival space drainage

The subconjunctival space is located between the outer sclera and overlying conjunctiva (Figure 2.2). During surgery, a passage is created for aqueous humour to drain from the anterior chamber into this space. This leads to the formation of a subconjunctival bleb. In the following discussion, we describe the trabeculectomy and glaucoma drainage devices separately, as one involves the creation of a biological valve from eye tissue and the other an implantation of a mechanical device.

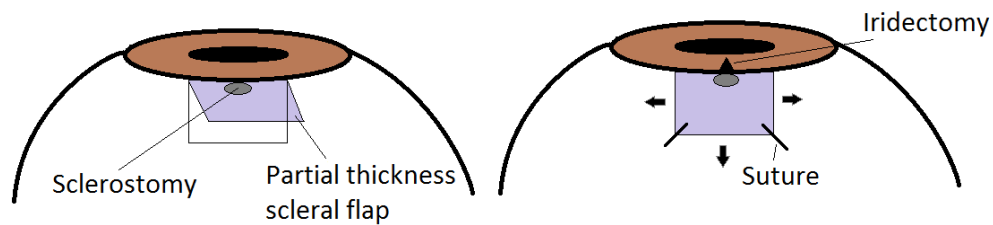
2.4.1 Trabeculectomy

A trabeculectomy involves the creation of a guarded drainage channel in the sclera, through which aqueous humour can flow out of the eye into a subconjunctival bleb in a controlled manner, thereby reducing the IOP (Figure 2.3). This procedure was developed because previous procedures such as iridencleisis, trephination and Scheie's procedure were full thickness (non-guarded) and nearly always led to post-operative hypotony and cataract (Elliot, 1909; Scheie, 1958; Spaeth, Joseph, & Fernandes, 1975; Razeghinejad & Spaeth, 2011). Since its description in 1968 (Cairns, 1968; Watson & Barnett, 1975), small variations in technique have been described, including different conjunctival incision sites (Shuster, Krupin, Kolker, & Becker, 1984; Jones, Clarke, & Khaw, 2005), scleral flap shapes and sizes (Clemente, 1980; Vernon, Gorman, & Zambarakji, 1998; Edmunds, Thompson, Salmon, & Wormald, 2001; Dhingra & Khaw, 2009), methods to create sclerostomies (Dellaporta, 1975; Dhingra et al., 2009), the use of anti-fibrotic agents (Khaw et al., 2001; Wong et al., 2009c) and the use of adjustable or releasable suture techniques (Wells, Bunce, & Khaw, 2004; de Barros, Gheith, Siam, & Katz, 2008). The effect of some of these variables will be tested and described in more detail in Chapters 3 and 4. A typical technique, the Moorfields Safer

a)



b)



c)



Figure 2.3 a) Schematic diagram of trabeculectomy showing the direction of aqueous humour outflow (broken arrow). b) Schematic diagram of trabeculectomy scleral flap. The conjunctival layer and bleb are not shown. Black arrows show aqueous humour outflow under the conjunctival bleb. c) Intra-operative photograph of trabeculectomy scleral flap.

Surgery System (Jones et al., 2005; Dhingra et al., 2009; Khaw et al., 2012) is described in more detail below.

In this system, a corneal traction suture is inserted with a spatulated 7/0 silk suture on a curved needle. This is better than placing a superior rectus suture which may cause superior rectus haematoma, globe perforation, subconjunctival haemorrhage, post-operative ptosis, and lesser treatment success (Edmunds, Bunce, Thompson, Salmon, & Wormald, 2004; Grehn et al., 2007). A conjunctival incision between 6-8 mm long is then made, preferably in the superior half to reduce the risk of subconjunctival haemorrhage, dysaesthesia, inflammation and endophthalmitis (Wells, Marks, & Khaw, 2005; Budenz, Hoffman, & Zacchei, 2001; Wolner et al., 1991). A fornix-based conjunctival incision is preferred as it is easier and faster to perform, allows good exposure of the surgical site, easier for re-operations when there is extensive scarring, and leads to more diffuse and less cystic blebs (Wells, Cordeiro, Bunce, & Khaw, 2003; Alwitry, Patel, & King, 2005; Fukuchi et al., 2006). However, there may be a higher risk of wound leakage with this type of incision and it is important to handle tissue gently, such as with the use of non-crushing conjunctival clamps. Following a generous dissection of Tenon's capsule with blunt scissors, haemostasis needs to be achieved with the minimum amount of wet-field diathermy. The correct creation of a partial-thickness (around 0.25 mm thick) scleral flap measuring 3-4 mm long and 4-5 mm wide is important as the flap provides the main resistance to aqueous humour outflow and hypotony in the early post-operative period (Birchall, Wakely, & Wells, 2006; Birchall, Bedgood, & Wells, 2007; Tse et al., 2012). The sides are not extended to the limbus as this helps to promote more posterior aqueous humour flow which is associated with larger and more diffuse blebs, less scarring and inflammation, and less hypotony (Birchall et al., 2006). Thinner flaps are avoided as they may lead to tears, dehiscence and cheese-wiring, all of which lead to reduced flap resistance and hypotony. Anti-fibrotics such as 5-fluorouracil

(5FU) 5% or Mitomycin C (MMC) 0.02-0.05% are applied under the conjunctiva and scleral flap with polyvinyl alcohol (PVA) sponges for 3 minutes in patients with high-risk of scarring and complications such as neovascular or inflammatory glaucoma, previous failed surgery, aphakia, and Afro-Caribbean descent. It is important to note that anti-metabolite application improve trabeculectomy outcomes but may also increase the risks of bleb leakage, hypotony and infection (Fluorouracil Filtering Surgery Study Group, 1996; Cheung, Wright, Murali, & Pederson, 1997; Khaw, 2001; Wilkins, Indar, & Wormald, 2005). Irrigation with at least 20 ml of Balanced Salt Solution (BSS) is needed to remove excess 5FU or MMC after the 3 minutes. A cannula is inserted into the anterior chamber via a paracentesis, and a balanced salt solution (BSS) infusion is started to prevent fluctuation in anterior chamber pressure and reduce the risk of suprachoroidal haemorrhage and further optic nerve compromise (Stalmans, 2006). The infusion rate is varied by positioning the infusion bottle at different levels above the patient's eye. A small part of the sclera and trabecular meshwork is then excised with a punch to make a standardised opening of 0.5 mm diameter for aqueous humour to flow under the scleral flap and into the subconjunctival space. Using a blade and scissors to create this sclerostomy is also possible but this may create a larger and irregular ostium with higher attendant risk of hypotony. A peripheral iridectomy is created to prevent pupillary block by incising a section of presenting iris horizontally. This iridectomy is placed at the 12 o'clock position so that it is hidden under the upper lid to prevent glare and diplopia. The partial-thickness scleral flap is preferably sutured down with adjustable or releasable sutures (Wells et al., 2004; de Barros et al., 2008), or alternatively with interrupted sutures which can be removed by laser lysis post-operatively (Melamed, Ashkenazi, Glovinski, & Blumenthal, 1990). Tight sutures are preferable as they prevent overfiltration from the scleral flap in the early post-operative period. The tightness of these sutures is adjusted according to the fluid flow from the infusion into the anterior

chamber. Finally, watertight closure of the conjunctival layer is performed with either purse-string or mattress sutures, with the knots tucked into corneal grooves. Round-bodied needles assist in the prevention of conjunctival tears and wound leaks. Post-operatively, suture adjustment can be performed from two weeks to a few months to titrate aqueous humour flow and IOP as needed.

2.4.1.1 Changes to the trabecular aqueous humour outflow pathway after trabeculectomy surgery

These changes include accumulation of extracellular material in the trabecular meshwork adjacent to the inner wall of Schlemm's canal (Lutjen-Drecoll & Barany, 1974) and decrease in diameter of Schlemm's canal (Johnson & Matsumoto, 2000), both seen from electron microscopy. As these changes were more obvious with clinically successful surgery (high facility of flow or presence of blebs and low IOP in the clinical history), the findings were attributed to lower aqueous humour flow through the trabecular meshwork as a result of the bypass. Changes to the uveoscleral pathway after trabeculectomy surgery have not been reported. However, uveoscleral outflow may increase if there is inflammation (Toris & Pederson, 1987), cyclodialysis (Toris & Pederson, 1985) or choroidal detachment (Joo, Ko, & Choe, 1989; Pederson, Gaasterland, & MacLellan, 1979).

2.4.1.2 Post-operative hypotony

There are many varied definitions of hypotony (Seah et al., 1995; Schubert, 1996; Rahman, Mendonca, Simmons, & Simmons, 2000; Costa & Arcieri, 2007), and one is low pressure (± 5 mmHg) [whether acute, transient, chronic or permanent] in an individual eye, leading to functional [whether asymptomatic or symptomatic] and structural changes [whether reversible or irreversible] (Schubert, 1996). The associated structural and functional changes include corneal oedema, shallow anterior chambers, cataracts, choroidal effusion, chorioretinal folds, papilloedema, maculopathy, visual loss and metamorphopsia (Costa et al., 2007). Additionally, hypotony may result in around 20% lower 5-year survival rates (Benson, Mandal, Bunce, & Fraser, 2005), thought to be due to reduced aqueous humour flow into the bleb and a relative increase in inflammatory mediators thus causing increased fibrosis. The occurrence rate of hypotony was higher when full thickness surgery was performed (17-74%) but reduced after the introduction of the guarded trabeculectomy procedure (10-23%) (Spaeth et al., 1975; Lamping, Bellows, Hutchinson, & Afran, 1986; Blondeau & Phelps, 1981). Younger age and myopia are risk factors for this condition, attributed to the reduced scleral rigidity in these conditions (Seah et al., 1995).

The possible causes of hypotony can be separated into early and late ones (Rahman et al., 2000; Benson et al., 2005). In the early stage, these are decreased aqueous humour production, increased uveoscleral outflow, overfiltration and wound leakage. Decreased aqueous humour production may be caused by post-operative ciliary body shutdown, which is associated with ocular inflammation (Toris et al., 1987) and the use of MMC (Nuyts et al., 1994; Gandolfi, Vecchi, & Braccio, 1995). Increased uveoscleral flow is caused by inflammation (Toris et al., 1987) cyclodialysis (Toris et al., 1985) and choroidal detachment (Joo et al., 1989; Pederson et al., 1979). Cyclodialysis is closely related to choroidal detachment, it occurs when the ciliary body detaches from the scleral spur after inadvertent

trauma during surgery, allowing aqueous humour into the suprachoroidal space. Early overfiltration occurs when there is too much aqueous humour flow passing under the scleral flap into the subconjunctival space, usually a result of inadequate or loose suture closure. Wound leakage occurs when there is inadequate closure or holes in the conjunctival layer. Other causes of early hypotony also include retinal detachment and globe perforation. In the late stage, cyclitic membranes can occur with inflammation and cover the ciliary body, which results in reduced aqueous humour production (Rahman et al., 2000). Overfiltration from an over-functioning bleb and leakage either through the bleb or wound dehiscence may also occur, particularly with the use of intra-operative MMC and 5FU (Shields, Scroggs, Sloop, & Simmons, 1993; Seah et al., 1995; Sihota et al., 2000).

Prevention of reduced aqueous humour production can be done by pre-operative steroid treatment in inflammatory cases (Rahman et al., 2000). For prevention of early overfiltration, placing tight scleral flap sutures which can be either adjusted, released, or removed by laser can limit the initial flow of aqueous humour (Wells et al., 2004; de Barros et al., 2008; Melamed et al., 1990). Meticulous suturing of the conjunctiva reduces the risk of wound leakage (Jones et al., 2005). Some cases of hypotony may be transient and need no treatment, but treatment may be necessary if it persists for more than 4-8 weeks to avoid permanent vision loss, particularly if maculopathy is present (Seah et al., 1995; Costa et al., 2007). To increase aqueous humour production, steroids may be needed to suppress inflammation of the ciliary body (Rahman et al., 2000). Cyclodialysis may need cycloplegia (whilst avoiding steroids), diathermy or laser treatment (Burchfield & Kolker, 1995), or cyclopexy (Spiegel, Katz, & McNamara, 1990) for it to close although choroidal detachment on its own is usually self-limiting (Pederson et al., 1979). Overfiltration can be treated with scleral flap re-suturing (Schwartz et al., 1996), a Simmons scleral shell (Simmons & Kimbrough, 1979), argon laser to shrink overly large blebs (Fink, Boys-Smith, & Brear, 1986) and injection of autologous

blood into blebs (Wise, 1993). Bleb leakage can be treated by using aqueous humour suppressants to reduce flow through the bleb (Costa et al., 2007), a Simmons scleral shell or symblepharon ring (Ruderman & Allen, 1985; Melamed, Hersh, Kersten, Lee, & Epstein, 1986; Hill, Aminlari, Sassani, & Michalski, 1990), a contact lens or shield (Blok, Kok, van Mil, Greve, & Kijlstra, 1990; Fourman & Wiley, 1989), topical gentamycin to stimulate wound healing (Tomlinson, Belcher, III, Smith, & Simmons, 1987), fibrin glue (Kajiwara, 1990), autologous blood injections (Wise, 1993; Smith, Magauran, III, Betchkal, & Doyle, 1995), conjunctival compression sutures to reduce leakage (Palmberg, 1996) or suturing donor scleral patches over areas of scleral maceration (Harizman, Ben Cnaan, Goldenfeld, Levkovitch-Verbin, & Melamed, 2005).

2.4.1.3 IOP outcomes and complications of trabeculectomy

Table 2.2 lists the IOP outcomes in recent trabeculectomy studies. The final reduction in IOP is 40-51% of the pre-operative value and it settles around 10-15 mmHg. Note that the majority of the studies involved the use of 5FU and MMC. Table 2.3 lists the commonest complications in the studies. It can be seen that most of the early complications are related to hypotony, including shallow anterior chambers (AC), choroidal effusion or detachment, maculopathy and cataracts, while bleb-related complications such as bleb leakage, infection and encapsulation are more common in the later period. Other reports also support this observation (Kangas, Greenfield, Flynn, Jr., Parrish, & Palmberg, 1997; DeBry, Perkins, Heatley, Kaufman, & Brumback, 2002). Overall, the findings highlight the fact that trabeculectomies still have only moderate long term results and a high risk profile, especially with the increased usage of anti-fibrotics. One main challenge is to eliminate early post-operative hypotony but yet still maintain enough aqueous humour drainage for satisfactory IOP reduction. It is here that the knowledge of pressure and flow control becomes important in trying to achieve the desired outcomes of this challenge.

Table 2.2 IOP outcomes after trabeculectomy in recent studies.

Authors	Follow-up (months)	Anti-fibrotic	Baseline mean IOP (mmHg)	Final mean IOP (mmHg)	Reduction in IOP (%)	Notes
(Wong et al., 2013)	96	5FU	24.4	13.7	43.9	Singapore 5FU trial, RCT
(Gedde et al., 2012b)	60	MMC	25.6	12.6	50.8	Tube vs Trabeculectomy Study, RCT
(Shah, Agrawal, Khaw, Shafi, & Sii, 2012)	48.6	MMC	33.7	13.1	41.1	ReGAE, Afro-Caribbean, prospective
(Lusthaus, Kubay, Karim, Wechsler, & Booth, 2010)	24	MMC	25.3	14.0	44.7	
(Tran et al., 2009)	60	MMC	22.0	11.1	49.5	Trabeculectomy vs Ahmed Glaucoma Valve, retrospective
(Law, Shih, Tran, Coleman, & Caprioli, 2009)	36	MMC	18.8	10.3	45.2	Initial vs repeat trabeculectomy study, retrospective
(Bevin, Molteno, & Herbison, 2008)	> 60	MMC/ 5FU (in 2% of cases)	24.9	14.8 (60 months)	40.6	Otago Glaucoma Surgery Outcome Study, prospective
(Stalmans, 2006)	16		21.2	12.8	39.6	Moorfields Safer Surgery System, retrospective
(Edmunds et al., 2001)	12	5FU, MMC	26.2	14.4	45.0	UK National Survey of Trabeculectomy
(Lichter et al., 2001)	60	MMC, 5FU	27	14-15	46.3	CIGTS, RCT

Table 2.3 List of common complications after trabeculectomy surgery in recent studies (early - < 4-6 weeks, late - > 4-6 weeks).

Authors	Anti-fibrotic	Hypotony	Shallow AC	Choroidal effusion/ detachment	Wound leakage	Hypotony maculopathy
(Gedde et al., 2012a)	MMC		10% (early), 0% (late)	13% (early), 4% (late)	11% (early)	5% (late)
(Jampel et al., 2012)	MMC/ 5FU	20% (total), 10% (late)				
(Shah et al., 2012)	MMC	10.6% (early), 0% (late)		14.9% (early)	8.5% (early)	0%
(Lusthaus et al., 2010)	MMC	55% (early), 3.3% (late)	56.7% (early), 1.7% (late)			
(Wong et al., 2009)	5FU		7%	9% (early)		0%
(Tran et al., 2009)	MMC	59% (early), 16% (late)		10% (early)		
(Law et al., 2009)	MMC	40% (early), 21% (late)	5%	1%	1%	4%
(Bevin et al., 2008)	MMC/ 5FU (in 2% of cases)	39% (early)	14% (early)	12% (early)		
(Stalmans, 2006)				8.9% (early)		
(Jampel et al., 2005)	MMC, 5FU	0.9% (early)	13% (early)	11% (early)	6% (early)	

(Continued) **Table 2.3** List of common complications after trabeculectomy surgery in recent studies (early - < 4-6 weeks, late - > 6 weeks).

Authors	Anti-fibrotic	Cataract progression	Bleb leakage	Blebitis/ endophthalmitis	Other
(Gedde et al., 2012a)	MMC		6% (late)	5% (late)	Hyphaema 8% (early), suprachoroidal haemorrhage 3%, malignant glaucoma 1% (early), bleb encapsulation 6% (late)
(Jampel et al., 2012)	MMC/ 5FU	55%	5.2% (late)	0.4% (early), 3.5% (late)	Oversized bleb 3.5%
(Shah et al., 2012)	MMC		2.1%	0%	Hyphaema 4.3% (early), suprachoroidal haemorrhage 0%
(Lusthaus et al., 2010)	MMC	1.7% (early), 1.7% (late)	1.7% (early)	0%	
(Wong et al., 2009)	5FU	50%	13%	0%	Oversized bleb 5%, uveitis 14%
(Tran et al., 2009)	MMC	13%			Hyphaema 4.5% (early)
(Law et al., 2009)	MMC			3%	Hyphaema 25%
(Bevin et al., 2008)	MMC/ 5FU (in 2% of cases)				Hyphaema 27% (early)
(Stalmans, 2006)				1.5% (early)	Hyphaema 5.4%, malignant glaucoma 1.5%, bleb encapsulation 14.3%
(Jampel et al., 2005)	MMC, 5FU			0%	Hyphaema 10% (early), suprachoroidal haemorrhage 0.7%, bleb encapsulation 12%

2.4.2 Subconjunctival space GDD

More recently, glaucoma drainage devices have evolved from being a second or third line surgical treatment for glaucoma to being proposed as first line surgical treatment. The Tube Versus Trabeculectomy (TVT) study is a randomised controlled trial to look at the differences between trabeculectomy with MMC (0.4 mg/ml for 4 minutes) and a Baerveldt 350 mm² device (Gedde et al., 2012b; Gedde et al., 2012a). Patients 18 to 85 years of age who had previous trabeculectomy and/or cataract extraction with intraocular lens implantation and uncontrolled glaucoma with IOP \geq 18 mmHg and \leq 40 mmHg on maximum tolerated medical therapy were included. From the total of 212 eyes, 107 were in the tube group and 105 were in the trabeculectomy group. At 5 years, IOP was 14.4 mmHg in the tube group and 12.6 mmHg in the trabeculectomy group, although this difference was not statistically significant. The number of glaucoma medications was 1.4 in the tube group and 1.2 in the trabeculectomy group, again the difference was not statistically significant. The cumulative probability of failure (IOP > 21 mmHg or not reduced by 20%, IOP \leq 5 mmHg, reoperation for glaucoma, or loss of light perception vision) was significantly higher in the trabeculectomy group (46.9% versus 29.8%; mainly due to inadequate IOP control but persistent hypotony was a larger component in the trabeculectomy group). The rate of re-operation for glaucoma (including suture lysis and post-operative 5FU injections) was significantly higher in the trabeculectomy group (29% versus 9%). Early post-operative complications were more common in the trabeculectomy group (37% versus 21%), mainly due to hyphaema and wound leaks in this group; hypotony related complications were similar between the groups. Late post-operative complications were similar in both groups (34% in the tube group, 36% in the trabeculectomy group; although choroidal effusion and hypotony maculopathy were more common in the trabeculectomy group), as was the rate of re-operation for complications (22% in the

tube group, 18% in the trabeculectomy group) and the rate of cataract extraction (54% in the tube group, 43% in the trabeculectomy group). The authors concluded that tube shunt surgery had a higher success rate compared to trabeculectomy with MMC. Both procedures were associated with similar IOP reduction and use of supplemental medical therapy but additional glaucoma surgery was needed more frequently after trabeculectomy with MMC. Surgical complications were common but most were transient and self-limiting. Although the rate of early post-operative complications was higher following trabeculectomy, the rates of late post-operative complications, re-operation for complications, and cataract extraction were similar with both surgical procedures.

The results of this study have attracted much discussion about its limitations (Caprioli, 2011; Singh & Gedde, 2011; Gross, 2012). Among them include that when the success rate was defined as < 14 mm Hg, there was no statistically significant difference between the groups. MMC dosage with trabeculectomy evolved during the time of the study, and lower dosages and durations used currently may result in less failure due to hypotony. The larger number of early post-operative complications in the trabeculectomy group comprised mainly of hyphaema and wound leaks, which were transient and self-limiting; serious complications requiring re-operation or loss of ≥ 2 lines of vision were similar between the groups. The findings are also limited to the Baerveldt device and not others like the Ahmed or Molteno ones. Comparison between Baerveldt and Ahmed devices will be discussed subsequently. Finally, this TVT study involved treatment of eyes with previous operations, in which device insertions are relatively well-established; results of trabeculectomy in un-operated eyes may be better. To conclude, the findings of the TVT study cannot be extrapolated to all trabeculectomies, all tubes, and all glaucoma patients. The relative merits of

trabeculectomy and glaucoma drainage device surgery should be considered individually for each patient in selecting the optimal glaucoma operation.

The first glaucoma drainage devices were reported in the early 1900s and employed horse hair and silk thread to drain the anterior chamber (Rollett & Moreau, 1907; Zorab, 1912; Lim, 1998). Subsequent attempts used various other materials, such as gold, platinum, tantalum and polyethylene but their long-term success was also limited (Stefansson, 1925; Row, 1934; Bick, 1949; Bietti, 1955). Most failed due to scar formation or seton migration and exposure. In 1969, Molteno described using a 1.0 mm long translimbal acrylic tube attached to an acrylic plate 8.5 mm in diameter and suturing the device to the sclera just beyond the limbus (Molteno, 1969). This device was intended to promote the formation of a juxtalimbal bleb and was then removed after a few months. The complications resulting from this procedure included uveitis, corneal irritation and discomfort due to the close proximity to the limbus. It was later modified to have a longer tube and its explant positioned at the equatorial region of the eye (Molteno, Straughan, & Ancker, 1976). Many of the currently available glaucoma drainage devices are still based on this concept of a long silicone tube of around 300 µm inner diameter connecting the anterior chamber (or vitreous cavity in the case of pars plana insertion) to a large explant or end-plate placed 9-10 mm posterior to the limbus. The explant would prevent conjunctival adhesion and develop an overlying fibrovascular capsule after 4-6 weeks. Once formed, all aqueous humour flow will be into this capsule before being absorbed by capillaries and lymphatic vessels in the lining. This capsule would provide the primary resistance to aqueous humour flow after its completion (Minckler, Shammam, Wilcox, & Ogden, 1987).

The earliest devices did not offer resistance to aqueous humour outflow, which resulted in a significant number of cases developing early post-operative hypotony, flat

anterior chambers and choroidal effusions. Subsequently, valved designs were introduced to reduce their occurrences. The first to offer a valve to limit overdrainage was the Krupin device (Krupin, 1976). This was followed later, among others, by the Ahmed Glaucoma Valve in 1993 (Lim, 1998). With the current non-valved devices, surgeons routinely restrict flow through them for 3-4 weeks after insertion, using external absorbable ligatures (Molteno, Polkinghorne, & Bowbyes, 1986) or internal removable suture stents (Egbert & Lieberman, 1989). Some early flow of aqueous humour to the outside of the eye is permitted by fenestrating the silicone tubes with a suture needle proximal to the ligation or occlusion site (Sherwood & Smith, 1993). Alternatively, some surgeons perform a 2-stage insertion where the device is sutured at its equatorial position but not connected to the anterior chamber. After about 6 weeks, when the fibrous capsule has developed then only is the tube inserted into the anterior chamber. During the time between both stages, either medical therapy or an ‘orphan’ trabeculectomy is used for IOP control (Molteno et al., 1986; Shaarawy, Sherwood, Hitchings, & Crowston, 2009).

Another major design modification was the increase in surface area of the explant to enhance the reduction in IOP. The double-plate Molteno implant was introduced in 1981 and this was followed by the Baerveldt device in 1992 which initially came in sizes of up to 500 mm². One study found that double-plate Molteno implants lowered IOP more than single-plate ones (Heuer et al., 1992). However, one Baerveldt study later showed that the 350 mm² device had a higher success rate when compared to the 500 mm² one (Britt et al., 1999). The current belief is that beyond an optimal size, any further increase in surface area might only be disadvantageous. Sizes between 250-350 mm² appear to offer the best trade-offs between IOP control and hypotony. In Table 2.4, we list the dimensions and materials of glaucoma drainage devices.

Table 2.4 Summary of glaucoma drainage devices and trabeculectomy.

Device	Drainage site	External dimensions	Explant surface area (mm ²)	Explant material	Valve	Tube material (inner/ outer diameter)
Trabeculectomy	A	Width 4 mm, length 3 mm (typical values but highly variable)	Variable bleb size	NA	Y (scleral flap)	NA
Ahmed Glaucoma Valve	A	Width 13 mm (184 mm ²), length 16 mm (184 mm ²), plate thickness 0.9 mm (silicone), 1.9 mm (polypropylene)	96, 184, 364	Silicone/ Polypropylene	Y	Silicone (300 µm, 640 µm)
Molteno	A	Circumferential diameter 13 mm (135 mm ²), plate thickness 1.65 mm	135, 270	Polypropylene	N	Silicone (340 µm, 640 µm)
Molteno 3	A	Width 15 mm, length 16 mm (175 mm ²), plate thickness 1.5 mm	175, 230	Silicone	N	Silicone (340 µm, 640 µm)
Baerveldt	A	Width 22 mm (250 mm ²), 32 mm (350 mm ²), length 13 mm, plate thickness 0.84 mm	250, 350	Silicone (barium-impregnated)	N	Silicone (300 µm, 640 µm)
ExPress	A	Length 2.64 mm (P50, P200), 2.96 mm (R50)	NA	NA	N	Stainless steel (50 µm [P50, R50] or 200 µm [P200], 380 µm)
MIDI-Arrow	A	Length 8.5 mm	NA	NA	N	SIBS (70 µm inner diameter)
AqueSys	A	Length 6 mm	NA	NA	N	Gelatine (50 µm inner diameter)

A – subconjunctival space, B – Schlemm’s canal, C – suprachoroidal space, NA – not applicable/ not available, Y – yes, N – no

(Continued) **Table 2.4** Summary of glaucoma drainage devices and trabeculectomy.

Device	Drainage site	External dimensions	Explant surface area (mm ²)	Explant material	Valve	Tube material (inner/ outer diameter)
Schocket	A	Width 4 mm (#20 band), 6 mm (#220 band), circumferential diameter 24 mm (at equator)	300 (#20 band), 450 (#220 band)	Silicone	N	Silicone (NA)
Krupin	A	Width 18 mm, length 13 mm, plate thickness 1.75 mm	180	Silicone	Y	Silicone (300 µm, 640 µm)
Optimed	A	Width 10 mm, length 14 mm, plate thickness 1.3 mm	140	PMMA	Y	Silicone (380 µm, 760 µm)
iStent	B	Length 1 mm (body), 250 µm (snorkel) [GTS100], length 360 µm [GTS400]	NA	Titanium	N	(120 µm, 180 µm) [GTS100] (230 µm outer diameter) [GTS400]
Hydrus	B	Length 15 mm	NA	Nitinol	N	NA
Gold Micro Shunt	C	Width 3.2 mm, length 5.2 mm, plate thickness 44 or 68 µm	NA	Gold (24-karat)	N	(9-19 × 24-40 µm high, 50 µm wide microchannels)
CyPass	C	Length 6.35 mm	NA	Polyimide	N	(300 µm, 510 µm)
Aquashunt	C	Width 4 mm, length 10 mm, plate thickness 0.75 mm	NA	Polypropylene	N	NA

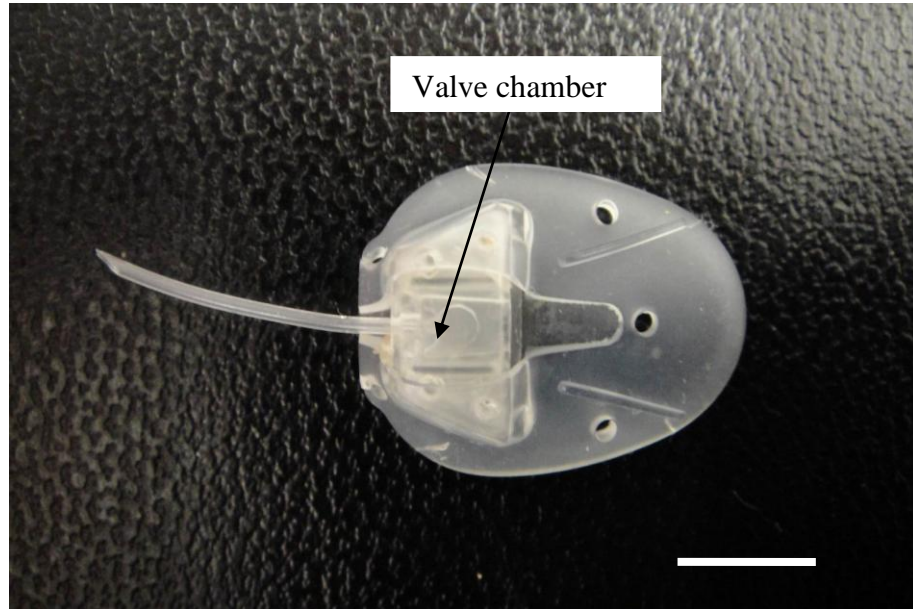
A – subconjunctival space, B – Schlemm's canal, C – suprachoroidal space, NA – not applicable/ not available, Y – yes, N - no

The Ahmed Glaucoma Valve consists of an explant with a trapezoid-shaped chamber which encloses a folded silastic sheet valve (Figure 2.4). The explants were first made of polypropylene but lower profile silicone ones were later introduced. These have been shown to provide better IOP reduction and fewer Tenon's cysts, attributed to the change in material and height (Ishida et al., 2006; Mackenzie, Schertzer, & Isbister, 2007). The manufacturer claims that the valve chamber design creates a Bernoulli's principle effect, although this has been refuted and the effect considered negligible (Lee, 1998). The valve is said to open at 8 mmHg or higher to prevent hypotony and works on the principle that pressure exerted by viscous forces controls its opening. However, there is variability in valve performance between individual devices, with each having different sensitivities of their response (Prata, Jr., Mermoud, LaBree, & Minckler, 1995; Moss, 2008) and this is likely to be due to the lack of consistency in manufacture. Finally, this valve was also claimed to become superfluous after a fibrovascular capsule had formed over the explant. However, subsequent studies showed that it added to the total resistance to aqueous humour flow and could get obstructed in the presence of excess anterior chamber inflammation and fibrin formation (Pan, 2002; Brown, Pan, & Ziaie, 2003).

Latest developments to the device include encasing in a polyethylene shell with pores to allow tissue integration and vascular ingrowth that gives resistance to infection, exposure, extrusion, and mechanical deformation (Kim et al., 2013). The 1-year report showed similar reductions in IOP and success rates compared to silicone and polypropylene devices. The long term results have not been reported however. Preliminary work is also being done on biodegradable sheets for the valve, designed to degrade at around 6 weeks when the hypertensive phase, which signifies device encapsulation, develops (Luong et al., 2013). Implantation in a small number of rabbits showed a more stable IOP profile during the first 12 weeks (signifying avoidance of the

hypertensive phase) after surgery and less collagen deposition around the device as compared to a 'normal' silicone Ahmed Glaucoma Valve.

a)



b)

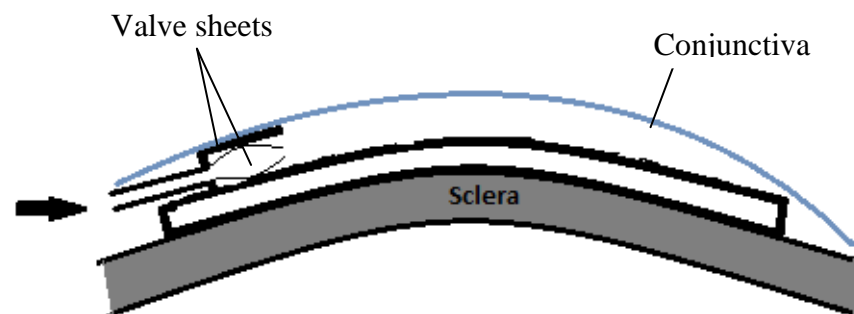


Figure 2.4 a) Photograph of Ahmed Glaucoma Valve (scale bar = 5 mm). b) Schematic cross-section diagram of the resistance mechanism (adapted from Lim (1998)). The valve sheets are said to separate at 8 mmHg or higher.

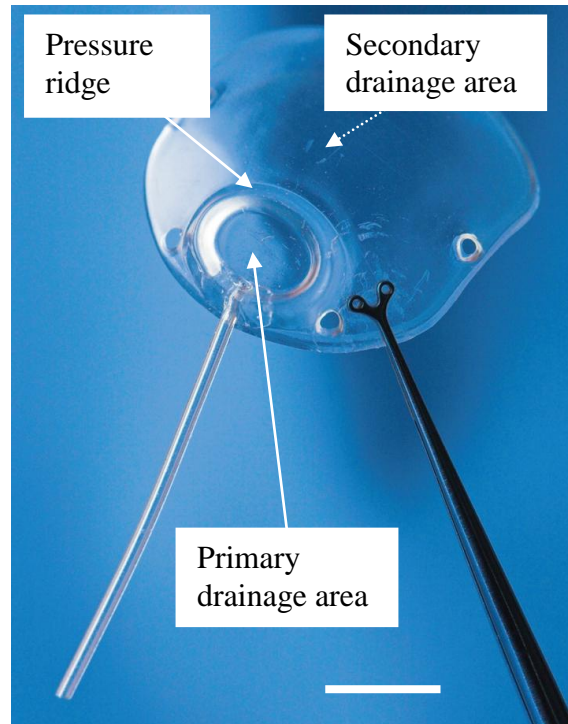
The Molteno devices include the single plate, double plate and Molteno 3 (Figure 2.5a). The double plate Molteno increases the effective surface area of a single plate from 135 mm² to 270 mm². The single and double plate devices are available with a pressure ridge design intended to reduce post-operative hypotony (Freedman, 1992). Aqueous humour would flow into the explant which is constrained by overlying conjunctival apposition. When IOP is sufficiently high, the conjunctiva will be lifted and then only can aqueous humour enter the surrounding bleb. However, one study reported that this effect was unpredictable (Gerber, Cantor, & Sponsel, 1997).

In a randomised controlled trial that compared the single-plate Molteno device with the silicone Ahmed Glaucoma Valve in 92 patients with refractory glaucoma (Nassiri et al., 2010), the decrease in IOP at two years was significantly higher with the Molteno (49.7%) than with the Ahmed devices (41.9%), but the number of glaucoma medications were not significantly different (1.41 for Molteno, 1.03 for Ahmed). Visual field deterioration was also similar between the groups. The rate of surgical failure (IOP > 21 mmHg, IOP < 5 mmHg, phthisis bulbi, loss of light perception vision, removal of the implant, reoperation for glaucoma, or any devastating intra-operative or post-operative complication) was similar at 16% for the Molteno and 18% for the Ahmed devices, all due to inadequate IOP reduction. Post-operative complications were comparable between the groups, with no reported cases of hypotony. However, one limitation of this study was that patients were removed from analysis at the time of failure, and mean IOP considering all the cases in each group was not reported (Gedde, Panarelli, Banitt, & Lee, 2013).

The Molteno 3, introduced in 2007, is made of silicone, more flexible, has a lower profile and comes in larger 175 mm² and 230 mm² single plate surface area sizes. It is also claimed to have an improved flow-restricting mechanism, aqueous humour flows into the primary drainage area but is prevented from flowing into the secondary

drainage area by conjunctival apposition (Figure 2.5b) until the IOP is sufficiently high. In a recent study comparing 175 mm² Molteno 3 and double plate Molteno (270 mm²) devices, the IOP and medication outcomes were similar at three years (13.9 mmHg with 0.9 medications for the Molteno 3 versus 14.5 mmHg with 0.7 medications for the double plate Molteno) (Thompson, Molteno, Bevin, & Herbison, 2013). Success rates were also similar between them at 79% each. Finally, post-operative hypotony rates were again similar at 35.6% with the Molteno 3 and 31.3% with the double plate Molteno, contributed mainly by cases which did not have initial tube restrictions. This final finding may also indicate a weakness in the claimed flow-restricting mechanism of the Molteno 3 device.

a)



b)

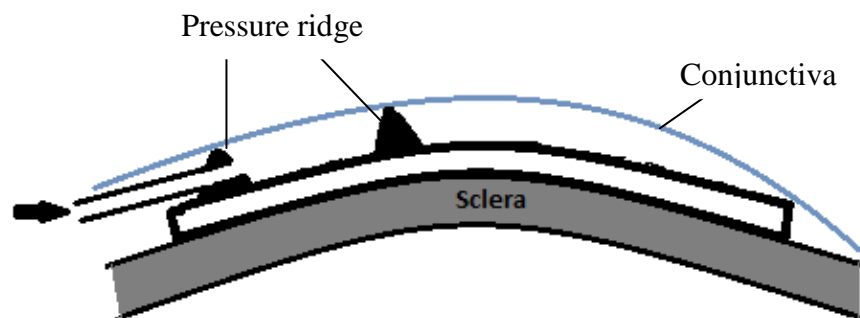


Figure 2.5 a) Photograph of Molteno 3 device (scale bar = 5 mm). b) Schematic cross-section diagram of the device (adapted from Lim (1998)). Aqueous humour flow from the primary drainage area to the secondary drainage area is limited by overlying conjunctiva to prevent continuous drainage leading to hypotony.

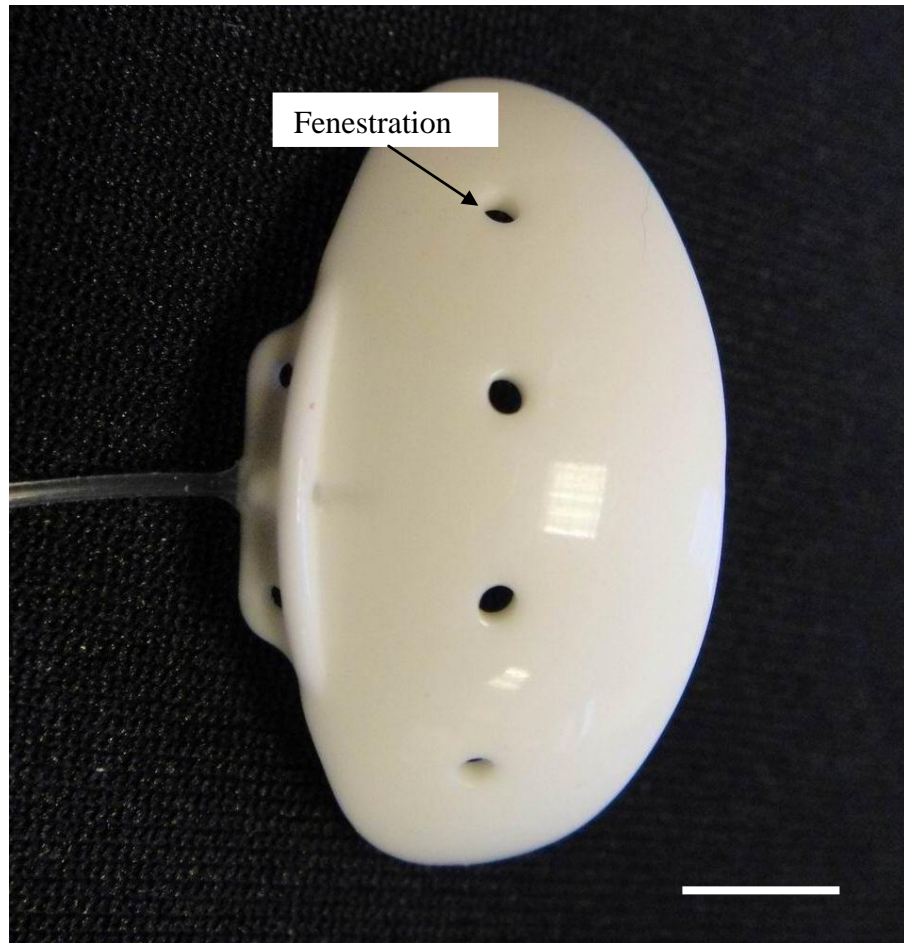
The Baerveldt device (Figure 2.6) has a wing-shaped explant made of radio-opaque barium-impregnated silicone and comes in 250 mm² and 350 mm² sizes. The larger surface area means that this device needs to be placed underneath 2 rectus muscles, leading to a higher profile of the bleb. An earlier 500 mm² size was discontinued due to a higher risk of diplopia and a lower success rate (Lloyd et al., 1994; Britt et al., 1999). The manufacturers subsequently improved on the original design by including fenestrations in the explant which enable fibrous tissue growth into the plate to reduce its height profile.

The Ahmed Baerveldt Comparison (ABC) study is a randomised controlled trial comparing the silicone Ahmed Glaucoma Valve and Baerveldt 350 mm² devices (Barton, Gedde, Budenz, Feuer, & Schiffman, 2011; Budenz et al., 2011; Gedde et al., 2013). 276 patients with refractory glaucoma requiring tube shunt implantation were enrolled. At the end of 1 year, mean IOP was lower in the Baerveldt group (13.2 mmHg versus 15.4 mmHg) but the use of number of glaucoma medications was similar (1.5 for the Baerveldt versus 1.8 for the Ahmed devices). Failure (IOP > 21 mmHg or not reduced > 20% from baseline, IOP < 5 mmHg, additional glaucoma surgery, removal of the implant, or loss of light perception vision) rates were similar between the two groups (14% for the Baerveldt versus 16% for the Ahmed devices). Post-operative complications during the first 3 months after surgery, such as tube occlusion and corneal oedema, were more common with the Baerveldt device (58% versus 43%), as was the rate of serious complications leading to reoperation and/ or vision loss of two or more Snellen lines (34% for Baerveldt versus 20% for Ahmed devices). There was no statistically significant difference in the rate of late post-operative complications observed between the two devices (37% for Baerveldt versus 29% for Ahmed devices).

The Ahmed Versus Baerveldt (AVB) Study group has reported longer term similarities and differences between the silicone Ahmed Glaucoma Valve and Baerveldt

350 mm² devices (Christakis et al., 2013; Gedde et al., 2013). From the 238 patients with refractory glaucoma, half of them had secondary glaucoma and 37% had a previously failed trabeculectomy. The mean pre-operative IOP was 31.4 mmHg on 3.1 glaucoma medications. At 3 years, the mean IOP was 15.7 mmHg in the Ahmed group and 14.4 mmHg in the Baerveldt group (reductions of 49% and 55% respectively) although the difference was not statistically significant. The use of medications was significantly higher in the Ahmed group (1.8) than in the Baerveldt group (1.1). The cumulative probability of failure (IOP > 18 mmHg or not reduced > 20% from baseline, IOP < 5 mmHg, vision-threatening complications, additional glaucoma procedures, or loss of light perception vision) was significantly higher in the Ahmed group (51% versus 34%). They had similar complication rates (52% for Ahmed group versus 62% for Baerveldt group) but the Baerveldt group had a higher rate of hypotony-related complications (6% versus 0%). The number of interventions was also not significantly different between them (38% for Ahmed group versus 50% for Baerveldt group). The authors concluded that both devices were effective in reducing IOP and glaucoma medications. The Baerveldt group had a lower failure rate and required fewer medications than the Ahmed group after 3 years, but it experienced more hypotony-related vision-threatening complications.

a)



b)

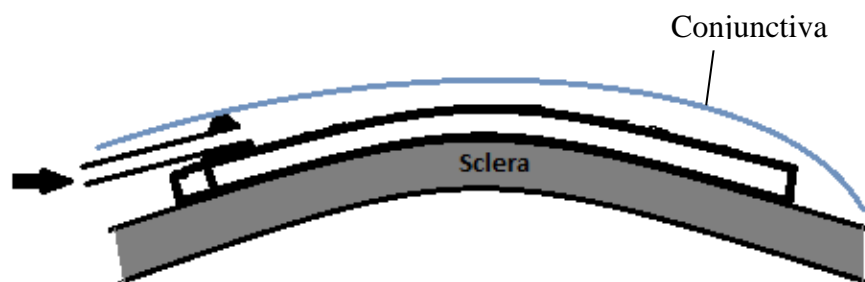


Figure 2.6 a) Photograph of Baerveldt device (scale bar = 5 mm). b) Schematic cross-section diagram of the device (adapted from Lim (1998)).

Table 2.5 lists the IOP outcomes in recent studies involving the above glaucoma drainage devices. The final IOP reduction with the majority of the devices is between 40-50% of the pre-operative value, and it settles between 13-17 mmHg. The overall IOP control between devices appears similar. The complications related to hypotony and bleb formation are listed in Table 2.6. It is evident that with these glaucoma drainage devices, hypotony also occurs in significant numbers despite the incorporation of valve mechanisms and preventative measures such as initial restriction of the tubes.

Table 2.5 IOP outcomes after GDD surgery in recent studies.

Authors	Device	Follow-up (months)	Baseline mean IOP (mmHg)	Final mean IOP (mmHg)	Reduction in IOP (%)	Notes
(Budenz et al., 2011)	Ahmed	12	31.2	15.4	50.6	Ahmed Baerveldt Comparison Study, RCT
(Nassiri et al., 2010)	Ahmed	24	33.0	15.4	53.3	Comparison between Ahmed Glaucoma Valve and single plate Molteno, RCT
(Souza et al., 2007)	Ahmed	60	30.4	15.9	47.7	Mixed glaucoma cases, retrospective
(Wilson, Mendis, Smith, & Paliwal, 2000)	Ahmed	10	25.7	17.2	33.1	Comparison between Ahmed Glaucoma Valve and trabeculectomy, RCT
(Gedde et al., 2012b)	Baerveldt	60	25.1	14.4	42.6	Tube vs Trabeculectomy Study, RCT
(Budenz et al., 2011)	Baerveldt	12	31.8	13.2	58.5	Ahmed Baerveldt Comparison Study, RCT
(Thompson, Molteno, Bevin, & Herbison, 2013)	Molteno 3	36	25.6	13.9	45.7	Comparison between Molteno 3 and double plate Molteno, retrospective
(Nassiri et al., 2010)	Molteno	24	30.8	17.0	44.8	Comparison between Ahmed Glaucoma Valve and single plate Molteno, RCT
(Every, Molteno, Bevin, & Herbison, 2006)	Molteno	36	40.1	21.9	45.4	Neovascular glaucoma, prospective
(Molteno, Bevin, Herbison, & Houlston, 2001)	Molteno	24	23.7	14.4	39.2	Prospective case series

Table 2.6 Incidences of hypotony and bleb-related complications after GDD surgery in recent studies (early - < 4-6 weeks, late - > 6 weeks).

Authors	Device	Hypotony	Shallow AC	Choroidal effusion/ detachment	Wound leakage	Hypotony maculopathy
(Budenz et al., 2011)	Ahmed		19% (early), 3% (late)	15% (early), 1% (late)		3% (early), 1% (late)
(Nassiri et al., 2010)	Ahmed		2.2%	4.3%	4.3%	0%
(Souza et al., 2007)	Ahmed	29% (early)	5% (early)	5% (early)		
(Wilson, Mendis, Smith, & Paliwal, 2000)	Ahmed	36% (early)	20% (early)	10.9% (early)	1.8% (early)	
(Gedde et al., 2012a)	Baerveldt		10% (early), 1% (late)	14% (early), 2% (late)	1% (early)	1% (late)
(Budenz et al., 2011)	Baerveldt		20% (early), 4% (late)	10% (early), 2% (late)		2% (early), 1% (late)
(Thompson, Molteno, Bevin, & Herbison, 2013)	Molteno 3	35.6% (early)	6.9% (early)	18.4% (early)		
(Nassiri et al., 2010)	Molteno		4.3%	8.7%	4.3%	2.2%
(Every et al., 2006)	Molteno		31% (early)	3% (early)		
(Molteno, Bevin, Herbison, & Houlston, 2001)	Molteno		8% (early)	15% (early)		

(Continued) **Table 2.6** Incidences of hypotony and bleb-related complications after GDD surgery in recent studies (early - < 4-6 weeks, late - > 6 weeks).

Authors	Device	Cataract progression	Bleb leakage	Endophthalmitis	Other
(Budenz et al., 2011)	Ahmed	13%		0%	Hyphaema 9% (early) 1% (late), suprachoroidal haemorrhage 0%
(Nassiri et al., 2010)	Ahmed	10.9%			Hyphaema 6.5%, bleb encapsulation 28.3%
(Souza et al., 2007)	Ahmed	22% (late)			Hyphaema 12% (early)
(Wilson, Mendis, Smith, & Paliwal, 2000)	Ahmed	0%		0%	Hyphaema 15% (early), suprachoroidal haemorrhage 0%
(Gedde et al., 2012a)	Baerveldt		0%	1% (late)	Hyphaema 2% (early), suprachoroidal haemorrhage 2% (early), malignant glaucoma 3% (early), bleb encapsulation 2%
(Budenz et al., 2011)	Baerveldt	20%		1% (early), 2% (late)	Hyphaema 17% (early) 2% (late), suprachoroidal haemorrhage 2% (early) 0% (late)
(Thompson, Molteno, Bevin, & Herbison, 2013)	Molteno 3				Hyphaema 17% (early)
(Nassiri et al., 2010)	Molteno	17.4%			Hyphaema 4.3%, bleb encapsulation 23.9%
(Every et al., 2006)	Molteno				Hyphaema 65% (early)
(Molteno, Bevin, Herbison, & Houlston, 2001)	Molteno	17% (late)		0%	Hyphaema 6% (early), suprachoroidal haemorrhage 0%

2.4.3 Other subconjunctival space GDD

The ExPress (Figure 2.7) is a stainless steel, non-valved device that was first approved by the FDA in 2002 (Gandolfi et al., 2002). It has a different design concept to the previously described devices, being a straight tube with a disc-like flange at the subconjunctival space end and a spur-like projection at the anterior chamber end to prevent extrusion. There are currently 2 versions, the P50 and P200, the numbers signifying their internal diameters in μm . Both are 2.64 mm in length. A previous R50 model has been discontinued, and it had a 50 μm internal diameter and 2.96 mm length. This device was designed for ease of insertion and the elimination of a sclerostomy and iridectomy, thus reducing post-operative inflammation and fibrosis when compared to a trabeculectomy.

In early cases, this device was implanted underneath bare conjunctiva but this resulted in complications such as hypotony, conjunctival erosion and endophthalmitis (Wamsley, Moster, Rai, Alvim, & Fontanarosa, 2004; Stewart, Diamond, Ashmore, & Ayyala, 2005; Rivier, Roy, & Mermoud, 2007). This implantation method was then changed to that under a trabeculectomy-style partial-thickness scleral flap (Dahan & Carmichael, 2005). In a subsequent retrospective study comparing 50 eyes with ExPress R50 devices and 50 eyes with trabeculectomies, IOP reduced from 26.2 mmHg to 13.7 mmHg after 11 months in the ExPress group and from 25.5 mmHg to 12.9 mmHg in the trabeculectomy group (Maris, Ishida, & Netland, 2007). Early postoperative hypotony rates were significantly lower in the ExPress group (4% vs 32%). In another comparative study of 15 eyes each, mean IOP reduced from 28.1 mmHg to 15.7 mmHg after a mean of 23.6 months in the ExPress P200 group and from 31.1 mmHg to 16.2 mmHg in the trabeculectomy group (Dahan, Ben Simon, & Lafuma, 2012). Complete success rates were significantly higher with the ExPress devices. Hypotony rates were also lower in this group

(7% vs 33%). One meta-analysis combined eight clinical trials and 605 eyes, and found the IOP reduction and success rates to be similar between the ExPress device and trabeculectomy (Wang, Zhou, Huang, & Zhang, 2013). However, the device was associated with significantly less hypotony and choroidal effusion than trabeculectomies, with pooled odds ratios of 0.29 and 0.65 respectively. Overall, current evidence does not support either superiority, equality or inferiority of this device over trabeculectomy surgery; however, the additional cost of the device itself should also be considered (Francis et al., 2011; Buys, 2013).

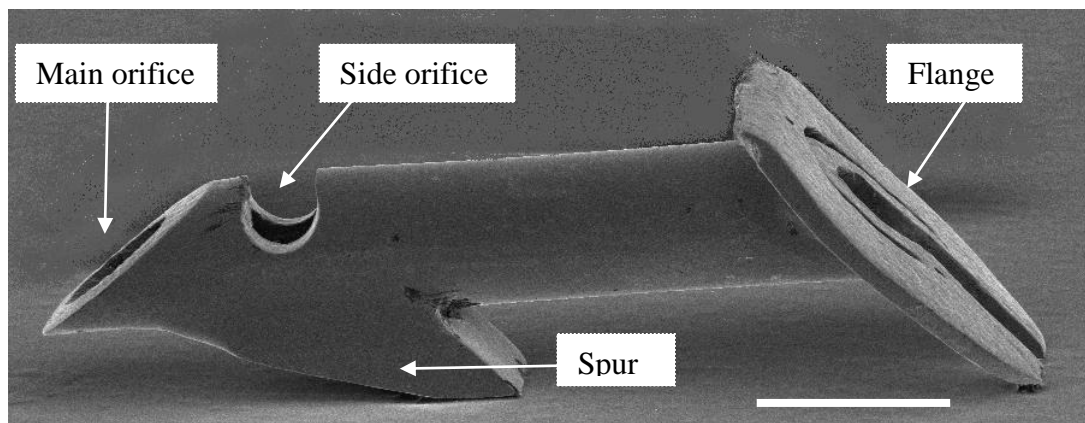


Figure 2.7 Scanning electron micrograph of ExPress P200 device (scale bar = 500 μm). The disc-like flange lies under the scleral flap in the subconjunctival space while the spur and labelled orifices lie in the anterior chamber.

The AqueSys tube (or Aquecentesis procedure, Figure 2.8) has dimensions of 50 μm internal diameter, 150 μm external diameter and 6 mm length. Made of cross-linked gelatine, it is claimed by the manufacturer to be soft, non-inflammatory and well-tolerated by the eye. This non-valved device is inserted using a specialised inserter via an *ab interno* (from the inside) approach to connect the anterior chamber and the subconjunctival space

without dissection or conjunctival disruption (Varma, Flynn, Marquis, Craven, & Bacharach, 2012). In a small study involving 15 patients, the mean pre-operative IOP of 21.3 mmHg reduced to 12.2 mmHg at 1 week. It was subsequently maintained at 15.0 mmHg at 1 month, 15.2 mmHg at 6 months and 15.3 mmHg at 12 months. The mean reduction in IOP was 9.1 mmHg at 1 week, 6.3 mmHg at 1 month, 6.5 mmHg at 6 months and 6.3 mmHg at 12 months (Kersten-Gomez & Dick, 2012).

The Miami InnFocus Drainage Implant (MIDI)-Arrow device is a 8.5 mm long, 70 μm internal diameter, 350 μm outer diameter, flexible non-valved tube made of poly(styrene-*b*-isobutylene-*b*-styrene) [SIBS]. This material is reported to be biostable and biocompatible, and can also be loaded with other pharmaceutical agents; it is also used to make coronary stents which can elute the anti-proliferative agent paclitaxel (Jim et al., 2010). In a study in rabbits, this device was found to avoid hypotony and elicit less collagen deposition and myofibroblasts differentiation than 300 μm internal diameter silicone tubes (Acosta et al., 2006). It is inserted through a scleral tunnel 3 mm from the limbus into the anterior chamber, leaving its distal end lying directly under the conjunctiva. It has two external fins to prevent migration into the anterior chamber (Figure 2.9). In one small study of 28 human eyes, IOP fell from a baseline of 24.0 \pm 5.4 mmHg to 10.5 \pm 2.8 mmHg at 12 months and maintained at 10.2 \pm 2.0 mmHg at 2 years. Complete and modified success rates were 91% and 96% at one year. Two subjects developed transient hypotony after day one but there were no cases of chronic hypotony or maculopathy (Palmberg et al., 2013).

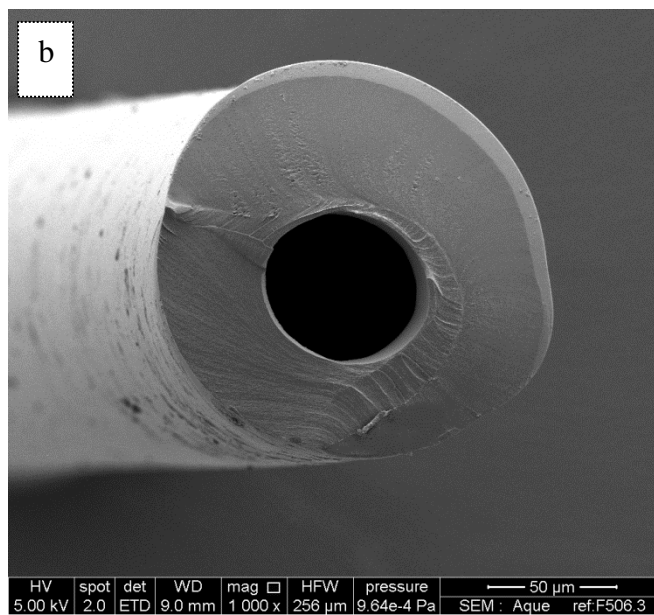
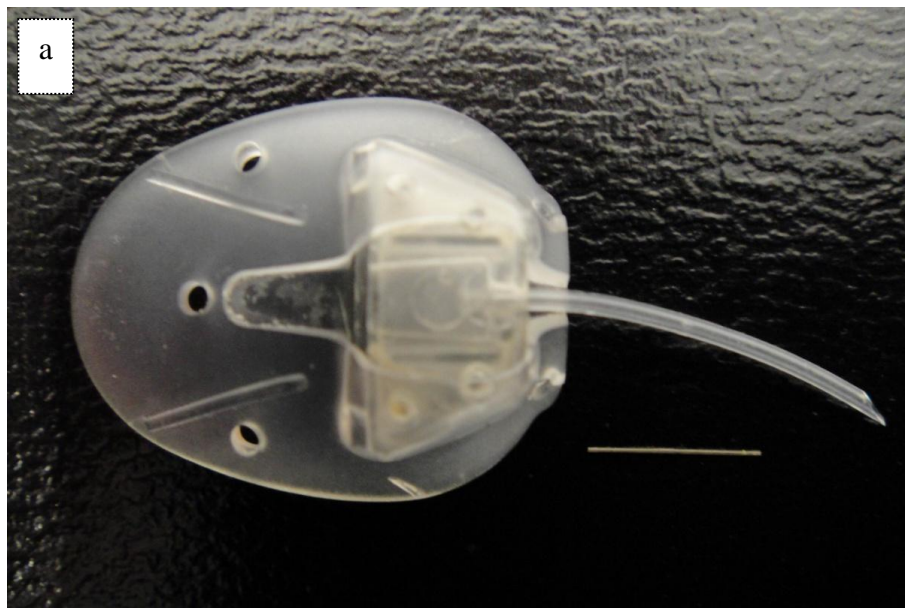


Figure 2.8 a) Photograph of 6 mm long AqueSys tube beside an Ahmed Glaucoma Valve.
b) Cross section of AqueSys tube on scanning electron micrograph (1000 × magnification).
The lumen diameter is 50 μm.

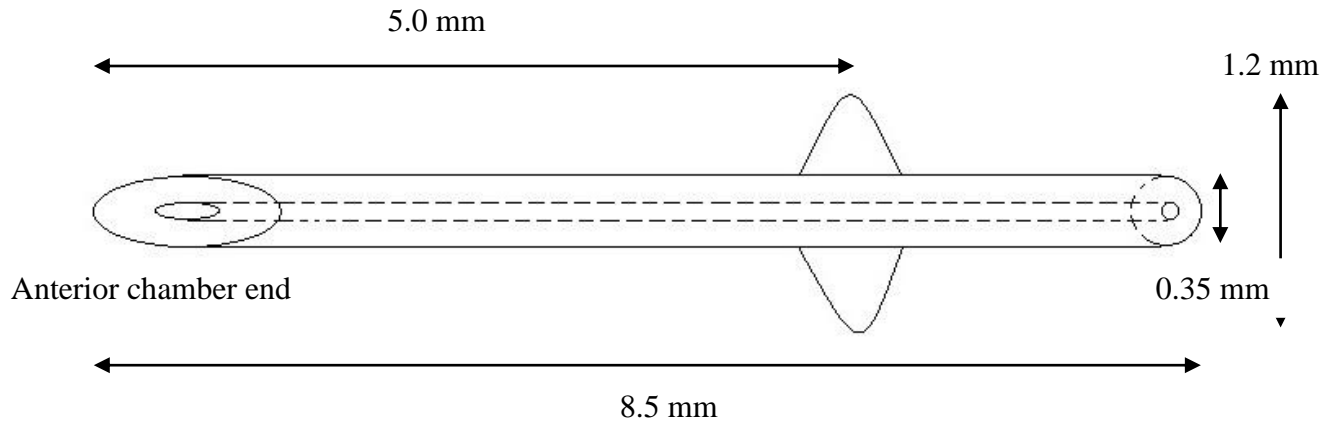


Figure 2.9 Plan view of MIDI-Arrow device. The lumen diameter is 70 μm .

It can be seen that the newer subconjunctival space glaucoma drainage devices i.e. the ExPress, AqueSys and MIDI-Arrow have non-valved, smaller inner diameter tube-without-explant designs. The main idea behind them seems to be to simplify the method of insertion, reduce the amount of tissue manipulation needed during insertion, and reduce surgery time. However, data on their (the AqueSys and MIDI-Arrow devices in particular) control of IOP is still limited. A study on this design of tube devices and its control of IOP is presented in Chapter 5 of this thesis.

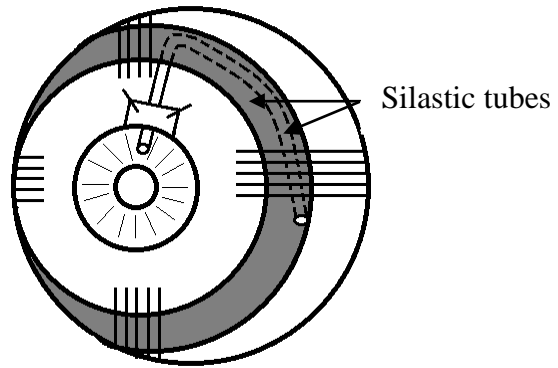
Certain devices appear to have fallen out of favour with current glaucoma surgeons. This is indicated by the substantial lack of peer-reviewed articles within the last 10-15 years. Among others, they include the Schocket, Krupin and OptiMed implants. Problems with inferior success rates and higher complication rates seem to have made them less popular, as discussed below. These following devices are either rarely used nowadays or not in production anymore.

The Schocket or anterior chamber tube shunt to encircling band (ACTSEB) procedure involves 2 silastic tubes normally used for nasolacrimal intubation (Figure 2.10a). The first tube is inserted in a globe-encircling manner under the recti muscles. The other tube, with one end in the anterior chamber, is tucked under this encircling band. Aqueous humour would drain into the capsule which forms and surrounds the band. In a modified Schocket procedure, a tube is inserted to connect the anterior chamber with a pre-existing retinal encircling band (Suh, Park, Kim, & Kim, 2007). Even though the procedure is lengthy, it is less expensive and its materials can be assembled in most operating rooms. Unfortunately, the success rate appeared less than that of other devices (Smith, Sherwood, & McGorray, 1992; Wilson et al., 1992). The two-piece nature of its construction made it prone to fail due to blockage at the distal end of the tube.

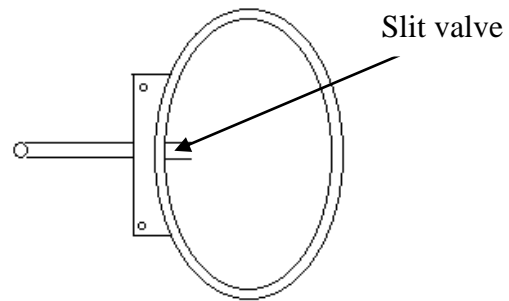
The Krupin device (Figure 2.10b) consisted of a silicone explant and tube. The explant plate incorporated a slit valve which was reported to open at 11 mmHg and close at 8 mmHg (Krupin, 1976). The reported success rate for this device was less than with the Molteno device and it was also more likely to lead to hypotony compared to the Ahmed Glaucoma Valve (Taglia, Perkins, Gangnon, Heatley, & Kaufman, 2002). This was likely to be due to its poor valve performance (Prata, Jr. et al., 1995; Francis, 1998; Eisenberg, Koo, Hafner, & Schuman, 1999).

The Optimed device had a 3 mm x 2 mm x 2 mm polymethylmethacrylate (PMMA) box section (Figure 2.10c) which contained 180-200 microtubules, each with an internal diameter of 60 μm for aqueous humour flow (Prata, Jr. et al., 1995). The microtubules made up the flow-restricting unit and provided a pressure gradient governed by Poiseuille's formula. Aqueous humour outflow occurred when IOP exceeded 10 mmHg and capillary action would draw fluid through the matrix as IOP increased. A cover over the box prevented fibrous tissue growth from blocking the holes. In laboratory tests, this device had minimal flow resistance, comparable to a unrestricted Baerveldt device in one report (Francis, 1998; Eisenberg et al., 1999). In a small study involving 7 eyes, the failure rate was around 40% after 3 years (Romaniuk, 1999).

a)



b)



c)

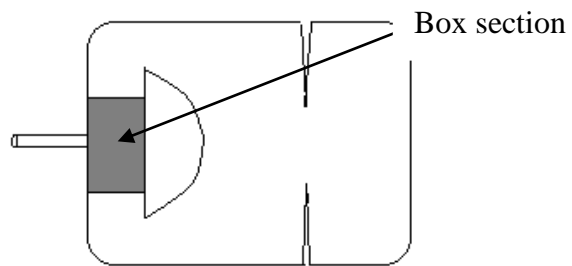


Figure 2.10 a) Schocket device. b) Krupin device. c) OptiMed device.

2.5 Schlemm's canal and suprachoroidal space drainage

In general, the devices here have been introduced after the subconjunctival space devices. These include the iStent, Hydrus, Gold Micro Shunt, CyPass and Aquashunt. The iStent and Hydrus are designed to facilitate aqueous humour drainage from the anterior chamber into the Schlemm's canal (Figure 2.2). The Gold Micro Shunt, CyPass and Aquashunt devices divert aqueous humour from the anterior chamber into the suprachoroidal space (Figure 2.2).

2.5.1 Schlemm's canal GDD

The iStent (trabecular micro-stent) GTS100 is an L-shaped, open half-pipe titanium tube (Figure 2.11a). The short snorkel inlet is designed to sit in the anterior chamber while the tube traverses the trabecular meshwork to end in Schlemm's canal. This device has its open side placed against the outer wall of Schlemm's canal and the closed side against its inner wall to prevent occlusion of the collector channels. Retention arches on the inner aspect prevent extrusion of the whole device. Surgery to insert the iStent is done through an *ab interno* approach without cutting any conjunctival tissue. The first benefit is that it can be performed through the same wound as that of phacoemulsification. If done together, the amount of inflammation and time for recovery is similar to that of phacoemulsification alone. The second benefit is that the conjunctiva is preserved in case further and more invasive glaucoma surgery e.g. trabeculectomy is needed. There is no bleb formation with this procedure (Samuelson, Katz, Wells, Duh, & Giamporcaro, 2011).

In a randomised controlled trial, patients had phacoemulsification with iStent implantation or phacoemulsification alone (Fea, 2010). After 15 months, IOP in the device

group (12 eyes) reduced from 17.9 mmHg to 14.8 mmHg (17.3%) while IOP in the control group (24 eyes) reduced from 17.3 mmHg to 15.7 mmHg (9%). In another study involving patients with open-angle glaucoma or ocular hypertension who were undergoing cataract surgery (Fernandez-Barrientos et al., 2010), 33 eyes of 33 patients were randomised to either two stents and cataract surgery (17 eyes) or cataract surgery alone (16 eyes). Mean IOP reduced from 24.2 to 17.6 mmHg (27.3%) in the device group and from 23.6 to 19.8 mmHg (16.1%) in the cataract surgery only group. In another randomised control trial, 240 eyes with mild to moderate open-angle glaucoma with IOP \leq 24 mmHg controlled on 1 to 3 medications were randomised to undergo cataract surgery with iStent implantation or cataract surgery only (Samuelson et al., 2011). At 1 year, reduction from the pre-operative, un-medicated IOP in both treatment groups were similar (8.4 mmHg vs 8.5 mmHg) and both significantly lower by \geq 30% from baseline values, although the reduction in number of medications was higher in the device group (1.4 vs 1.0). The number of \geq 20% IOP reduction without medication was higher in the device group (66% vs 48%), as was the number of \leq 21 mmHg (72% vs 50%). Stent obstruction occurred in 4% but there were no cases of hypotony. In a prospective case series (Arriola-Villalobos et al., 2012), 19 subjects with mild or moderate open-angle glaucoma (including pseudoexfoliative and pigmentary types) and cataract underwent phacoemulsification and intraocular lens implantation along with implantation of one iStent. IOP was reduced from 19.4 mmHg to 16.2 mmHg at the end of follow up (53.7 months), a 16.3% decrease in IOP. There was no incidence of hypotony, choroidal effusion or shallow anterior chambers.

The newer iStent Inject or GTS400 has a flanged anterior chamber end, a narrow thorax portion, and a head with 4 outflow orifices (Figure 2.11b). It is 360 μ m in length, 230 μ m in external diameter and is also made of titanium. In a study using human anterior

segments placed in perfusion organ culture, one or 2 iStent Inject devices were inserted into the trabecular meshwork (Bahler et al., 2012). Insertion of 1 device increased outflow facility from 0.16 $\mu\text{l}/\text{min}/\text{mmHg}$ to 0.38 $\mu\text{l}/\text{min}/\text{mm Hg}$, with concurrent pressure reduction from 16.7 mmHg to 8.6 mmHg. Addition of a second device increased outflow facility to 0.78 $\mu\text{l}/\text{min}/\text{mm Hg}$. In humans, these devices have been implanted in conjunction with phacoemulsification. In one report, 25 subjects who had received cataract surgery and stents were followed up for 2 years (Bacharach, 2012). 68% had an IOP of 18 mmHg or less and $> 20\%$ reduction without medication, compared to 24% in cataract surgery only controls.

The Hydrus device is a Schlemm's canal scaffold with an open structure to facilitate aqueous humour movement into the collector channels (Figure 2.11c). It is 15 mm long, curved to fit inside the canal and increases the canal's cross-sectional area by 4-5 times for up to 5 clock hours. It is made of Nitinol or nickel titanium alloy (Camras et al., 2012). In one study, 40 patients received the Hydrus without cataract extraction and their IOP reduced by 21.8% from 21.6 mmHg on an average of 1.7 medications to 16.9 mmHg on 0.6 medications after 6 months (Samuelson, Pfeiffer, & Lorenz, 2012). Minor complications were reported, including mild iris damage and transient hyphaema lasting less than one week.

From the clinical evidence, we can see that the IOP reduction with Schlemm's canal devices is less than 20% after deducting the reduction from cataract removal alone, and lower than that with subconjunctival space devices. They are however associated with minimal risks of hypotony.

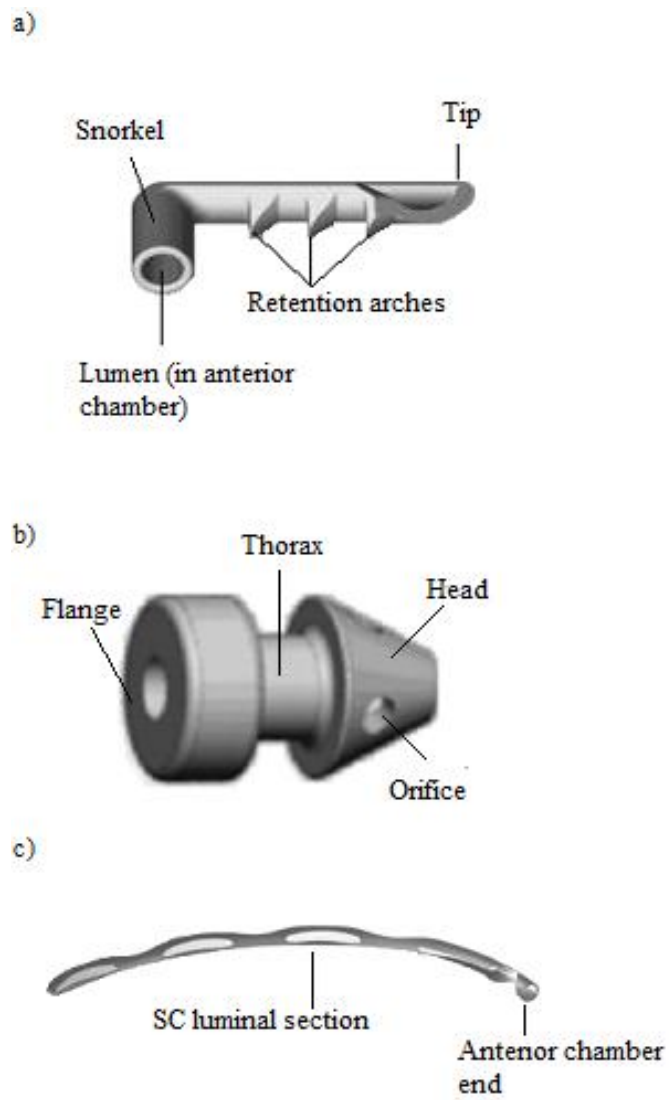


Figure 2.11 a) iStent GTS100 device. b) iStent Inject (GTS 400) device. c) Hydrus device.

2.5.2 Suprachoroidal space GDD

The suprachoroidal space is a potential space between the inner surface of the sclera and the outer surface of the choroid. It is not present under normal physiological conditions. The theoretical advantages of draining aqueous humour into this space is its natural counter-pressure helps to prevent severe post-operative hypotony, the potential capacity of transport afforded by the excellent blood supply of the metabolically active choroid, and the negative hydrostatic pressure gradient which facilitates drainage (Emi, Pederson, & Toris, 1989; Jordan et al., 2006). From this space, there are 2 possible drainage pathways, one through scleral pores and to the episcleral venous plexus, and the other through choroidal resorption.

The Gold Micro Shunt (GMS) is a flat device designed to connect the anterior chamber with the suprachoroidal space (Figure 2.12a). Its anterior and posterior ends have multiple inlet and exit holes 100 μm in diameter and these are connected by microchannels. Additionally, there are lateral channels 50 μm in diameter for increased aqueous humour movement and fin-like tabs posteriorly for anchoring the device in the suprachoroidal space. To reduce hypotony, only half of the microchannels are initially open. If further IOP reduction is needed after implantation, the rest can be opened by using a titanium-sapphire 790 nm wavelength laser (Melamed, Ben Simon, Goldenfeld, & Simon, 2009). Clinical outcomes with this device are discussed subsequently.

The CyPass (Figure 2.12b) is a 6.35 mm long, 300 μm ID hollow polyimide tube with microchannels along its side. It is inserted via an *ab interno* approach and usually performed along with phacoemulsification. The aim is to create a controlled cyclodialysis with a stented outflow conduit to the suprachoroidal space. In a prospective case-series, 81 patients were implanted with this device and followed-up for 6 months (Ianchulev, Ahmed,

Hoeh, Rau, & DeJuan, 2010). There was a 29% decrease in IOP from 22.9 mmHg to 16.2 mmHg and a similar reduction in medication requirements. There were two cases of transient hyphaema which resolved by one week and one case of a shallow anterior chamber which resolved by 1 month.

The iStent Supra is the third model in the iStent family and has an insertion method similar to that of the CyPass. It is made of non-magnetic, heparin-coated polyethersulphone and has a titanium sleeve. The interim results of one on-going study have been reported (Junemann, 2013). However, it is being tested along with the use of travoprost so its individual effect cannot be ascertained. In the study, open angle glaucoma patients with IOP not controlled with 2 medications were implanted with the device and started on travoprost post-operatively. The IOP reduction in the 42 subjects was from 24.8 mmHg to 13.2 mmHg (46.8%) after 1 year. 98% of cases had a reduction in IOP of 20%.

The Aquashunt is another suprachoroidal drainage device and is made of polypropylene (Figure 2.12c). During insertion, a full thickness scleral incision is made before the device is advanced into the suprachoroidal space and then into the anterior chamber. The insertion tool also serves as an obturator to keep tissue from blocking the lumen as it is advanced. The device's leading edge separates the adhesion between the ciliary body and scleral spur with a shearing effect. Excessive movement into the anterior chamber is limited by the shunt's shoulders, which are set 3 mm back from the leading edge (Rao, 2009). Data regarding this device in human use has not been reported, but one study did report the differences in aqueous humour dynamics, IOP and fibrosis between this device and the GMS in rabbits (Oatts et al., 2013). Fluorophotometric aqueous humour flow and both tonographic and fluorophotometric outflow facility were not changed with both devices without antifibrotic use. Morning IOP was decreased through 15 weeks in

both groups. At the end of 15 weeks, morning IOP was lower with the Aquashunt (41% reduction from baseline of 23.7 mmHg) than with the GMS (18% reduction from baseline). The reductions in evening IOP were smaller with the Aquashunt and not significant with the GMS. Both shunts were devoid of foreign body reaction but exhibited fibrosis, and the GMS showed fibrovascular invasion into its holes and microchannels. Thickness of fibrosis was greater in the GMS group (246 μm) than the Aquashunt group (188 μm). Antifibrotics reduced fibrosis around the devices but also diminished shunt performance at the end of the study. This latter effect was thought to be due to some aqueous humour exiting into an overlying bleb and thus bypassing the suprachoroidal space, which subsequently led to narrowing and failure of the space. The Aquashunt resulted in more cases of hyphaema (40% vs 10%) and was also liable to device migration (20%) and retinal detachment (10%). Overall, it may be that it provides better IOP control and incites less fibrosis than the GMS in humans.

2.5.2.1 Suprachoroidal space drainage and fibrosis

The initial report of GMS implantation showed satisfactory performance (Melamed et al., 2009). In the case of 38 patients with POAG, pseudoexfoliative glaucoma, pigment dispersion glaucoma and uveitic glaucoma on maximal medical therapy, IOP decreased by 9 mmHg (33%) from 27.6 mmHg to 18.2 mmHg after 11.7 months. Surgical and complete success (IOP between 5 mmHg and 22 mmHg with and without anti-glaucoma medication) was achieved in 79% and 13.2% respectively. However, subsequent reports indicate how this device may be liable to failure due to excessive fibrosis. One report showed how 5 correctly-placed GMS devices failed due to the presence of thick connective tissue capsules surrounding both their proximal and distal ends, and invading into the anterior and

posterior holes (Agnifili et al., 2012). Connective tissue was also observed within the inner microchannels although these were more loosely arranged. The mean time of failure was 6.8 months and the mean IOP at that time was 30.4 mmHg. The suggested causes leading to the fibrosis were direct activation and proliferation of suprachoroidal space fibroblasts induced by the intra-operative manipulation of the space, and migration of Tenon's fibroblasts through the scleral incision. The scleral incision was also thought to permit some direct subconjunctival filtration in the early post-operative period; reduced washout of fibroblasts from the inner microchannels by aqueous humour as a result of the bypass could allow proliferation of the cells. These findings are supported by another study that reported qualified and complete success rates (IOP < 21 mmHg and reduction > 33%) of 67.3% and 5.5% after 2 years in 55 eyes. The change in IOP in all cases was not reported but in the failure cases (32.7%), the authors mentioned that thin membranes obstructed the anterior and posterior holes in 66.7% and 16.7% respectively (Figus et al., 2011). Another report described the experience of implanting the GMS into 31 eyes; after 7.3 months, 97% of them were classified as failures due to inadequate IOP reduction, serious complications or the need for additional surgery (Hueber, Roters, Jordan, & Konen, 2013). 77% needed further surgery due to inadequate IOP reduction, the mean IOP increased from 26.6 mmHg to 27.2 mmHg during the study. The overall 1-year and 2-year failure rates were 71% and 90% respectively. However, the cause of failure could not be exactly ascertained from the report.

Long term reports of the other suprachoroidal space devices are not available at the moment but it may be that high fibrosis rates, perhaps contributed by the excellent blood supply of the metabolically active choroid will downplay the role of drainage into this space. Further investigation and reports will help provide this important information.

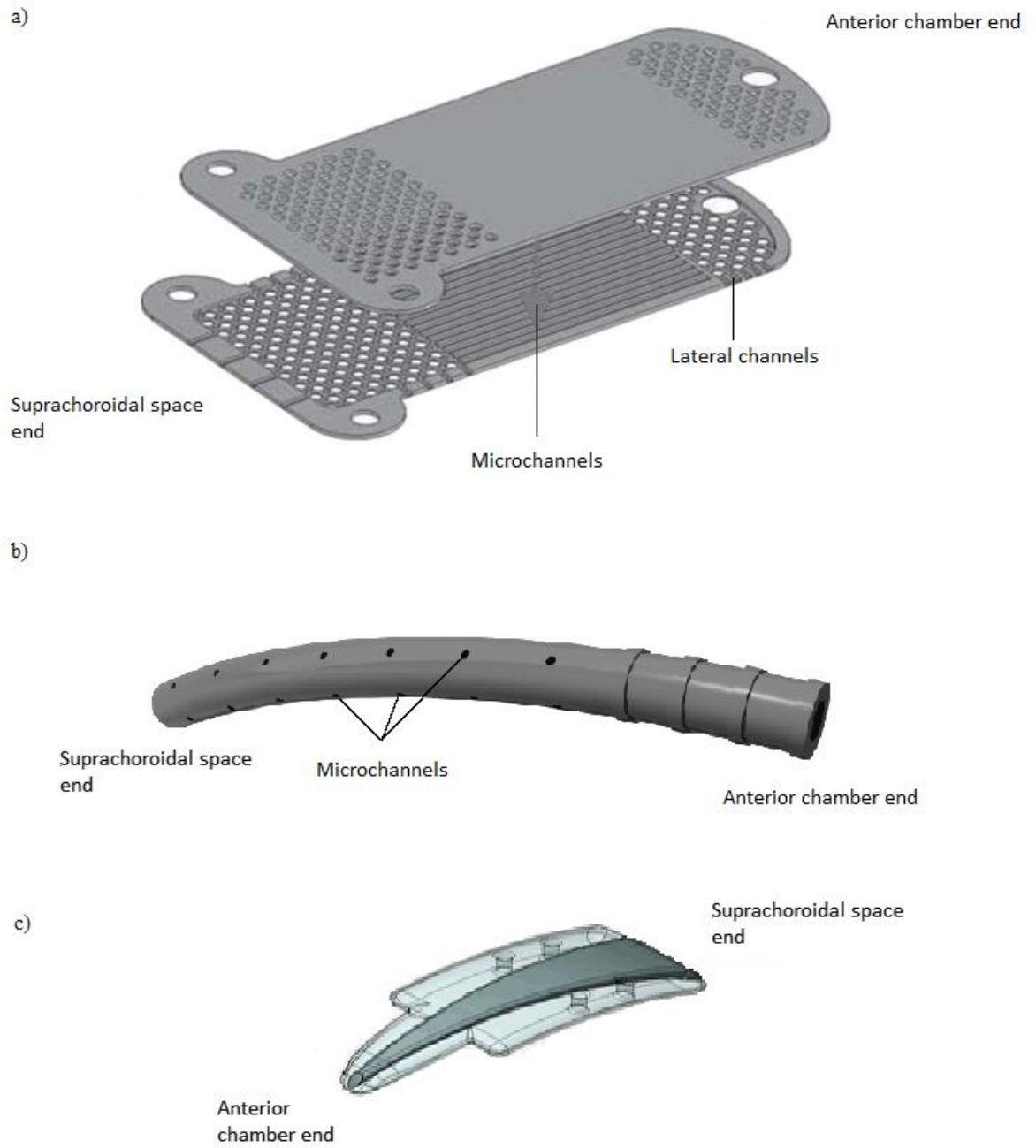


Figure 2.12 a) Gold Micro Shunt device. b) CyPass device. c) Aquashunt device.

2.6 Fluid mechanics of trabeculectomy and glaucoma drainage devices

The control of aqueous humour flow and IOP is important for successful glaucoma surgery. In many clinical studies, the criteria for success include IOP of between 6 and 21 mmHg (Gedde et al., 2009; Budenz et al., 2011). As such, there is a fine balance between obtaining successful results, or unwanted hypotony/ hypertony. It is acknowledged that in the later post-operative stage, resistance and flow are determined mainly by the bleb or fibrous scarring beyond the device, but post-operative control by the flap or device in the early post-operative stage is important in limiting overfiltration and setting the stage for effective long-term drainage. The knowledge of how these interventions affect resistance and flow is then useful in making clinical decisions to obtain the best outcomes. The characteristics are determined by the form and function of the procedures and devices, which in turn depend on their drainage pathways. In this section, we will describe the fluid mechanical aspects related to trabeculectomy and glaucoma drainage devices. We first introduce some of the critical concepts in fluid mechanics.

Aqueous humour flow through a GDD is characterised by a Reynolds number, Re , which expresses the relative strength of inertial to viscous forces in the fluid, and is defined as

$$Re = \frac{ul}{\nu}, \quad (2.2)$$

where u is a characteristic flow speed, l a characteristic length scale and ν the kinematic viscosity (10^{-6} m²/s for aqueous humour). For a typical device (e.g. Ahmed or Baerveldt device with a 300 μ m inner diameter tube), $u \sim 10^{-4}$ m/s and $l \sim 10^{-4}$ m, giving $Re \sim 10^{-2}$. When Re is < 2000 , as in this situation, the flow is viscously dominated or laminar and inertial forces can be completely neglected (Batchelor, 2000).

2.6.1 Electrical circuit analogy

The purpose of a glaucoma drainage device is to provide an intervention strategy that, given an initial aqueous humour flow rate Q and pre-operative pressure P_{pre} , gives a post-operative pressure P_{post} . The drainage of aqueous humour can be through routes that act in series or in parallel to the normal physiological route. The contrasting drainage routes put constraints on the resistance required of the procedure or device which can be understood using an electrical circuit analogy based on Ohm's law (Akers, Gassman, & Smith, 2006). This approach has been used before to discuss glaucoma procedures and drainage devices but not to classify them in this manner (Fankhauser & Giger, 1994; Pan, 2005). The basis of the electrical circuit analogy is that pressure (voltage) P is equal to the product of flow rate (current) Q and resistance R (which is the inverse of outflow facility C). The important assumptions here are that aqueous humour production and trabecular outflow resistance remain constant after surgery (which may be more accurate in the early post-operative stage, before development of the changes described in section 2.4.1.1), and uveoscleral outflow U is similarly constant, pressure-independent and drains only 10% of total aqueous humour. From the Goldmann equation (Equation 2.1), the pressure difference between IOP and EVP, $\Delta P = P - EVP$ is proportional to $Q - U$. Since $U/Q \leq 0.1$, then $\Delta P \cong \frac{Q}{C}$. In the engineering community, C is usually termed as permeability K , so

$$\Delta P = \frac{Q}{K}. \quad (2.3)$$

Figure 2.13a shows the electrical circuit analogy of the physiological resistances of the trabecular meshwork and Schlemm's canal operating in series. The pre-operative pressure is related to the flow rate by

$$\Delta P_{pre} = \frac{Q}{K_{tm+sc}}, \quad (2.4)$$

where K_{tm+sc} is the permeability of the trabecular meshwork and Schlemm's canal.

Intervention using a trabeculectomy/ GDD introduces an alternative subconjunctival route which operates in parallel to and bypassing the trabecular meshwork and Schlemm's canal, as in Figure 2.13b. The effect of introducing a parallel pathway for drainage into the subconjunctival space, which has a permeability K_{gdd} , requires the conditions

$$Q_{gdd}/K_{gdd} = Q/(K_{tm+sc} + K_{gdd}) \quad (2.5)$$

and conservation of mass

$$Q_{tm+sc} + Q_{gdd} = Q. \quad (2.6)$$

The results can be expressed as

$$\Delta P_{post} = \frac{Q}{K_{tm+sc} + K_{gdd}} \quad (2.7)$$

and

$$Q_{gdd} = \frac{Q(K_{gdd})}{K_{tm+sc} + K_{gdd}}. \quad (2.8)$$

The ratio of the post-operative pressure to the pre-operative pressure is

$$\frac{\Delta P_{post}}{\Delta P_{pre}} = \frac{1}{1 + \frac{K_{gdd}}{K_{tm+sc}}} \quad (2.9)$$

and

$$\frac{Q_{gdd}}{Q} = \frac{\left(\frac{K_{gdd}}{K_{tm+sc}}\right)}{1 + \left(\frac{K_{gdd}}{K_{tm+sc}}\right)}. \quad (2.10)$$

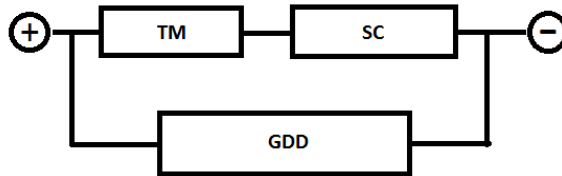
Figure 2.14a shows the variation of the post-operative pressure with the ratio of the permeability of the device to that of the physiological route. Assuming an average EVP of 9 mmHg, we see that for a reduction in IOP from 25-50 mmHg to 15 mmHg i.e. $\Delta P_{post}/\Delta P_{pre}$ of 0.15-0.38, the permeability of the device needs to be about 1.5-6.0 times the permeability of the physiological route. This correlates to around 55-85% of total flow

passing through the device (Figure 2.14b). For a typical Q of 3 $\mu\text{l}/\text{min}$, the estimated flow rate through the GDD is in the range of 1.7-2.6 $\mu\text{l}/\text{min}$.

a)



b)



c)

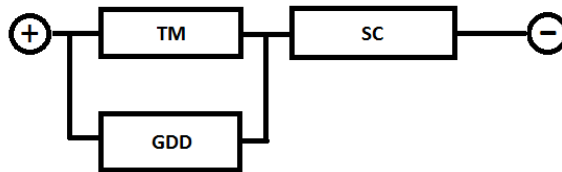
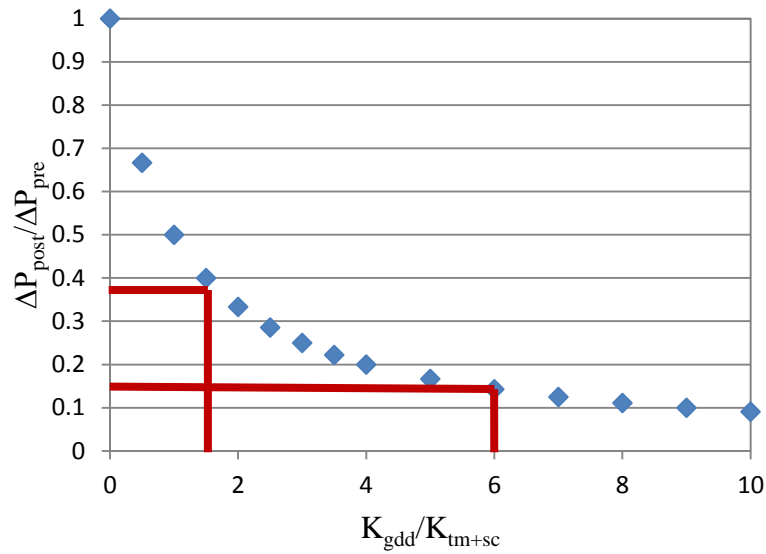


Figure 2.13 a) Electrical circuit diagram of pre-operative outflow pathway. b) Electrical circuit diagram of post-operative outflow pathway (subconjunctival and suprachoroidal drainage). c) Electrical circuit diagram of post-operative outflow pathway (Schlemm's canal drainage).

a)



b)

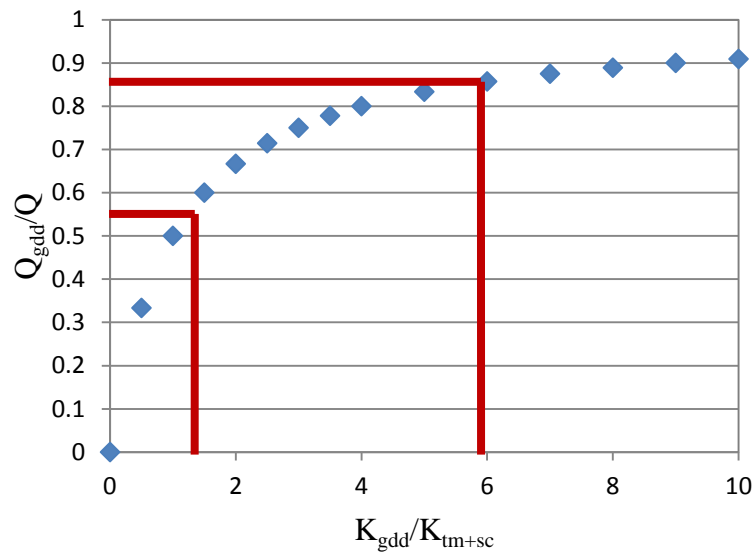


Figure 2.14 a) Calculated variation of post-operative pressure with ratio of permeability of a subconjunctival drainage device to that of the physiological route (from Equation 2.9). A reduction of IOP from 25-50 mmHg to 15 mmHg ($\Delta P_{post}/\Delta P_{pre}$ of 0.15-0.38) requires the permeability of the device to be about 1.5-6.0 times the permeability of the physiological route. b) The same permeability ratio correlates to around 55-85% of total flow passing through the device (from Equation 2.10).

From data reported in other studies, we derived K values by direct conversion of outflow facility or the inverse of resistance for the devices which were investigated. These are shown in Table 2.7. Note that in some of these *in vitro* studies, the flow rates involved were much higher than normal physiological aqueous humour flow rates. As permeability of valved devices depends on flow rate, the values reported may not be representative of one in an actual living eye with lower flow rates. Additionally, the lengths of the tube sections of the devices during testing were not stated. As these lengths affect resistance, the permeability values indicated here may be less accurate.

Table 2.7 Permeability (K) values for Ahmed Glaucoma Valve, Baerveldt, Krupin, Optimed and ExPress devices compared to that of normal eyes. The values in brackets are the flow rates used during testing.

Device	K ($\mu\text{l}/\text{min}/\text{mmHg}$)	References
Ahmed Glaucoma Valve	0.4 (2 $\mu\text{l}/\text{min}$) – 20 (50 $\mu\text{l}/\text{min}$); 0.7 (2 $\mu\text{l}/\text{min}$); 1.2 (10.8 $\mu\text{l}/\text{min}$)	(Francis, 1998; Prata, Jr. et al., 1995; Eisenberg et al., 1999)
Baerveldt (partially ligated)	10 (2 $\mu\text{l}/\text{min}$)	(Prata, Jr. et al., 1995)
Krupin	4.0 (2 $\mu\text{l}/\text{min}$) – 11.1 (10 $\mu\text{l}/\text{min}$); 5.0 (2 $\mu\text{l}/\text{min}$)	(Francis, 1998; Prata, Jr. et al., 1995)
Optimed	12.5 (2 $\mu\text{l}/\text{min}$) – 25.0 (10 $\mu\text{l}/\text{min}$); 1.1 (2 $\mu\text{l}/\text{min}$); 6.2 (10.8 $\mu\text{l}/\text{min}$)	(Francis, 1998; Prata, Jr. et al., 1995; Eisenberg et al., 1999)
ExPress	16.4-19.6 [P50], 20.4-22.7 [R50] (97 - 512 $\mu\text{l}/\text{min}$); 90.9-142.9 [P200] (664 - 2241 $\mu\text{l}/\text{min}$)	(Estermann, Yuttitham, Chen, Lee, & Stamper, 2012)
Normal eye	0.2-0.4	(Toris et al., 2008; Gulati et al., 2011; Liu et al., 2011)

If we take K as being $\leq 0.2 \mu\text{l}/\text{min}/\text{mmHg}$ in a glaucomatous eye, we see at the relatively low flow rate of $2 \mu\text{l}/\text{min}$, K of the Ahmed Glaucoma Valve is only 2-3 times that of the eye. This is advantageous as the reduction in IOP is lower and there is a reduced likelihood of hypotony. At higher flow rates, K increases as the valve opens to allow more aqueous humour flow. The other devices have permeabilities at least 10 times higher which may lead to overdrainage and hypotony. To avoid this, in the early post-operative stage before the development of resistance by the bleb or fibrous scarring, flow restricting measures need to be employed. These include temporary internal or external occlusion of tubes such as with the Baerveldt and Molteno devices and implantation under the scleral flap in the case of the ExPress device.

When drainage is into the Schlemm's canal, the route is in parallel with the trabecular meshwork and in series with the canal (Figure 2.13c). Placing a GDD in parallel with the meshwork leads to a post-operative pressure of

$$\Delta P_{post} = \frac{Q}{\frac{(K_{tm}+K_{gdd}) \times K_{sc}}{(K_{tm}+K_{gdd})+K_{sc}}} . \quad (2.11)$$

The ratio of the post-operative pressure to the pre-operative pressure,

$$\frac{\Delta P_{post}}{\Delta P_{pre}} = \frac{K_{tm+sc}}{\frac{(K_{tm}+K_{gdd}) \times K_{sc}}{(K_{tm}+K_{gdd})+K_{sc}}} , \quad (2.12)$$

can also be expressed as

$$\frac{\Delta P_{post}}{\Delta P_{pre}} = \left(\frac{\frac{K_{tm}}{K_{tm+sc}} + \frac{K_{gdd}}{K_{tm+sc}}}{\frac{K_{tm}}{K_{sc}} + \frac{K_{tm+sc}}{K_{sc}} \left(\frac{K_{gdd}}{K_{tm+sc}} \right) + 1} \right)^{-1} . \quad (2.13)$$

In this case, since the highest resistance is encountered at the juxtacanalicular trabecular meshwork and inner wall of Schlemm's canal, we estimate that $K_{tm}/K_{sc} \sim 1$. Figure 2.15 shows the variation of the post-operative pressure with the ratio of the permeability of the device to that of the physiological route. Here we see that the pressure drop is always less

than 50%, which is in keeping with the more modest IOP reductions seen clinically (Fea, 2010; Fernandez-Barrientos et al., 2010; Arriola-Villalobos et al., 2012). The permeabilities of these devices need also be higher than those for subconjunctival drainage devices. For example, a reduction of IOP from 24 mmHg to 18 mmHg ($\Delta P_{post}/\Delta P_{pre}$ of 0.6) requires the permeability of the device to be around 8 times the permeability of the physiological route.

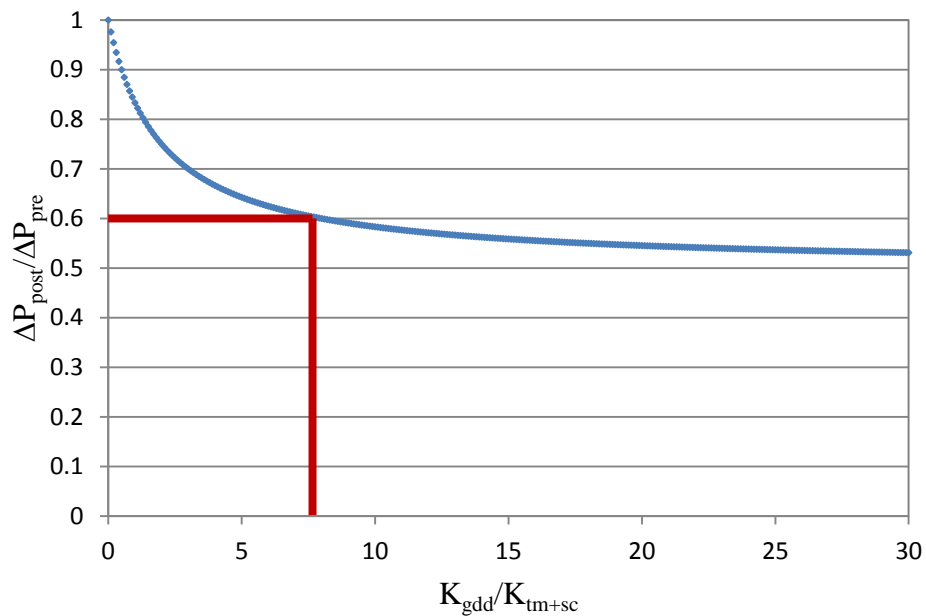


Figure 2.15 Calculated variation of post-operative pressure with ratio of permeability of a Schlemm's canal device to that of the physiological route (from Equation 2.13). The pressure drop is less than 50% and a reduction of IOP from 24 mmHg to 18 mmHg ($\Delta P_{post}/\Delta P_{pre}$ of 0.6) requires the permeability of the device to be around 8 times the permeability of the physiological route.

In the absence of data on actual devices, we can estimate their K using scaling analysis. Defining Q as flow rate, d as internal diameter, L as length, μ as dynamic

viscosity, and u and ΔP as characteristic velocity and pressure scales, the conservation of mass requires that

$$Q \sim u d^2 \quad (2.14)$$

while the balance between resistance caused by viscous forces and the driving pressure gradient,

$$\frac{\mu u}{d^2} \sim \frac{\Delta P}{L}. \quad (2.15)$$

Combining both,

$$Q \sim \Delta P \frac{d^4}{\mu L}, \text{ or } K \sim \frac{d^4}{\mu L}. \quad (2.16)$$

For circular sections of tubing, Poiseuille's Law is applicable. This law gives the pressure drop in a fluid flowing through a long cylindrical pipe (Batchelor, 2000). Its assumptions are that the flow is laminar through a pipe of constant circular cross-section substantially longer than its diameter; the fluid is incompressible and Newtonian; and there is no acceleration of fluid in the pipe. This law gives

$$K = \frac{\pi d^4}{128 \mu L}. \quad (2.17)$$

In Figure 2.16, the black shaded area indicates the range for an ideal device based on our calculations, the red shaded area the range of reported experimental values for the ExPress P50 and R50 (data in Table 2.7), and the blue shaded area the range of reported experimental values for the ExPress P200. The expected value for the ExPress P200 (200 μm ID, 2.64 mm length) is within the range found experimentally. The expected value for the ExPress R50 (50 μm ID, 2.64 mm length) is lower than its experimental value. One possible explanation for this is the actual device having a larger internal diameter than the stated 50 μm , and this will be explored in Chapter 5 of this thesis. As $K \sim d^4$, small changes in diameter will affect the permeability significantly. For comparison, we have also

superimposed the expected values for the MIDI-Arrow, AqueSys and CyPass devices. We can see that the first two devices have dimensions which are comparable to our ideal device.

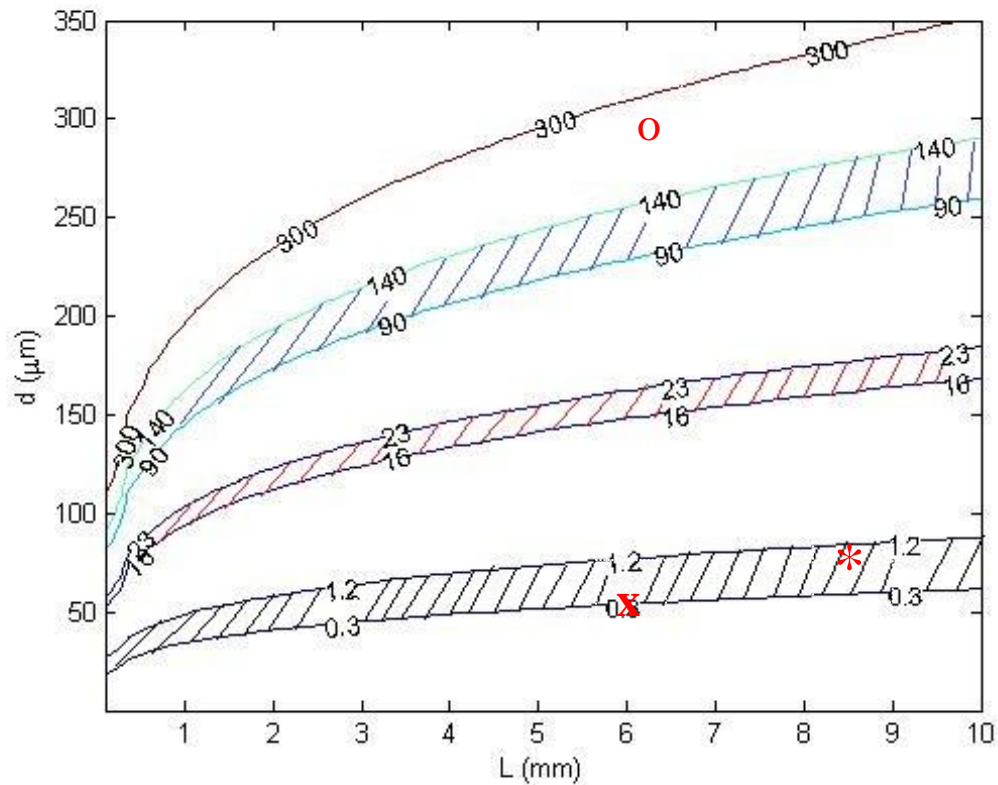


Figure 2.16 Normogram for assessing K values (in $\mu\text{l}/\text{min}/\text{mmHg}$). The black shaded area indicates the range for an ideal device while the red and blue shaded areas indicate the range of experimental values for the ExPress P50/ R50 and ExPress P200 respectively. The values for the MIDI-Arrow (*), AqueSys (x) and CyPass (o) devices are superimposed.

When drainage is into the suprachoroidal space, the electrical circuit analogy is similar to that of drainage into the subconjunctival space (Figure 2.13b). The calculated K value of the CyPass device is much larger in comparison to the subconjunctival space

devices. This may potentially lead to excessive aqueous humour outflow and hypotony, although a degree of restriction may be afforded by the natural counter-pressure of the space (Jordan et al., 2006).

2.6.2 Pressure-flow response of GDD

To characterise a GDD, it is important to be able to estimate the relationship between the pressure across the device and the flow rate through it. GDD can be divided into non-valved and valved categories, with different pressure-flow responses between them (Francis, 1998; Stay, Pan, Brown, Ziaie, & Barocas, 2005). For non-valved or fixed resistance devices,

$$P = QR. \tag{2.18}$$

At low flow rates, resistances of these devices are lower than with valved devices (Figure 2.17a), which may lead to problems with hypotony. Pressure is also sensitive to small variations in flow rate through the device (Figure 2.17b). These characteristics may be more suitable for devices which drain into areas such as the Schlemm's canal (with resistance from the EVP distally) and the suprachoroidal space (with its natural counter-pressure) to maintain IOP over a certain level.

With valved devices, resistance is a function of flow rate, where it is initially high but falls with increasing flow rate (Figure 2.17a). At low flow rates, it is higher than with fixed resistance devices, which may help to reduce hypotony. Pressure is weakly dependent on flow rate, and is maintained at a relatively stable level over a wider range of flow rates (Figure 2.17b). These characteristics are advantageous for devices which drain into areas with less resistance such as the subconjunctival space.

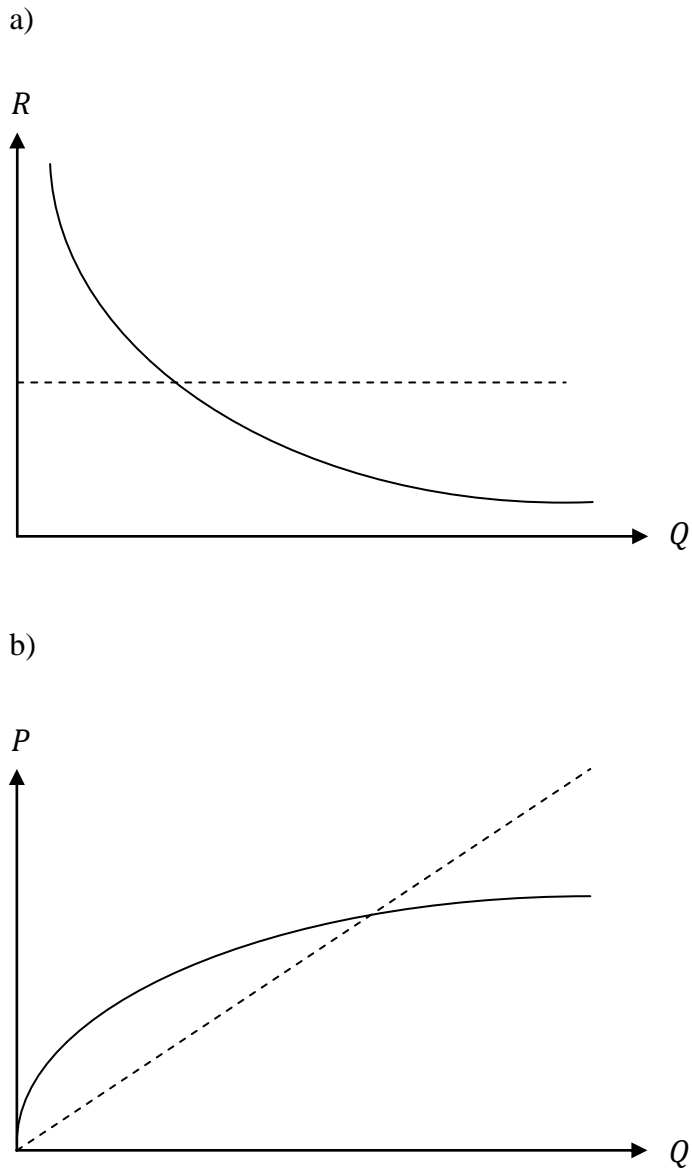


Figure 2.17 a) Expected resistance-flow rate response curves of a fixed resistance device (dashed line) and a valved device (solid line). b) Expected pressure-flow rate response curves of a fixed resistance device (dashed line) and a valved device (solid line). (R – resistance, P – pressure, Q – flow rate).

For a valved device, the dependence of pressure on flow rate is based on its material properties (Young's modulus E , Poisson's ratio ν) and sheet thickness T . From the bending equation (Landau & Lifshitz, 1986; described in more detail in Chapter 3),

$$\frac{ET^3\nabla^4h}{12(1-\nu^2)} = p, \quad (2.19)$$

where h is the gap separation. The scaling for flow rate,

$$Q \sim P \frac{H^3}{\mu}. \quad (2.20)$$

From Equation 2.19, the scaling for deformation,

$$\frac{ET^3H}{L^4} \sim P. \quad (2.21)$$

Combining the scaling for flow rate with the scaling for deformation, we obtain

$$P \sim \left(\frac{Q\mu}{EL^3}\right)^{\frac{1}{4}} \left(\frac{T}{L}\right)^{\frac{9}{4}}. \quad (2.22)$$

The response of Ahmed Glaucoma Valves to flow rate has been analysed using finite element analysis and experiments on actual devices (Stay et al., 2005). The authors inferred that the valve material had a Young's modulus E of 4.2 MPa and the pressure across the valve varied as $P \sim Q^{1/4}$. Along with Equation 2.22, we see that pressure has a stronger dependence on the physical dimensions of the valve (T and L) than it does on the flow rate and material properties. This may explain the reported difficulty in reproducing its pressure-flow characteristics (Prata, Jr. et al., 1995; Moss, 2008) as it may occur due to manufacturing issues related to the sensitivity of pressure to T , which has a $T^{\frac{9}{4}}$ dependence.

In the case of a trabeculectomy, it is essentially another flap valve formed from the superficial scleral flap and sutures. Therefore, the pressure-flow response should be similar to that of the Ahmed Glaucoma Valve, where $P \sim Q^{1/4}$. In one recent study, the response was found to be similar to that of a fixed resistance device, with a linear increase in

pressure with increasing flow rate (Tse et al., 2012). In the study, which also utilised finite element analysis, the scleral flap was modelled as having a fixed initial gap separation. This assumption may be inaccurate and would explain the different pressure-flow response that the authors found. In this thesis, we will explore the pressure-flow response of a trabeculectomy.

2.7 Conclusion and Research Questions

An understanding of fluid mechanics principles may be useful in making clinical decisions or improving upon the procedures and devices used in glaucoma surgery. Hypothetically, the designs depend on where the aqueous humour drains into. Devices which drain into the subconjunctival space, in parallel to the trabecular outflow pathway, should be slightly more permeable (1.5-6.0 times) than the glaucomatous eye or weakly dependent on the flow rate for adequate pressure reduction while still maintaining low incidences of hypotony. Valved devices satisfy this latter constraint as pressures have a weak dependence on flow rate ($P \sim Q^{1/4}$). Devices which drain into the Schlemm's canal work partially in series with the trabecular outflow pathway, and the operative conditions are different. As flow is limited by the resistance of the distal outflow structures and EVP, the devices should have higher permeabilities and can be of fixed geometry with a stronger dependence on flow rate ($P \sim Q^1$). Suprachoroidal drainage devices operate similarly to the subconjunctival space devices and thus need similar constraints. Current devices have the highest permeabilities and fixed geometry which may be disadvantageous but this may be partially accommodated by the natural counter-pressure restricting excessive aqueous humour outflow.

At the moment, trabeculectomy and subconjunctival space drainage devices still offer the most reductions in IOP and are likely to be continued in use for the treatment of glaucoma refractory to medical and laser therapy. However, they are still associated with large numbers of complications, of which the majority in the early post-operative period are related to hypotony. The findings of this review and analysis have prompted that a better understanding of the trabeculectomy and glaucoma drainage devices is needed to improve the outcome of glaucoma surgery. One of the main research questions in this thesis is how the trabeculectomy scleral flap performs as a valve, from a fluid mechanical perspective; and how it affects flow of aqueous humour and the pressure outcome. The other research question is whether small inner diameter fixed resistance tubes with permeabilities 1.5-6.0 times more than a glaucomatous eye are able to provide controlled aqueous humour flow into the subconjunctival space with avoidance of overfiltration and hypotony. The approach taken in testing these hypotheses is described in the following chapters.

Chapter 3

3 Fluid-structure characteristics of the scleral flap and the influence of the scleral flap and sutures on intraocular pressure (IOP) and aqueous humour flow direction

3.1 Introduction

Fluid mechanics is based on a combination of physical analysis and experimental observations (Binder, 1973). The general objective is to provide dependable practical results and a thorough understanding of fundamental flow features. To aid this effect, scaling (dimensional) analysis is useful for checking equations, changing units, determining a convenient arrangement of variables of a physical relationship, and planning systematic experiments. It frequently aids in making an easier description of the phenomena. However, reference to experimental data need to be made to obtain the necessary constants or coefficients for a complete numerical expression.

In the brief analysis of trabeculectomy at the end of Chapter 2, we suggested that the procedure creates a flap valve, formed by the partial thickness scleral flap and sutures. As such, both the resistance-flow and pressure-flow relationships would be non-linear. In this chapter, we describe the fluid-structure characteristics of the scleral flap as determined through scaling analysis, and then compare them with experimental results with a large scale trabeculectomy model. With the scaling analysis, the characteristics of interest were the dependences of both flap displacement H and pressure P on flap dimensions L and T , and aqueous humour flow rate Q . We then use the physical model to objectively measure

the influence of flap thickness, shape, suture number and position on the pressure under the model scleral flap. In the final part of the experiment, we perform a qualitative assessment of how the variables determine aqueous humour flow under the scleral flap. The intended outcome was an enhanced understanding of how the different variables could affect the outcome of surgery. As far as we know, there has never been an approach such as this to understand the trabeculectomy procedure.

3.2 Methods

3.2.1 Scaling analysis

The scleral flaps are characterised by the geometrical dimensions length L , width W and thickness T (Figure 3.1). The aqueous humour is characterised by flow rate Q and dynamic viscosity μ . The flaps are subjected to small amounts of strain so a linearly elastic model is appropriate, where for a small strain, they are characterised by Poisson's ratio ν and Young's modulus E .

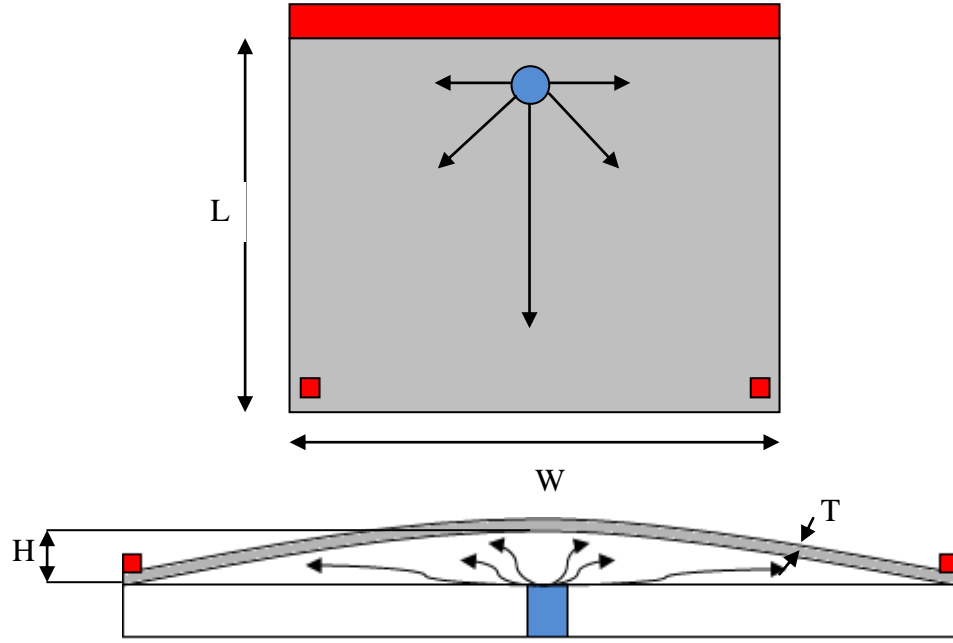


Figure 3.1 Schematic diagram of scleral flap from above and a cross section view. In the physical model, the silicone sheet (scleral flap) is indicated in grey and the back plate (limbus) and ‘sutures’ in red. The inlet hole (sclerostomy) is indicated in blue and the bottom plate in white. W – width, L - length, T - sheet thickness, H - fluid height.

Aqueous humour flow below the scleral flap is characterised by low Reynolds numbers ($\sim 10^{-2}$, this calculation is explained in the following section) and can be described by lubrication theory where the flow of fluids is in a thin layer over a wide area. The depth-averaged velocity,

$$\mathbf{u} = -\frac{\lambda h^2}{\mu} \nabla p \quad (3.1)$$

where λ is a coefficient for the boundary conditions. This is solved subject to the constraint that the flux of aqueous humour through the sheet is Q . The characteristic size of the flap is L (since $W/L \sim 1$), so we have $\frac{\partial}{\partial x} \sim 1/L$ and $\frac{\partial}{\partial y} \sim 1/L$. The integral form of mass conservation requires that flow rate out of the rectangular flap,

$$Q = \underbrace{\int_{-W/2}^{W/2} \frac{\lambda h^2}{\mu} \nabla p \cdot \hat{n} dS}_{\frac{H^3 P}{\mu}} \quad (3.2)$$

where the integral is taken over the exit from the flap (the order of magnitude estimates of the terms are indicated below the underbrace). The characteristics of the flaps depend on whether they are bending (the initial deflection perpendicular to the mid-surface of the flap) or stretching (when further deformation from transverse loads results in a change in the area of the mid-surface) (Ribe, 2001). γ is the Airy stress function. The coupled equations for bending and stretching (Landau & Lifshitz, 1986) are

$$\underbrace{\frac{ET^3 \nabla^4 h}{12(1-\nu^2)}}_{\frac{ET^3 H}{L^4}} - \underbrace{T \left(\frac{\delta^2 \gamma}{\delta y^2} \frac{\delta^2 h}{\delta x^2} + \frac{\delta^2 \gamma}{\delta x^2} \frac{\delta^2 h}{\delta y^2} - 2 \frac{\delta^2 h}{\delta x \delta y} \frac{\delta^2 \gamma}{\delta y \delta x} \right)}_{\frac{TH\Gamma}{L^4}} = p \quad (3.3)$$

and

$$\underbrace{\nabla^4 \gamma}_{\frac{\Gamma}{L^4}} + E \underbrace{\left(\frac{\delta^2 h}{\delta y^2} \frac{\delta^2 h}{\delta x^2} - \left(\frac{\delta^2 h}{\delta y \delta x} \right)^2 \right)}_{\frac{EH^2}{L^4}} = 0. \quad (3.4)$$

The following is a modification of the coupled equations. For low flow rates, balancing pressure against bending forces from Equation 3.3 gives

$$\frac{ET^3 H}{L^4} \sim P \sim \frac{Q\mu}{H^3}, \quad (3.5)$$

or

$$\frac{H}{T} \sim \left(\frac{Q\mu L^4}{ET^7} \right)^{\frac{1}{4}}. \quad (3.6)$$

For high flow rates, stretching is important and $\Gamma \sim EH^2$. Balancing stretching and pressure gives

$$\frac{ETH^3}{L^4} \sim \frac{Q\mu}{H^3}, \quad (3.7)$$

or

$$\frac{H}{T} \sim \left(\frac{Q\mu L^4}{ET^7} \right)^{\frac{1}{6}}. \quad (3.8)$$

The transition from bending to stretching occurs when $\frac{H}{T} \sim 1$, which occurs when the critical flow rate,

$$Q_c \sim \frac{ET^7}{\mu L^4}. \quad (3.9)$$

The pressure can be related to the flap displacement. Below the critical flow rate, the pressure is

$$\frac{P}{E} \sim \left(\frac{Q\mu}{EL^3} \right)^{\frac{1}{4}} \left(\frac{T}{L} \right)^{\frac{9}{4}}. \quad (3.10)$$

At higher flow rates, in the stretching state, the pressure shows a weaker dependence on flow rate, i.e.

$$\frac{P}{E} \sim \left(\frac{Q\mu}{EL^3} \right)^{\frac{1}{6}} \left(\frac{T}{L} \right)^{\frac{17}{6}}. \quad (3.11)$$

This tells us what the pressure response of a flap is and how it depends on flow rate, flap thickness, flap size and elastic modulus.

The flap is typically characterised by a length $L = 3$ mm in the sclera which has a Young's modulus $E \sim 1 \times 10^6$ Pa. At the limbus, the sclera is approximately 0.5 mm thick, and the flap formed is typically half thickness $T = 0.25$ mm. Such flaps are sutured in position so that aqueous humour ($\mu \sim 10^{-3}$ Pa.s) can leak from 3 sides. The critical flow rate Q_c (from Equation 3.9) is 7.5×10^{-7} m³/s, which is significantly higher than that of normal aqueous humour flow rate (1.5-3 μ l/min or 2.5 - 5.0×10^{-11} m³/s). Therefore, this flap also works in the bending regime.

3.2.2 Physical model

The physical model exploits the principle of geometric and dynamic similarity or similitude which is commonly used in the area of engineering to test fluid flow conditions with scaled models (Binder, 1973). In order to obtain information regarding the flow phenomena in or around a structure, called the original or prototype, it is often convenient, economical and sound engineering to experiment with a copy or model of the prototype. The model may be geometrically smaller than, equal to, or larger than the prototype in size. These provide an advantage in research, design and performance-prediction work which cannot be obtained from theoretical calculations alone. Certain laws of similarity need to be observed in order to ensure that the model test data can be applied to the prototype. These laws in turn provide means for correlating and interpreting the test data. In addition to geometric similarity, dynamic (i.e. forces acting on the flow) similarity need also be considered, where the velocity and streamlines of flow are matched. The dimensionless Reynolds number (Re) determines the ratio of viscous versus inertial forces acting on the body. Dynamic similarity between a prototype and its model is realised when the Re for the model equals that of the prototype. The Re can be determined from

$$Re = ul/v \quad (3.12)$$

or

$$Re = Ql/Av, \quad (3.13)$$

where u is velocity, l is a characteristic length or hydraulic diameter, v is kinematic viscosity, Q is volumetric flow rate and A is cross-sectional area. For example, taking a simple case where a model is tested in the same fluid as that of the prototype flow (i.e. with the same kinematic viscosity), a larger model than the prototype will need a higher associated velocity. Another application of the principle is to replace the operating fluid

with a different test fluid, which can be for convenience, cost or safety reasons. However, it is often impossible to achieve strict similitude during a model test (Heller, 2011). The greater the departure from the application's operating conditions, the more difficult achieving similitude is. In these cases, some aspects of similitude may be neglected, focusing on only the most important parameters. For aqueous humour flow under a scleral flap, with typical values of $Q \sim 3\mu\text{l}/\text{min}$, $W \sim 4\text{ mm}$, $L \sim 3\text{ mm}$, $H \sim 0.5\text{ mm}$ and $\nu \sim 10^{-6}\text{ m}^2/\text{s}$ (see Figure 3.1), the Re is $\sim 2.5 \times 10^{-2}$. In our model, with typical values of $Q \sim 400\text{ml}/\text{h}$, $W \sim 12\text{ cm}$, $L \sim 9\text{ cm}$, $H \sim 2\text{ mm}$ and $\nu \sim 10^{-3}\text{ m}^2/\text{s}$, the Re is $\sim 1.9 \times 10^{-2}$. As such, while the model is much larger than a scleral flap, the flow properties are similar.

The main assembly consisted of 9 mm thick transparent acrylic upper and lower plates separated by an intermediate section. The intermediate section comprised of a back plate (to represent the limbus) and 1 cm x 1 cm x 1 cm cuboidal 'sutures' to adequately restrain the silicone sheets at their edges but allow space for their deformation (Figure 3.1). The lower plate had a 10 mm inlet hole through which the working fluid flowed in underneath the sheet, injected using a syringe driver (Cole-Parmer, IL, USA). The upper plate applied uniform pressure on the intermediate section and lower plate. This assembly was then mounted on top of a light box to enhance visualisation of flow (Figure 3.2).

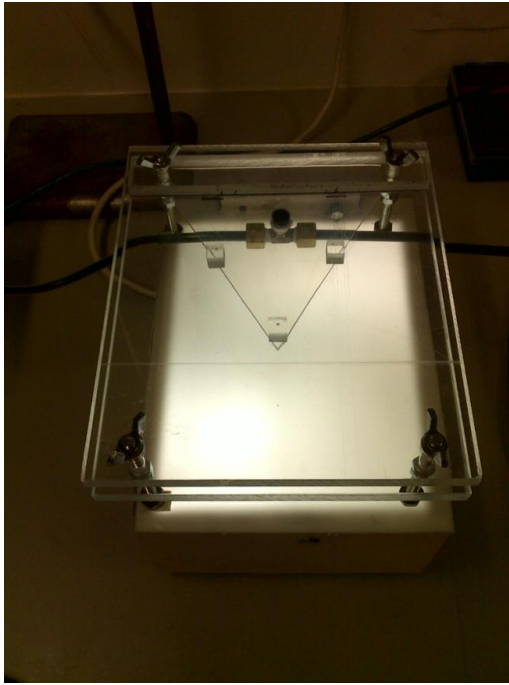


Figure 3.2 Elevated view photograph of the main assembly with a triangular sheet in position.

In our experiment, transparent silicone sheets (HT-6240; Rogers Corporation, CT, USA) of 0.3, 0.5, 0.8, 1.6 and 3.2 mm thicknesses were used to model the scleral flap; in relation to a typical actual scleral flap thickness of 250 μm , they were up to $12 \times$ thicker. The range of thicknesses allowed us to test pressure and flow as a function of flap thickness. Prior to the experiment, the material properties of the silicone sheets were determined using a materials tester (model H5KS; Hounsfield Test Equipment, Surrey, UK). A 1.6 mm thick sheet was mounted and incrementally loaded with up to 75 N of force. High resolution images were taken, which showed the axial extension and transverse contraction of the sheet. The Young's (elastic) modulus E was determined from the initial slope of the stress-strain curve and the Poisson's ratio ν from the transverse contraction strain to axial extension strain ratio. We found $E = 1.0$ MPa (which is comparable to

reported scleral values of 1.2-1.3 MPa (Asejczyk-Widlicka, Srodka, Kasprzak, & Pierscionek, 2007) and 1.8-2.9 MPa (Friberg & Lace, 1988)) and $\nu = 0.495$ (which is close to the 0.5 expected for an incompressible material).

These sheets were cut into 12 cm x 12 cm squares, 12 cm x 9 cm rectangles and 12 cm equilateral triangles. In relation to typical actual scleral flap dimensions, they were around $30 \times$ larger. They were fixed at the 'limbus' end using the back plate of the intermediate section (Figure 3.1). Additionally, they were also fixed in various suture configurations including 2 sutures, 4 sutures or 5 sutures for rectangular and square flaps; and 1 suture or 3 sutures for triangular flaps (Figure 3.3). These configurations are the ones commonly seen in experimental and clinical practice (Birchall et al., 2006; Tse et al., 2012; de Barros et al., 2008; Kobayashi & Kobayashi, 2011).

For the working fluid, we used 100% glycerine (VWR International Limited, UK) and undiluted Parker black ink (as a dye) in a ratio of 100:1. The dye was necessary for visualising fluid flow underneath the sheet. The kinematic viscosity of the glycerine and dye fluid, ν was $\sim 1.15 \times 10^{-3} \text{ m}^2/\text{s}$ which enabled us to maintain dynamic similarity to aqueous humour flow under a scleral flap. The solution was homogeneously mixed and the whole system ensured to be free of air bubbles before each run.

Before placement of each silicone sheet, a thin layer of glycerine was spread out on the bottom plate to aid subsequent removal of air bubbles. The sheet was then placed and restrained with the back plate and 'sutures'. Next, the glycerine was squeezed out to create an air tight seal between the sheet and the lower plate. The upper plate was then placed on top of the back plate and 'sutures' and tightened down with wing nuts (Figure 3.2). To prevent air from getting under the sheets again, the nuts were not over-tightened. The assembly was also checked to be level before the start of the experiment.

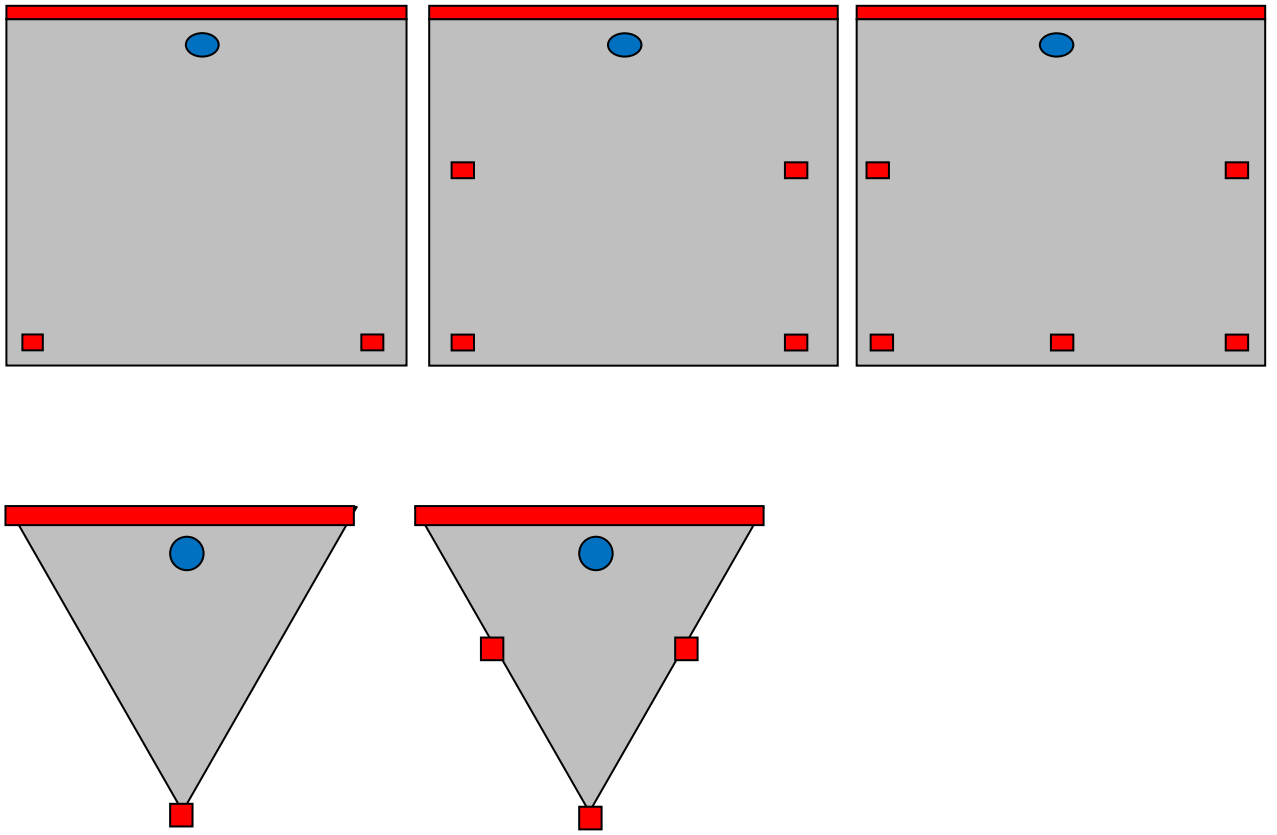


Figure 3.3 Configurations of sheets and sutures. Top row shows rectangles and squares with 2 sutures (left), 4 sutures (middle) and 5 sutures (right). Bottom row shows triangles with 1 suture (left) and 3 sutures (right).

Our model utilised separate pressure measurement and image recording circuits (Figure 3.4). These circuits are described separately in the following sections.

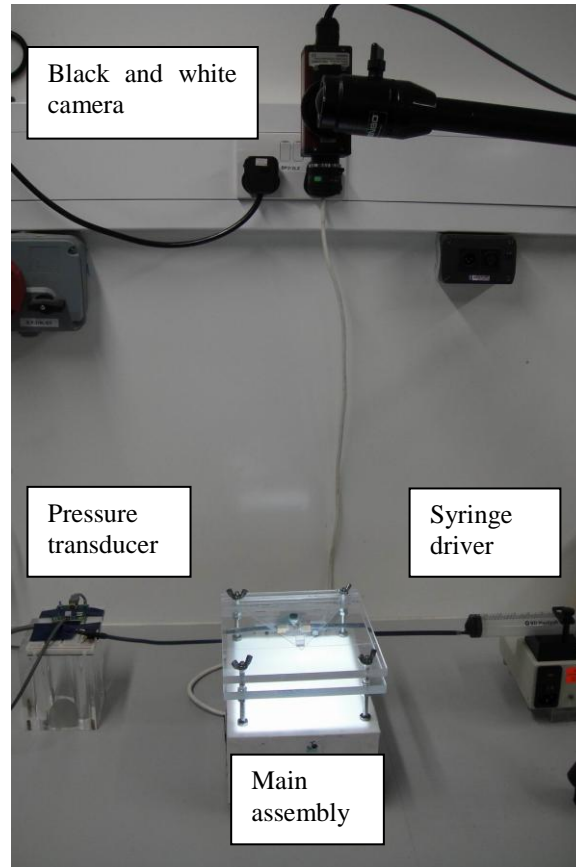


Figure 3.4 Photograph of complete setup. The syringe driver pumped dyed fluid and the pressure transducer measured pressure under the transparent sheet on the main assembly. The black and white camera recorded images for analysis of the direction of flow.

3.2.2.1 Pressure measurement

For the pressure measurement circuit, we used a pressure transducer (model 26PCAFA6D, 15V excitation; Honeywell International, NJ, USA) connected to a signal conditioner/ amplifier (Mantracourt Electronics Ltd, Exeter, UK) and personal computer. Non-expansile tubing (outer diameter 6 mm, internal diameter 4 mm) was used throughout the system. This setup was connected to the inlet hole of the main assembly and syringe driver with a 3-way connector. The level of the pressure inlet port on the pressure transducer was the same as the level of the lower plate and the syringe driver. Prior to the actual experiment, calibration of the pressure transducer was performed using a water manometer which was a 1 m long hollow glass rod with an outer diameter of 6 mm and internal diameter of 3 mm. The voltage readings for various levels from 0 – 70 cm H₂O (and the equivalent values in mmHg, 1 cm H₂O = 0.7355 mmHg) were noted and plotted in a graph. A least squares linear fit to the relationship between voltage and pressure was calculated (Figure 3.5). The equation derived was then used to convert voltage into pressure readings.

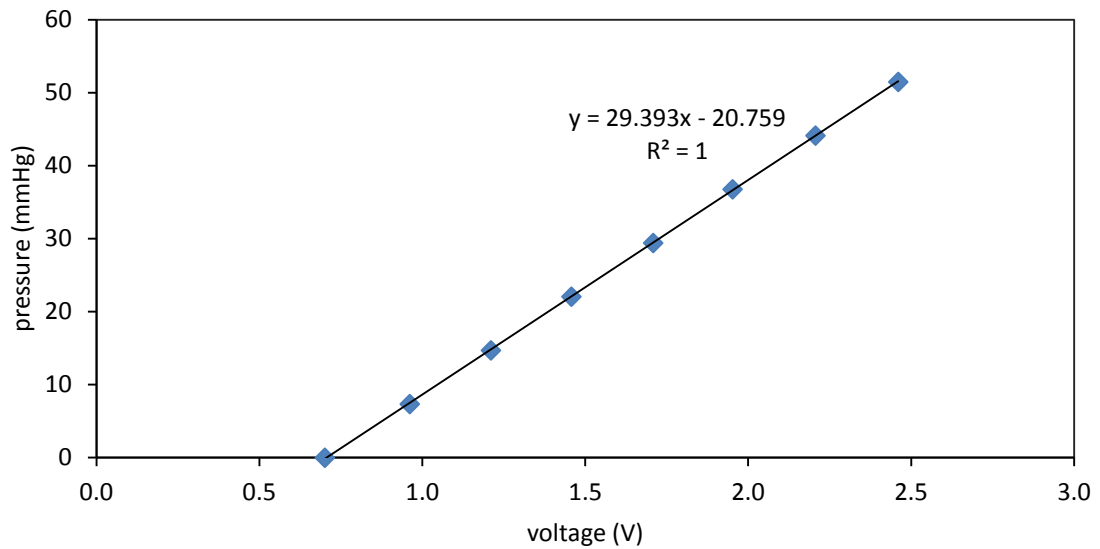


Figure 3.5 Calibration of pressure transducer showing linear response to change in pressure. The pressure transducer provided a ‘base’ voltage reading even with 0 mmHg pressure.

Measurement of the resistance of the tubing and connections was also performed. We infused the working fluid through the system at 100, 200, 300 and 400 ml/h without a silicone sheet in place and measured the voltage changes. From a simplified version of Poiseuille’s equation,

$$P = QR, \tag{3.14}$$

the resistance was determined from the slope of the pressure versus flow rate graph and it was 0.004 mmHg/ml/h. This baseline resistance was deducted from the pressure readings from each run.

In the actual experiment with silicone sheets in place, the syringe driver was started and the pressure recorded and plotted. The flap, suture and flow rate combinations used are

stated in section 3.2.2.3. A typical pressure curve obtained is shown in Figure 3.6, the outcome of interest was the equilibrium pressure.

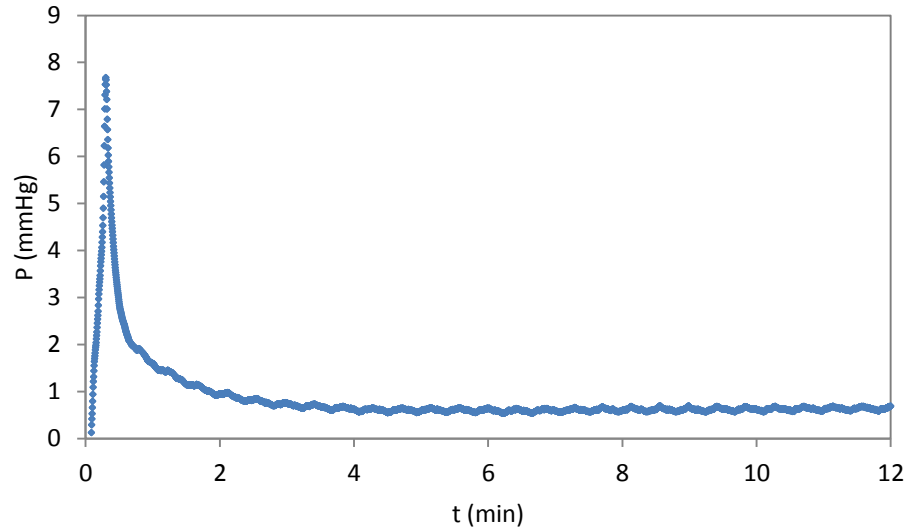


Figure 3.6 Typical pressure curve showing an initial spike, before equilibration after the silicone sheet flap valve opened.

3.2.2.2 Image recording and processing

Images were recorded using a black and white camera (Dolphin F145B; Allied Vision Technologies GmbH, Germany) connected to a personal computer. Experiments were carried out in a darkened room to enhance contrast for the image analysis.

Prior to the actual experiment, calibration was performed by adding dyed glycerine into an empty beaker in increments of 0.5 ml up to a total of 20 ml, with serial images being taken (Figure 3.7). With a known beaker diameter (59.0 mm), the average height of the fluid as the volume increased could be calculated. MATLAB was used to measure the average intensity of each pixel in each image and correlated this with the average height of the fluid. As the intensity increased with fluid height, a corresponding fluid height could be

attributed to all areas in an image (Cenedese & Dalziel, 1998). The calibration curve indicated a linear relationship between the change in intensity (I_0/I) and the height of fluid (thickness) up to around 4 mm (Figure 3.8). The curve levelled out after that as the intensity became saturated and the program could not register any further change. From this information, the maximum reading of the fluid height in the MATLAB script was set to 4 mm.

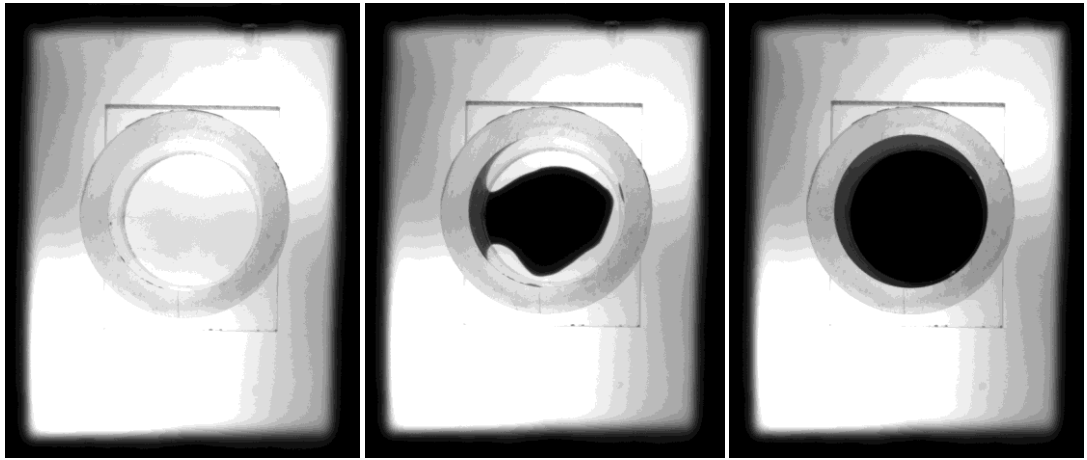


Figure 3.7 Calibration using dyed glycerine increments. Serial images are taken after each addition and analysed using MATLAB.

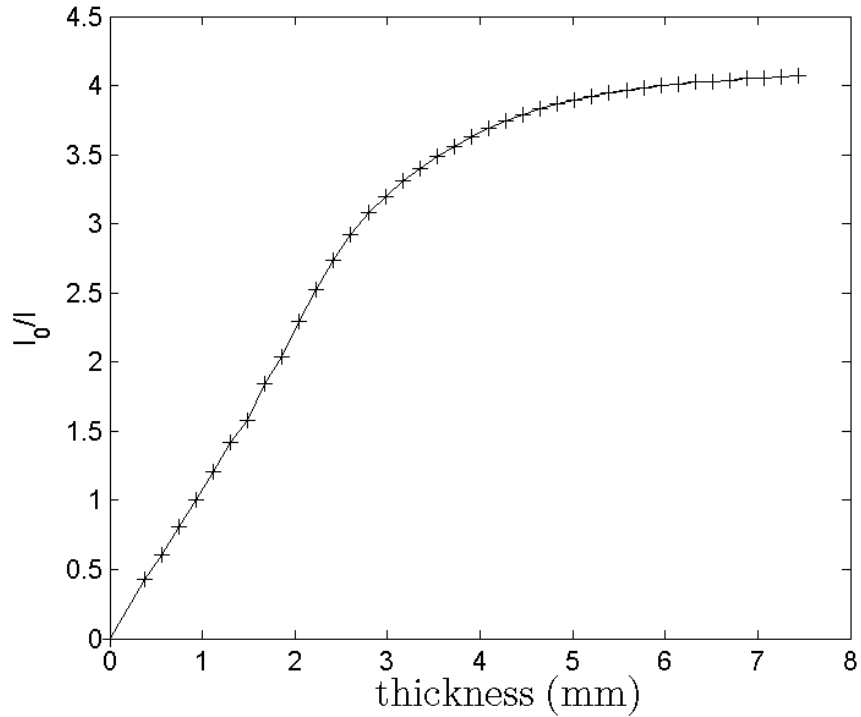


Figure 3.8 Calibration curve for image processing. The curve levelled out after around 4 mm thickness.

In the actual experiment, an initial image was recorded before flow was started, and then at pre-determined intervals of between 1 to 4 seconds after the start of flow. With these images, MATLAB measured the average intensity of each pixel in the individual images. The difference in intensity was then converted into fluid height under the sheet. For the comparison with the scaling analysis, a H/T versus $Q\mu L^4/ET^7$ plot was produced (see Results section) while for the assessment of fluid flow under the flap, the final image was processed as a false-colour image (Figure 3.9).

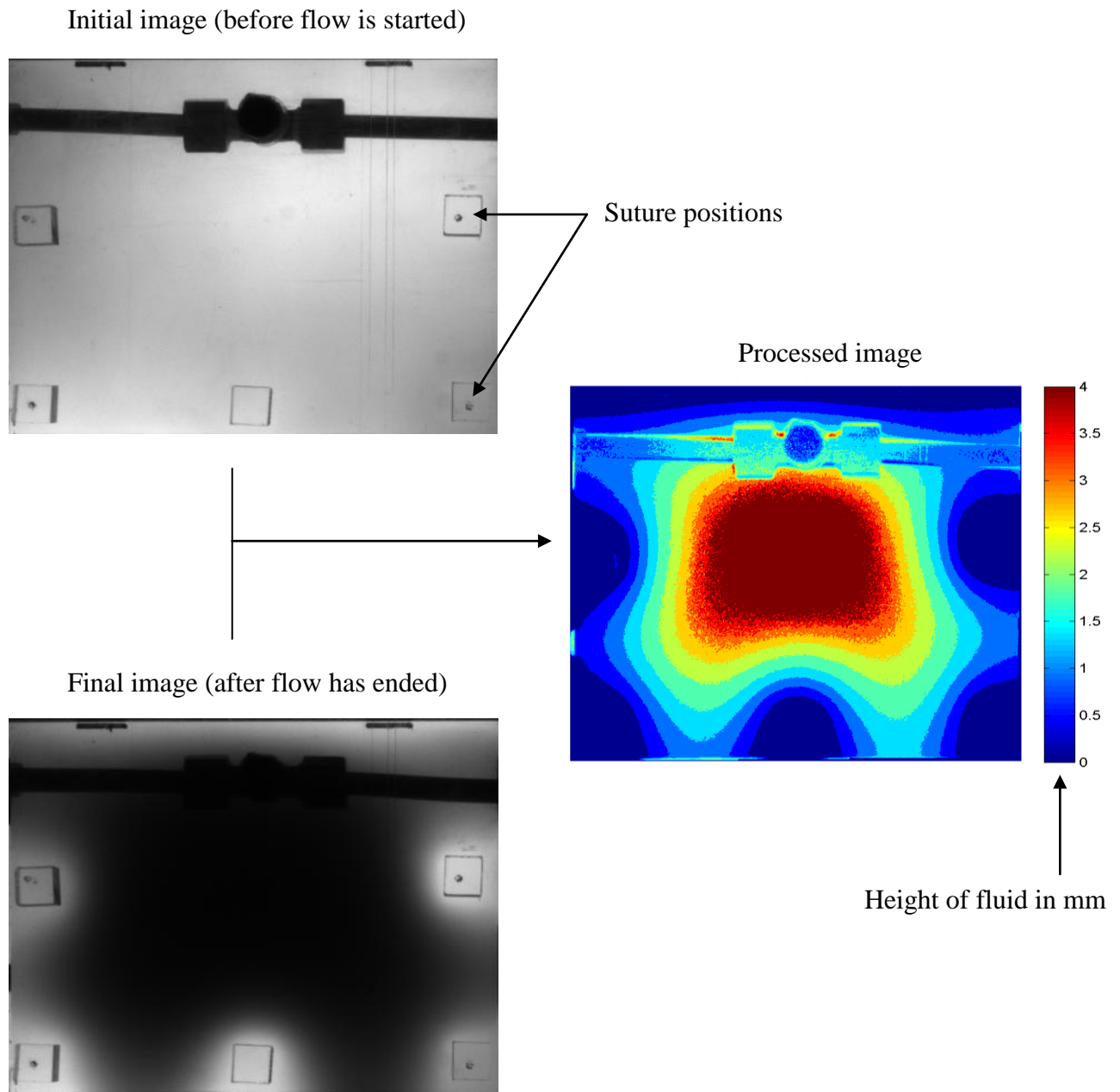


Figure 3.9 Method of processing false colour image by MATLAB. The initial image is compared with the final image and the difference in intensity converted into fluid height in the processed image. Suture positions can just be visualised in the processed image.

3.2.2.3 Experimental combinations

For the comparison between scaling analysis and physical model section, 0.3, 0.5, 0.8, 1.6 and 3.2 mm thick rectangle (with 2 sutures) and triangle (with 3 sutures) sheets were used with flow rates of 50, 100, 200, 300 and 400 ml/h. Additional flow rates of 10 and 20 ml/h were also used with the 1.6 and 3.2 mm thick sheets. This was to test a wide range of T and Q values.

For the pressure under the scleral flap and flow of fluid flow under the scleral flap sections, we utilised 0.8 and 1.6 mm thick sheets in all the configurations shown in Figure 3.3. This was to test a wide range of configurations which may exist in clinical practice. However, only flow rates of 100, 200 and 400 ml/h were used, to maintain dynamic similarity to aqueous humour flow.

For all experimental runs, we ran 50 ml of fluid for the rectangle and square flaps and 35 ml for the triangle ones. This was pre-determined through pilot runs to be sufficient for the pressure and flow to reach equilibrium.

3.2.2.4 Statistical analysis

Statistical analysis was performed using Prism 4 software (GraphPad Software, Inc., CA, USA). The paired t-test was used when comparing 2 groups while repeated measures ANOVA with Bonferroni's multiple comparison post-test was used when comparing 3 groups. $P < 0.05$ was considered statistically significant.

3.3 Results

3.3.1 Comparison between scaling analysis and physical model

The experimental variation of $\frac{H}{T}$ with $\frac{Q\mu L^4}{ET^7}$ is shown in Figure 3.10. The experiments cover a significant range of $\frac{Q\mu L^4}{ET^7}$ (over 10 decades) because of the sensitivity of the results to T . The experimental results support the scaling analysis, with a 1/4 gradient for $\frac{H}{T} < 1$ (bending state) and 1/6 gradient for $\frac{H}{T} > 1$ (stretching state), confirming the predictions of Equations 3.6 and 3.8 respectively. The experimental variation of $\frac{P}{E}$ with $\frac{Q\mu}{EL^3}$ is shown in Figure 3.11. There was a wide scattering of the data points, indicating a poor correlation between the analysis and the measured pressure values.

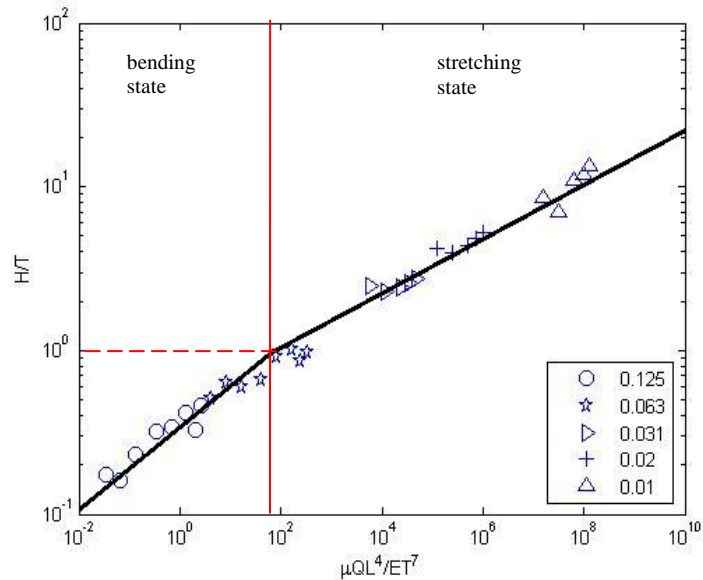


Figure 3.10 Experimental variation of $\frac{H}{T}$ with $\frac{Q\mu L^4}{ET^7}$ (see Equations 3.6 and 3.8), showing 1/4 and 1/6 gradients corresponding to the bending and stretching states.

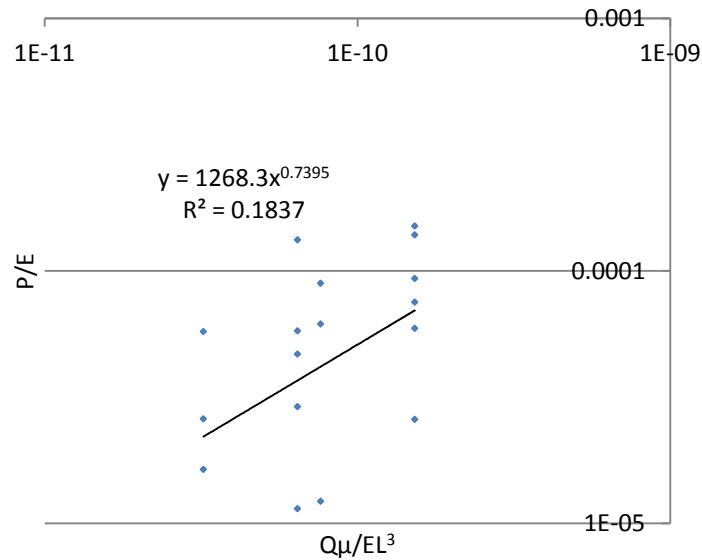


Figure 3.11 Experimental variation of $\frac{P}{E}$ with $\frac{Q\mu}{EL^3}$ (see Equations 3.10 and 3.11), showing the wide scattering of data points.

3.3.2 Pressure under the scleral flap

Note that the pressure readings do not correlate with actual IOP. They are however indicative of the relative differences in IOP with different scleral flap configurations in the actual trabeculectomy procedure.

The pressure readings were heavily influenced by flow rate and sheet thickness. With our setup, the lowest flow rate of 100 ml/h generally gave small pressure changes (< 0.1 mmHg) which were affected more by experimental errors. When the rate of 200 ml/h was used, this problem was reduced. The thinner 0.8 mm sheet also tended to provide low readings. The biggest differences were seen with the thicker 1.6 mm sheet and rate of 400 ml/h.

A total of six experimental runs were performed for each setting. In the following graphs, pressure drops are inversely related to the pressure values shown. Error bars indicate 1 standard deviation (SD) and asterisks (*) indicate where differences are statistically significant ($p < 0.05$).

Influence of flap thickness

Pressures under the thicker sheets were higher than those under the thinner sheets i.e. the pressure drops were smaller. When there were 3 sutures for triangles and 2 sutures for rectangles and squares (Figure 3.12), pressures under the thinner sheets were between 35.6-48.9% of pressures under the thicker sheets. When there were 3 sutures for triangles and 5 sutures for rectangles and squares (Figure 3.13), pressures under the thinner sheets were between 27.2-42.8% of pressures under the thicker sheets.

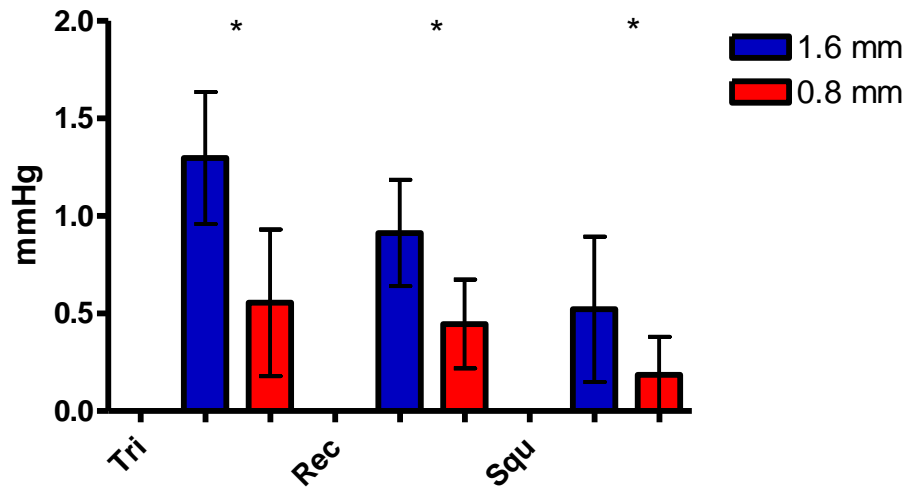


Figure 3.12 Comparison between thicknesses when there were 3 sutures for triangles and 2 sutures for rectangles and squares. With all 3 shapes, pressures were higher with the thicker sheet.

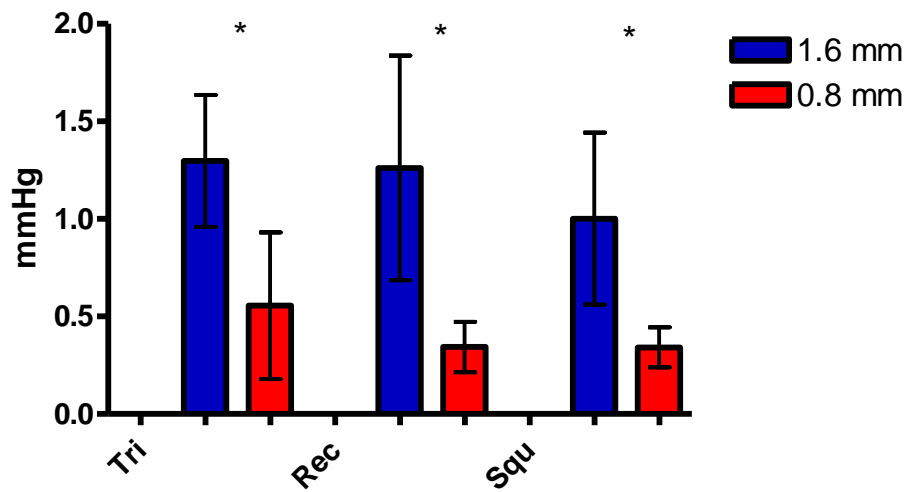


Figure 3.13 Comparison between thicknesses when there were 3 sutures for triangles and 5 sutures for rectangles and squares. With all 3 shapes, pressures were higher with the thicker sheet.

Influence of flap shape

When there were 3 sutures for triangles and 2 sutures for rectangles and squares, we found that triangles maintained higher pressures, followed by rectangles and squares (Figure 3.14). The pressures under the rectangular sheets were between 48.6-80.3% of pressures under the triangular sheets and pressures under the square sheets were 29.7-40.2% of pressures under the triangular sheets. When there were 3 sutures for triangles and 5 sutures for rectangles and squares, a similar pattern was seen but the differences were all not statistically significant (Figure 3.15). Pressures under the rectangular sheets were between 61.8-108.9% of pressures under the triangular sheets and pressures under the square sheets were 61.4-88.5% of pressures under the triangular sheets.

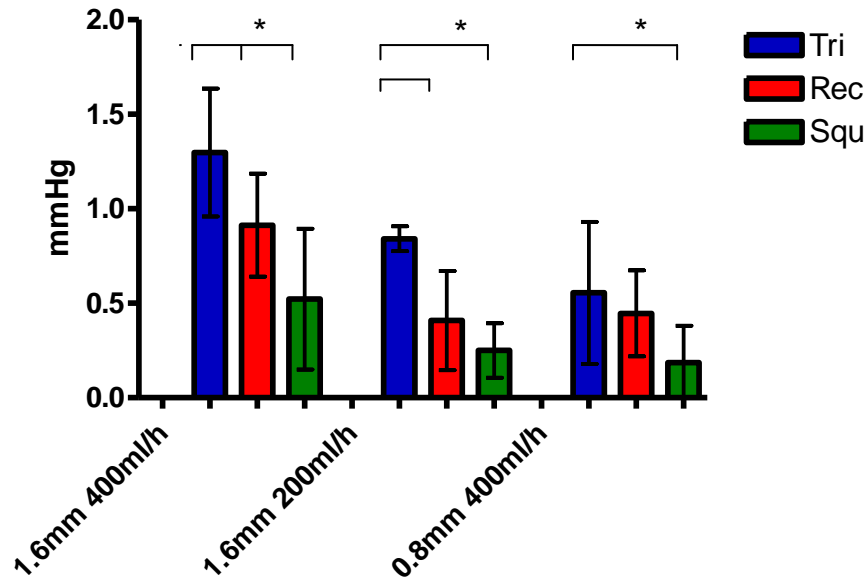


Figure 3.14 Comparison between shapes when there were 3 sutures for triangles and 2 sutures for rectangles and squares. Triangles maintained higher pressures, followed by rectangles and squares.

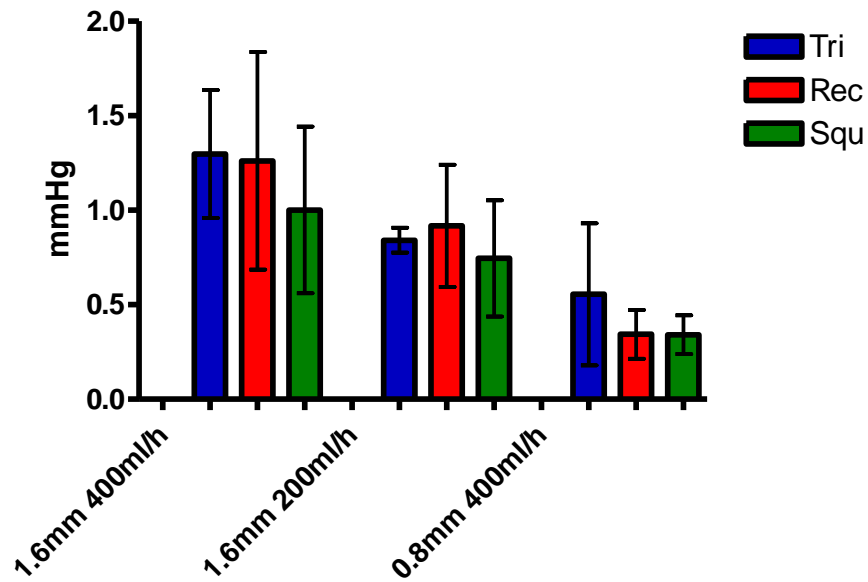


Figure 3.15 Comparison between shapes when there were 3 sutures for triangles and 5 sutures for rectangles and squares. There were no statistically significant differences between the shapes.

Influence of suture numbers and positions

With increasing numbers of sutures, the pressure drop became smaller (Figures 3.16-3.18). With the rectangular sheets, 4 sutures provided between 58.7-84.2% of the pressures with 5 sutures and 2 sutures provided between 44.6-130% of the pressures with 5 sutures. With the square sheets, 4 sutures provided between 45.3-98.4% of the pressures with 5 sutures and 2 sutures provided between 49.9-54.5% of the pressures with 5 sutures. With the triangular sheets, 1 suture provided between 52.5-81.0% of the pressures with 3 sutures.

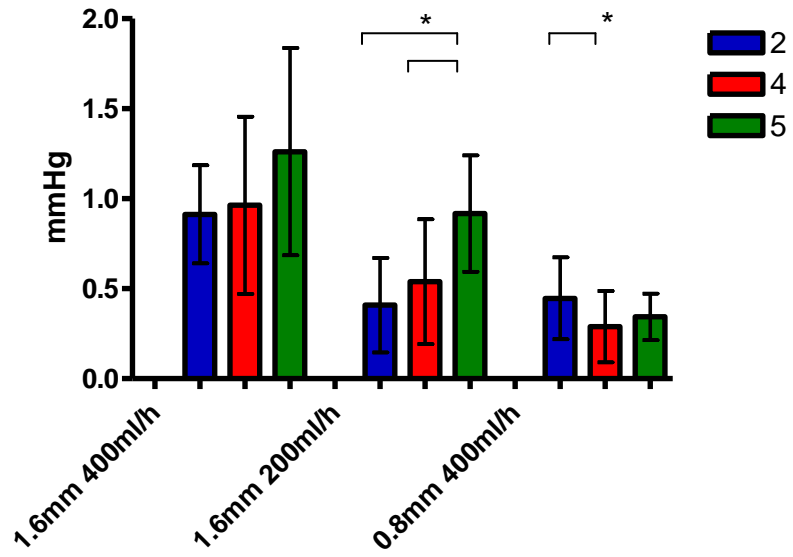


Figure 3.16 Comparison between number of sutures in the rectangle group. Generally, higher pressures were maintained with more sutures.

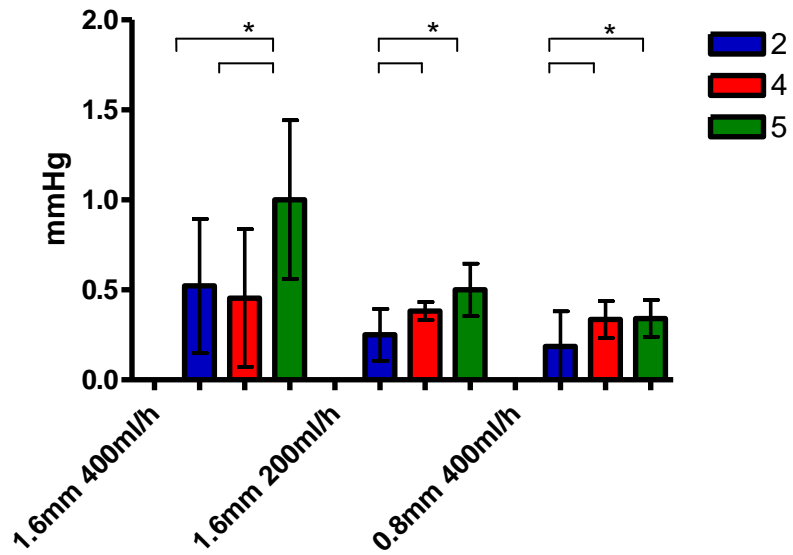


Figure 3.17 Comparison between number of sutures in the square group. Generally, higher pressures were maintained with more sutures.

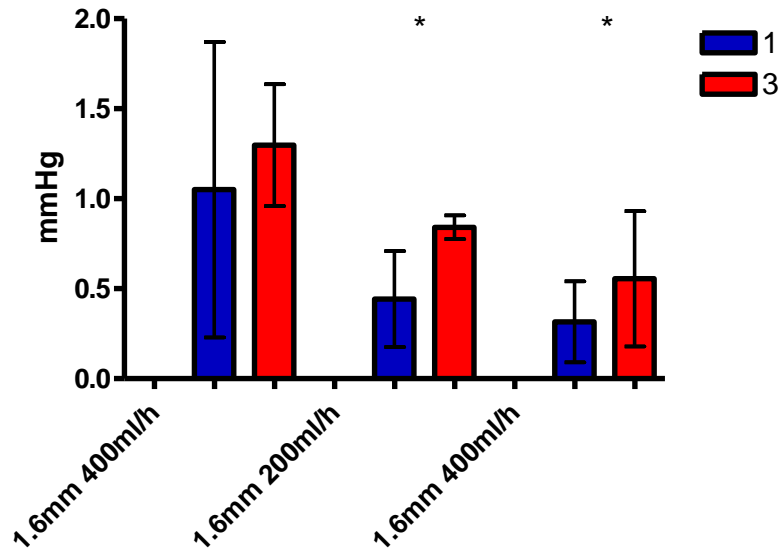


Figure 3.18 Comparison between number of sutures in the triangle group. Higher pressures were maintained with more sutures.

3.3.3 Fluid flow under the scleral flap

For this part of the experiment, we determine the flow under the flap using the height and spread of fluid in the final image. There may be differences between our findings and actual aqueous humour flow under the scleral flap due to other differences between the silicone sheet used in our model and actual sclera such as wettability characteristics.

Influence of flap thickness

When comparing between the different thicknesses, we found fluid height under the thinner sheets to be higher and wider for all three sheet shapes (Figure 3.19). The difference was small with the rectangle and square sheets but larger with the triangle sheet. The direction of flow was similar between thicknesses.

Influence of flap shape

Our results were inconclusive when considering rectangles and squares with 5 sutures (see next section). With the 4-suture rectangle and square sheets, we found that the direction of flow was away from the limbus towards the opposite edge (Figures 3.20a and b). With the 2-suture rectangle sheet (Figure 3.20c), the direction of flow was away from the limbus and also to the sides. With the 2-suture square sheet (Figure 3.20d), the direction of flow was to the sides. With 3-suture triangles, the flow was also away from the limbus (Figure 3.20e) but when there was only 1 suture then the flow was to the sides (Figure 3.20f).

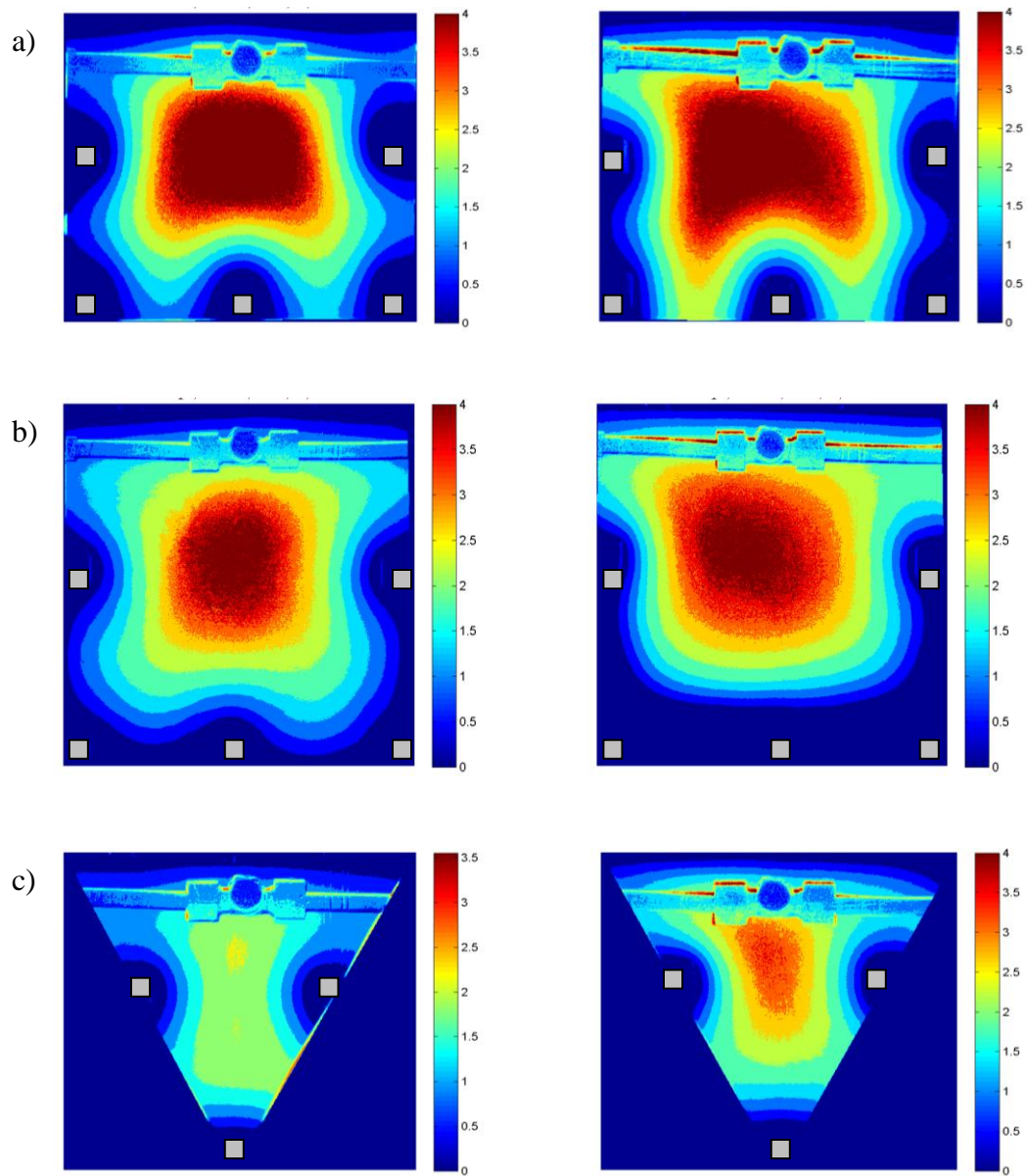


Figure 3.19 False colour final images showing fluid height under a) rectangle (b) square and (c) triangle sheets. Suture positions (grey boxes) are superimposed on the images. The images on the left are for 1.6 mm thickness while those on the right are for 0.8 mm thickness. Fluid heights under the thinner sheets were higher and wider for all three sheet shapes.

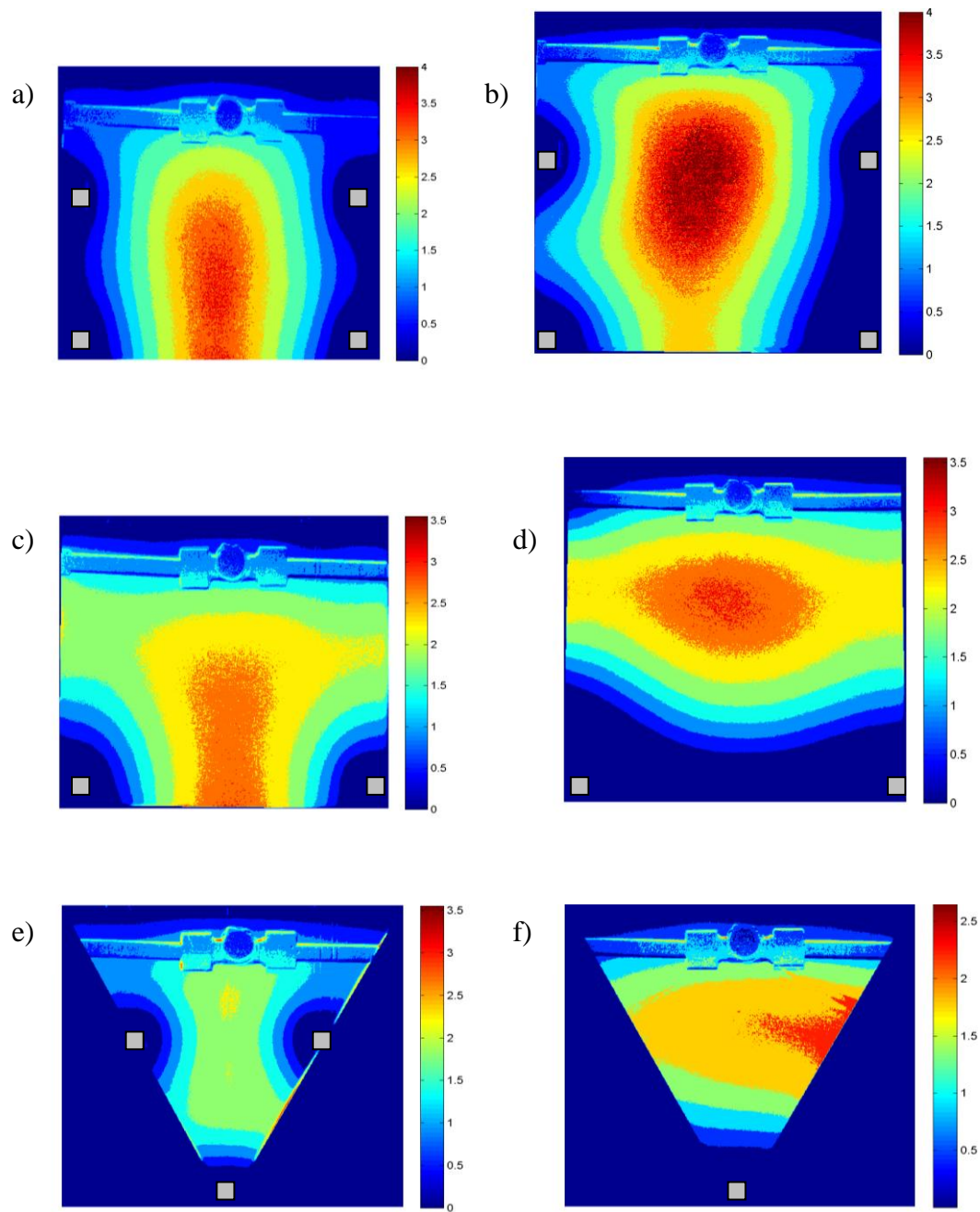


Figure 3.20 False colour final images showing fluid movement under a (a) rectangle with 4 sutures, (b) square with 4 sutures, (c) rectangle with 2 sutures, (d) square with 2 sutures, (e) triangle with 3 sutures and (f) triangle with 1 suture. Suture positions (grey boxes) are superimposed on the images. With 4-suture rectangle and square sheets, the direction of flow was away from the limbus towards the opposite edge. With the 2-suture rectangle sheet the flow was away from the limbus and also to the sides. With the

(Continued) **Figure 3.20**

2-suture square sheet, the direction of flow was to the sides. With 3-suture triangles, the flow was also away from the limbus but when there was only 1 suture then the flow was to the sides.

Influence of suture numbers and positions

With the 5-suture rectangle and square configurations, fluid tended to accumulate under the sheets as they were well constrained. With 4 sutures, the flow was directed more posteriorly while with 2 sutures the flow was directed mainly to the sides (Figures 3.21 and 3.22). With 3-suture triangles, the flow was away from the limbus but when there was only 1 suture then the flow was to the sides (Figure 3.23).

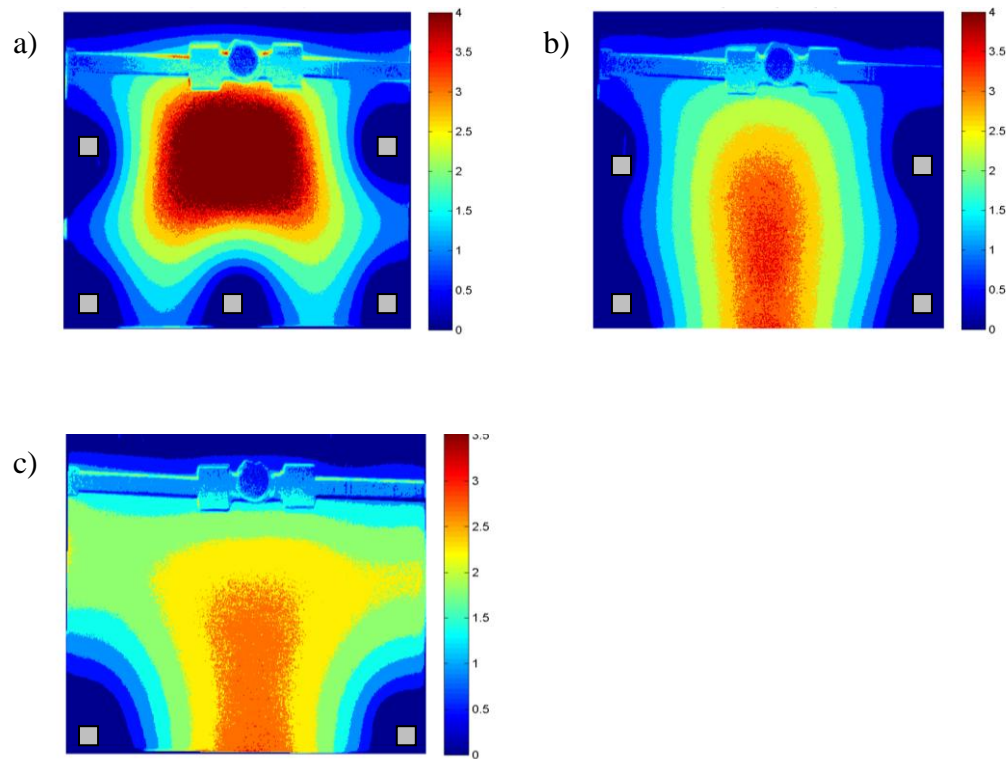


Figure 3.21 False colour final images showing fluid movement under a rectangular sheet with (a) 5, (b) 4 and (c) 2 sutures. Suture positions (grey boxes) are superimposed on the images. With 5 sutures, fluid accumulated under the sheet as it was well constrained. With 4 sutures, the flow was directed posteriorly while with 2 sutures the flow was directed posteriorly and to the sides.

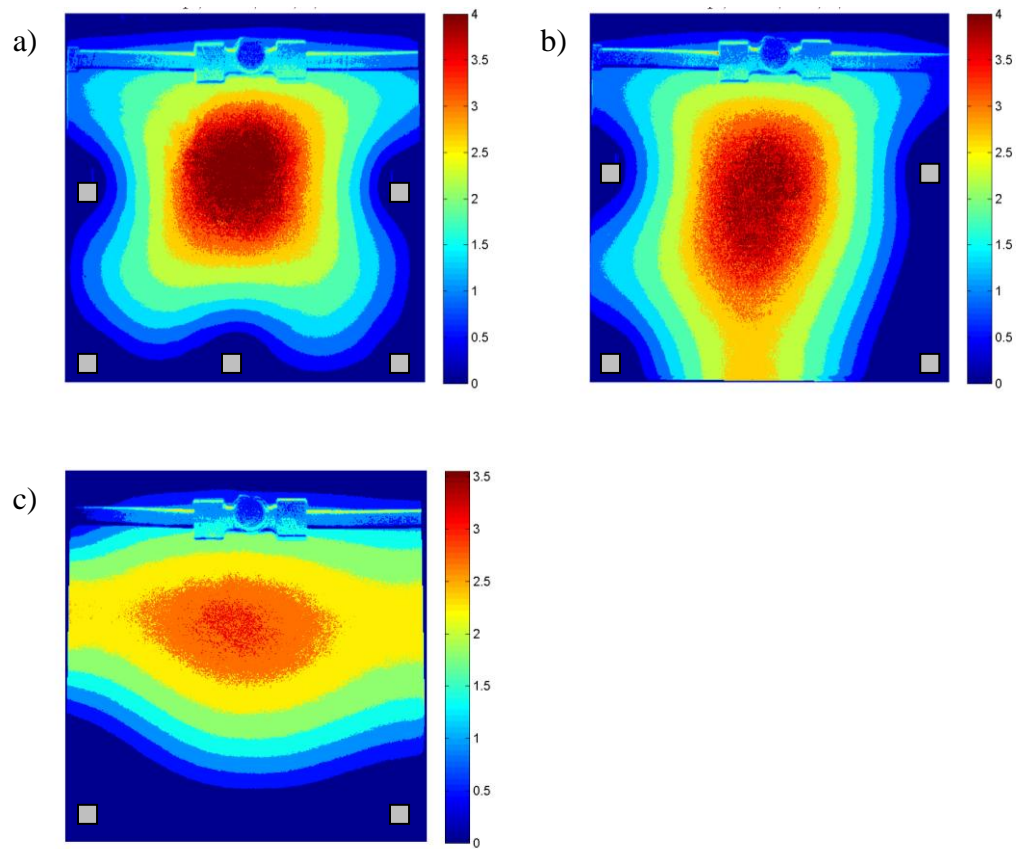


Figure 3.22 False colour final images showing fluid movement under a square sheet with (a) 5, (b) 4 and (c) 2 sutures. Suture positions (grey boxes) are superimposed on the images. With 5 sutures, fluid accumulated under the sheet as it was well constrained. With 4 sutures, the flow was directed posteriorly while with 2 sutures the flow was directed to the sides.

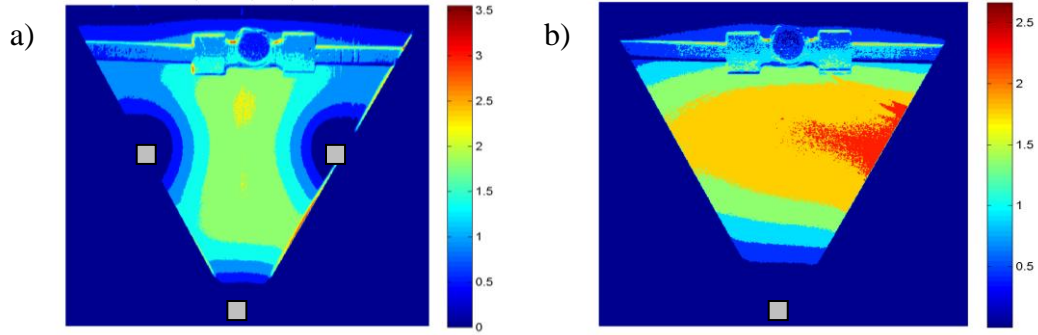


Figure 3.23 False colour final images showing fluid movement under a triangular sheet with (a) 3 sutures and (b) 1 suture. Suture positions (grey boxes) are superimposed on the images. With 3 sutures, the flow was away from the limbus but with 1 suture it was to the sides.

3.4 Discussion

3.4.1 Comparison between scaling analysis and physical model

The scaling analysis showed that the displacement generated by fluid flow scaled as $\frac{H}{T} \sim \left(\frac{Q\mu L^4}{ET^7}\right)^{\frac{1}{4}}$ when the elastic sheet was bending and $\frac{H}{T} \sim \left(\frac{Q\mu L^4}{ET^7}\right)^{\frac{1}{6}}$ when it was stretching, which was the same as that of the Ahmed Glaucoma Valve in our previous study (Appendix A). We were able to confirm this non-linear, valvular relationship (Oosterbroek et al., 1998) between scleral flap displacement and flow rate with our experimental findings. Stay et al. (2005) reported that pressure scaled as $P \sim Q^{\frac{1}{4}}$ with Ahmed Glaucoma Valves. From our theoretical calculations, we also expected the trabeculectomy scleral flap to have the same dependence, with $\frac{P}{E} \sim \left(\frac{Q\mu}{EL^3}\right)^{\frac{1}{4}} \left(\frac{T}{L}\right)^{\frac{9}{4}}$ in the bending state and

$\frac{P}{E} \sim \left(\frac{Q\mu}{EL^3}\right)^{\frac{1}{6}} \left(\frac{T}{L}\right)^{\frac{17}{6}}$ in the stretching state. However, we could not confirm this relationship due to the poor correlation between the calculations and the experimental data, and believe this to be due mainly to a weakness with our recording equipment. With the flow rates used, most of the net pressure changes were low (≤ 1 mmHg) and this was at the lower limit of sensitivity and precision of the pressure transducer. The lack of precision was especially significant as very small differences in P were expected from the experiment (between 10^{-4} and 10^{-5} [dimensionless quantities], as can be seen in Figure 3.11).

3.4.2 Pressure and fluid flow under the scleral flap

A trabeculectomy involves the creation of a guarded drainage channel in the sclera, through which aqueous humour can flow out of the eye in a controlled manner into a subconjunctival bleb, thereby reducing the IOP. In the early post-operative period, the scleral flap serves as the principal resistance to aqueous humour outflow (Birchall et al., 2006; Birchall et al., 2007; Tse et al., 2012). This makes it important as a regulator to reduce the risk of overfiltration and hypotony, and conversely it may also result in inadequate reduction in IOP. In addition, this flap may also have an important role in the posterior diversion of aqueous humour flow, which is desirable (Jones et al., 2005; Birchall et al., 2006; Dhingra et al., 2009). All these factors provided the motivation to look at pressure changes and aqueous humour flow direction afforded by this flap after the procedure.

Influence of flap thickness

As flap thickness increases, its rigidity and resistance to lifting also increases (Birchall et al., 2007). This is seen in our case, with thinner flaps there is more fluid flow below it and to the outside thus creating a larger pressure drop (50-70% lower pressures with the thinner 0.8 mm sheets). In a recent computational study, trabeculectomy surgery was modelled using finite element simulation to compare the effect of various scleral flap and sclerostomy shapes and sizes on aqueous humour outflow rate in an objective manner (Tse et al., 2012). Computations were performed based on fluid-solid interaction involving theoretical flap deformation caused by the flow of aqueous humour under it. In their comparison with 250 μm thick flaps, the authors found a marginal reduction (-4.8%) in aqueous humour outflow rate with 300 μm thick flaps but a much larger increase (+188.4%) with 200 μm thick flaps.

The results indicate that the thickness of the scleral flap created during trabeculectomy may be tailored according to the desired IOP outcome. In clinical practice, half thickness (around 250 μm) flaps are recommended (Jones et al., 2005; Stalmans, 2006; Salim, 2012). To facilitate more aqueous humour flow, thinner flaps can be created, and vice versa. However, only very small changes should be made as when scleral flap thickness gets closer to 200 μm there may not be sufficient tension to control aqueous humour flow and also a higher risk of dehiscence or cheese-wiring of the flap (Tse et al., 2012; Dhingra et al., 2009; Khaw et al., 2012).

Influence of flap shape

In the 3-suture triangle versus 2-suture rectangle and square comparison, there were statistically significant higher pressures with the triangles, by around 20-70%. The differences were not statistically significant in the 3-suture triangle versus 5-suture rectangle and square comparison. This discrepancy could be due to the 3-suture triangle flaps having more sutures and thus more resistance to flow than the 2-suture rectangle and square flaps. However, in this same configuration group, there were also statistically significant differences between the rectangle and square flaps, so the effect of sutures cannot completely account for the results. We believe that triangular flaps of the same width and length result in lower pressure drops than rectangular or square ones. This is due to the smaller surface area of the triangular flap, being half of that of a rectangle or square with similar dimensions. Although not statistically significant, the rectangles in our experiment also had lower pressure drops compared to squares, a difference likely to be due to the smaller surface area (108 cm² versus 144 cm²).

Our pressure findings support the findings reported by Tse et al. which showed that triangular flaps led to lower aqueous humour outflow rates and higher pressures when compared to square ones. For example, the rate for a 4 mm × 4 mm triangle flap was 57.6% lower than that of a 4 mm × 4 mm square flap. They also found that smaller scleral flaps result in lower aqueous humour outflow rates. For example, the rate for a 3 mm × 2 mm rectangle flap was 32.7% lower than that of a 4 mm × 4 mm square flap. Interestingly, when they compared a 4 mm × 4 mm square flap with a 5.65 mm × 5.65 mm triangle flap which had the same surface area, the aqueous humour outflow rate was 26.6% lower with the triangle flap. However, the triangles in their study all had 3 sutures compared to 2

sutures for the squares and rectangles, the difference which could explain the lower flow rates with the triangles. This effect of sutures will be discussed in the next section.

The evidence points to that if larger reductions in IOP are needed, then the scleral flap should be made square or larger. However, this effect does not seem to be reflected in clinical findings. In a study to compare a triangular flap in one eye versus a square-shaped one in the other eye of the same patient, there was no long-term difference in the post-operative IOP and complication rates (Kimbrough, Stewart, Decker, & Praeger, 1982). Another study comparing triangular and square scleral flaps found that there was a pressure difference (2.5 mmHg lower for triangular flaps) for the first two post-operative days although this difference became non-significant after that. Additionally, in this study the triangular flaps only had one suture for 'high flow' of aqueous humour, compared to four sutures for the square flaps for 'low flow' conditions (Batterbury & Wishart, 1993). The exact dimensions of the flaps could not be ascertained in these reports for us to examine the effect of size.

Other studies considered the effect of varying the size of the scleral flap. In a laboratory study modelling trabeculectomy on cadaver eyes with real time monitoring of the IOP, there was no significant effect of changing flap sizes from 4 mm × 4 mm to 3 mm × 2 mm on the eventual IOP (Birchall et al., 2007). Two clinical studies showed no clear advantage or disadvantage of 4 mm × 4 mm scleral flaps compared to 2 mm × 2 mm ones (Starita, Fellman, Spaeth, & Poryzees, 1984; Vernon et al., 1998). However, there are potential advantages of smaller flaps, there being a larger area of undisturbed tissue (which might be important in reducing overall bleb scarring or if repeat surgery is required) and a reduced astigmatic effect on the cornea (Vernon et al., 1998; Vernon, Zambarakji, Potgieter, Evans, & Chell, 1999).

We found that the direction of flow was influenced less by shape but more by the number and position of sutures, which will be discussed in the next section. With different shapes, the small difference between them could be due to the similarity in their width:length aspect ratios, which in our experiment were 1.33 for rectangles, 1.00 for squares and 1.15 for triangles. In a previous computational and experimental study by our group (unpublished data), we found that the width:length aspect ratio of a scleral flap was important in determining the direction of aqueous humour flow. Changing the shape of the flap from a square (aspect ratio 1.0) to wide rectangle (aspect ratio 2.5) would increase the fraction of fluid moving posteriorly by a factor of 6. Additionally, with width:length aspect ratios of < 2 , triangular flaps created more posterior flow. When this aspect ratio increased to > 2 , the effect was reversed. However, as far as we know, there have not been any clinical studies to compare these theoretical and experimental results with.

Influence of suture numbers and positions

Our results show that the pressure drop becomes smaller when more sutures are inserted. With more sutures, there is more resistance under the scleral flap, leading to less aqueous humour escape through the flap gap and thus a higher pressure is maintained. Careful control of the pressure drop is important, especially to avoid hypotony after trabeculectomy. In certain cases such as in inflammatory glaucoma where there may be postoperative ciliary body shutdown and increased uveoscleral outflow (Rahman et al., 2000; Schubert, 1996; Toris et al., 1987), the number of sutures may need to be increased to allow for the higher risk of hypotony.

We were unable to determine flow direction with the 5-suture configuration as the fluid accumulated under the well-constrained sheets. With 4 sutures, the flow was directed

more posteriorly while with 2 sutures the flow was directed more to the sides. In the triangle group, this pattern was also seen with 3 sutures and 1 suture respectively. The direction of flow naturally avoids the suture positions due to the higher resistance encountered. In the case of 2 sutures (for rectangles and squares) or 1 suture (for triangles), it is also affected by the distance to the closest edge of the sheet. A larger portion of fluid flows to the sides as they are closer to the sclerostomy as compared to the opposite edge.

From our results, we support the intra-operative use of an anterior chamber infusion via a paracentesis to titrate flow during scleral flap closure (Jones et al., 2005; Dhingra et al., 2009; Khaw et al., 2012). The number and position of sutures can be varied by observing fluid flow, of which amount and direction can be a good estimate of the post-operative outcome. However, it is also important to note that if there is too little flow underneath the scleral flap, such as when having too many sutures, there might be increased scarring and resistance underneath it and this will lead to even less aqueous humour outflow and high IOP (Haynes & Alward, 1999; Bettin, 2012). A good strategy around this is to use adjustable or releasable sutures to titrate pressure postoperatively (Wells et al., 2004; Jones et al., 2005; de Barros et al., 2008; Kobayashi et al., 2011). With this strategy, a slightly higher initial post-operative IOP is still acceptable as this can be lowered by adjusting or removing sutures a few days to a few weeks after the initial surgery.

There was a number of limitations in our experiment. Suture tension can be an influential factor in determining pressure and direction of flow (Wells et al., 2004; Birchall & Wells, 2008). However, in clinical practice the exact amounts of tension applied are variable among surgeons, and indeed many surgeons put in adjustable or releasable sutures. We therefore did not look into this effect and designed our experiment such that there was

standardised and adequate but not tight suture tension at the edges of the scleral flap in our model. The effect of the sclerostomy size was also not considered. Tse et al. (2012) looked into this and reported that smaller sclerostomy surface areas, and thus larger flap-to-sclerostomy surface area ratios increased aqueous humour outflow rate.

Additionally, our experimental setup also did not include a fluid capacitor, as used in flow experiments with actual glaucoma drainage devices on their own i.e. not mounted into eyes (Eisenberg et al., 1999; Lim, Wells, & Khaw, 2002). In retrospect, compliance provided by this capacitor could eliminate the initial spike in pressure before the valve opened (Figure 3.6). However, we do not think we were significantly disadvantaged as we were looking at the subsequent steady state equilibrium pressures and not valve opening or closing pressures (Gilbert & Bond, 2007). Finally, we also acknowledge that in the actual procedure, numerous other variables come into play, especially in the longer term e.g. wound healing and scarring under the conjunctival bleb (Azura-Blanco & Katz, 1998; Khaw et al., 2001). As such, our study only provides information on the early post-operative control of IOP and aqueous humour flow.

3.5 Conclusion

The scaling analysis and experimental data show that the trabeculectomy scleral flap has a valve-like, non-linear dependence of displacement as a function of flow rate. The dependence of pressure as a function of flow rate could not be determined. Flap thickness, shape and the number and position of sutures can affect pressure and aqueous humour flow under the scleral flap. Thinner and larger scleral flaps, as well as lower number of sutures provide higher pressure drops, with the effect of the sutures being clinically more significant. Similarly, flow direction is affected mainly by suture number and position, aqueous humour moves away from areas of the flap under tension from the sutures and more towards the nearest free edge of the flap. Posterior flow of aqueous humour is promoted by placing sutures along the sides while leaving the posterior edge free.

Chapter 4

4 The effect of scleral flap shapes, suture numbers and aqueous humour protein content and viscosity on equilibrium pressure under the trabeculectomy scleral flap in a porcine model

4.1 Introduction

This experiment was designed to compare and validate the equilibrium pressure findings from our physical model in Chapter 3 to that of a porcine scleral flap model. A trabeculectomy scleral flap is created on mounted porcine sclera and the resulting equilibrium pressures with different scleral flap shapes and suture numbers are measured. Porcine eyes have been used as trabeculectomy and non-penetrating glaucoma surgery models, and in other glaucoma-related experiments such as to assess uveoscleral outflow and to investigate the change in IOP during LASIK surgery (Jacobi, Dietlein, Colling, & Krieglstein, 2000; Lee, Chiang, & Shah, 2006; Shaarawy, Wu, Mermoud, Flammer, & Haefliger, 2004; Xu, Yao, Wu, Li, & Ye, 2010; Wagner, Edwards, & Schuman, 2004; Hernandez-Verdejo, Teus, Roman, & Bolivar, 2007). This is in view of their low cost, easy availability and the fact that their size and volume, particularly of the anterior chamber (0.3 ml), are closer to the human than any other species reported (Sanchez, Martin, Ussa, & Fernandez-Bueno, 2011). The sclera is $2 \times$ thicker than human sclera but both have similar histology and collagen bundle arrangement (Nicoli et al., 2009). The particular model that we employed was based on that of the AGFID project team (2001) which used porcine

corneoscleral buttons mounted on an artificial anterior chamber to assess fluid leakage and pressure control after making stab incisions through the sclera.

Additionally, we also used this model to look at the influence of aqueous humour protein content and viscosity on equilibrium pressures under the scleral flap, to see if higher IOP could be expected soon after trabeculectomies for example in eyes affected by secondary glaucoma due to inflammation (Panek, Holland, Lee, & Christensen, 1990; Herbert, Viswanathan, Jackson, & Lightman, 2004; Siddique, Suelves, Baheti, & Foster, 2013). Changes in aqueous humour protein content may occur in inflammation, due to the breakdown of the blood-aqueous barrier, leading to increased levels of albumin, globulin and fibrinogen. In normal aqueous humour the protein content is around 10-20 mg/ 100 ml, and in cases of uveitis this can increase to 1000-2000 mg/ 100 ml (Krause & Raunio, 1969; Krause & Raunio, 1970; Tripathi, Millard, & Tripathi, 1989). For comparison, the protein content of plasma is 6000-7000 mg/ 100 ml (Gornall, Bardawill, & David, 1949). Previous studies have reported that increased aqueous humour protein content and its subsequent aggregation and precipitation can increase the resistance of the trabecular meshwork and reduce outflow facility (Epstein, Hashimoto, & Grant, 1978; Johnson et al., 1986; Ladas et al., 2001). As such, we can see how this is a possible mechanism of raised IOP and glaucoma.

Another potential determinant of outflow facility is aqueous humour viscosity or its resistance to flow, which is increased by higher protein contents. Viscosity is a measure of the friction between layers in a fluid which are travelling at different velocities, with velocity being highest in the centre and lowest in the periphery. With higher viscosity, more stress i.e. pressure is needed to overcome this friction to maintain movement of the fluid with the same velocity pattern. Although there have been reports of aqueous humour

viscosity not changing significantly in the presence of excess protein in inflammation (McEwen, 1958) or in POAG (Vass et al., 2004), one study found that it affected outflow facility in cadaveric eyes more than expected when measured differences between infusion fluids were analysed (Epstein et al., 1978). The authors reported that diluted serum had less viscosity than undiluted, but interfered with outflow facility more than anticipated on the basis of viscosity alone. They concluded that serum proteins interfere with outflow in a more complex way than through abnormal viscosity alone. As far as we know, there are no repeat or similar studies that have been subsequently reported.

When there is a breakdown of the blood-aqueous barrier, the trabecular meshwork may also be blocked by inflammatory cells. As the trabecular meshwork pore size goes down to $< 15 \mu\text{m}$ in diameter (Bill & Svedbergh, 1972), $10 \mu\text{m}$ diameter red blood cells and $10\text{-}20 \mu\text{m}$ diameter white blood cells (Young, Lowe, Stevens, & Heath, 2006) may cause blockage and a reduction in aqueous humour outflow. However, in a clinical study by Ladas et al. (2001), there was no correlation between outflow facility as determined by Schiotz tonography and the amount of anterior chamber cells as determined by slit-lamp microscopy. The authors did however find a correlation between outflow facility and aqueous humour protein levels inferred from laser flare photometry. They suggested that the effect of cells on aqueous humour outflow facility was smaller than the effect of its protein content.

4.2 Methods

Eyes from 6-12 month old mixed breed pigs were used. Whole pig heads were obtained from an abattoir and the eyes enucleated and used within 36 hours of slaughter (Johnson, 2005). The eyes were discarded if they had any discernible damage on them. These eyes were sectioned horizontally and the iris, lens, vitreous and choroid removed (Figure 4.1). The scleral segments were then cut into 18 mm diameter asymmetrical discs, to include a small section of limbus and cornea. These discs were then mounted on a Barron artificial anterior chamber, normally used in corneal transplant surgery (Katena Products, Inc., NJ, USA) [Figure 4.2]. Room temperature was maintained around 21 °C.

One inlet port of the artificial anterior chamber was attached to the infusion pump (Cole-Parmer, IL, USA) and pressure transducer (model 162PC01D, 8V excitation; Honeywell International, NJ, USA). This pressure transducer was connected to an interface board/ voltmeter (model VM110; Velleman NV, Gavere, Belgium) and personal computer (PC) [Figure 4.3]. The other inlet port of the artificial anterior chamber was closed. Non-expansile, low compliance silicone tubing (outer diameter 6 mm, internal diameter 3 mm) was used throughout the system. The working fluid used to mimic aqueous humour was Balanced Salt Solution (BSS; Alcon Laboratories, Inc., Texas, USA) unless stated otherwise. BSS is used in ophthalmic surgery for irrigation and to replace aqueous humour (Edelhauser & Macrae, 1995). It has similar pH, osmolality and concentrations of sodium, potassium, calcium, magnesium and chloride to aqueous humour.



Figure 4.1 Enucleated porcine eye before sectioning (left), after sectioning and removal of iris, lens, vitreous and choroid (right).



Figure 4.2 Barron artificial anterior chamber used to mount corneoscleral segments.

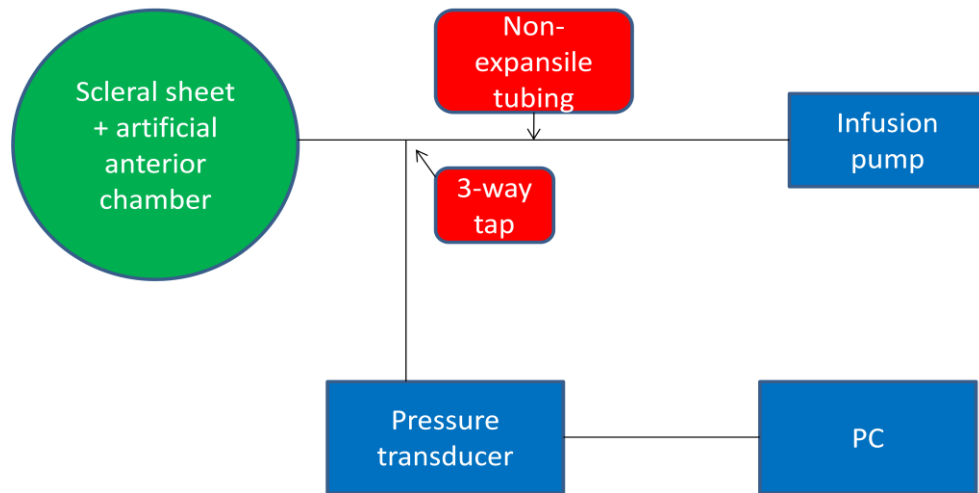


Figure 4.3 Experimental setup. The artificial anterior chamber was connected to the infusion pump and pressure transducer using non-expansile tubing and a 3-way tap.

Before the actual experiment, we calibrated the pressure transducer (see Chapter 3) and measured the resistance of the Barron artificial anterior chamber and silicone tubing. This was done by infusing BSS at 50, 100, 200, 300 and 400 ml/h through the system with the two tissue pedestal openings open to the atmosphere. The tissue pedestal openings and the pressure transducer inlet port were positioned at the same level. The resistance was determined from the slope of the pressure vs. flow rate line. Compliance of the silicone tubing was also measured. We infused 10, 20, 30 and 40 μ l of BSS into the system with the pinch clamps closed and measured the resulting pressure changes. The compliance was derived from the slope of the volume infused vs. pressure line.

At the start of each experimental run, the infusion rate was set at 3 μ l/min (0.18 ml/h) to mimic normal aqueous humour production rate. When the pressure was around 20 mmHg, a scleral flap was fashioned on the mounted sclera (Figure 4.4). A 250 μ m Accurate Depth blade (BD, NJ, USA) was used to outline either 4 mm x 3 mm rectangles, 4 mm x 4 mm squares or 4 mm x 4 mm triangles (Figure 4.5). A crescent knife was then used to

dissect below the flap up to the limbus. This flap was then reflected and a stab incision with an MVR blade performed at the limbus. After this step, a 0.75 mm in diameter sclerostomy was performed with a Kelly Descemet's membrane punch. Any remaining air in the anterior chamber was removed through the sclerostomy by a gentle bolus of BSS. The flap was then repositioned and sutured down with 2 10/0 nylon sutures. In Chapter 3, we found that sutures played the most important role in determining pressure, so an equal number of sutures for all 3 shapes was chosen to prevent spurious results due to discrepancy in suture numbers. For the rectangular and square flaps, the sutures were positioned at the 2 far corners while for the triangular flaps these were midway along the 2 free edges. The sutures were tied to achieve adequate tightness while avoiding creasing or stretching of the scleral flap. Time was then reset to zero and the equilibrium pressure in the chamber recorded. This was defined as a steady pressure with fluctuations within 0.5 mmHg of each other for > 5 minutes (Figure 4.6). The tracing was expected to typify the rise in IOP after the scleral flap was sutured in a trabeculectomy.

For the comparison between different fluids, to standardise the shape we only used 4 mm wide x 3 mm long rectangular scleral flaps. However, these rectangular flaps had either 4 or 2 sutures each (Figure 4.5) and the groups were compared separately.

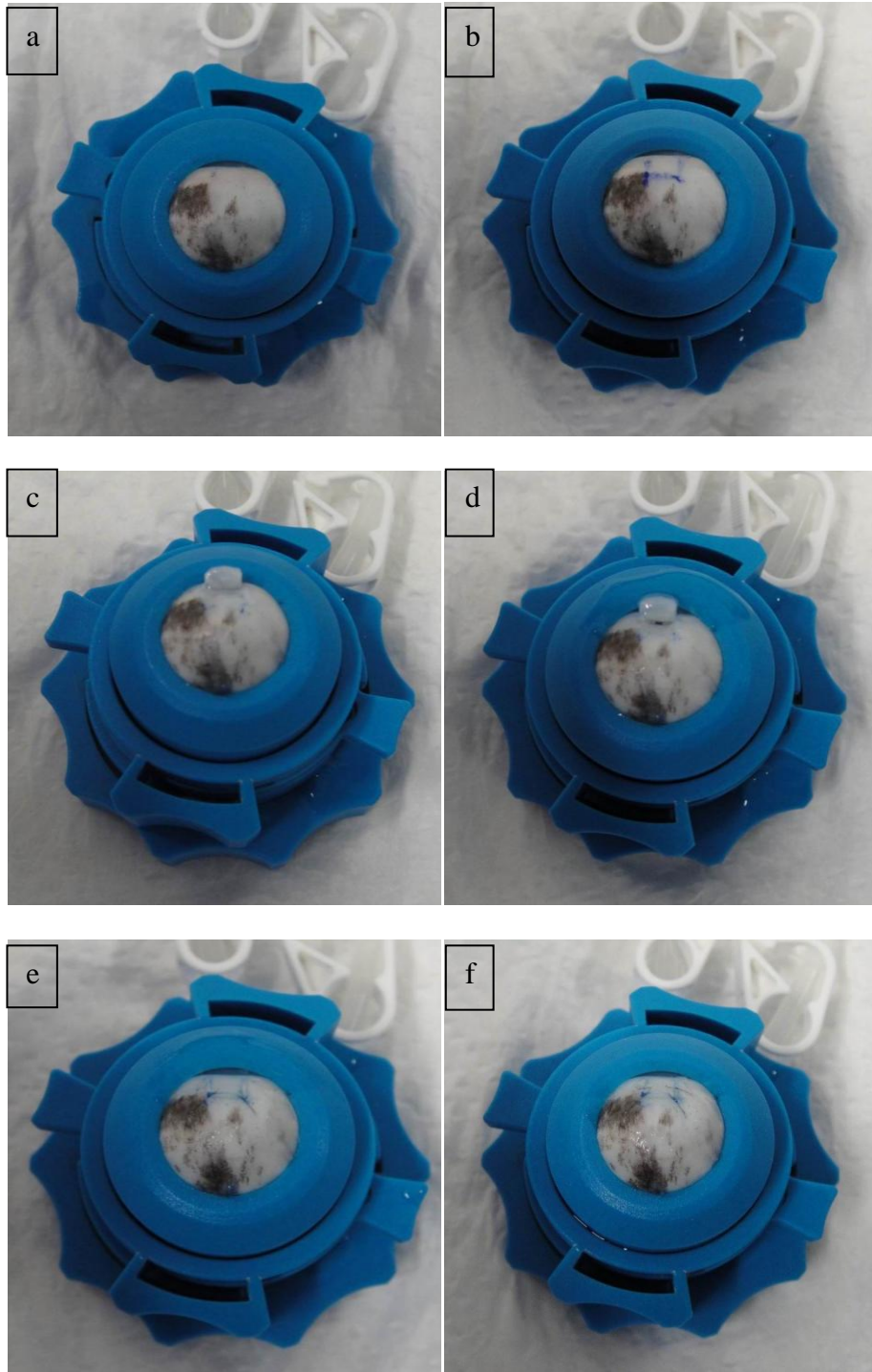


Figure 4.4 a) Porcine eye mounted on artificial anterior chamber, b) scleral flap margin demarcated, c) scleral flap created and reflected, d) after sclerostomy, e) after resuturing (2 sutures), f) after resuturing (4 sutures).

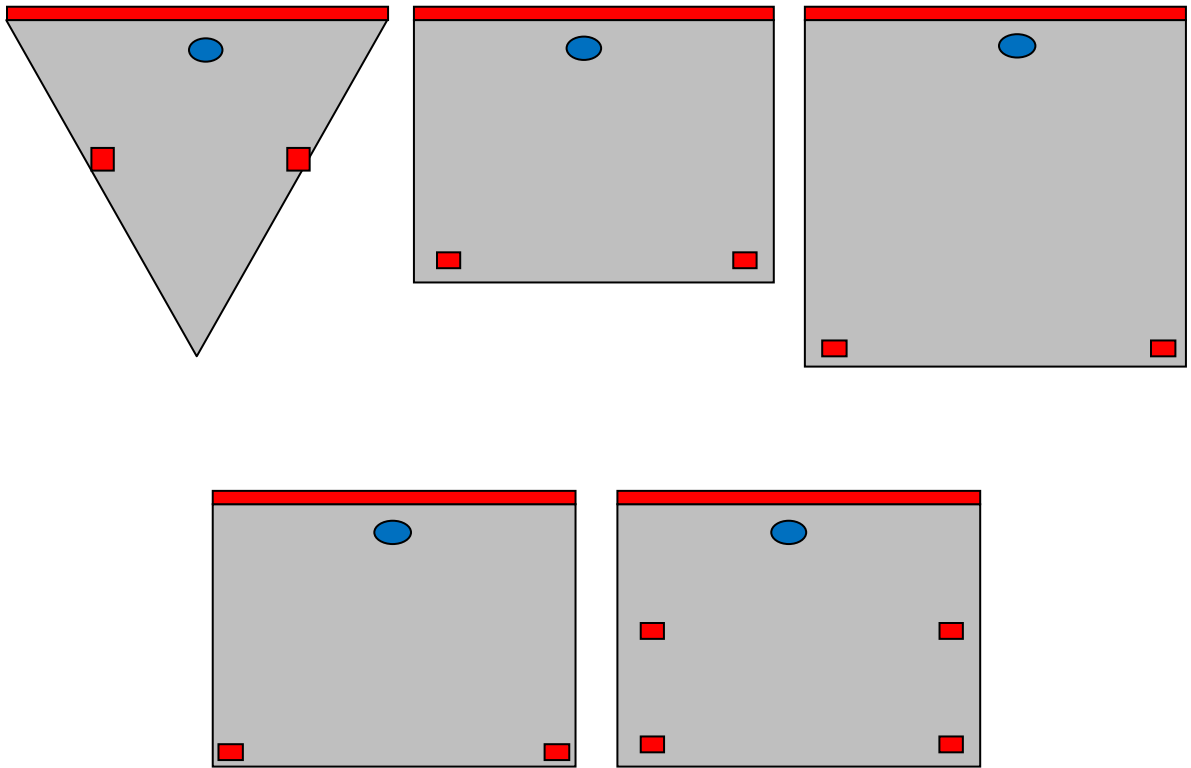


Figure 4.5 Configurations of scleral flaps and sutures. Top row shows 2 sutures each in the comparison between different scleral flap shapes. Bottom row shows rectangles with 2 and 4 sutures each, used in the comparison between different fluids.

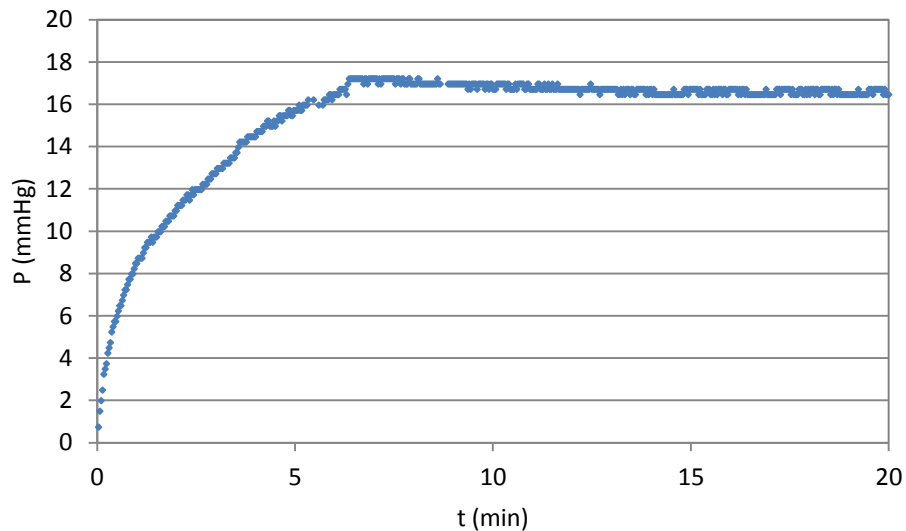


Figure 4.6 Typical pressure curve after resuturing the scleral flap, showing equilibrium as fluid flows out under the scleral flap. Due to compliance of the sclera and chamber space, there was no spike in the increase in pressure.

We used three different infusion fluids in this part of the experiment. The first was plain BSS as a control, the second was albumin in BSS in a concentration of 300 mg/ 100 ml to model a moderate amount of abnormal aqueous humour protein (Shah, Spalton, & Taylor, 1992). For this, 1 ml of 30% Bovine Serum Albumin (BSA) was added to 99 ml of BSS. The third solution contained albumin in BSS at a concentration of 3000 mg/ 100 ml to simulate a maximal amount of abnormal aqueous humour protein (Krause et al., 1970). For this, 10 ml of 30% Bovine Serum Albumin (BSA) was added to 90 ml of BSS. We chose albumin as the source of protein because it constitutes the majority (55% by mass fraction) of aqueous humour protein (Krause et al., 1969; Shah et al., 1992).

The viscosities of these fluids were measured with a U-tube viscometer (size A; VWR International Limited, UK). This was to enable us to directly compare our viscosity results with those of Epstein et al. (1978). The following steps were taken according to the manufacturer's guidelines and that in the European Pharmacopoeia 5.0 (European

Directorate for the Quality of Medicines, 2005a). The viscometer was partially immersed and kept upright in a water bath at 21 °C. 12 ml of the fluid to be tested was pipetted into the viscometer and left for 30 minutes for temperature equilibration. Suction was applied to the other limb to raise the fluid level beyond the upper mark, and then released. The time required for the level of the fluid to drop from the upper mark to the lower one was measured with a digital stopwatch to the nearest tenth of a second. 5 readings were taken for each fluid and compared to that of distilled water, to get the relative viscosity. The viscometer was rinsed with distilled water and acetone before drying in air between fluids.

In all groups, n = 8. Statistical analysis was performed using Prism 4 software (GraphPad Software, Inc., CA, USA). The unpaired t-test was used when comparing 2 groups while one-way ANOVA with Bonferroni's multiple comparison post-test was used when comparing 3 groups. $P < 0.05$ was considered statistically significant.

4.3 Results

The resistance of the Barron artificial anterior chamber and silicone tubing was 0.0002 mmHg/ μ l/min and this was taken into consideration when calculating the actual pressure. The compliance of the silicone tubing was 1.60 μ l/mmHg. The relative viscosities of the various working fluids (compared to distilled water at 21 °C) were 1.02 +/- 0.002 (mean +/- SD) for plain BSS, 1.04 +/- 0.001 for albumin in BSS (300 mg/ 100 ml) and 1.12 +/- 0.001 for albumin in BSS (3000 mg/ 100 ml) [p < 0.001].

As our model here is still quite dissimilar from an actual eye (e.g. not having the same ocular compliance in the absence of the majority of the sclera and cornea, and other eye structures such as the iris and trabecular meshwork), the pressure readings may not correlate exactly with actual IOP. Instead this model gives an indication of the relative difference in IOP. The advantage of this model is that we are able to isolate the effect of the variables solely on the scleral flap.

In the following bar charts, error bars indicate 1 SD and * indicates a statistically significant difference. When comparing the different shapes (Figure 4.7), the mean for triangles was 19.6 +/- 7.3 mmHg, for rectangles was 18.7 +/- 5.1 mmHg and for squares was 16.5 +/- 5.3 mmHg. The differences between them were not statistically significant (p = 0.755).

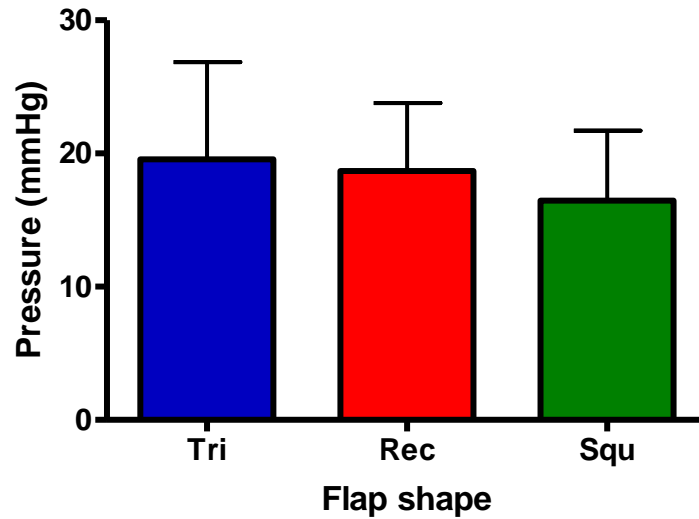


Figure 4.7 Comparison between different shapes, using BSS as the working fluid. There was no statistically significant difference between the shapes.

When comparing the different fluids, in the 4 suture group (Figure 4.8), the mean equilibrium pressure with plain BSS was 31.9 +/- 5.0 mmHg, for albumin in BSS (300 mg/ 100 ml) was 31.6 +/- 5.5 mmHg and for albumin in BSS (3000 mg/ 100 ml) was 33.1 +/- 6.2 mmHg. There was no statistically significant difference between the fluids ($p = 0.859$). In the 2 suture group (Figure 4.9), the mean equilibrium pressure with plain BSS was 18.7 +/- 5.1 mmHg, for albumin in BSS (300 mg/ 100 ml) was 19.4 +/- 5.0 mmHg and for albumin in BSS (3000 mg/ 100 ml) was 20.4 +/- 4.7 mmHg. Again, there was no statistically significant difference between the fluids ($p = 0.841$).

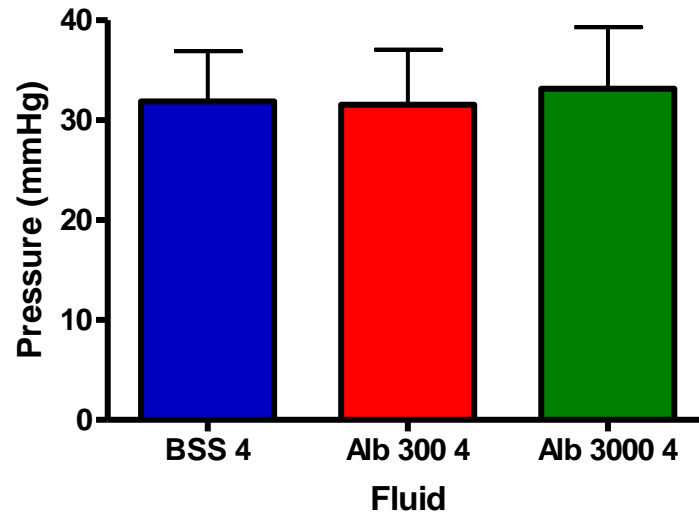


Figure 4.8 Comparison between fluids in the 4-suture group. There was no statistically significant difference between the fluids.

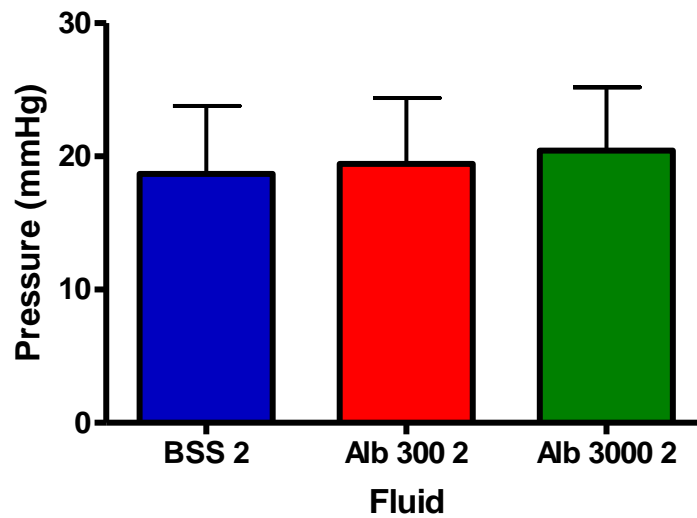


Figure 4.9 Comparison between fluids in the 2-suture group. There was no statistically significant difference between the fluids.

When comparing the same fluid with 4 or 2 sutures (Figure 4.10), all groups showed statistically significant differences. In the BSS group, 4 sutures yielded 31.9 +/- 5.0 mmHg while 2 sutures yielded 18.7 +/- 5.1 (p = 0.002). In the albumin in BSS (300 mg/ 100 ml) group, 4 sutures yielded 31.6 +/- 5.5 mmHg while 2 sutures yielded 19.4 +/- 5.0 mmHg (p < 0.001). Finally, in the albumin in BSS (3000 mg/ 100 ml) group, 4 sutures yielded 33.1 +/- 6.2 mmHg while 2 sutures yielded 20.4 +/- 4.7 mmHg (p = 0.002).

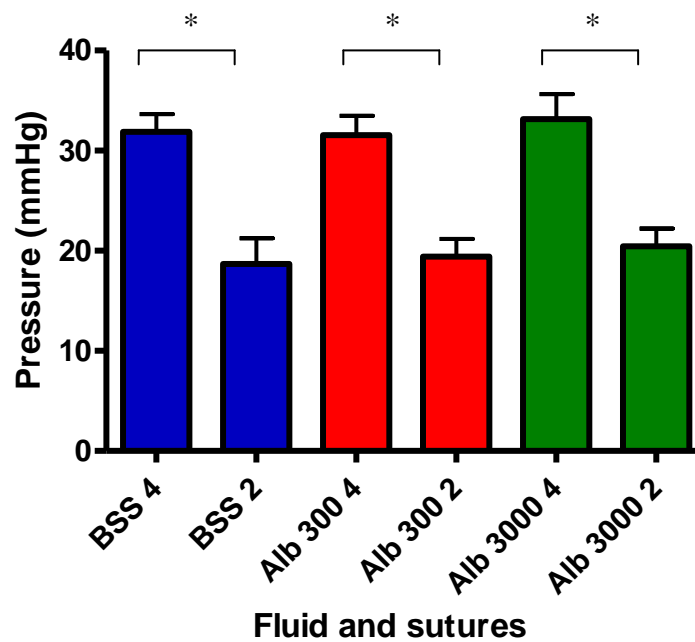


Figure 4.10 Comparisons between same fluids with 4 or 2 sutures. When considering the same fluid, 4 sutures always maintained higher pressures.

4.4 Discussion

In this experiment, we looked at the influence of scleral flap shapes and suture numbers on equilibrium pressure under the scleral flap in trabeculectomies. This was to enable a comparison with some findings from our physical model experiment in Chapter 3. As this porcine scleral flap model more closely resembles an actual eye as compared to the previous physical model, we also employed it to look at the influence of aqueous humour protein content and viscosity, which may increase in anterior chamber inflammation.

In contrast to our findings in Chapter 3 and that of Tse et al. (2012), with this porcine model we found no differences in equilibrium pressures with the different shaped scleral flaps. This finding is in keeping with the clinical findings reported by Kimbrough et al. (1982) and Batterbury et al. (1993) as discussed in Chapter 3. There was also no statistically significant difference between the different sizes and surface areas. In this study, the surface areas of our porcine flaps were 8 mm² (triangle), 12 mm² (rectangle) and 16 mm² (square). Birchall et al. (2007) found no difference in IOP between 16 mm² and 6 mm² flaps made in enucleated human eyes. Starita et al. (1984) and Vernon et al. (1998) found no difference between 16 mm² flaps and 4 mm² microtrabeculectomy flaps in actual patients.

The discrepancy between physical/ computational models and actual eye tissue could be due to factors such as ocular rigidity or compliance (Pallikaris, Dastiridou, Tsilimbaris, Karyotakis, & Ginis, 2010) and sclerocorneal elasticity (Johnson et al., 2007). These are measures of tissue distensibility and indicate how much volume can be introduced before a change in pressure occurs. With the porcine sclera and artificial anterior chamber in place, there is more compliance in the system which results in less change in

pressure with change in volume. As such, statistically significant differences with the physical model might not translate similarly in the porcine model.

Additionally, surface tension of aqueous humour may affect trabecular outflow, such as with the vacuolation of aqueous humour into Schlemm's canal (Ross, Blake, & Ayyala, 2010). In a liquid, attractive forces exist between the molecules. The majority of molecules are surrounded by other molecules and there is no net force acting on each of them. Molecules on the surface, however, are pulled inwards with little or no opposite force. The surface layer thus acts as a tense membrane resisting external force. The surface tension of glycerine is 63 mN/m at 20 °C (National Physical Laboratory, 2013), lower than that of BSS which is 71 mN/m (Ross et al., 2010); this difference in character between the fluids could also affect flap function and pressures between our models. In summary, there is a more complex interaction between the actual eye tissue, 'aqueous humour' and sutures in the porcine model which most likely explains the differences between it and the physical model.

In this porcine model, when comparing the number of sutures, equilibrium pressures with 4 sutures were around 40% higher than with 2 sutures. This is because of the increased resistance of the scleral flap, needing a higher pressure for aqueous humour to lift and open it. This supports our finding in Chapter 3 and strengthens our belief that sutures play the most important role in determining pressure outcomes after trabeculectomy.

We found no differences in equilibrium pressures between the different fluids, in both the 4-suture and 2-suture groups. Although they did not perform trabeculectomies, we compare our results with that of Epstein et al. (1978) which showed significant reduction (36-42%) in outflow facility in enucleated human eyes when using diluted human serum as the infusion fluid. The obvious difference between our model and theirs is they used whole

eyes with intact trabecular meshwork. As juxtacanalicular trabecular meshwork pore size goes down to $< 15 \mu\text{m}$ in diameter (Bill et al., 1972), these structures are more likely to be blocked by precipitation of excess protein, as compared to the larger sclerostomy and space under the scleral flap, especially in the initial period before fibrosis and wound healing develop.

In their study, Epstein et al. obtained relative viscosities of 1.12 for diluted 25% human serum, 1.29 for diluted 50% human serum and 1.70 for whole human serum, while we obtained values of 1.02 for BSS, 1.04 for albumin in BSS (300 mg/ 100 ml) [which is expected to be approximately equivalent to diluted 5% human serum] and 1.12 for albumin in BSS (3000 mg/ 100 ml) [approximately equivalent to diluted 50% human serum]. The relative viscosity values for Epstein et al.'s whole human serum and our BSS were similar to that found in another study looking at the viscosity of normal aqueous humour (Beswick & McCulloch, 1956). The discrepancy between relative viscosity values of Epstein et al.'s diluted 50% human serum and its equivalent in our experiment may be due to differences between using serum or albumin. Knowing the relative viscosity of actual uveitic aqueous humour could help determine the better model of it, but this has not been reported. This knowledge would be helpful for future studies exploring the link between aqueous humour protein content, viscosity and subsequent pressure outcomes.

Taking into account all the evidence, it does not appear that increased aqueous humour protein levels and viscosities affect the control of pressure by the scleral flap in the initial stages after trabeculectomy before wound healing has developed. However, their effect in the long term, or on the trabeculectomy procedure in a whole eye is still inconclusive and further studies in this area are indicated.

We would like to discuss some features of this model. We were unable to assess the effect of scleral flap thickness, due to the technical difficulty in ensuring a precise and consistent flap thickness across the whole scleral flap. An attempt to minimise this problem was made with the usage of 250 μm Accurate Depth and crescent knives to create the flap. Perhaps one way of ensuring a consistent thickness is with the use of a femtosecond laser, as has been utilised in a previous laboratory study (Bahar, Kaiserman, Trope, & Rootman, 2007). However, at the present time, there would likely be cost and availability issues with this modality. Our model also does not incorporate the trabecular meshwork or the conjunctival bleb. Some authors have previously modelled the trabecular meshwork using in-line membrane filters with 0.2 μm and 1.0 μm pores, which are similar to the smallest pores of the juxtacanalicular trabecular meshwork (Johnson et al., 1986). However, we did not include this in our setup as we wanted to isolate the flow through the trabeculectomy; interaction between the infusion fluid and membrane filter could add to another source of variable resistance, which would affect our pressure findings. The conjunctival bleb is thought to form the main resistance to aqueous humour outflow a few weeks after surgery (Azulara-Blanco et al., 1998; Khaw et al., 2001). However, fibrosis and wound healing below the bleb are difficult to predict and model accurately (Tse et al., 2012) so we also left this feature absent. As such, our model is more suitable for examining the results of intervention in the early post-operative stage, when the subconjunctival space is not yet the main barrier to flow.

Our experimental setup here did not include a fluid capacitor, as discussed in the preceding chapter. We think this additional component was superfluous as there was sufficient compliance in the system and we were measuring equilibrium values for pressure, and not valve opening pressures when any surges in pressure can affect

measurements (Gilbert et al., 2007). As seen in Figure 4.6, there was no spike in the pressure curves we obtained. Finally, the effect of anterior chamber inflammation on the aqueous outflow channels may be masked by associated hyosecretion of aqueous humour (Sen et al., 2012; Toris et al., 1987) and the IOP may vary depending on the predominance of outflow obstruction or hyosecretion. Aqueous humour production may also be similarly affected by the surgery itself (Schubert, 1996). These make it difficult to predict the outcome after trabeculectomy surgery. With our model, we set the aqueous humour ‘production’ rate constant at 3 $\mu\text{l}/\text{min}$. We predict that the pressure differences when using lower flow rates would be even smaller.

4.5 Conclusion

Equilibrium pressures under the scleral flap are affected by the number of sutures but not by typical scleral flap shapes and sizes. Differences between the physical and actual eye tissue models are due to a more complex interaction between the scleral flap, aqueous humour and sutures. The control of pressure by the scleral flap in the initial stage after trabeculectomy is not affected by the different aqueous humour protein contents and viscosities encountered in anterior chamber inflammation.

Chapter 5

5 An evaluation of fixed resistance tubes for drainage into the subconjunctival space

5.1 Introduction

In Chapter 2 (section 2.6.1), we calculated that subconjunctival space devices with permeabilities 1.5-6.0 \times more than the glaucomatous eye could provide reductions in IOP from 25-50 mmHg to 15 mmHg. Figure 5.1 shows permeability, K by dimensions of tube devices as derived from Poiseuille's Law (see Chapter 2),

$$K = \frac{1}{R} = \frac{\pi d^4}{128\mu L} \quad (5.1)$$

where R is resistance, d is internal diameter, μ is dynamic viscosity and L is device length. The black shaded area covers the range of values for our ideal device (assuming a glaucomatous eye with an outflow facility of 0.2 $\mu\text{l}/\text{min}/\text{mmHg}$). From Figure 5.1, we predict that for a fixed resistance device of around 5 mm in length, a 50-75 μm internal diameter (ID) lumen could provide the required aqueous humour flow from the anterior chamber to the subconjunctival space. However, with diameters such as these, it is conceivable that there is an increased risk of obstruction by protein or fibrin deposition post-surgery.

The pressure drop across the device itself is shown in Figure 5.2. From Poiseuille's Law,

$$P = \frac{128\mu L Q}{\pi d^4}, \quad (5.2)$$

at a flow rate, Q of 3 $\mu\text{l}/\text{min}$, a 5 mm long device with an ID of 50 μm would have a pressure drop of 12.2 mmHg. The relationship is such that if the flow rate is halved to 1.5 $\mu\text{l}/\text{min}$ then the pressure drop will also be halved to 6.1 mmHg as well. These pressure drops can also be taken as the differences between pressures in the anterior chamber and subconjunctival space ends (Acosta et al., 2006). It can be seen that if the pressure in the subconjunctival space is zero, as can be expected in the early post-operative stage before wound healing develops, then the pressure in the anterior chamber or the IOP will be the same as the pressure drop across the tube, thus hypotony is avoided.

In this chapter, we test these predictions and also compare the results with those of the ExPress P50 and P200 devices.

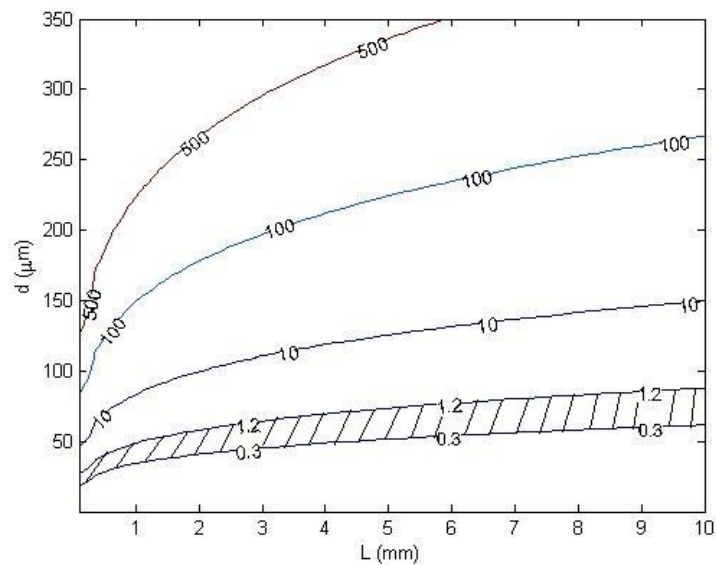


Figure 5.1 Permeability (K , in $\mu\text{l}/\text{min}/\text{mmHg}$). The black shaded area covers our desired values for an ideal device. L - length of tube, d – diameter of tube.

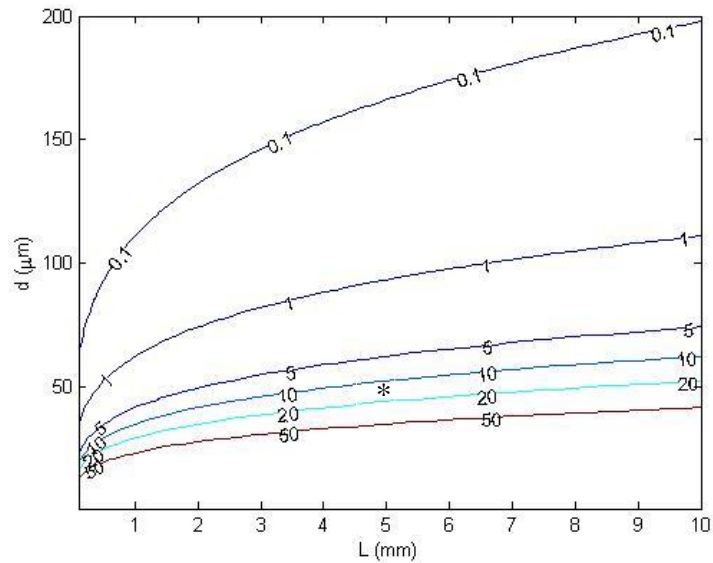


Figure 5.2 Pressure drop across a tube (in mmHg, at a flow rate of 3 $\mu\text{l}/\text{min}$). * indicates the value for a 5 mm long, 50 μm ID tube. If the flow rate is halved, the pressure drop is also halved.

For the experiments, we used 50 μm and 100 μm ID tubes bought from Cole-Parmer (IL, USA) and ExPress P50 and P200 devices (4 units each) which were provided by Alcon, Inc. (TX, USA). The 50 μm and 100 μm ID tubes were made from polytetrafluoroethylene (PTFE), a synthetic fluoropolymer of tetrafluoroethylene. We chose to use these extruded tubes as our model as they were readily available in the dimensions we wanted to test, with small tolerances in manufacture. There was limited availability in manufacturing our own tubes to the exacting dimensions and tolerances; an available alternative was to produce tubes through a manual dip-coating process, but this is associated with much higher dimensional variability in the tubes produced (Siewert et al., 2012). In the study by Siewert et al., when they used this process of dip-coating, there was between 19-42% deviation when trying to make tubes with 60-160 μm wall thicknesses. As

such, we were unable to test using other materials such as silicone which is used in current glaucoma drainage devices such as the Ahmed and Baerveldt devices.

PTFE is a high-molecular-weight compound consisting wholly of carbon and fluorine atoms covalently bonded to each other (The Merck Index, 1976). PTFE molecules at the surface also repel other molecules that come close to them. Its contact angle or measure of surface wettability/ surface tension is the lowest among polymers, including silicone, which may make it less prone to protein adsorption (Butt, Graf, & Kappl, 2006). As such, PTFE is hydrophobic, stable, non-reactive and non-toxic. Because of its chemical inertness, PTFE cannot be cross-linked like an elastomer. It has one of the lowest coefficients of friction and is used medically to make vascular stents and artificial heart valves (Sayers, Raptis, Berce, & Miller, 1998; Quintessenza, Jacobs, Chai, Morell, & Lindberg, 2010). Although the use of a PTFE tube on its own as a glaucoma drainage device has not been reported, a heat-stretched, semi-permeable membrane version of PTFE (expanded-PTFE) has been tested as a material to make subconjunctival space glaucoma drainage explants attached to silicone tubes leading into the anterior chamber (Boswell, Noecker, Mac, Snyder, & Williams, 1999; Kim, Kim, Choi, Lee, & Ahn, 2003). Although Boswell et al. found that the resulting post-implantation fibrosis in their rabbit model was thinner and more vascularised with the expanded-PTFE explants than with silicone Baerveldt devices, Kim et al. subsequently reported that the IOP control and complications seen in their human study were similar to those reported from using Ahmed, Baerveldt and Molteno implants.

We started off with material testing of the PTFE tubes. This was done to look at the Young's Modulus or stiffness of the PTFE, for a brief comparison with other materials used

to make subconjunctival space glaucoma drainage devices. Scanning electron microscopy was performed next to look at the dimensions and details of the tubes and ExPress devices. This was followed by flow studies to look at resistance of the tubes and devices. Resistance is the inverse of facility, and we looked at these values to enable a comparison with other published studies. The effect of higher protein and fibrin content in the fluid flowing through the lumens was also investigated, to see how they may affect flow and pressure. We then incorporated the tubes and devices into our porcine sclera model from Chapter 4 to test and compare their control of pressure, with and without overlying scleral flaps. Finally, we looked at the most suitable stab incision sizes for their insertion, as a measure to minimise external leakage which could lead to additional drops in pressure.

5.2 Methods

5.2.1 Material testing

Samples of the 100 μm ID PTFE tubes were subjected to uni-axial tensile testing using a H5KS materials tester (Hounsfield Test Equipment, Surrey, UK) with a 250N load cell. The 50 μm ID tubes are assumed to have the same material properties since they are made of the same material. 38 mm lengths of the 100 μm ID tube were attached to the upper and lower grips, with care taken to avoid slippage. The cross-sectional area of each tube was calculated to be 0.118 mm^2 . Force was applied at a strain rate of 1 mm/min and the elongation noted. The machine produced a force-elongation curve, and a stress-strain curve was then plotted. The Young's modulus of the PTFE material was determined from the gradient of the secant between 0 and 1% strain. At these limits, we assumed a linear stress-strain relationship for the polymer as the load applied was small.

5.2.2 Electron microscopy

Samples of the PTFE tubes and ExPress devices were imaged using a scanning electron microscope (Quanta 200F; FEI, OR, USA). We had an AqueSys glaucoma drainage device available, which we also imaged. The PTFE tubes and collagen AqueSys device were coated with an ultrathin 20nm layer of gold prior to scanning while the stainless steel ExPress tubes were uncoated. We selected the most perpendicular images to minimise parallax errors when measuring the relevant dimensions using ImageJ software (US National Institutes of Health, MA, USA). At least 6 measurements in different orientations or positions were taken for each dimension and the mean and SD obtained.

5.2.3 Flow studies

The following experiments were all performed at room temperature (20-21°C).

5.2.3.1 Fixed flow rate method

We measured the resistance of the 50 μm and 100 μm tubes by first cutting 5 mm long segments using a microtome, to avoid luminal deformation. The first 2.5 mm of these segments were then glued on the outside with cyanoacrylate glue before mounting in the lumen of 21G needles (0.51 mm inner diameter; BD, NJ, USA) [Figure 5.3]. To minimise the amount of resistance in the needles themselves, they were cut down to 5 mm in length from the hilt before the tubes were glued to them. Water-tightness was checked by injecting BSS through the mounted tubes while looking for leaks around the attachment site.

Based on the setup in Chapter 4, using a 3-way tap and non-expansile, low compliance silicone tubing, the mounted tubes were attached to a 1 ml syringe (BD, NJ, USA) on a syringe driver (Cole-Parmer, IL, USA) and a pressure transducer (162PC01D; Honeywell International, NJ, USA). This pressure transducer was connected to an interface board/ voltmeter (VM110; Velleman NV, Gavere, Belgium) and personal computer. Balanced Salt Solution (BSS) [Alcon Laboratories, Inc., TX, USA] was used with this method unless stated otherwise, and all air bubbles were removed from the system prior to the start of each run.

Prior to the actual runs, the resistance of the 21G needle itself was measured. This was done by infusing BSS at 10, 20, 30, 40 and 50 $\mu\text{l}/\text{min}$ through a needle without a tube and recording the pressure. Resistance was deduced from the slope of a pressure versus

flow rate graph. There was no discernible pressure increase with flow rates up to 50 $\mu\text{l}/\text{min}$, so we took the resistance to be negligible. In the actual runs with the tubes mounted to the needles, flow rate was increased from 0 to 35 $\mu\text{l}/\text{min}$ (50 μm tubes) or 40 $\mu\text{l}/\text{min}$ (100 μm tubes) in steps of 5-10 $\mu\text{l}/\text{min}$. Each flow rate was maintained for 5 minutes and the stabilised pressure recorded (Figure 5.4). Again, resistance was derived from the slope of the pressure against flow rate graph.

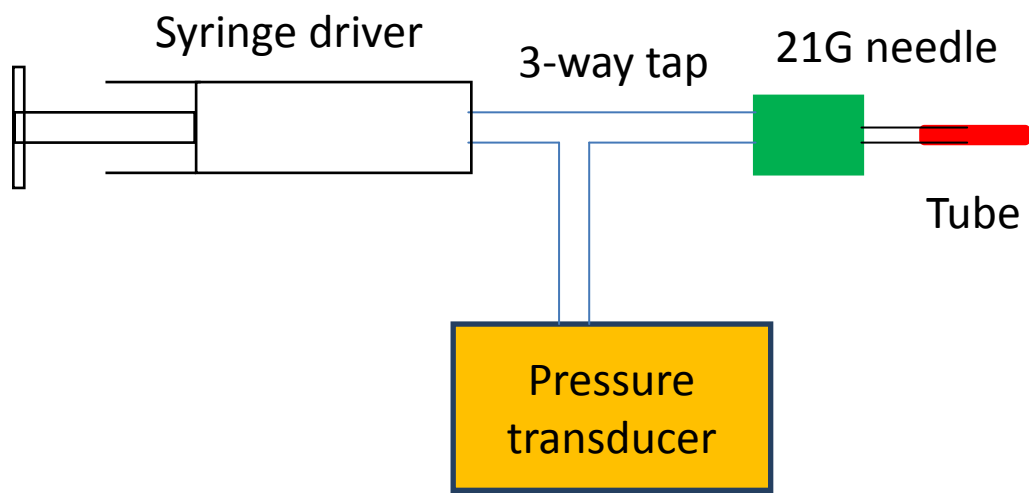


Figure 5.3 Setup for fixed flow rate method.

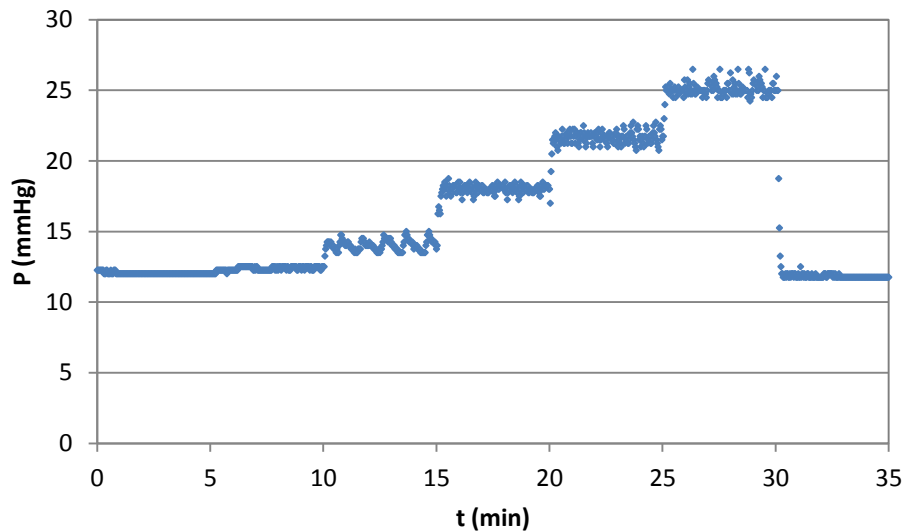


Figure 5.4 Typical steps in pressure when flow rates were increased.

5.2.3.2 Fixed pressure method

This method was used primarily to compare the resistance of ExPress devices in our study with those reported in another study (Estermann, Yuttitham, Chen, Lee, & Stamper, 2013). We also used this method to test our 50 μm and 100 μm tubes, to compare with the results with the fixed flow rate method.

Manometers or standpipes are attached to the system without a syringe driver in place, the pressure from the head of water would provide flow through the tube or device tested. The amount of fluid collected enabled calculation of flow rate and resistance values. The manometers were constructed from three 60 ml syringe barrels which were cut and glued together. For the tubes, the 21G needle mountings (from the previous section) were attached to the syringe tip at the bottom of the manometer (Figure 5.5).

As for the ExPress devices, we slightly modified the method described by Estermann et al. We implanted the devices using their pre-loaded injectors onto 0.8 mm

thick silicone sheets (HT-6240; Rogers Corporation, CT, USA). These sheets were then bound with rubber bands to a similar manometer as described before but which had the bottom end removed (Figure 5.6). In initial tests, we found that there were more incidences of leakage around the ExPress devices when using laboratory film, as used by Estermann et al.

After attaching the tubes or ExPress devices, the manometer was filled with BSS, which was then allowed to flow and flush the system for 15 minutes. Water-tightness around the ExPress devices were checked with a microscope during this time, if in doubt the devices were implanted in new silicone sheets and re-mounted to the manometer. The height of BSS was then set at 6.8, 13.6, 20.4, 27.2 and 34.0 cm (equivalent to 5, 10, 15, 20 and 25 mmHg) and the dripping fluid was collected in a beaker on a precision scale (GF-300; A&D Instruments Ltd., Abingdon, UK) over a period of 15 minutes for each level. During the test, the level of BSS in the manometer, and thus pressure was kept constant by addition from a BSS bottle and tube. From the amount of BSS collected, we derived the flow rate, which in turn enabled us to derive resistance.

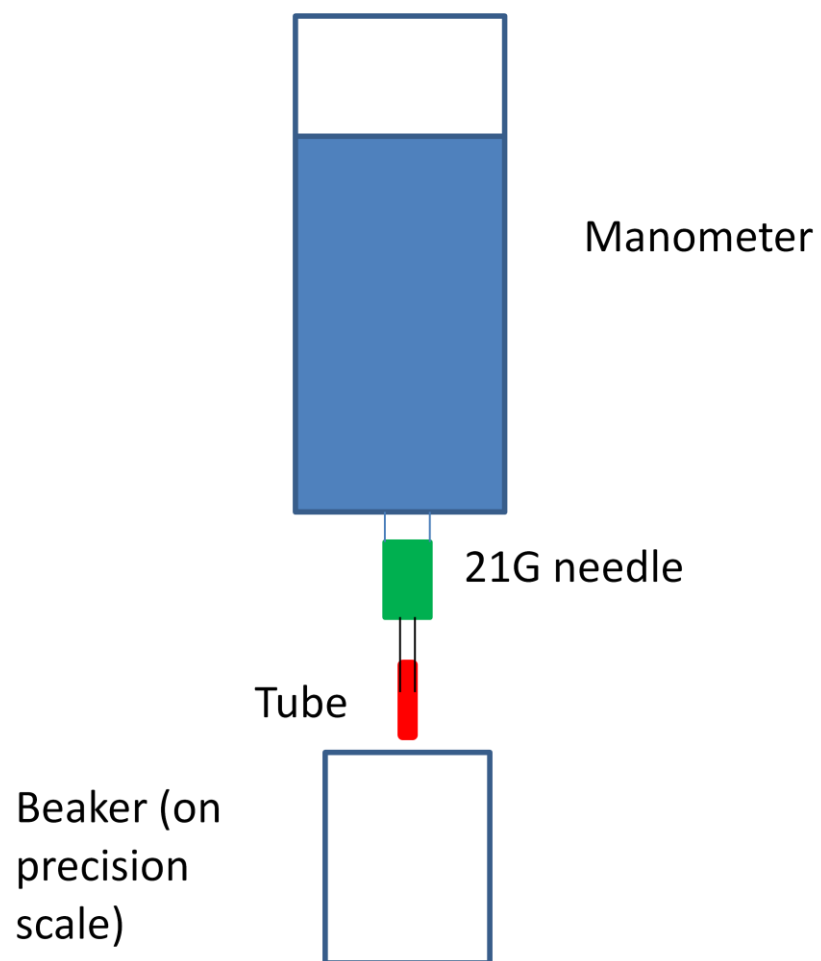


Figure 5.5 Setup for fixed pressure method (tubes). The manometer level was kept constant by addition from a BSS bottle and tube (not shown).

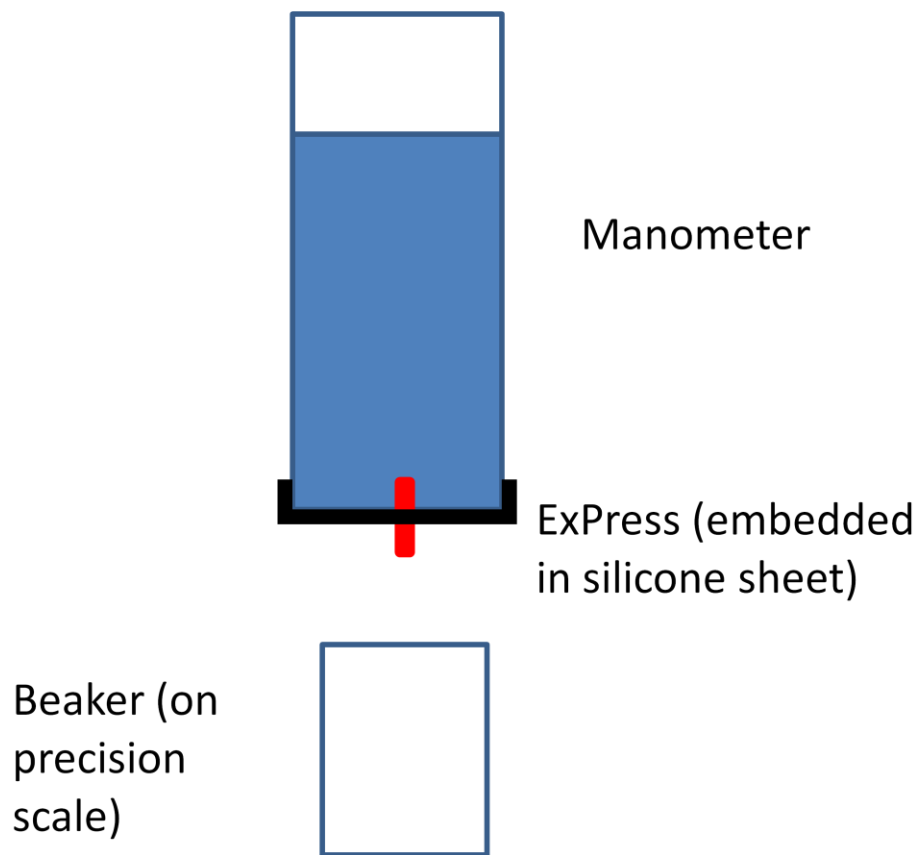


Figure 5.6 Setup for fixed pressure method (ExPress devices). The manometer level was kept constant by addition from a BSS bottle and tube (not shown).

5.2.3.3 Effect of higher protein and fibrin content

Resistance values of the tubes and devices when using BSS, albumin in BSS (300 mg/ 100 ml), albumin in BSS (3000 mg/ 100 ml), fibrin in BSS (0.5 mg/ ml) and fibrin in BSS (1.0 mg/ ml) were determined. The concentrations of albumin used in this experiment were to model moderate and maximal amounts of abnormal aqueous humour protein, as in Chapter 4, and the method for preparing them was described in that chapter. The concentrations of fibrin in BSS were chosen based on estimation, as we could not find in the literature typical values for the concentration of fibrin in aqueous humour during

inflammation. These concentrations provided cloudy solution appearances similar to that seen in fibrinoid aqueous humour, with sedimentation much like that seen in hypopyon formation. The fibrin in BSS solutions were prepared by adding 25 mg and 50 mg of fibrin (insoluble powder from human plasma; Sigma Aldrich, Dorset, UK) with BSS to make up volumes of 50 ml. Separate syringes were used for the different fluids.

As the insoluble fibrin tended to sink down in the gravity-dependant fixed pressure experimental setups (Figures 5.5 and 5.6) and could easily block the tubes and devices, we employed the fixed flow rate method as in Figure 5.3. The only difference was when testing the ExPress devices; to enable water-tight attachment to the 3-way tap, they were glued to the lumens of 24G (0.51 mm inner diameter; BD, NJ, USA) IV cannulas which were also cut down to 5 mm in length. These cannulas on their own also had negligible resistances when tested.

With the tubes and ExPress devices *in situ*, flow rate was increased from 0 to 35 $\mu\text{l}/\text{min}$ (50 μm tubes) or 40 $\mu\text{l}/\text{min}$ (100 μm tubes) in steps of 5-10 $\mu\text{l}/\text{min}$, or 0 to 166.7 $\mu\text{l}/\text{min}$ (ExPress devices) in steps of 33.3 $\mu\text{l}/\text{min}$. The higher flow rates were necessary with the ExPress devices as they had lower resistances and thus produced lower pressure readings with the lower flow rates. Each flow rate was maintained for 5 minutes and the stabilised pressure recorded. The resistance was deduced from the slope of a pressure versus flow rate graph.

5.2.4 Porcine sclera model

We incorporated the tubes and ExPress devices into our porcine sclera model as described in chapter 4. With this model, with the corneoscleral disc mounted on the Barron artificial anterior chamber and physiological flow rates of 1.5-3.0 $\mu\text{l}/\text{min}$, we were unable to obtain a stable pressure as it continually increased as the infusion progressed; pressure was only released when stab incisions were performed. In contrast, the AGFID project team (2001) found that stable pressures of between 15-28 mmHg could be maintained with a similar setup. Their flow rates were not reported, but besides this, the difference could also be due to less water-tightness in their different artificial anterior chamber. We also created 4 mm wide \times 3 mm long, 250 μm thick scleral flaps before proceeding to apply the relevant interventions. This was to obtain closer scleral bed thickness to human eyes (Chapter 4) and improve the fit of the ExPress devices. Any air remaining in the anterior chamber was removed after each stab incision by a gentle bolus of BSS.

5.2.4.1 Equilibrium pressure without an overlying scleral flap

This was to compare the control of pressures by the different tubes and devices on their own, without the effect of an overlying flap. Patent 50 μm tubes or ExPress devices were inserted after a 27G stab incision while 100 μm tubes were inserted after a 26G stab incision (Figures 5.7 and 5.8). Scleral flaps were not repositioned or sutured after device insertion. The flow rate was set at 3 $\mu\text{l}/\text{min}$ and the pressure tracing reset. The resulting equilibrium pressures were observed. Each ExPress device was used for two runs.

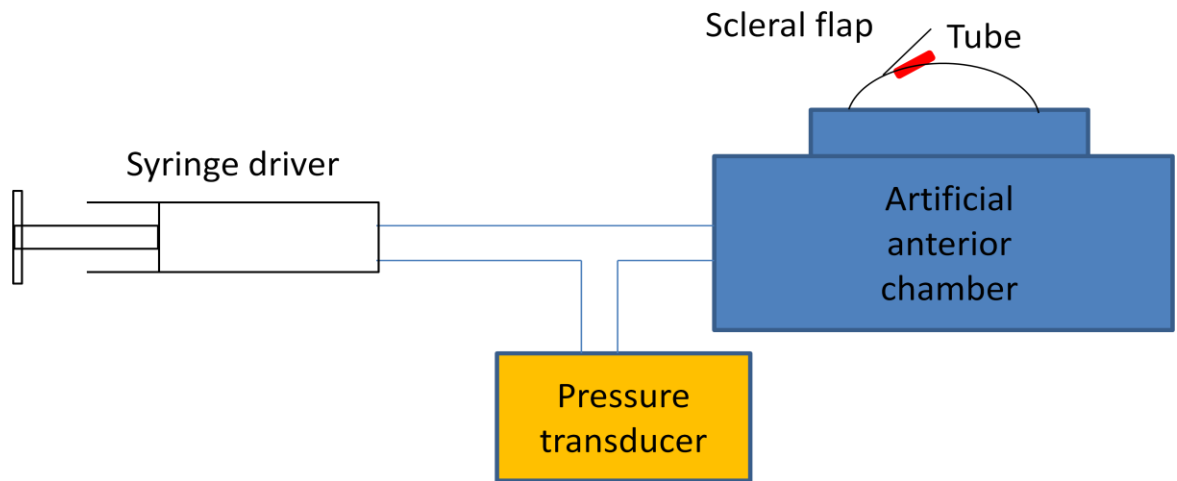


Figure 5.7 Setup for equilibrium pressure without a flap experiment. The scleral flap was not repositioned or sutured after device insertion.

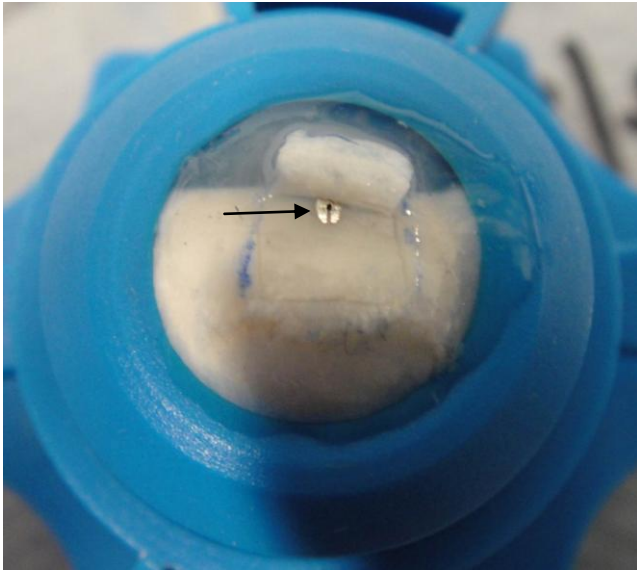


Figure 5.8 Photograph of ExPress device *in situ* (arrow) and reflected scleral flap.

5.2.4.2 Equilibrium pressure with an overlying scleral flap

Here we compared equilibrium pressures between ExPress devices and a trabeculectomy. The 50 μm (and 100 μm) tubes were not tested as they are aimed for insertion without scleral flaps. For the ExPress devices, a 27G stab incision through the scleral bed was performed after which they were inserted using their injector. Each device was used for two runs. For the trabeculectomy, after creating a scleral flap, a sclerostomy was performed using a 0.75 mm diameter scleral punch. In all cases, the scleral flaps were sutured down adequately with 2 10/0 nylon sutures, as in Figure 5.9. The flow rate was set at 3 $\mu\text{l}/\text{min}$ and the pressure tracing reset. A typical trace is shown in Figure 5.10, showing a gradual increase in pressure until the flap opened to allow flow.

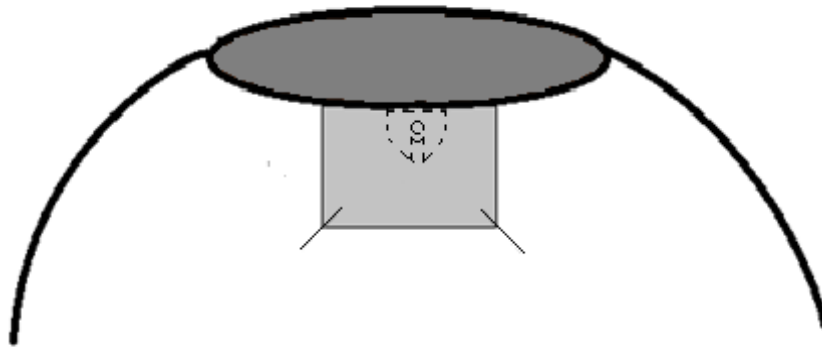


Figure 5.9 Diagram of ExPress device under a sutured flap.

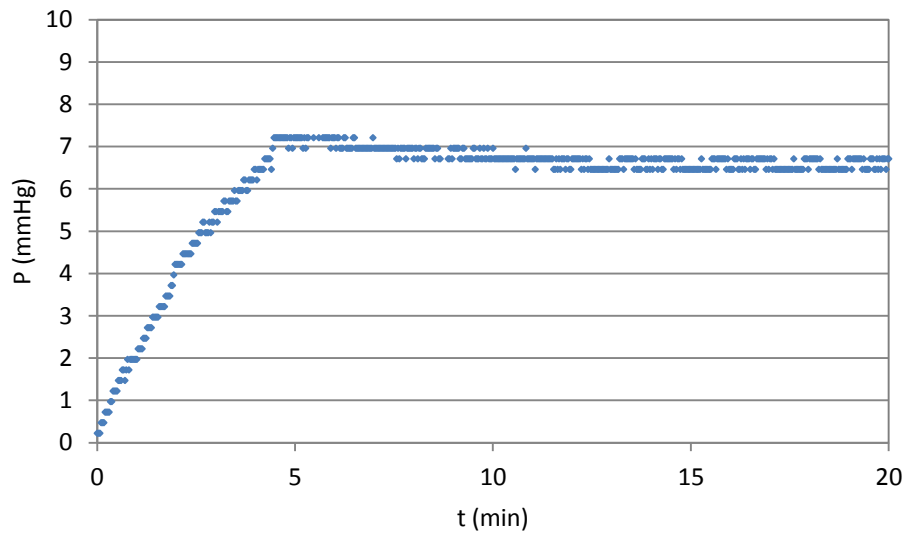


Figure 5.10 Typical pressure curve in equilibrium pressure with an overlying flap experiment. The pressure levelled out after the flap opened to allow flow.

5.2.4.3 Index of external leakage with different stab incision sizes

Occluded tubes or ExPress devices were inserted after making stab incisions in the scleral bed with 27G (50 μm tubes and ExPress devices), 26G (100 μm tubes) or 25G (ExPress devices) needle stabs (Figure 5.11). The nominal outer diameters (OD) of these needles were as follows – 27G 0.41 mm, 26G 0.46 mm and 25G 0.51 mm. The tubes were occluded with cyanoacrylate glue at their tips. The ExPress P50 and P200 devices (1 each) were occluded with short segments of broken-off introducer wire in their lumens. The occlusions were supplemented by using cyanoacrylate glue to cover the flanged external (subconjunctival space) ends. Each of these devices was used twice for each subgroup.

After the devices were inserted through the incisions, pressure in the manometer was increased to 20 mmHg. Scleral flaps were not repositioned or sutured after device insertion. This time, no BSS was added to the manometer during the test. The whole apparatus was left for 1 hour for pressure to stabilise, after which the pressure was noted.

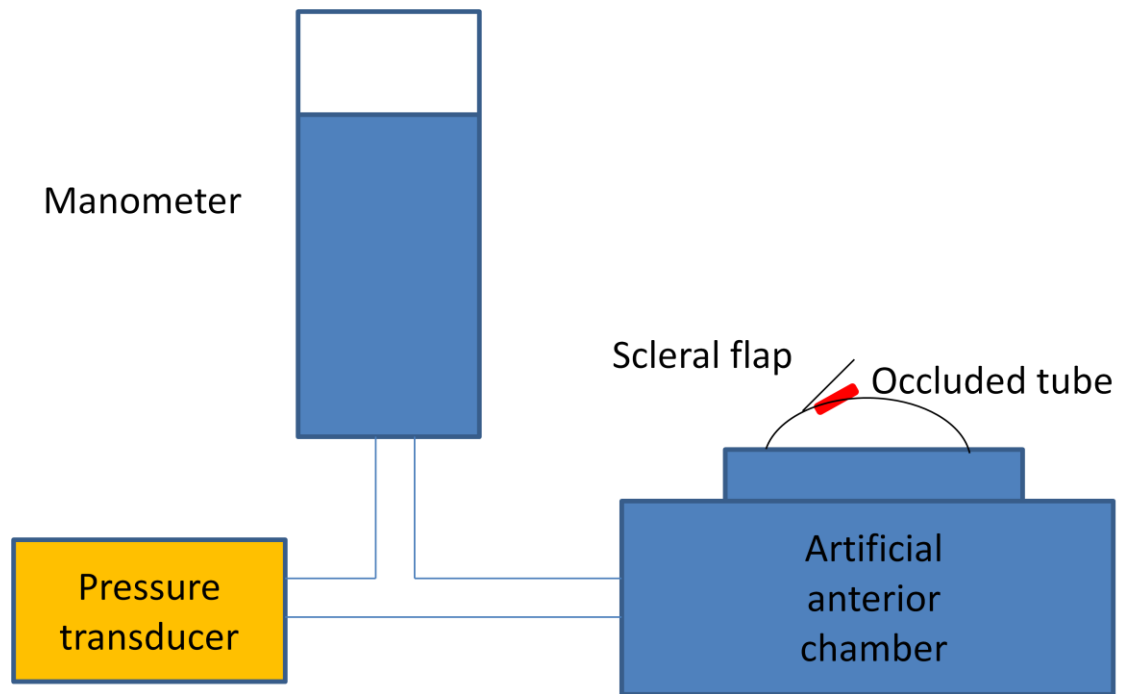


Figure 5.11 Setup for index of external leakage experiment. Scleral flaps were not repositioned or sutured, and no BSS was added to the manometer during the test.

Statistical analysis was performed using Prism 4 software (GraphPad Software, Inc., CA, USA). The unpaired t-test was used when comparing 2 groups while one-way ANOVA +/- Bonferroni's multiple comparison post-test was used when comparing 3 groups. $P < 0.05$ was considered statistically significant.

5.3 Results

5.3.1 Material testing

From the stress-strain curve that was produced, the gradient of the secant between 0 and 1% strain showed that the Young's modulus of the PTFE material was 663 +/- 38 MPa (n = 3).

5.3.2 Electron microscopy

A summary of dimensions of the tubes and devices is shown in Table 5.1. Some actual images are shown in Figures 5.12-5.16.

Table 5.1 Summary of tube and device dimensions.

PTFE tubes			
	50 μm	100 μm	Notes
Internal diameter (μm)	56.3 +/- 2.3	106.8 +/- 1.4	Examples in Figure 5.12
External diameter (μm)	354.2 +/- 4.6	397.0 +/- 7.0	
ExPress devices			
	P50	P200	
Length, whole (mm)	2.56 +/- 0.01		Example in Figure 5.13
Width, tube section (μm)	377.0 +/- 8.5		
Length, complete tube section (mm)	1.36 +/- 0.02		
Internal diameter, subconjunctival space end (μm)	205.0 +/- 5.8	206.4 +/- 3.3	P = 0.564 Examples in Figure 5.14
Internal diameter, anterior chamber end (μm)	206.9 +/- 3.7	204.5 +/- 0.9	P = 0.434 Examples in Figure 5.15
AqueSys device			
Internal diameter (μm)	55.9 +/- 2.6		Example in Figure 5.16
External diameter (μm)	147.7 +/- 1.9		

Note: For the electron microscope we used, the manufacturer quotes an error in magnification (and measurement) of +/- 1.5%.

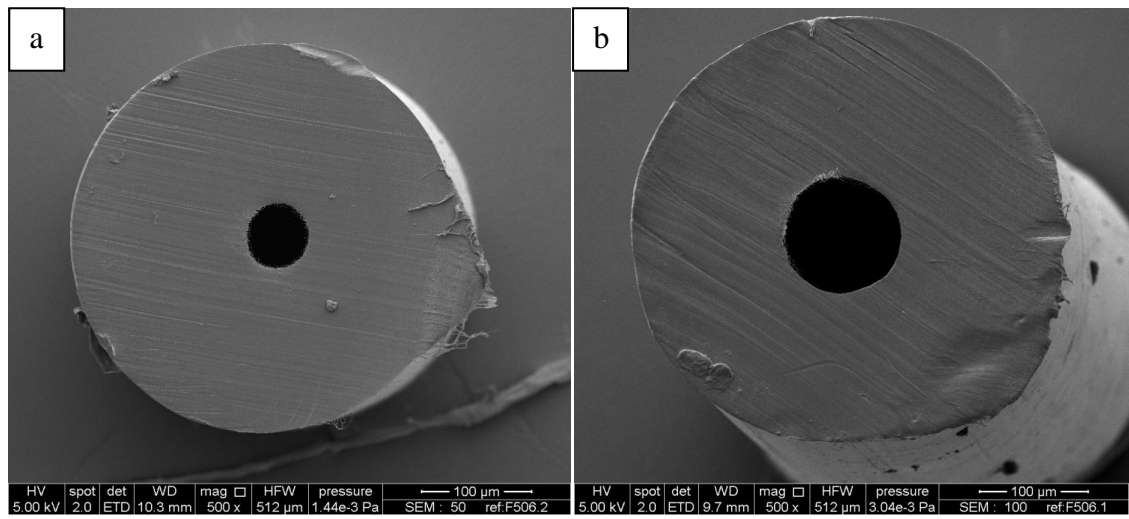


Figure 5.12 Cross-sections of (a) 50 μm and (b) 100 μm tubes (500 × magnification).

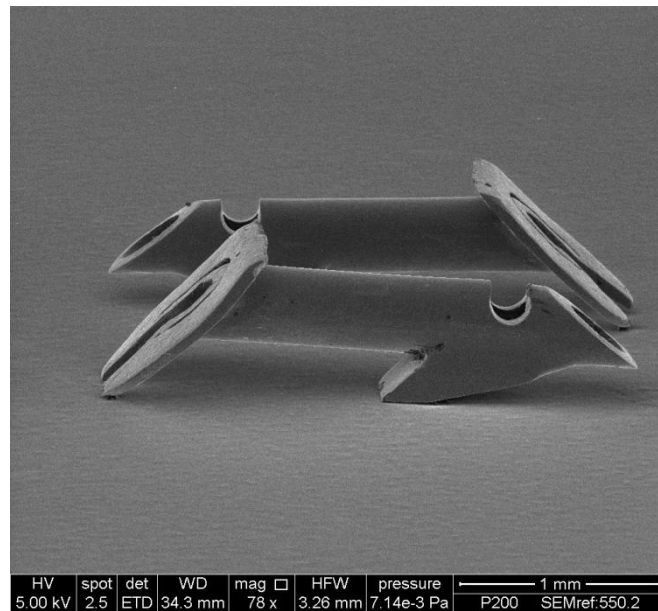


Figure 5.13 Profile of two ExPress P200 devices (78 × magnification).

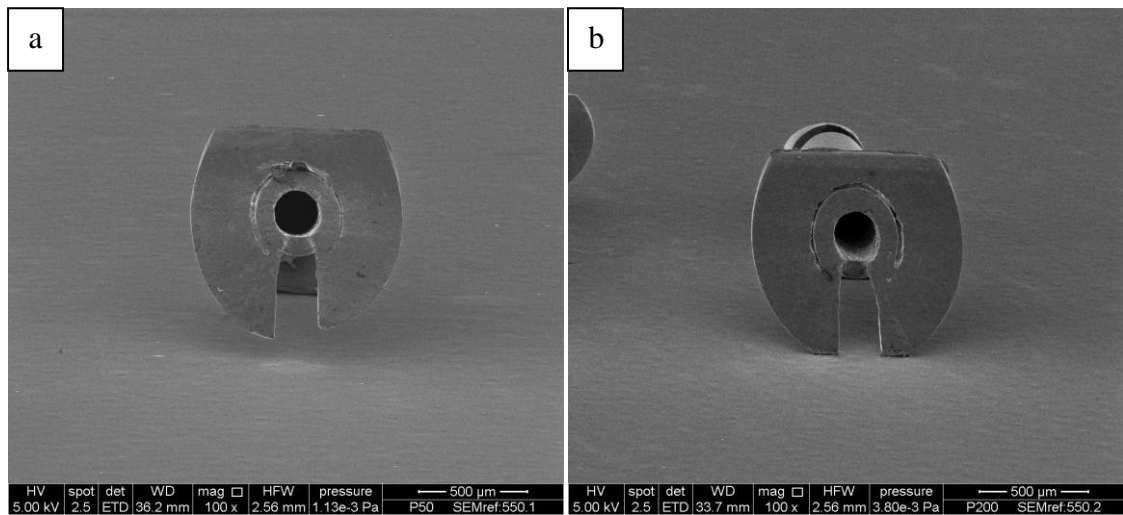


Figure 5.14 Subconjunctival space ends of (a) P50 and (b) P200 devices (100 × magnification). The external dimensions and lumens are similarly sized.

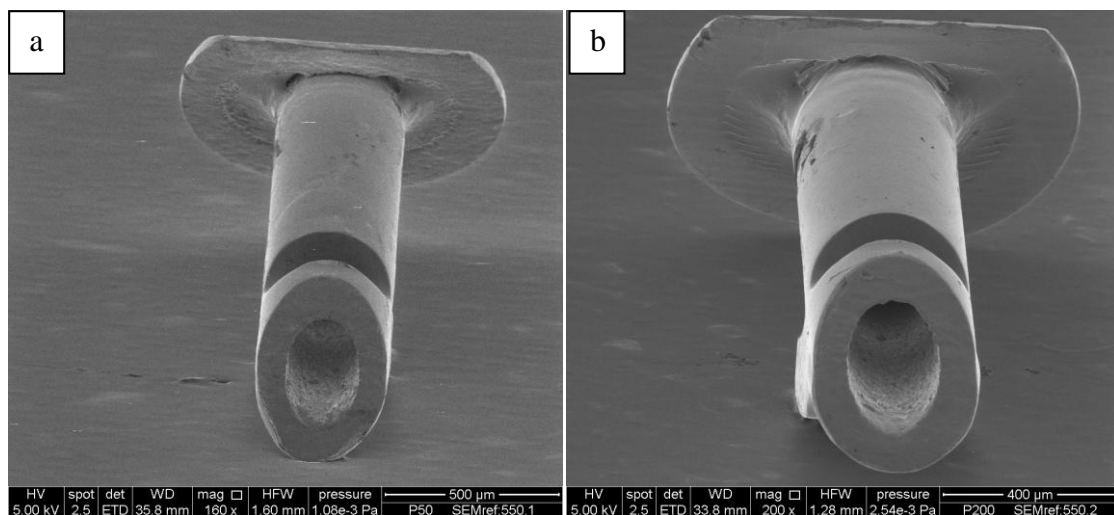


Figure 5.15 Anterior chamber ends of (a) P50 (160 × magnification) and (b) P200 devices (200 × magnification). The external dimensions and lumens are similarly sized.

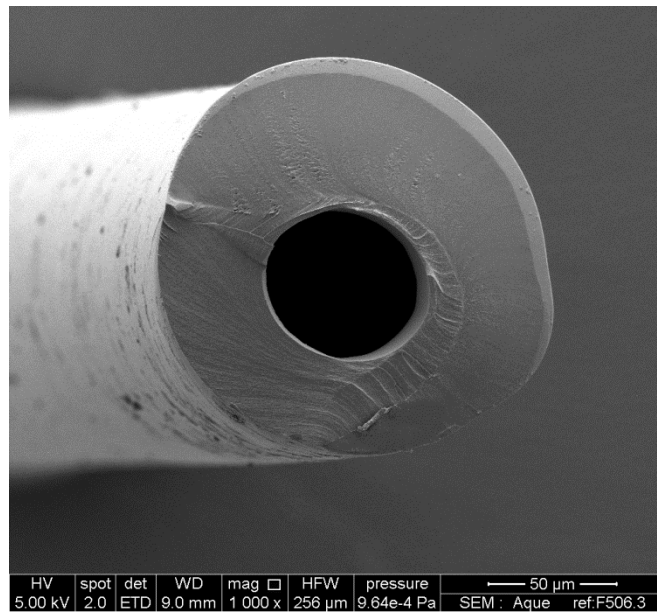


Figure 5.16 AquSys device (1000 × magnification).

5.3.3 Flow studies

5.3.3.1 Resistance of 50 μm and 100 μm tubes

With the fixed flow rate method (Figure 5.17a), resistance of the 50 μm tubes was 1.52 +/- 0.12 mmHg/μl/min and for the 100 μm tubes was 0.17 +/- 0.02 mmHg/μl/min (mean +/- SD, n = 6 each). Comparatively, with the fixed pressure method (Figure 5.17b), resistance of the 50 μm tubes was 1.48 +/- 0.15 mmHg/μl/min and for the 100 μm tubes was 0.19 +/- 0.01 mmHg/μl/min (n = 6 each). There was no statistically significant difference in resistance values between fixed flow rate and fixed pressure methods (P = 0.659 for 50 μm, P = 0.334 for 100 μm).

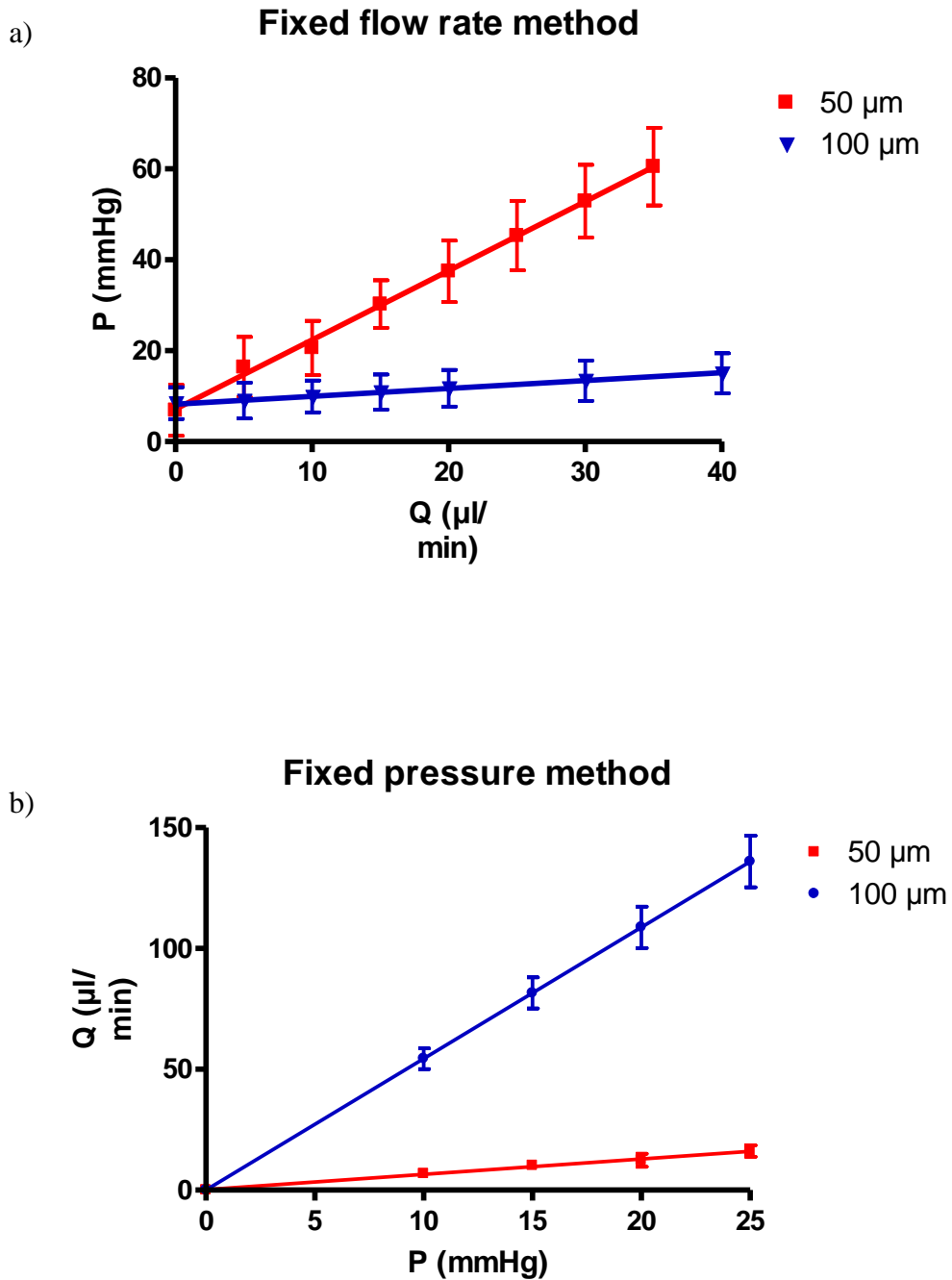


Figure 5.17 (a) Pressure-flow rate relationship with fixed flow rate method. Resistance is calculated from the gradient of the best-fit line. (b) Flow rate-pressure relationship with fixed pressure method. The gradient reflects the facility i.e. the inverse of resistance.

5.3.3.2 Resistance of ExPress devices

Resistance of the P50 devices was 0.054 ± 0.002 mmHg/ μ l/min and for the P200 devices was 0.010 ± 0.001 mmHg/ μ l/min ($n = 4$ each) [Figure 5.18].

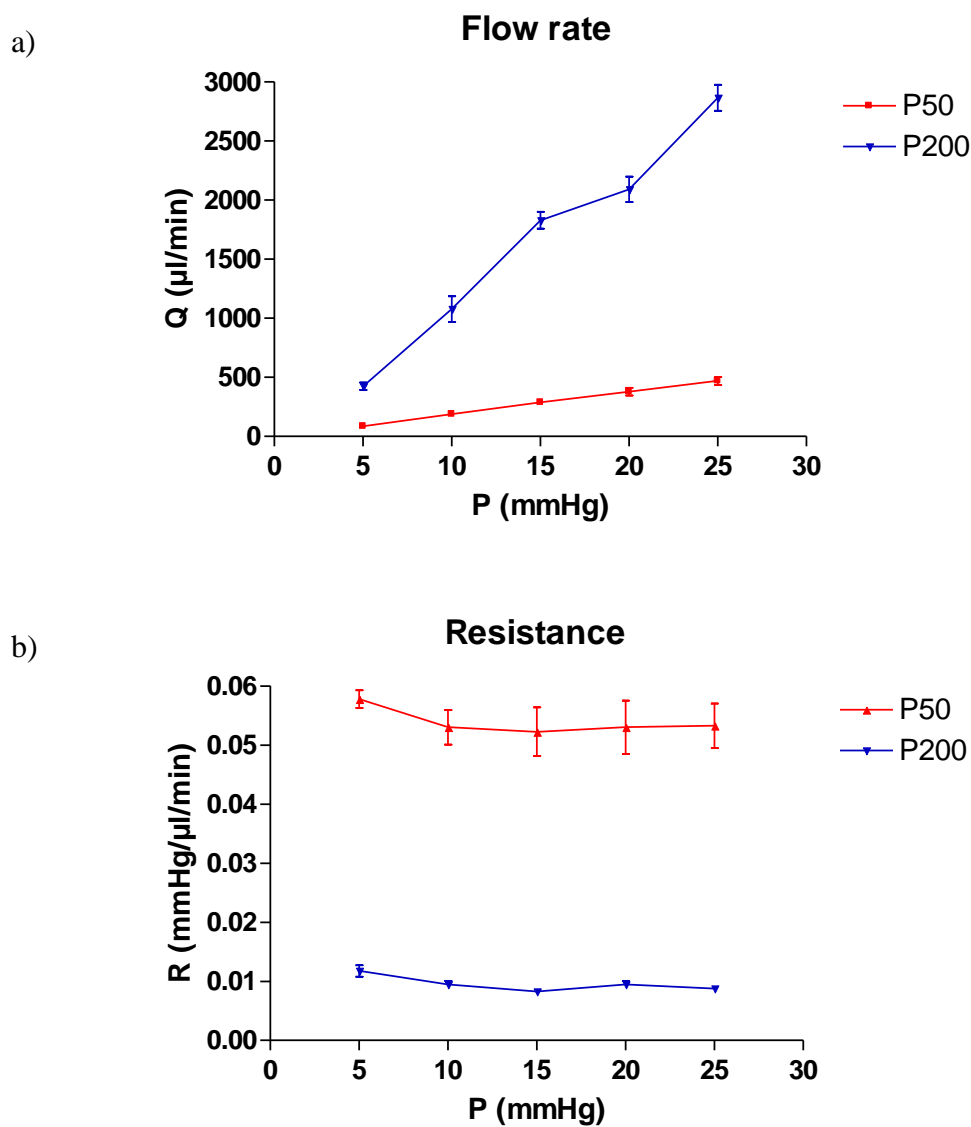


Figure 5.18 (a) Flow rate and (b) resistance of ExPress devices with fixed pressure method. The devices demonstrated fixed resistance characteristics.

5.3.3.3 Comparison between experimental and predicted permeability values

Differences between experimental and predicted permeability values from the fixed pressure method are shown in Table 5.2 below.

Table 5.2 Experimental and predicted permeability of devices.

	Permeability, experimental ($\mu\text{l}/\text{min}/\text{mmHg}$)	Permeability, predicted ($\mu\text{l}/\text{min}/\text{mmHg}$)
50 μm tube	0.66 +/- 0.05	0.40
100 μm tube	5.44 +/- 0.17	5.11
P50	18.57 +/- 0.76	Poiseuille's Law not applicable as lumens do not have constant
P200	104.71 +/- 14.68	circular cross-section.

5.3.3.4 Effect of higher protein and fibrin content

With the 50 μm tube (Figure 5.19), there was a significant difference in resistance between BSS and albumin in BSS (3000 mg/ 100 ml). With that level of albumin, resistance was increased by 26.1%. Fibrin in BSS (0.5 mg/ ml and 1.0 mg/ ml) did not affect resistance in this experiment. With the 100 μm tube and both ExPress devices (Figures 5.19 and 5.20), there were no statistically significant differences in resistance values between all the different fluids.

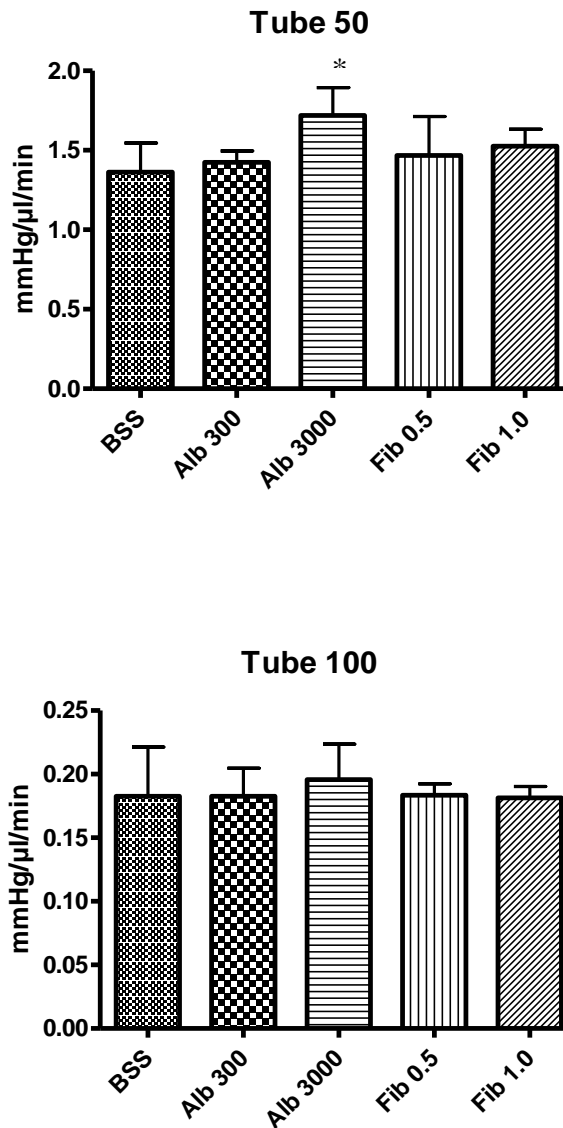


Figure 5.19 Resistance of PTFE tubes with different fluids (n = 6 each). * indicates a statistically significant difference compared to BSS. In the 50 μm tubes, only albumin in BSS (3000 mg/ 100 ml) resulted in higher tube resistance than BSS. In the 100 μm tubes, there were no statistically significant differences between fluids.

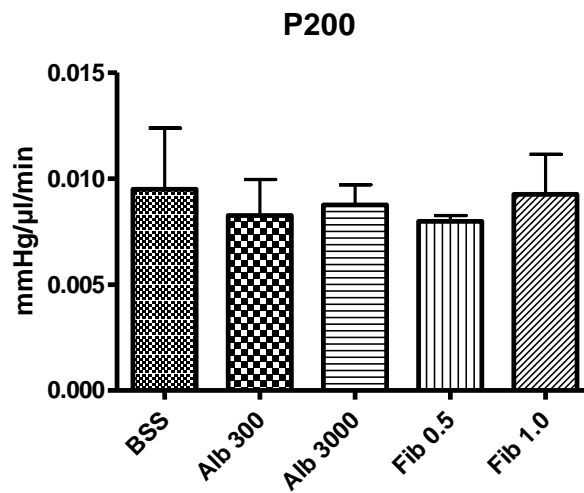
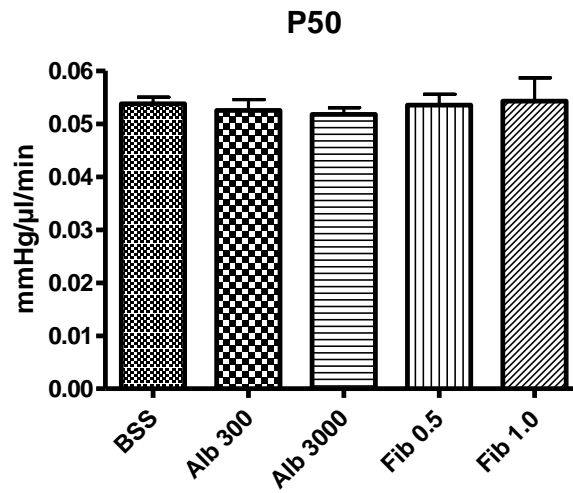


Figure 5.20 Resistance of ExPress devices with different fluids (n = 4 each). There were no statistically significant differences between fluids in both devices.

5.3.4 Porcine sclera model

5.3.4.1 Equilibrium pressure without an overlying scleral flap

Equilibrium pressures were 6.71 +/- 0.34 mmHg for the 50 µm tube, 4.54 +/- 0.89 mmHg for the 100 µm tube, 0.63 +/- 0.59 mmHg for the ExPress P50 and 0.25 +/- 0.38 mmHg for the ExPress P200 (n = 8 each). There were statistically significant differences between all devices, apart from that between the ExPress P50 and ExPress P200.

5.3.4.2 Equilibrium pressure with an overlying scleral flap

Equilibrium pressures were 17.81 +/- 3.30 mmHg for the ExPress P50, 17.31 +/- 4.24 mmHg for the ExPress P200 and 16.28 +/- 6.67 mmHg for the trabeculectomy (n = 8 each, P = 0.850) [Figure 5.21].

5.3.4.3 Index of external leakage with different stab incision sizes

Pre and post-insertion pressure values with the different combinations of tubes and devices are shown in Table 5.3.

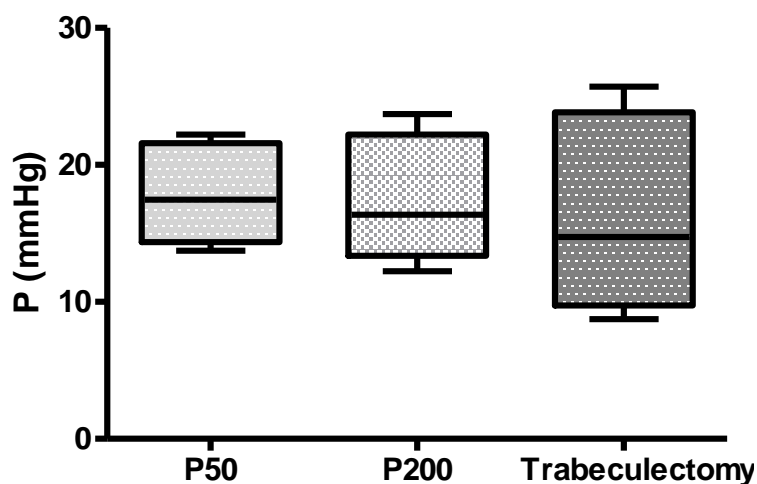


Figure 5.21 There was no statistically significant difference in equilibrium pressures between the ExPress devices and a trabeculectomy. However, the standard deviation with a trabeculectomy was larger, indicating a wider variability in readings. This may be due to lumen size variations in the trabeculectomy.

Table 5.3 Pre and post insertion pressures in index of external leakage experiment.

Tube/ device, size of stab incision	Pre insertion pressure, mmHg	Post insertion (60 mins) pressure, mmHg	Difference, mmHg	P value
50 μ m tube, 27G	20.24 +/- 0.25	19.82 +/- 0.26	0.43 +/- 0.15 #	< 0.001
100 μ m tube, 26G	20.22 +/- 0.12	20.04 +/- 0.12	0.19 +/- 0.01 #	< 0.001
ExPress, 27G	20.26 +/- 0.16	19.22 +/- 0.21	1.03 +/- 0.26 *	< 0.001
ExPress, 25G	20.20 +/- 0.22	19.17 +/- 0.59	1.03 +/- 0.58 *	0.008

N = 6 (tubes), 4 (ExPress). No statistically significant difference between pre insertion pressures.

Statistically significant differences between # and *.

5.4 Discussion

5.4.1 Material testing

We compared our findings with data from MATBASE (<http://www.matbase.com>). On the database, Young's moduli are given as 1-5 MPa for silicone, 410-750 MPa for PTFE, 1.5-2.0 GPa for polypropylene and 200 GPa for stainless steel. The Young's modulus of our PTFE tubes was thus consistent with that listed and is more stiff than silicone (which is used to make many current glaucoma drainage devices) but less so than polypropylene (earlier Ahmed and Molteno devices) and stainless steel (ExPress devices).

Material stiffness should be considered in the design of glaucoma drainage devices. It has been suggested that the more rigid polypropylene undergoes micro-movement which increases inflammation (Ayyala, Michelini-Norris, Flores, Haller, & Margo, 2000). Clinical studies have shown that silicone Ahmed Glaucoma Valves have lower rates of the hypertensive phase (24% vs 32%) as well as failure (4-6% vs 13-18%) compared to polypropylene ones (Ishida et al., 2006). Another study also found differences in encapsulation rate (0% vs 20%) between silicone and polypropylene Ahmed Glaucoma Valves in their paediatric glaucoma population (Sayed & Awadein, 2013). Along the same lines of reasoning, PTFE being stiffer than silicone may also cause more inflammation and thus be less suitable as glaucoma drainage device material.

Stainless steel, as used in ExPress devices is the stiffest among the materials mentioned above. As such, it may also cause more inflammation than silicone. This may be the reason why in the initial period when ExPress devices were implanted without cover under a scleral flap, a significant number of conjunctival erosions (11-12%) were reported, particularly if they were malpositioned (Traverso et al., 2005;

Rivier et al., 2007; Stewart, Diamond, Ashmore, & Ayyala, 2005). Following this, implantation of the devices under the scleral flap was recommended (Dahan et al., 2005; Maris et al., 2007), and is the current practice today (de Jong, Lafuma, Aguade, & Berdeaux, 2011; Good & Kahook, 2011; Dahan et al., 2012). Long term results may show whether this effect of stiffness is important for implantation under the scleral flap too, although in one study which has reported 5-year outcomes, no cases of conjunctival erosion were reported (de Jong et al., 2011).

5.4.2 Electron microscopy

For the PTFE tubes we used, the SEM measurements were consistent with the nominal dimensions supplied by the manufacturer, which were 50 μm ID/ 350 μm OD for 50 μm tubes and 100 μm ID/ 400 μm OD for 100 μm tubes. For the ExPress devices, the external dimensions of the P50 and P200 devices were similar to each other and consistent with the nominal dimensions supplied by the manufacturer. Most strikingly, we found that the lumens of both models also had the same dimensions, at both subconjunctival space and anterior chamber ends. We subsequently approached Alcon, Inc. to enquire about this finding. They confirmed our findings and showed how the P50 differs from the P200 only in having a 150 μm diameter bar lying across its lumen in the middle of the device, as in Figure 5.22. This design has interesting implications on fluid flow and pressure, as will be discussed in the next section.

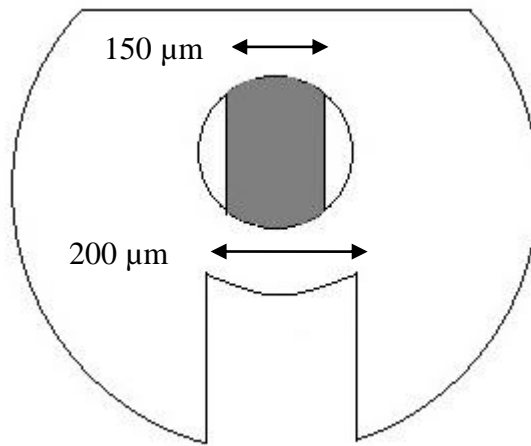


Figure 5.22 Inner bar (in grey) in the lumen of the P50 device. This bar is located centrally in the device.

5.4.3 Flow studies

Studies on flow in glaucoma drainage devices have employed both fixed flow rate (Prata, Jr. et al., 1995; Eisenberg et al., 1999; Lim et al., 2002; Pan, 2002) and fixed pressure methods (Breckenridge, Bartholomew, Crosson, & Kent, 2004; Estermann et al., 2013). We compared the different methods and found no statistically significant difference in the resistance values they produced. One article suggested that while the fixed flow rate method was useful for assessing device performance and validation, the gravity-dependant fixed pressure method usually took less time and could be useful as a manufacturing line test (Porter, Krawczyk, & Carey, 1997). However, we would like to point out that the fixed pressure method generated flow rates of up to 3000 $\mu\text{l}/\text{min}$ in the case of the ExPress P200 devices. This high flow rate is an unlikely representation of actual conditions in the eye and may also lead to erroneous results when testing flow-rate sensitive devices such as valves, due to the more turbulent flow generating larger resistance values (Batchelor, 2000).

The resistances and flow rates of the two ExPress models were consistent with fixed resistance characteristics, and similar to that reported by Estermann et al. (2013) which were 0.056 mmHg/ μ l/min for the P50 and 0.009 mmHg/ μ l/min for the P200. We too found that the difference in resistance values between the P50 and P200 could not be explained just on the basis of their descriptions, where from Poiseuille's Law a four-fold decrease in inner diameter from 200 μ m to 50 μ m would increase resistance by 256 times. In our experiment, the P50 device resistance was only around five times more than that of the P200 device, and around 28 times more than that of the 50 μ m ID tube. However, we now know that the P50 device has 200 μ m diameter circular lumens at both ends and 2 smaller half-circle shaped ones centrally (Figure 5.22), thus making Poiseuille's Law inapplicable to its case. In fact, this law is also not applicable for ExPress devices in general as the side orifice disrupts the constant circular cross section assumption. Instead, there is no single law to calculate the resistance of these more complex devices and experimental determination is indicated.

Experimental permeability values of the tubes were higher than those predicted from Poiseuille's Law. The difference was marked with the 50 μ m ID tube (65%) but small with the 100 μ m ID tube (6%). The error could be due to small unnoticed leakage around the smaller tube, or in determining its internal diameter (by a difference of up to 8 μ m) as permeability has a dependence on diameter to the fourth power, as compared to linear dependences on the other dimensions i.e. viscosity, length and flow rate. Despite the higher experimental permeability values, the one for the 50 μ m ID tube (0.66 μ l/min/mmHg) still meets the requirement we predict for reduction in IOP from 25-50 mmHg to 15 mmHg.

The MIDI-Arrow device has an ID of 70 μ m and length of 8.5 mm, thus making its calculated permeability 0.55 μ l/min/mmHg. In a small study in 23 humans, IOP fell from a baseline of 24.0 +/- 5.4 mmHg to 10.5 +/- 2.8 mmHg at 12 months and

maintained at 10.2 +/- 2.0 mmHg at 2 years (Palmberg et al., 2013). Complete and modified success rates were 91% and 96% at one year. Two subjects developed transient hypotony after day one but there were no cases of chronic hypotony or maculopathy. Another device, the AqueSys has a 50 μm ID and a 6 mm length, making its calculated permeability value 0.32 $\mu\text{l}/\text{min}/\text{mmHg}$. In a study where AqueSys devices were inserted into 15 patients, the mean pre-operative IOP of 21.3 mmHg reduced to 12.2 mmHg at 1 week. It was subsequently maintained at 15.0 mmHg at 1 month, 15.2 mmHg at 6 months and 15.3 mmHg at 12 months. No cases of hypotony were reported (Kersten-Gomez et al., 2012). The favourable clinical data with the two devices can be taken as an encouraging sign that fixed resistance devices with permeability values in the region we predicted are able to provide adequate reductions in IOP whilst minimising hypotony. If we consider the 5 mm long and 50 μm ID tube we tested, with its calculated permeability of 0.40 $\mu\text{l}/\text{min}/\text{mmHg}$, the IOP drop would be intermediate between that with the MIDI-Arrow (~ 14 mmHg at 12 months) and that with the AqueSys (~ 6 mmHg at 12 months). The hypotony rate would also be intermediate between those reported in the 2 studies. These predictions will need to be tested in actual living eyes.

5.4.3.1 Effect of higher protein and fibrin content

With the 50 μm tube, resistance was higher with albumin in BSS (3000 mg/ 100 ml) than with plain BSS. The increase of 26.1% is an indicator of potential blockage of the smaller diameter tube by fluids with high protein concentrations, and could be due to increased viscosity [relative viscosity of 1.12 for albumin in BSS (3000 mg/ 100 ml) as found in Chapter 4] or protein deposition. Although PTFE has features that promote stability and non-reactivity, in a previous study which compared fibrinogen, fibrin and cellular adhesion on polymers, PTFE was found to be less resistant than

phosphorylcholine-coated polymethylmethacrylate [PC-PMMA] (Lim, 1999). As such, besides the potential problem with its stiffness, this is another which may make it less suitable for use to make glaucoma drainage devices.

There was no statistically significant difference in generated resistance between BSS and 0.5 or 1.0 mg/ ml fibrin in BSS solutions. However, in an earlier pilot study where we used a constant pressure setup (Figures 5.5 and 5.6), we found that the insoluble fibrin tended to sink to the bottom of the apparatus and could block both 50 μm and 100 μm tubes. Even with the constant flow rate setup (Figure 5.3), we could see most of the fibrin gravitating below the level of the syringe hub (outlet), thus it was mostly 'clear' BSS that flowed through the mountings and devices. However, since most glaucoma drainage devices are inserted in the superior half of the eye, we felt that our constant flow rate model was still a good representative. In future, a more refined model incorporating a convection effect in the anterior chamber (Siggers & Ethier, 2011) to allow a more realistic movement of fibrin should enable us to understand fibrin's effect better. Additionally, improvement on this model we used may be realised with the use of *in situ* polymerised fibrin (produced by mixing fibrinogen and thrombin solutions) *in lieu* of the insoluble powder, as it is a more realistic representation of fibrin in the anterior chamber.

At this moment, the evidence suggests that caution is appropriate with the use of devices with internal diameters less than 100 μm for cases such as inflammatory glaucoma where aqueous humour protein concentrations are frequently raised (Herbert et al., 2004; Siddique et al., 2013).

5.4.4 Porcine sclera model

5.4.4.1 Equilibrium pressure without an overlying scleral flap

The 50 μm tubes maintained pressure above 6 mmHg without overlying scleral flaps. At the lower physiological aqueous humour flow rate of 1.5 $\mu\text{l}/\text{min}$, this pressure is expected to be around 3 mmHg. This suggests that the tubes may offer a degree of protection against hypotony after insertion in actual eyes. Contrarily, the ExPress devices offered virtually no resistance to flow. This is in keeping with the results of our flow studies and initial clinical ExPress device implantations without cover under a scleral flap, when significant numbers of hypotony (up to 91%) occurred (Wamsley et al., 2004; Rivier et al., 2007). Following the findings, implantation of the devices under the scleral flap was recommended (Dahan et al., 2005; Maris et al., 2007).

5.4.4.2 Equilibrium pressure with an overlying scleral flap

We found that pressures did not differ between the ExPress devices and a typical trabeculectomy. This finding is consistent with those of many clinical studies (Maris et al., 2007; de Jong et al., 2011; Dahan et al., 2012). However, we can say that ExPress device implantations result in less variability in pressure readings. This may be due to lumen size variations (Buys, 2013); ExPress devices have lumen size measurements with small tolerances (Table 5.1), as compared to making a sclerostomy with a punching device or knife. In practice, even with same-sized punching devices, variations in sclerostomy sizes occur due to differences in scleral tissue tension or sharpness of the instruments (for example, if the cutting process is performed more than once).

5.4.4.3 Index of external leakage with different stab incision sizes

We looked at the amount of para-tubal leakage which occurs after insertion of the devices. In the case of the ExPress devices, we also compared the amounts after 27G and 25G stab incisions (sizes stated in the packaging leaflet). The least amount of leakage occurred with the 100 μm tube (397 μm OD) after a 26G (0.46 mm nominal OD) needle stab, followed by the 50 μm tube (354 μm OD) after a 27G (0.41 mm nominal OD) needle stab. When we tried to insert a 100 μm tube after a 27G needle stab (to try to improve the fit), a significant amount of manipulation was needed which could deform the tube.

There was more para-tubal leakage with the ExPress devices than with the tubes, but the amounts were similar after either 27G or 25G (0.50 mm nominal OD) needle stabs. It is likely that the spur enlarges the scleral opening during insertion, which leads to a poorer fit around the body and increased leakage. However, we found that subjectively more manipulation was needed to insert the device after the smaller 27G needle stab, which could traumatise surrounding local tissue. We therefore think that 25G needle stabs are better for inserting ExPress devices.

Overall, this experiment has provided insight into some issues related to material selection, dimensions and shapes of potential and current glaucoma drainage devices, and their control of flow and pressure. These need to be taken into consideration when designing new devices. One next step is to identify potentially better materials in respect to biocompatibility for the production of prototypes, to be used for insertion into living eyes. Such materials may be those with fibrosis-modifying (Lobler et al., 2011) or drug elution (Sahiner et al., 2009; Ponnusamy, Yu, John, Ayyala, & Blake, 2013) capabilities. Other physical designs can also be explored, such as a device with multiple channels, some with removable occlusions which can be removed post-operatively to

titrate flow and pressure; and larger diameter but longer tubes (to have the same permeability values) which can deposit aqueous humour more posteriorly in the subconjunctival space.

The knowledge of the actual pressure drops with the tubes in the porcine sclera model could support our theoretical prediction. However, we were unable to measure them due to the inability to maintain stable pressures before intervention i.e. making stab incisions and inserting the tubes. Additionally, the resistance of the overlying conjunctiva and bleb are not considered, making our findings realistic only for the early post-operative stage of surgery before wound healing has developed. Finally, another limitation of this study is that the *in vitro* findings may not correlate exactly with results in actual living eyes, where other issues such as total ocular compliance and tissue hydration come into play. As such, the findings from this experiment need to be corroborated by those from experiments with actual living eyes.

5.5 Conclusion

The 50 μm ID tubes we used have resistance and permeability values that we predict can provide the required aqueous humour flow and IOP reduction, while still preventing low IOP without insertion under a scleral flap. However, they may be blocked by fluids with high protein content. Poiseuille's Law is not applicable for estimating resistance in ExPress devices. Their low resistance values make them unlikely to prevent hypotony on their own and they lead to similar equilibrium pressure as the trabeculectomy procedure when inserted under the scleral flap. Insertion of these devices after a 25G stab incision allows less tissue manipulation. Finally, the stiffness of PTFE may be disadvantageous for its use as a material for glaucoma drainage devices.

Chapter 6

6 General discussion, conclusion and future work

There are a number of surgical methods for treating glaucoma, including the trabeculectomy and the insertion of glaucoma drainage devices. At the current time, these procedures are still associated with post-operative complications for a significant number of patients, particularly related to the control of aqueous humour flow in the early post-operative period. In this thesis, a fluid mechanics approach was taken to understand better some aspects of the surgery and devices with the aim to improve their outcomes.

The trabeculectomy scleral flap acts as a valve or guard to control aqueous humour outflow, particularly in the early post-operative period before resistance develops in the subconjunctival bleb through the process of wound healing (Birchall et al., 2006; Birchall et al., 2007; Tse et al., 2012). This is important for the prevention of overfiltration and subsequent hypotony, of which significant numbers were shown after non-guarded filtering procedures such as iridencleisis, trephination and Scheie's procedure (Elliot, 1909; Scheie, 1958; Spaeth et al., 1975; Razeghinejad et al., 2011). Sutures, and to a lesser extent, scleral flap geometry affect aqueous humour outflow and the change in pressure. Less overfiltration and higher IOP can be achieved with a higher number of sutures, thicker scleral flaps, and flaps with smaller surface areas. Tight scleral flap closure at the end of surgery is preferable as the sutures can be adjusted or removed by the surgeon in the post-operative period to titrate aqueous humour outflow and IOP (Wells et al., 2004; Jones et al., 2005; de Barros et al., 2008; Kobayashi et al., 2011). Additionally, diversion of aqueous humour flow more posteriorly into the subconjunctival space can encourage the formation of larger and more diffuse blebs, less scarring and inflammation, and less hypotony (Jones et al., 2005; Birchall et al.,

2006; Dhingra et al., 2009); thoughtful positioning of the sutures, such as putting them along the sides of the flap while avoiding the posterior free margin can facilitate this diversion.

With glaucoma drainage devices, single fixed-resistance tubes with inner diameters in the range of 50-75 μm can potentially improve the control of aqueous humour flow into the subconjunctival space with adequate reduction of IOP and less risk of overfiltration and hypotony, without needing additional flow-restricting measures such as temporary internal or external sutures, or insertion under scleral flaps. The 50 μm internal diameter tubes that were tested in Chapter 5 showed particular promise as a basis of new glaucoma drainage devices as they maintained pressure > 5 mmHg in the porcine sclera model, although the actual drop in pressure was not tested. This will need further investigation by means of *in vivo* experiments which have the added benefit of being able to measure pressure drops in the short and longer terms after device implantation. Additional results from implantation of similar devices such as the MIDI-Arrow and AqueSys in human eyes are expected to corroborate the findings in this thesis.

One potential problem with smaller inner diameter tubes is that their resistance may be increased by higher aqueous humour protein or fibrin content, and viscosities such as when there is significant anterior chamber inflammation. While the larger space under scleral flap in the early post-operative period may not be affected as much, the smaller lumens within the tubes may get obstructed by protein or fibrin deposition. Additionally, the effect of protein and fibrin on the trabecular meshwork (Johnson et al., 1986) may add to even more aqueous humour outflow resistance and this will add to a bigger effect on the overall outcome. It may be prudent to consider this potential weakness if the smaller diameter devices are to be inserted in inflamed eyes. Additional testing in living eyes will be needed to confirm or refute the observation that was found.

When considering the experimental approach in this thesis, the large scale physical analogue and *ex vivo* porcine corneoscleral models allowed a cost-effective, efficient and convenient way to assess the effect of variables on the isolated scleral flap, as well as performance of model and actual drainage devices. The experimental setups enabled the control of parameters such as aqueous humour flow rates and viscosity to simplify and standardise conditions to find general principles about the investigated procedure and devices. This approach is analogous to recognised methods such as those used in tablet dissolution or drug release studies, which are conducted in glass containers with paddle wheels or baskets, or flow-through chambers (European Directorate for the Quality of Medicines, 2005b). While the apparatus are dissimilar to the stomach or gastrointestinal tract, they can provide important information in the evaluation and development of new therapies and medicines.

While the experimental setups in this thesis provided a physical understanding of flow and pressure control in idealised situations, they were unable to assess the more complex, global *in vivo* effect, which is affected by other variables such as ocular compliance, wound healing and resistance of the overlying conjunctiva and bleb. There were differences even between the two setups that were used, which supports the notion that there is less relevance of findings to clinical outcomes when utilising models that are distinctly dissimilar to the actual tissues and conditions (Weinreb et al., 2005; Johnson, 2005). As such, the findings in this thesis still need testing for reproducibility in real eyes, of animals or preferably humans.

Conclusion

The trabeculectomy scleral flap acts as a valve to guard from excessive aqueous humour outflow and hypotony, and parameters such as the number and position of sutures and scleral flap geometry can be tailored to alter aqueous humour outflow and IOP outcomes. Tubes with internal diameters around 50 μm show promise for controlled aqueous humour flow into the subconjunctival space with avoidance of low IOP. However, their performance may be limited by obstruction of the small lumens by particles such as protein and fibrin.

Applying engineering principles to glaucoma surgical procedures and drainage devices have provided novel insight into their function. The analyses and models used in this thesis mimic trabeculectomies and glaucoma drainage devices, and can be used to assess aqueous humour flow in the development of new treatments or devices. The advantages include efficiency, cost-effectiveness and the ability to test many variables. However, their main limitation is that the results may not translate exactly into the more complex living eye.

Future work

There is a need to improve the outcome of surgical procedures for glaucoma. The process of developing new procedures or devices can start with physical analysis and Computational Fluid Dynamics (CFD). These may help to predict the resultant outcomes in an efficient way as they enable the control of many variables which can otherwise be difficult in *in vivo* settings. These techniques simplify and standardise conditions to tell us general principles about the procedures and devices, to guide their evolution. Their analyses can be followed up by using experimental models with similar

physical and geometrical properties to the procedures and devices. With the experimental models, more realistic specifications and conditions enable the results to be closer to those in the actual clinical situation.

Although not explored in this thesis, CFD is another technique to analyse fluid flow with the procedures and devices (Gardiner et al., 2010; Villamarin et al., 2012). With this technique, numerical methods and algorithms are employed to analyse situations. The calculations required to simulate the interaction of fluids with surfaces are performed using advanced and high-speed computers, resulting in software which may predict the results in complex scenarios with reasonable accuracy. In the case of this research project, CFD could possibly simulate the flow of aqueous humour under the scleral flap in a 3-dimensional manner, and the flow of aqueous humour along the channels of devices with more complicated designs such as the ExPress. However, the main difficulty with this technique is in characterising the geometry and structural interactions of the procedures and devices; these are intrinsically complex and challenging, and may affect the validity of the predicted outcomes.

In the process of designing a new glaucoma drainage device, consideration should also be given to the types of materials used in their manufacture. The ideal glaucoma drainage device should be made of materials which can be integrated into the surgical site without causing significant inflammation, foreign body reaction or other damage to the surrounding tissue. At the same time, they should also have a degree of resistance to adhesion and blockage from the fluid and cellular material flowing through the device. Biodegradable forms could provide the alternative outflow pathway initially, and then degrade to leave a fistula or tract behind, and they may also be used as drug delivery vehicles providing pressure-lowering or anti-scarring pharmacological support. Current and new research into biocompatibility is expected to produce materials which have these capabilities. Polymer and biomaterial technology is advancing rapidly and

have been used, among others, as scaffolds for tissue engineering and regeneration as well as controlled release drug delivery vehicles (Nair & Laurencin, 2007). It is conceivable then, that a suitable material derived from this polymer group could be used in the manufacture of glaucoma drainage devices.

Once a potential material is found, suitable designs and dimensions need to be investigated further. These may involve experimenting with different physical designs such as combinations of inner diameters and lengths of channels, for better control of resistance, aqueous humour flow and subsequent pressure. Adjustable valve openings which can be modified post-operatively to titrate aqueous humour flow and pressure can also be explored. Alternatively, tubes with multiple channels may also provide controlled aqueous humour flow, some of the channels could be occluded at the time of surgery but then opened in the post-operative stage to titrate flow and pressure according to the initial outcome. The external design of these devices may also be investigated, for example having different appendages such as those to prevent excessive external movement or leakage; or to ease their insertion techniques.

Finally, a prototype incorporating all these desirable characteristics can be manufactured and tested in *in vivo* animal studies. The animal model could be the rabbit; it has a large eye relative to its body, is easy to handle and breed, and more economical than with using dogs or primates (Gwon, 2008). It is already used to assess procedures such as cataract surgery, corneal transplantation, laser refractive surgery, retinal detachment surgery and intravitreal drug delivery. However, young rabbits have a more robust post-operative inflammatory response, greater than that seen in adult human eyes. This needs to be taken into account when assessing the post-operative stage.

If the results prove to be favourable, then the final stage would be to introduce the device in humans to see if the translation from 'bench-to-bedside' is successful.

References

Acosta, A. C., Espana, E. M., Yamamoto, H., Davis, S., Pinchuk, L., Weber, B. A. et al. (2006). A newly designed glaucoma drainage implant made of poly(styrene-b-isobutylene-b-styrene): biocompatibility and function in normal rabbit eyes. *Archives of Ophthalmology*, *124*, 1742-1749.

Advanced Glaucoma Intervention Study Investigators (2000). The Advanced Glaucoma Intervention Study (AGIS): 7. The relationship between control of intraocular pressure and visual field deterioration. *American Journal of Ophthalmology*, *130*, 429-440.

Agnifili, L., Costagliola, C., Figus, M., Iezzi, G., Piattelli, A., Carpineto, P. et al. (2012). Histological findings of failed gold micro shunts in primary open-angle glaucoma. *Graefes Archive for Clinical and Experimental Ophthalmology*, *250*, 143-149.

Akers, A., Gassman, M., & Smith, R. (2006). Flow Division. In *Hydraulic Power System Analysis* (pp. 299-334). New York: Taylor & Francis.

Allingham, R. R., Damji, K., Freedman, S., Moroi, S., & Shafranov, G. (2005). *Shield's Textbook of Glaucoma*. (5th ed.) Philadelphia: Lippincott Williams & Wilkins.

Alm, A. & Nilsson, S. F. (2009). Uveoscleral outflow - A review. *Experimental Eye Research*, *88*, 760-768.

Alodhayb, S., Morales, J., Edward, D. P., & Abu-Amero, K. K. (2013). Update on pediatric glaucoma. *Seminars in Ophthalmology*, *28*, 131-143.

Alwitry, A., Patel, V., & King, A. W. (2005). Fornix vs limbal-based trabeculectomy with mitomycin C. *Eye, 19*, 631-636.

Arriola-Villalobos, P., Martinez-de-la-Casa JM, Diaz-Valle, D., Fernandez-Perez, C., Garcia-Sanchez, J., & Garcia-Feijoo, J. (2012). Combined iStent trabecular micro-bypass stent implantation and phacoemulsification for coexistent open-angle glaucoma and cataract: a long-term study. *British Journal of Ophthalmology, 96*, 645-649.

Asejczyk-Widlicka, M., Srodka, D. W., Kasprzak, H., & Pierscionek, B. K. (2007). Modelling the elastic properties of the anterior eye and their contribution to maintenance of image quality: the role of the limbus. *Eye, 21*, 1087-1094.

Ayyala, R. S., Michelini-Norris, B., Flores, A., Haller, E., & Margo, C. E. (2000). Comparison of different biomaterials for glaucoma drainage devices: part 2. *Archives of Ophthalmology, 118*, 1081-1084.

Azuara-Blanco, A. & Katz, L. J. (1998). Dysfunctional filtering blebs. *Survey of Ophthalmology, 43*, 93-126.

Bacharach, J. (2012). Results through two years postoperative from prospective, randomized studies of second generation stents and cataract surgery in mild-moderate open-angle glaucoma. Poster presented at the 22nd Annual AGS Meeting; March 1, 2012; New York.

Bahar, I., Kaiserman, I., Trope, G. E., & Rootman, D. (2007). Non-penetrating deep sclerectomy for glaucoma surgery using the femtosecond laser: a laboratory model. *British Journal of Ophthalmology, 91*, 1713-1714.

Bahler, C. K., Hann, C. R., Fjield, T., Haffner, D., Heitzmann, H., & Fautsch, M. P. (2012). Second-generation trabecular meshwork bypass stent (iStent inject) increases outflow facility in cultured human anterior segments. *American Journal of Ophthalmology*, *153*, 1206-1213.

Barton, K., Gedde, S. J., Budenz, D. L., Feuer, W. J., & Schiffman, J. (2011). The Ahmed Baerveldt Comparison study. Methodology, baseline patient characteristics, and intraoperative complications. *Ophthalmology*, *118*, 435-442.

Batchelor, G. K. (2000). *An introduction to fluid mechanics*. Cambridge University Press.

Batterbury, M. & Wishart, P. K. (1993). Is high initial aqueous outflow of benefit in trabeculectomy? *Eye*, *7*, 109-112.

Benson, S. E., Mandal, K., Bunce, C. V., & Fraser, S. G. (2005). Is post-trabeculectomy hypotony a risk factor for subsequent failure? A case control study. *BMC Ophthalmology*, *5*, 7.

Beswick, J. A. & McCulloch, C. (1956). Effect of hyaluronidase on the viscosity of the aqueous humour. *British Journal of Ophthalmology*, *40*, 545-548.

Bettin, P. (2012). Postoperative management of penetrating and nonpenetrating external filtering procedures. *Developments in Ophthalmology*, *50*, 48-63.

Bevin, T. H., Molteno, A. C., & Herbison, P. (2008). Otago Glaucoma Surgery Outcome Study: long-term results of 841 trabeculectomies. *Clinical and Experimental Ophthalmology*, *36*, 731-737.

Bick, M. W. (1949). Use of tantalum for ocular drainage. *Archives of Ophthalmology*, *42*, 373-388.

Bietti, G. B. (1955). The present state of the use of plastics in eye surgery. *Acta Ophthalmologica*, 33, 337-370.

Bill, A. & Phillips, C. I. (1971). Uveoscleral drainage of aqueous humour in human eyes. *Experimental Eye Research*, 12, 275-281.

Bill, A. & Svedbergh, B. (1972). Scanning electron microscopic studies of the trabecular meshwork and the canal of Schlemm - an attempt to localize the main resistance to outflow of aqueous humor in man. *Acta Ophthalmologica*, 50, 295-320.

Binder, R. C. (1973). Dimensional Analysis and Dynamic Similarity. In *Fluid Mechanics* (5 ed., pp. 87-104). New Jersey: Prentice-Hall.

Birchall, W., Bedggood, A., & Wells, A. P. (2007). Do scleral flap dimensions influence reliability of intraocular pressure control in experimental trabeculectomy? *Eye*, 21, 402-407.

Birchall, W., Wakely, L., & Wells, A. P. (2006). The influence of scleral flap position and dimensions on intraocular pressure control in experimental trabeculectomy. *Journal of Glaucoma*, 15, 286-290.

Birchall, W. & Wells, A. P. (2008). The effect of scleral flap edge apposition on intraocular pressure control in experimental trabeculectomy. *Clinical and Experimental Ophthalmology*, 36, 353-357.

Blok, M. D., Kok, J. H., van Mil, C., Greve, E. L., & Kijlstra, A. (1990). Use of the Megasoft Bandage Lens for treatment of complications after trabeculectomy. *American Journal of Ophthalmology*, 110, 264-268.

Blondeau, P. & Phelps, C. D. (1981). Trabeculectomy vs thermosclerostomy. A randomized prospective clinical trial. *Archives of Ophthalmology*, 99, 810-816.

Boey, P. Y., Singhal, S., Perera, S. A., & Aung, T. (2012). Conventional and emerging treatments in the management of acute primary angle closure. *Clinical Ophthalmology*, 6, 417-424.

Boswell, C. A., Noecker, R. J., Mac, M., Snyder, R. W., & Williams, S. K. (1999). Evaluation of an aqueous drainage glaucoma device constructed of ePTFE. *Journal of Biomedical Materials Research*, 48, 591-595.

Breckenridge, R. R., Bartholomew, L. R., Crosson, C. E., & Kent, A. R. (2004). Outflow resistance of the Baerveldt glaucoma drainage implant and modifications for early postoperative intraocular pressure control. *Journal of Glaucoma*, 13, 396-399.

Britt, M. T., LaBree, L. D., Lloyd, M. A., Minckler, D. S., Heuer, D. K., Baerveldt, G. et al. (1999). Randomized clinical trial of the 350-mm² versus the 500-mm² Baerveldt implant: longer term results: is bigger better? *Ophthalmology*, 106, 2312-2318.

Broadway, D. C., Grierson, I., O'Brien, C., & Hitchings, R. A. (1994). Adverse effects of topical antiglaucoma medication. I. The conjunctival cell profile. *Archives of Ophthalmology*, 112, 1437-1445.

Brown, J., Pan, T., & Ziaie, B. (2003). In Vitro Simulation of Flow Characteristics of Valved Glaucoma Drainage Devices After Fibrous Capsule Formation. *Investigative Ophthalmology & Visual Science*, 44, 3308.

Brubaker, R. F. (1991). Flow of aqueous humor in humans [The Friedenwald Lecture]. *Investigative Ophthalmology & Visual Science*, 32, 3145-3166.

Brubaker, R. F. (2004). Goldmann's equation and clinical measures of aqueous dynamics. *Experimental Eye Research*, 78, 633-637.

Budenz, D. L., Barton, K., Feuer, W. J., Schiffman, J., Costa, V. P., Godfrey, D. G. et al. (2011). Treatment Outcomes in the Ahmed Baerveldt Comparison Study after 1 Year of Follow-up. *Ophthalmology*, *118*, 443-452.

Budenz, D. L., Hoffman, K., & Zacchei, A. (2001). Glaucoma filtering bleb dysesthesia. *American Journal of Ophthalmology*, *131*, 626-630.

Burchfield, J. C. & Kolker, A. E. (1995). Diagnosis and treatment of cyclodialysis clefts. *Journal of Glaucoma*, *4*, 207-213.

Butt, H. J., Graf, K., & Kappl, M. (2006). Contact angle phenomena and wetting. In *Physics and Chemistry of Interfaces* (2 ed., pp. 118-144). Wiley-VCH.

Buys, Y. M. (2013). Trabeculectomy with ExPRESS: weighing the benefits and cost. *Current Opinion in Ophthalmology*, *24*, 111-118.

Cairns, J. E. (1968). Trabeculectomy. Preliminary report of a new method. *American Journal of Ophthalmology*, *66*, 673-679.

Camras, L. J., Yuan, F., Fan, S., Samuelson, T. W., Ahmed, I. K., Schieber, A. T. et al. (2012). A novel Schlemm's Canal scaffold increases outflow facility in a human anterior segment perfusion model. *Investigative Ophthalmology & Visual Science*, *53*, 6115-6121.

Caprioli, J. (2011). The tube versus trabeculectomy study: why its findings may not change clinical practice? *American Journal of Ophthalmology*, *151*, 742-744.

Caprioli, J. & Coleman, A. L. (2010). Blood pressure, perfusion pressure, and glaucoma. *American Journal of Ophthalmology*, *149*, 704-712.

Cenedese, C. & Dalziel, S. (1998). Concentration and depth field determined by the light transmitted through a dyed solution. In *Proceedings of the 8th International Symposium on Flow Visualization*. G.M. Carlomagno & I. Grant (Eds.), (pp. 61.1-61.5).

Chai, C. & Loon, S. C. (2010). Meta-analysis of viscocanalostomy versus trabeculectomy in uncontrolled glaucoma. *Journal of Glaucoma*, 19, 519-527.

Cheng, J. W., Xi, G. L., Wei, R. L., Cai, J. P., & Li, Y. (2010). Efficacy and tolerability of nonpenetrating filtering surgery in the treatment of open-angle glaucoma: a meta-analysis. *Ophthalmologica*, 224, 138-146.

Cherecheanu, A. P., Garhofer, G., Schmidl, D., Werkmeister, R., & Schmetterer, L. (2013). Ocular perfusion pressure and ocular blood flow in glaucoma. *Current Opinion in Pharmacology*, 13, 36-42.

Cheung, J. C., Wright, M. M., Murali, S., & Pederson, J. E. (1997). Intermediate-term outcome of variable dose mitomycin C filtering surgery. *Ophthalmology*, 104, 143-149.

Christakis, P. G., Tsai, J. C., Kalenak, J. W., Zurakowski, D., Cantor, L. B., Kammer, J. A. et al. (2013). The Ahmed Versus Baerveldt Study - Three-Year Treatment Outcomes. *Ophthalmology*, 120, 2232-2240.

Clemente, P. (1980). [Goniotrepanation with Triangular Scleral Flap]. *Klinische Monatsblätter für Augenheilkunde*, 177, 455-458.

Collaborative Normal-Tension Glaucoma Study Group (1998a). Comparison of glaucomatous progression between untreated patients with normal-tension glaucoma

and patients with therapeutically reduced intraocular pressures. *American Journal of Ophthalmology*, 126, 487-497.

Collaborative Normal-Tension Glaucoma Study Group (1998b). The effectiveness of intraocular pressure reduction in the treatment of normal-tension glaucoma. *American Journal of Ophthalmology*, 126, 498-505.

Costa, V. P. & Arcieri, E. S. (2007). Hypotony maculopathy. *Acta Ophthalmologica Scandinavica*, 85, 586-597.

Czudowska, M. A., Ramdas, W. D., Wolfs, R. C., Hofman, A., De Jong, P. T., Vingerling, J. R. et al. (2010). Incidence of glaucomatous visual field loss: a ten-year follow-up from the Rotterdam Study. *Ophthalmology*, 117, 1705-1712.

Dahan, E., Ben Simon, G. J., & Lafuma, A. (2012). Comparison of trabeculectomy and Ex-PRESS implantation in fellow eyes of the same patient: a prospective, randomised study. *Eye*, 26, 703-710.

Dahan, E. & Carmichael, T. R. (2005). Implantation of a miniature glaucoma device under a scleral flap. *Journal of Glaucoma*, 14, 98-102.

Damji, K. F., Bovell, A. M., Hodge, W. G., Rock, W., Shah, K., Buhrmann, R. et al. (2006). Selective laser trabeculoplasty versus argon laser trabeculoplasty: results from a 1-year randomised clinical trial. *British Journal of Ophthalmology*, 90, 1490-1494.

Dandona, L., Dandona, R., Srinivas, M., Mandal, P., John, R. K., McCarty, C. A. et al. (2000). Open-angle glaucoma in an urban population in southern India: the Andhra Pradesh eye disease study. *Ophthalmology*, 107, 1702-1709.

de Barros, D. S., Gheith, M. E., Siam, G. A., & Katz, L. J. (2008). Releasable suture technique. *Journal of Glaucoma*, *17*, 414-421.

de Jong, L., Lafuma, A., Aguade, A. S., & Berdeaux, G. (2011). Five-year extension of a clinical trial comparing the EX-PRESS glaucoma filtration device and trabeculectomy in primary open-angle glaucoma. *Clinical Ophthalmology*, *5*, 527-533.

DeBry, P. W., Perkins, T. W., Heatley, G., Kaufman, P., & Brumback, L. C. (2002). Incidence of late-onset bleb-related complications following trabeculectomy with mitomycin. *Archives of Ophthalmology*, *120*, 297-300.

Dellaporta, A. (1975). Experiences with trepano-trabeculectomy. *Transactions - Section on Ophthalmology. American Academy of Ophthalmology and Otolaryngology*, *79*, OP362-OP371.

Dhingra, S. & Khaw, P. T. (2009). The Moorfields Safer Surgery System. *Middle East African Journal of Ophthalmology*, *16*, 112-115.

Downs, J. C., Roberts, M. D., & Sigal, I. A. (2011). Glaucomatous cupping of the lamina cribrosa: A review of the evidence for active progressive remodeling as a mechanism. *Experimental Eye Research*, *93*, 133-140.

Edelhauser, H. F. & Macrae, S. M. (1995). Irrigating and viscous solutions. In M. Sears & A. Tarkkeanen (Eds.), *Surgical Pharmacology of the Eye* (pp. 363-368). New York: Raven Press.

Edmunds, B., Bunce, C. V., Thompson, J. R., Salmon, J. F., & Wormald, R. P. (2004). Factors associated with success in first-time trabeculectomy for patients at low risk of failure with chronic open-angle glaucoma. *Ophthalmology*, *111*, 97-103.

Edmunds, B., Thompson, J. R., Salmon, J. F., & Wormald, R. P. (2001). The National Survey of Trabeculectomy. II. Variations in operative technique and outcome. *Eye, 15*, 441-448.

Egbert, P. R. & Lieberman, M. F. (1989). Internal suture occlusion of the Molteno glaucoma implant for the prevention of postoperative hypotony. *Ophthalmic Surgery, 20*, 53-56.

Eisenberg, D. L., Koo, E. Y., Hafner, G., & Schuman, J. S. (1999). In vitro flow properties of glaucoma implant devices. *Ophthalmic Surgery and Lasers, 30*, 662-667.

Elliot, R. H. (1909). Preliminary note on a new operative procedure for the establishment of a filtering cicatrix in the treatment of glaucoma. *Ophthalmoscope, 7*, 804-806.

Emi, K., Pederson, J. E., & Toris, C. B. (1989). Hydrostatic pressure of the suprachoroidal space. *Investigative Ophthalmology & Visual Science, 30*, 233-238.

Epstein, D. L., Hashimoto, J. M., & Grant, W. M. (1978). Serum obstruction of aqueous outflow in enucleated eyes. *American Journal of Ophthalmology, 86*, 101-105.

Estermann, S., Yuttitham, K., Chen, J. A., Lee, O. T., & Stamper, R. L. (2013). Comparative in vitro flow study of 3 different Ex-PRESS miniature glaucoma device models. *Journal of Glaucoma, 22*, 209-214.

European Directorate for the Quality of Medicines (2005a). Capillary Viscometer Method. In *European Pharmacopoeia* (5.0 ed., pp. 29-30). Council of Europe.

European Directorate for the Quality of Medicines (2005b). Dissolution Test For Solid Dosage Forms. In *European Pharmacopoeia* (5.0 ed., pp. 228-230). Council of Europe.

Every, S. G., Molteno, A. C., Bevin, T. H., & Herbison, P. (2006). Long-term results of Molteno implant insertion in cases of neovascular glaucoma. *Archives of Ophthalmology*, *124*, 355-360.

Fankhauser, F. & Giger, H. (1994). A model for fluid mechanisms in sclerostomy. *Graefes Archive for Clinical and Experimental Ophthalmology*, *232*, 379-385.

Fea, A. M. (2010). Phacoemulsification versus phacoemulsification with microbypass stent implantation in primary open-angle glaucoma: randomized double-masked clinical trial. *Journal of Cataract and Refractive Surgery*, *36*, 407-412.

Feiner, L. & Piltz-Seymour, J. R. (2003). Collaborative Initial Glaucoma Treatment Study: a summary of results to date. *Current Opinion in Ophthalmology*, *14*, 106-111.

Fernandez-Barrientos, Y., Garcia-Feijoo, J., Martinez-de-la-Casa, J. M., Pablo, L. E., Fernandez-Perez, C., & Sanchez, J. G. (2010). Fluorophotometric Study of the Effect of the Glaukos Trabecular Microbypass Stent on Aqueous Humor Dynamics. *Investigative Ophthalmology & Visual Science*, *51*, 3327-3332.

Figus, M., Lazzeri, S., Fogagnolo, P., Iester, M., Martinelli, P., & Nardi, M. (2011). Supraciliary shunt in refractory glaucoma. *British Journal of Ophthalmology*, *95*, 1537-1541.

Fink, A. J., Boys-Smith, J. W., & Brear, R. (1986). Management of large filtering blebs with the argon laser. *American Journal of Ophthalmology*, *101*, 695-699.

Fluorouracil Filtering Surgery Study Group (1996). Five-year follow-up of the Fluorouracil Filtering Surgery Study. *American Journal of Ophthalmology*, *121*, 349-366.

Foster, P. J., Buhrmann, R., Quigley, H. A., & Johnson, G. J. (2002). The definition and classification of glaucoma in prevalence surveys. *British Journal of Ophthalmology*, *86*, 238-242.

Fourman, S. & Wiley, L. (1989). Use of a collagen shield to treat a glaucoma filter bleb leak. *American Journal of Ophthalmology*, *107*, 673-674.

Francis, B. A. (1998). Characteristics of glaucoma drainage implants during dynamic and steady-state flow conditions. *Ophthalmology*, *105*, 1708-1714.

Francis, B. A., Singh, K., Lin, S. C., Hodapp, E., Jampel, H. D., Samples, J. R. et al. (2011). Novel glaucoma procedures: a report by the American Academy of Ophthalmology. *Ophthalmology*, *118*, 1466-1480.

Freedman, J. (1992). Clinical experience with the Molteno dual-chamber single-plate implant. *Ophthalmic Surgery*, *23*, 238-241.

Friberg, T. R. & Lace, J. W. (1988). A comparison of the elastic properties of human choroid and sclera. *Experimental Eye Research*, *47*, 429-436.

Fukuchi, T., Ueda, J., Yaoeda, K., Suda, K., Seki, M., & Abe, H. (2006). Comparison of fornix- and limbus-based conjunctival flaps in mitomycin C trabeculectomy with laser suture lysis in Japanese glaucoma patients. *Japanese Journal of Ophthalmology*, *50*, 338-344.

Gandolfi, S., Traverso, C. F., Bron, A., Sellem, E., Kaplan-Messas, A., & Belkin, M. (2002). Short-term results of a miniature draining implant for glaucoma in combined surgery with phacoemulsification. *Acta Ophthalmologica Scandinavica Supplement*, 236, 66.

Gandolfi, S. A., Vecchi, M., & Braccio, L. (1995). Decrease of intraocular pressure after subconjunctival injection of mitomycin in human glaucoma. *Archives of Ophthalmology*, 113, 582-585.

Gardiner, B.S., Smith, D.W., Coote, M., & Crowston, J.G. (2010). Computational Modeling of Fluid Flow and Intra-Ocular Pressure following Glaucoma Surgery. *PLoS ONE*, 5, e13178. doi:10.1371/journal.pone.0013178

Gedde, S. J., Herndon, L. W., Brandt, J. D., Budenz, D. L., Feuer, W. J., & Schiffman, J. C. (2012a). Postoperative complications in the Tube Versus Trabeculectomy (TVT) study during five years of follow-up. *American Journal of Ophthalmology*, 153, 804-814.

Gedde, S. J., Panarelli, J. F., Banitt, M. R., & Lee, R. K. (2013). Evidenced-based comparison of aqueous shunts. *Current Opinion in Ophthalmology*, 24, 87-95.

Gedde, S. J., Schiffman, J. C., Feuer, W. J., Herndon, L. W., Brandt, J. D., & Budenz, D. L. (2009). Three-year follow-up of the tube versus trabeculectomy study. *American Journal of Ophthalmology*, 148, 670-684.

Gedde, S. J., Schiffman, J. C., Feuer, W. J., Herndon, L. W., Brandt, J. D., & Budenz, D. L. (2012b). Treatment outcomes in the Tube Versus Trabeculectomy (TVT) study after five years of follow-up. *American Journal of Ophthalmology*, 153, 789-803.

Gerber, S. L., Cantor, L. B., & Sponsel, W. E. (1997). A comparison of postoperative complications from pressure-ridge Molteno implants versus Molteno implants with suture ligation. *Ophthalmic Surgery and Lasers*, 28, 905-910.

Gilbert, D. & Bond, B. (2007). Intraluminal pressure response in Baerveldt tube shunts: A comparison of modification techniques. *Journal of Glaucoma*, 16, 62-67.

Glaucoma Laser Trial Research Group (1990). The Glaucoma Laser Trial GLT 2. Results of Argon Laser Trabeculoplasty Versus Topical Medicines. *Ophthalmology*, 97, 1403-1413.

Glaucoma Laser Trial Research Group (1995). The Glaucoma Laser Trial (GLT) and glaucoma laser trial follow-up study: 7. Results. *American Journal of Ophthalmology*, 120, 718-731.

Goldmann, H. A. (1951). [Out-flow pressure, minute volume and resistance of the anterior chamber flow in man]. *Documenta Ophthalmologica*, 5-6, 278-356.

Good, T. J. & Kahook, M. Y. (2011). Assessment of bleb morphologic features and postoperative outcomes after Ex-PRESS drainage device implantation versus trabeculectomy. *American Journal of Ophthalmology*, 151, 507-513.

Gornall, A. G., Bardawill, C. J., & David, M. M. (1949). Determination of serum proteins by means of the biuret reaction. *Journal of Biological Chemistry*, 177, 751-766.

Grant, W. M. (1963). Experimental aqueous perfusion in enucleated human eyes. *Archives of Ophthalmology*, 69, 783-801.

Grehn, F., Hollo, G., Khaw, P., Overton, B., Wilson, R., Vogel, R. et al. (2007). Factors affecting the outcome of trabeculectomy: an analysis based on combined data

from two phase III studies of an antibody to transforming growth factor beta2, CAT-152. *Ophthalmology*, 114, 1831-1838.

Grieshaber, M. C. & Flammer, J. (2005). Blood flow in glaucoma. *Current Opinion in Ophthalmology*, 16, 79-83.

Gross, R. L. (2012). Glaucoma filtration surgery: trabeculectomy or tube shunt? *American Journal of Ophthalmology*, 153, 787-788.

Gulati, V., Ghate, D. A., Camras, C. B., & Toris, C. B. (2011). Correlations between parameters of aqueous humor dynamics and the influence of central corneal thickness. *Investigative Ophthalmology & Visual Science*, 52, 920-926.

Gwon, A. (2008). The Rabbit in Cataract/ IOL Surgery. In: Tsonis, P.A. (Ed.), *Animal Models in Eye Research* (pp. 184-204). Elsevier.

Harizman, N., Ben Cnaan, R., Goldenfeld, M., Levkovitch-Verbin, H., & Melamed, S. (2005). Donor scleral patch for treating hypotony due to leaking and/or overfiltering blebs. *Journal of Glaucoma*, 14, 492-496.

Haynes, W. L. & Alward, W. L. (1999). Control of intraocular pressure after trabeculectomy. *Survey of Ophthalmology*, 43, 345-355.

Heijl, A., Leske, M. C., Bengtsson, B., Hyman, L., Bengtsson, B., & Hussein, M. (2002). Reduction of intraocular pressure and glaucoma progression: results from the Early Manifest Glaucoma Trial. *Archives of Ophthalmology*, 120, 1268-1279.

Heller, V. (2011). Scale effects in physical hydraulic engineering models. *Journal of Hydraulic Research*, 49, 293-306.

Herbert, H. M., Viswanathan, A., Jackson, H., & Lightman, S. L. (2004). Risk factors for elevated intraocular pressure in uveitis. *Journal of Glaucoma*, 13, 96-99.

Hernandez-Verdejo, J. L., Teus, M. A., Roman, J. M., & Bolivar, G. (2007). Porcine Model to Compare Real-Time Intraocular Pressure during LASIK with a Mechanical Microkeratome and Femtosecond Laser. *Investigative Ophthalmology & Visual Science*, 48, 68-72.

Heuer, D. K., Lloyd, M. A., Abrams, D. A., Baerveldt, G., Minckler, D. S., Lee, M. B. et al. (1992). Which is better? One or two? A randomized clinical trial of single-plate versus double-plate Molteno implantation for glaucomas in aphakia and pseudophakia. *Ophthalmology*, 99, 1512-1519.

Hill, R. A., Aminlari, A., Sassani, J. W., & Michalski, M. (1990). Use of a symblepharon ring for treatment of over-filtration and leaking blebs after glaucoma filtration surgery. *Ophthalmic Surgery*, 21, 707-710.

Hondur, A. (2008). Nonpenetrating glaucoma surgery: Meta-analysis of recent results. *Journal of Glaucoma*, 17, 139-146.

Hueber, A., Roters, S., Jordan, J. F., & Konen, W. (2013). Retrospective analysis of the success and safety of Gold Micro Shunt Implantation in glaucoma. *BMC Ophthalmology*, 13, 35.

Ianchulev, T., Ahmed, I. K., Hoeh, H., Rau, M., & DeJuan, E. (2010). Minimally invasive ab interno suprachoroidal device (CyPass) for IOP control in open-angle glaucoma. AAO Annual Meeting; October 18-19, 2010; Chicago, IL.

Ishida, K., Netland, P. A., Costa, V. P., Shiroma, L., Khan, B., & Ahmed, I. I. (2006). Comparison of polypropylene and silicone Ahmed Glaucoma Valves. *Ophthalmology*, 113, 1320-1326.

Jacobi, P. C., Dietlein, T. S., Colling, T., & Krieglstein, G. K. (2000). Photoablative laser-grid trabeculectomy in glaucoma filtering surgery: histology and outflow facility measurements in porcine cadaver eyes. *Ophthalmic Surgery and Lasers*, 31, 49-54.

Jampel, H. D., Musch, D. C., Gillespie, B. W., Lichter, P. R., Wright, M. M., & Guire, K. E. (2005). Perioperative complications of trabeculectomy in the collaborative initial glaucoma treatment study (CIGTS). *American Journal of Ophthalmology*, 140, 16-22.

Jampel, H. D., Solus, J. F., Tracey, P. A., Gilbert, D. L., Loyd, T. L., Jefferys, J. L. et al. (2012). Outcomes and bleb-related complications of trabeculectomy. *Ophthalmology*, 119, 712-722.

Jim, M. H., Ho, H. H., Ko, R. L., Siu, C. W., Yiu, K. H., Lau, C. P. et al. (2010). Paclitaxel-eluting stents for chronically occluded saphenous vein grafts (EOS) study. *Journal of Interventional Cardiology*, 23, 40-45.

Johnson, C. S., Mian, S. I., Moroi, S., Epstein, D., Izatt, J., & Afshari, N. A. (2007). Role of corneal elasticity in damping of intraocular pressure. *Investigative Ophthalmology & Visual Science*, 48, 2540-2544.

Johnson, D. H. (2005). Trabecular meshwork and uveoscleral outflow models. *Journal of Glaucoma*, 14, 308-310.

Johnson, D. H. & Matsumoto, Y. (2000). Schlemm's canal becomes smaller after successful filtration surgery. *Archives of Ophthalmology*, 118, 1251-1256.

Johnson, M. (2006). 'What controls aqueous humour outflow resistance?'. *Experimental Eye Research*, 82, 545-557.

Johnson, M., Ethier, C. R., Kamm, R. D., Grant, W. M., Epstein, D. L., & Gaasterland, D. (1986). The flow of aqueous humor through micro-porous filters. *Investigative Ophthalmology & Visual Science*, 27, 92-97.

Jones, E., Clarke, J., & Khaw, P. T. (2005). Recent advances in trabeculectomy technique. *Current Opinion in Ophthalmology*, 16, 107-113.

Joo, S. H., Ko, M. K., & Choe, J. K. (1989). Outflow of aqueous humor following cyclodialysis or ciliochoroidal detachment in rabbit. *Korean Journal of Ophthalmology*, 3, 65-69.

Jordan, J. F., Engels, B. F., Dinslage, S., Dietlein, T. S., Ayertey, H. D., Roters, S. et al. (2006). A novel approach to suprachoroidal drainage for the surgical treatment of intractable glaucoma. *Journal of Glaucoma*, 15, 200-205.

Junemann, A. (2013). Twelve Month Outcomes Following Ab Interno Implantation of Suprachoroidal Stent and Postoperative Administration of Travoprost to Treat Open Angle Glaucoma. Poster presentation at the XXXI Congress of the ESCRS 5-9 October 2013, Amsterdam.

Juzych, M. S., Chopra, V., Banitt, M. R., Hughes, B. A., Kim, C., Goulas, M. T. et al. (2004). Comparison of long-term outcomes of selective laser trabeculoplasty versus argon laser trabeculoplasty in open-angle glaucoma. *Ophthalmology*, 111, 1853-1859.

Kajiwara, K. (1990). Repair of a leaking bleb with fibrin glue. *American Journal of Ophthalmology*, 109, 599-601.

Kangas, T. A., Greenfield, D. S., Flynn, H. W., Jr., Parrish, R. K., & Palmberg, P. (1997). Delayed-onset endophthalmitis associated with conjunctival filtering blebs. *Ophthalmology*, *104*, 746-752.

Kass, M. A., Gordon, M. O., Gao, F., Heuer, D. K., Higginbotham, E. J., Johnson, C. A. et al. (2010). Delaying treatment of ocular hypertension: the ocular hypertension treatment study. *Archives of Ophthalmology*, *128*, 276-287.

Kass, M. A., Heuer, D. K., Higginbotham, E. J., Johnson, C. A., Keltner, J. L., Miller, J. P. et al. (2002). The Ocular Hypertension Treatment Study: a randomized trial determines that topical ocular hypotensive medication delays or prevents the onset of primary open-angle glaucoma. *Archives of Ophthalmology*, *120*, 701-713.

Kersten-Gomez, I. & Dick, H. (2012). First results of the innovative minimal-invasive glaucoma surgery technique: the AqueSys Aquecentesis procedure. Presented at the Congress of the ESCRS; Sept 8-12 2012; Milan, Italy.

Khaw, P. T. (2001). Advances in glaucoma surgery: evolution of antimetabolite adjunctive therapy. *Journal of Glaucoma*, *10*, S81-S84.

Khaw, P. T., Chang, L., Wong, T. T., Mead, A., Daniels, J. T., & Cordeiro, M. F. (2001). Modulation of wound healing after glaucoma surgery. *Current Opinion in Ophthalmology*, *12*, 143-148.

Khaw, P. T., Chiang, M., Shah, P., Sii, F., Lockwood, A., & Khalili, A. (2012). Enhanced trabeculectomy: the Moorfields Safer Surgery System. *Developments in Ophthalmology*, *50*, 1-28.

Kim, C., Kim, Y., Choi, S., Lee, S., & Ahn, B. (2003). Clinical experience of e-PTFE membrane implant surgery for refractory glaucoma. *British Journal of Ophthalmology*, *87*, 63-70.

Kim, J., Allingham, R. R., Hall, J., Klitzman, B., Stinnett, S., & Asrani, S. (2013). Clinical Experience With a Novel Glaucoma Drainage Implant. *Journal of Glaucoma*. [Epub ahead of print].

Kimbrough, R. L., Stewart, R. H., Decker, W. L., & Praeger, T. C. (1982). Trabeculectomy: square or triangular scleral flap? *Ophthalmic Surgery*, *13*, 753.

Klein, B. E., Klein, R., Sponsel, W. E., Franke, T., Cantor, L. B., Martone, J. et al. (1992). Prevalence of glaucoma. The Beaver Dam Eye Study. *Ophthalmology*, *99*, 1499-1504.

Kobayashi, H. & Kobayashi, K. (2011). A comparison of the intraocular pressure lowering effect of adjustable suture versus laser suture lysis for trabeculectomy. *Journal of Glaucoma*, *20*, 228-233.

Krause, U. & Raunio, V. (1969). Proteins of the normal human aqueous humour. *Ophthalmologica*, *159*, 178-185.

Krause, U. & Raunio, V. (1970). The proteins of the pathologic human aqueous humour. An in vivo investigation. *Ophthalmologica*, *160*, 280-287.

Krupin, T. (1976). Valve implants in filtering surgery. *American Journal of Ophthalmology*, *81*, 232-235.

Kwon, Y. H., Fingert, J. H., Kuehn, M. H., & Alward, W. L. (2009). Primary open-angle glaucoma. *New England Journal of Medicine*, *360*, 1113-1124.

Ladas, J. G., Yu, F., Loo, R., Davis, J. L., Coleman, A. L., Levinson, R. D. et al. (2001). Relationship between aqueous humor protein level and outflow facility in patients with uveitis. *Investigative Ophthalmology & Visual Science*, 42, 2584-2588.

Lamping, K. A., Bellows, A. R., Hutchinson, B. T., & Afran, S. I. (1986). Long-term evaluation of initial filtration surgery. *Ophthalmology*, 93, 91-101.

Landau, L. D. & Lifshitz, E. M. (1986). *Theory of Elasticity. Course of Theoretical Physics*. (3 ed.) (vols. 7) Oxford: Elsevier.

Law, S. K., Shih, K., Tran, D. H., Coleman, A. L., & Caprioli, J. (2009). Long-term outcomes of repeat vs initial trabeculectomy in open-angle glaucoma. *American Journal of Ophthalmology*, 148, 685-695.

Lee, G. A., Chiang, M. Y., & Shah, P. (2006). Pig eye trabeculectomy-a wet-lab teaching model. *Eye*, 20, 32-37.

Lee, V. W. (1998). Glaucoma "Valves" - Truth versus Myth. *Ophthalmology*, 105, 567-568.

Leske, M. C., Heijl, A., Hussein, M., Bengtsson, B., Hyman, L., & Komaroff, E. (2003). Factors for glaucoma progression and the effect of treatment: the Early Manifest Glaucoma Trial. *Archives of Ophthalmology*, 121, 48-56.

Leydhecker, W., Akiyama, K., & Neumann, H. G. (1958). [Intraocular pressure in normal human eyes]. *Klin Monatsblätter Augenheilkd Augenarztl Fortbild*, 133, 662-670.

Lichter, P. R., Musch, D. C., Gillespie, B. W., Guire, K. E., Janz, N. K., Wren, P. A. et al. (2001). Interim clinical outcomes in the Collaborative Initial Glaucoma

Treatment Study comparing initial treatment randomized to medications or surgery. *Ophthalmology*, 108, 1943-1953.

Lim, K. S. (1998). Glaucoma drainage devices; past, present, and future. *British Journal of Ophthalmology*, 82, 1083-1089.

Lim, K. S. (1999). Cell and protein adhesion studies in glaucoma drainage device development. *British Journal of Ophthalmology*, 83, 1168-1171.

Lim, K. S., Wells, A. P., & Khaw, P. T. (2002). Needle perforations of Molteno tubes. *Journal of Glaucoma*, 11, 434-438.

Liu, H., Fan, S., Gulati, V., Camras, L. J., Zhan, G., Ghate, D. et al. (2011). Aqueous humor dynamics during the day and night in healthy mature volunteers. *Archives of Ophthalmology*, 129, 269-275.

Lloyd, M. A., Baerveldt, G., Fellenbaum, P. S., Sidoti, P. A., Minckler, D. S., Martone, J. F. et al. (1994). Intermediate-term results of a randomized clinical trial of the 350- versus the 500-mm² Baerveldt implant. *Ophthalmology*, 101, 1456-1463.

Lobler, M., Sternberg, K., Stachs, O., Allemann, R., Grabow, N., Roock, A. et al. (2011). Polymers and drugs suitable for the development of a drug delivery drainage system in glaucoma surgery. *Journal of Biomedical Materials Research Part B: Applied Biomaterials*, 97, 388-395.

Luntz, M. H. & Livingston, D. G. (1977). Trabeculotomy ab externo and trabeculectomy in congenital and adult-onset glaucoma. *American Journal of Ophthalmology*, 83, 174-179.

Luong, Q. M., Shang, L., Ang, M., Kong, J. F., Peng, Y., Wong, T. T. et al. (2013). A New Design and Application of Bioelastomers for Better Control of

Intraocular Pressure in a Glaucoma Drainage Device. *Advanced Healthcare Materials* [Epub ahead of print].

Lusthaus, J., Kubay, O., Karim, R., Wechsler, D., & Booth, F. (2010). Primary trabeculectomy with mitomycin C: safety and efficacy at 2-years. *Clinical & Experimental Ophthalmology*, *38*, 831-838.

Lutjen-Drecoll, E. & Barany, E. H. (1974). Functional and electron microscopic changes in the trabecular meshwork remaining after trabeculectomy in cynomolgus monkeys. *Investigative Ophthalmology & Visual Science*, *13*, 511-524.

Mackenzie, P. J., Schertzer, R. M., & Isbister, C. M. (2007). Comparison of silicone and polypropylene Ahmed glaucoma valves: two-year follow-up. *Canadian Journal of Ophthalmology*, *42*, 227-232.

Maeda, M., Watanabe, M., & Ichikawa, K. (2013). Evaluation of trabectome in open-angle glaucoma. *Journal of Glaucoma*, *22*, 205-208.

Maepea, O. & Bill, A. (1989). The pressures in the episcleral veins, Schlemm's canal and the trabecular meshwork in monkeys: effects of changes in intraocular pressure. *Experimental Eye Research*, *49*, 645-663.

Maris, P. J. G., Ishida, K., & Netland, P. A. (2007). Comparison of trabeculectomy with Ex-PRESS miniature glaucoma device implanted under scleral flap. *Journal of Glaucoma*, *16*, 14-19.

McEwen, W. K. (1958). Application of Poiseuille's law to aqueous outflow. *Archives of Ophthalmology*, *60*, 290.

Melamed, S., Ashkenazi, I., Glovinski, J., & Blumenthal, M. (1990). Tight scleral flap trabeculectomy with postoperative laser suture lysis. *American Journal of Ophthalmology*, *109*, 303-309.

Melamed, S., Ben Simon, G. J., Goldenfeld, M., & Simon, G. (2009). Efficacy and safety of gold micro shunt implantation to the supraciliary space in patients with glaucoma: a pilot study. *Archives of Ophthalmology*, *127*, 264-269.

Melamed, S., Hersh, P., Kersten, D., Lee, D. A., & Epstein, D. L. (1986). The use of glaucoma shell tamponade in leaking filtration blebs. *Ophthalmology*, *93*, 839-842.

Mendicino, M. E., Lynch, M. G., Drack, A., Beck, A. D., Harbin, T., Pollard, Z. et al. (2000). Long-term surgical and visual outcomes in primary congenital glaucoma: 360 degrees trabeculotomy versus goniotomy. *Journal of the American Association for Pediatric Ophthalmology and Strabismus*, *4*, 205-210.

Mendrinis, E. & Shaarawy, T. (2008). Nonpenetrating Glaucoma Surgery: Indications, Techniques, Complications, and Results. In D.M. Albert, J. W. Miller, D. T. Azar, & B. A. Blodi (Eds.), *Albert & Jakobiec's Principles & Practice of Ophthalmology* (3 ed., Saunders Elsevier).

Minckler, D. S., Shamma, A., Wilcox, M., & Ogden, T. E. (1987). Experimental studies of aqueous filtration using the Molteno implant. *Transactions of the American Ophthalmological Society*, *85*, 368-392.

Mitchell, P., Smith, W., Attebo, K., & Healey, P. R. (1996). Prevalence of open-angle glaucoma in Australia. The Blue Mountains Eye Study. *Ophthalmology*, *103*, 1661-1669.

Molteno, A. C. (1969). New implant for drainage in glaucoma. Clinical trial. *British Journal of Ophthalmology*, 53, 606-615.

Molteno, A. C., Bevin, T. H., Herbison, P., & Houliston, M. J. (2001). Otago glaucoma surgery outcome study: long-term follow-up of cases of primary glaucoma with additional risk factors drained by Molteno implants. *Ophthalmology*, 108, 2193-2200.

Molteno, A. C., Polkinghorne, P. J., & Bowbyes, J. A. (1986). The vicryl tie technique for inserting a draining implant in the treatment of secondary glaucoma. *Australian and New Zealand Journal of Ophthalmology*, 14, 343-354.

Molteno, A. C., Straughan, J. L., & Ancker, E. (1976). Long tube implants in the management of glaucoma. *South African Medical Journal*, 50, 1062-1066.

Mosaed, S., Dustin, L., & Minckler, D. S. (2009). Comparative outcomes between newer and older surgeries for glaucoma. *Transactions of the American Ophthalmological Society*, 107, 127-133.

Moss, E. (2008). Assessment of Closing Pressure in Silicone Ahmed FP7 Glaucoma Valves. *Journal of Glaucoma*, 17, 489-493.

Nair, L.S., & Laurencin, C.T. (2007). Biodegradable polymers as biomaterials. *Progress in Polymer Science*, 32, 762–798.

Nassiri, N., Kamali, G., Rahnavardi, M., Mohammadi, B., Nassiri, S., Rahmani, L. et al. (2010). Ahmed glaucoma valve and single-plate Molteno implants in treatment of refractory glaucoma: a comparative study. *American Journal of Ophthalmology*, 149, 893-902.

National Physical Laboratory (2013). Kaye and Laby Tables of Physical and Chemical Constants. National Physical Laboratory [On-line]. Available: <http://www.kayelaby.npl.co.uk/>

Nicoli, S., Ferrari, G., Quarta, M., Macaluso, C., Govoni, P., Dallatana, D. et al. (2009). Porcine sclera as a model of human sclera for in vitro transport experiments: histology, SEM, and comparative permeability. *Molecular Vision*, 15, 259-266.

Nouri-Mahdavi, K., Hoffman, D., Coleman, A. L., Liu, G., Li, G., Gaasterland, D. et al. (2004). Predictive factors for glaucomatous visual field progression in the Advanced Glaucoma Intervention Study. *Ophthalmology*, 111, 1627-1635.

Nuyts, R. M., Felten, P. C., Pels, E., Langerhorst, C. T., Geijssen, H. C., Grossniklaus, H. E. et al. (1994). Histopathologic effects of mitomycin C after trabeculectomy in human glaucomatous eyes with persistent hypotony. *American Journal of Ophthalmology*, 118, 225-237.

Oatts, J. T., Zhang, Z., Tseng, H., Shields, M. B., Sinard, J. H., & Loewen, N. A. (2013). In vitro and in vivo comparison of two suprachoroidal shunts. *Investigative Ophthalmology & Visual Science*, 54, 5416-5423.

Oosterbroek, R. E., Berenschot, J. W., Schlautmann, S., Lammerink, T. S. J., Berg, A. V. D., & Elwenspoek, M. C. (1998). Modeling and Validation of Fluid Structure Interactions in Passive Micro Valves. Presented at MSM International Conference on Modeling and Simulation of Microsystems; April 6-8, 1998, Santa Clara, CA, USA.

Pallikaris, I. G., Dastiridou, A. I., Tsilimbaris, M. K., Karyotakis, N. G., & Ginis, H. S. (2010). Ocular rigidity. *Expert Review of Ophthalmology*, 5, 343-351.

Palmberg, P. F. (1996). Compression sutures - A new treatment for leaking or painful filtering blebs [ARVO abstract]. *Investigative Ophthalmology & Visual Science*, 37.

Palmberg, P. F., Battle, J. F., Albuquerque, R., Corona-Peralta, A., Riss, I., Parrish, R. et al. (2013). A Novel Minimally Invasive Drainage Implant (the MIDI-Arrow): One-Two Year Follow Up. Presented at the Meeting of the Association for Research in Vision and Ophthalmology; Seattle, USA; 5-9 May 2013.

Pan, T. (2002). A microfluid test-bed with nanopore membranes for in-vitro simulation of flow characteristics of glaucoma drainage devices. *Annual International Conference of the IEEE Engineering in Medicine and Biology - Proceedings*, 3, 1830-1831.

Pan, T. (2005). Modeling and characterization of a valved glaucoma drainage device with implications for enhanced therapeutic efficacy. *IEEE transactions on bio-medical engineering*, 52, 948-951.

Panek, W. C., Holland, G. N., Lee, D. A., & Christensen, R. E. (1990). Glaucoma in patients with uveitis. *British Journal of Ophthalmology*, 74, 223-227.

Pederson, J. E., Gaasterland, D. E., & MacLellan, H. M. (1979). Experimental ciliochoroidal detachment. Effect on intraocular pressure and aqueous humor flow. *Archives of Ophthalmology*, 97, 536-541.

Ponnusamy, T., Yu, H., John, V. T., Ayyala, R. S., & Blake, D. A. (2013). A Novel Antiproliferative Drug Coating for Glaucoma Drainage Devices. *Journal of Glaucoma*. [Epub ahead of print].

Porter, J. M., Krawczyk, C. H., & Carey, R. F. (1997). In vitro flow testing of glaucoma drainage devices. *Ophthalmology*, *104*, 1701-1707.

Prata, J. A., Jr., Mermoud, A., LaBree, L., & Minckler, D. S. (1995). In vitro and in vivo flow characteristics of glaucoma drainage implants. *Ophthalmology*, *102*, 894-904.

Quaranta, L., Katsanos, A., Russo, A., & Riva, I. (2013). 24-hour intraocular pressure and ocular perfusion pressure in glaucoma. *Survey of Ophthalmology*, *58*, 26-41.

Quigley, H. A. (2011). Glaucoma. *Lancet*, *377*, 1367-1377.

Quigley, H. A. & Broman, A. T. (2006). The number of people with glaucoma worldwide in 2010 and 2020. *British Journal of Ophthalmology*, *90*, 262-267.

Quintessenza, J. A., Jacobs, J. P., Chai, P. J., Morell, V. O., & Lindberg, H. (2010). Polytetrafluoroethylene Bicuspid Pulmonary Valve Implantation: Experience with 126 Patients. *World Journal for Pediatric and Congenital Heart Surgery*, *1*, 20-27.

Rahman, A., Mendonca, M., Simmons, R. B., & Simmons, R. J. (2000). Hypotony after glaucoma filtration surgery. *International Ophthalmology Clinics*, *40*, 127-136.

Rao, K. (2009). New devices in glaucoma surgery. *Expert Review of Ophthalmology*, *4*, 491-504.

Razeghinejad, M. R. & Spaeth, G. L. (2011). A history of the surgical management of glaucoma. *Optometry & Vision Science*, *88*, E39-E47.

Ribe, N. M. (2001). Bending and stretching of thin viscous sheets. *Journal of Fluid Mechanics*, 433, 135-160.

Rivier, D., Roy, S., & Mermoud, A. (2007). Ex-PRESS R-50 miniature glaucoma implant insertion under the conjunctiva combined with cataract extraction. *Journal of Cataract and Refractive Surgery*, 33, 1946-1952.

Rollett, M. & Moreau, M. (1907). Le drainage au crin de la chambre anteriure contre l'hypotonie et la douleur. *Rev Gen Ophtal*, 26, 289-292.

Romaniuk, W. (1999). Valve implants of glaucoma pressure regulator for refractory glaucoma: own experience. *Klinika Oczna*, 101, 459-461.

Rosenquist, R. (1989). Outflow resistance of enucleated human eyes at two different perfusion pressures and different extents of trabeculotomy. *Current Eye Research*, 8, 1233-1240.

Ross, A., Blake, R. C., & Ayyala, R. S. (2010). Surface tension of aqueous humor. *Journal of Glaucoma*, 19, 456-459.

Row, H. (1934). Operation to control glaucoma. *Archives of Ophthalmology*, 12, 325-329.

Ruderman, J. M. & Allen, R. C. (1985). Simmons' tamponade shell for leaking filtration blebs. *Archives of Ophthalmology*, 103, 1708-1710.

Sahiner, N., Kravitz, D. J., Qadir, R., Blake, D. A., Haque, S., John, V. T. et al. (2009). Creation of a drug-coated glaucoma drainage device using polymer technology: in vitro and in vivo studies. *Archives of Ophthalmology*, 127, 448-453.

Salim, S. (2012). Current variations of glaucoma filtration surgery. *Current Opinion in Ophthalmology*, 23, 89-95.

Samuelson, T. W., Katz, L. J., Wells, J. M., Duh, Y. J., & Giamporcaro, J. E. (2011). Randomized evaluation of the trabecular micro-bypass stent with phacoemulsification in patients with glaucoma and cataract. *Ophthalmology*, 118, 459-467.

Samuelson, T. W., Pfeiffer, N., & Lorenz, K. (2012). Six month results from a prospective, multicenter study of a nickel-titanium Schlemm's canal scaffold for IOP reduction in open angle glaucoma. Poster presented at the 22nd Annual Meeting of the American Glaucoma Society; March 1, 2012; New York.

Sanchez, I., Martin, R., Ussa, F., & Fernandez-Bueno, I. (2011). The parameters of the porcine eyeball. *Graefes Archive for Clinical and Experimental Ophthalmology*, 249, 475-482.

Sayed, Y. E. & Awadein, A. (2013). Polypropylene vs silicone Ahmed valve with adjunctive mitomycin C in paediatric age group: a prospective controlled study. *Eye*, 27, 728-34.

Sayers, R. D., Raptis, S., Berce, M., & Miller, J. H. (1998). Long-term results of femorotibial bypass with vein or polytetrafluoroethylene. *British Journal of Surgery*, 85, 934-938.

Scheie, H. G. (1958). Retraction of scleral wound edges as a fistulizing procedure for glaucoma. *Transactions - American Academy of Ophthalmology and Otolaryngology*, 62, 803-811.

Schubert, H. D. (1996). Postsurgical hypotony: relationship to fistulization, inflammation, chorioretinal lesions, and the vitreous. *Survey of Ophthalmology*, 41, 97-125.

Schwartz, G. F., Robin, A. L., Wilson, R. P., Suan, E. P., Pheasant, T. R., & Prensky, J. G. (1996). Resuturing the scleral flap leads to resolution of hypotony maculopathy. *Journal of Glaucoma*, 5, 246-251.

Seah, S. K., Prata, J. A., Jr., Minckler, D. S., Baerveldt, G., Lee, P. P., & Heuer, D. K. (1995). Hypotony following trabeculectomy. *Journal of Glaucoma*, 4, 73-79.

Sen, H. N., Drye, L. T., Goldstein, D. A., Larson, T. A., Merrill, P. T., Pavan, P. R. et al. (2012). Hypotony in patients with uveitis: The Multicenter Uveitis Steroid Treatment (MUST) Trial. *Ocular Immunology and Inflammation*, 20, 104-112.

Shaarawy, T., Wu, R., Mermoud, A., Flammer, J., & Haefliger, I. O. (2004). Influence of non-penetrating glaucoma surgery on aqueous outflow facility in isolated porcine eyes. *British Journal of Ophthalmology*, 88, 950-952.

Shaarawy, T. M., Sherwood, M. B., Hitchings, R. A., & Crowston, J. G. (2009). *Glaucoma: Expert Consult. Volume 2 Surgical Management*. Philadelphia: Saunders Elsevier.

Shah, P., Agrawal, P., Khaw, P. T., Shafi, F., & Sii, F. (2012). ReGAE 7: long-term outcomes of augmented trabeculectomy with mitomycin C in African Caribbean patients. *Clinical and Experimental Ophthalmology*, 40, e176-e182.

Shah, S. M., Spalton, D. J., & Taylor, J. C. (1992). Correlations between laser flare measurements and anterior chamber protein concentrations. *Investigative Ophthalmology & Visual Science*, 33, 2878-2884.

Sherwood, M. B. & Smith, M. F. (1993). Prevention of early hypotony associated with Molteno implants by a new occluding stent technique. *Ophthalmology*, *100*, 85-90.

Shields, M. B., Scroggs, M. W., Sloop, C. M., & Simmons, R. B. (1993). Clinical and histopathologic observations concerning hypotony after trabeculectomy with adjunctive mitomycin C. *American Journal of Ophthalmology*, *116*, 673-683.

Shuster, J. N., Krupin, T., Kolker, A. E., & Becker, B. (1984). Limbus- v fornix-based conjunctival flap in trabeculectomy. A long-term randomized study. *Archives of Ophthalmology*, *102*, 361-362.

Siddique, S. S., Suelves, A. M., Baheti, U., & Foster, C. S. (2013). Glaucoma and uveitis. *Survey of Ophthalmology*, *58*, 1-10.

Siewert, S., Schultze, C., Schmidt, W., Hinze, U., Chichkov, B., Wree, A. et al. (2012). Development of a micro-mechanical valve in a novel glaucoma implant. *Biomedical Microdevices*, *14*, 907-920.

Sigal, I. A. & Ethier, C. R. (2009). Biomechanics of the optic nerve head. *Experimental Eye Research*, *88*, 799-807.

Siggers, J. H. & Ethier, C. R. (2011). Fluid Mechanics of the Eye. *Annual Review of Fluid Mechanics*, *44*, 347-372.

Sihota, R., Dada, T., Gupta, S. D., Sharma, S., Arora, R., & Agarwal, H. C. (2000). Conjunctival dysfunction and mitomycin C-induced hypotony. *Journal of Glaucoma*, *9*, 392-397.

Simmons, R. J. & Kimbrough, R. L. (1979). Shell tamponade in filtering surgery for glaucoma. *Ophthalmic Surgery*, *10*, 17-34.

Singh, K. & Gedde, S. J. (2011). Interpretation and misinterpretation of results from the tube versus trabeculectomy study. *International Ophthalmology Clinics*, 51, 141-154.

Smith, M. F., Magauran, R. G., III, Betchkal, J., & Doyle, J. W. (1995). Treatment of postfiltration bleb leaks with autologous blood. *Ophthalmology*, 102, 868-871.

Smith, M. F., Sherwood, M. B., & McGorray, S. P. (1992). Comparison of the double-plate Molteno drainage implant with the Schocket procedure. *Archives of Ophthalmology*, 110, 1246-1250.

Souza, C., Tran, DH., Loman, J., Law, SK., Coleman, AL., & Caprioli, J. (2007). Long-term Outcomes of Ahmed Glaucoma Valve Implantation in Refractory Glaucomas. *American Journal of Ophthalmology*, 144, 893-900.

Spaeth, G. L., Joseph, N. H., & Fernandes, E. (1975). Trabeculectomy: a re-evaluation after three years and a comparison with Scheie's procedure. *Ophthalmic Surgery*, 6, 27-38.

Spiegel, D., Katz, L. J., & McNamara, J. A. (1990). Surgical repair of a traumatic cyclodialysis cleft after laser failure. *Ophthalmic Surgery*, 21, 372-373.

Stalmans, I. (2006). Safe trabeculectomy technique: long term outcome. *British Journal of Ophthalmology*, 90, 44-47.

Starita, R. J., Fellman, R. L., Spaeth, G. L., & Poryzees, E. M. (1984). Effect of varying size of scleral flap and corneal block on trabeculectomy. *Ophthalmic Surgery*, 15, 484-487.

Stay, M. S., Pan, T., Brown, J. D., Ziaie, B., & Barocas, V. H. (2005). Thin-film coupled fluid-solid analysis of flow through the Ahmed glaucoma drainage device. *Journal of Biomechanical Engineering*, *127*, 776-781.

Stefansson, J. (1925). An operation for glaucoma. *American Journal of Ophthalmology*, *8*, 681-693.

Stewart, R. M., Diamond, J. G., Ashmore, E. D., & Ayyala, R. S. (2005). Complications following Ex-press glaucoma shunt implantation. *American Journal of Ophthalmology*, *140*, 340-341.

Suh, M. H., Park, K. H., Kim, T. W., & Kim, D. M. (2007). The efficacy of a modified ACTSEB (anterior chamber tube shunt to an encircling band) procedure. *Journal of Glaucoma*, *16*, 622-626.

Taglia, D. P., Perkins, T. W., Gangnon, R., Heatley, G. A., & Kaufman, P. L. (2002). Comparison of the Ahmed Glaucoma Valve, the Krupin Eye Valve with Disk, and the double-plate Molteno implant. *Journal of Glaucoma*, *11*, 347-353.

Tamm, E. R. (2009). The trabecular meshwork outflow pathways: structural and functional aspects. *Experimental Eye Research*, *88*, 648-655.

The Merck Index (1976). *The Merck Index: An Encyclopedia of Chemicals, Drugs, and Biologicals*. (9 ed.) New Jersey: Merck & Co.

Thomas, R., Sekhar, G. C., & Kumar, R. S. (2004). Glaucoma management in developing countries: medical, laser, and surgical options for glaucoma management in countries with limited resources. *Current Opinion in Ophthalmology*, *15*, 127-131.

Thompson, A. M., Molteno, A. C., Bevin, T. H., & Herbison, P. (2013). Otago glaucoma surgery outcome study: comparative results for the 175-mm² Molteno 3 and double-plate Molteno implants. *JAMA Ophthalmology*, *131*, 155-159.

Tomlinson, C. P., Belcher, C. D., III, Smith, P. D., & Simmons, R. J. (1987). Management of leaking filtration blebs. *Annals of Ophthalmology*, *19*, 405-8, 411.

Toris, C. B. & Camras, C. B. (2008). Aqueous Humor Dynamics II. Clinical Studies. In M. Civan (Ed.), *The Eye's Aqueous Humor* (2 ed., pp. 231-272). Salt Lake City: Academic Press.

Toris, C. B. & Pederson, J. E. (1985). Effect of intraocular pressure on uveoscleral outflow following cyclodialysis in the monkey eye. *Investigative Ophthalmology & Visual Science*, *26*, 1745-1749.

Toris, C. B. & Pederson, J. E. (1987). Aqueous humor dynamics in experimental iridocyclitis. *Investigative Ophthalmology & Visual Science*, *28*, 477-481.

Toris, C. B., Yablonski, M. E., Wang, Y. L., & Camras, C. B. (1999). Aqueous humor dynamics in the aging human eye. *American Journal of Ophthalmology*, *127*, 407-412.

Tran, D. H., Souza, C., Ang, M. J., Loman, J., Law, S. K., Coleman, A. L. et al. (2009). Comparison of long-term surgical success of Ahmed Valve implant versus trabeculectomy in open-angle glaucoma. *British Journal of Ophthalmology*, *93*, 1504-1509.

Traverso, C. E., De Feo, F., Messas-Kaplan, A., Denis, P., Levartovsky, S., Sellem, E. et al. (2005). Long term effect on IOP of a stainless steel glaucoma drainage

implant (Ex-PRESS) in combined surgery with phacoemulsification. *British Journal of Ophthalmology*, 89, 425-429.

Tripathi, R. C., Millard, C. B., & Tripathi, B. J. (1989). Protein composition of human aqueous humor: SDS-PAGE analysis of surgical and post-mortem samples. *Experimental Eye Research*, 48, 117-130.

Tse, K. M., Lee, H. P., Shabana, N., Loon, S. C., Watson, P. G., & Thean, S. Y. L. H. (2012). Do shapes and dimensions of scleral flap and sclerostomy influence aqueous outflow in trabeculectomy? A finite element simulation approach. *British Journal of Ophthalmology*, 96, 432-437.

Varma, R., Flynn, W. J., Marquis, R., Craven, E. R., & Bacharach, J. (2012). Devices in Development. *Glaucoma Today*, 10, 44-54.

Vass, C., Hirn, A. E., Unger, B. W., Mayr, B. M., Georgopoulos, A. G., Rainer, A. et al. (2004). Human aqueous humor viscosity in cataract, primary open angle glaucoma and pseudoexfoliation syndrome. *Investigative Ophthalmology & Visual Science*, 45, E-Abstract 503.

Vernon, S. A., Gorman, C., & Zambarakji, H. J. (1998). Medium to long-term intraocular pressure control following small flap trabeculectomy (microtrabeculectomy) in relatively low risk eyes. *British Journal of Ophthalmology*, 82, 1383-1386.

Vernon, S. A., Zambarakji, H. J., Potgieter, F., Evans, J., & Chell, P. B. (1999). Topographic and keratometric astigmatism up to 1 year following small flap trabeculectomy (microtrabeculectomy). *British Journal of Ophthalmology*, 83, 779-782.

Villamarina, A., Roya, S., Hasballaa, R., Vardoulisa, O., Reymonda, P., & Stergiopoulos, N. (2012). 3D simulation of the aqueous flow in the human eye. *Medical Engineering & Physics* 34, 1462–1470.

Wagner, J. A., Edwards, A., & Schuman, J. S. (2004). Characterization of uveoscleral outflow in enucleated porcine eyes perfused under constant pressure. *Investigative Ophthalmology & Visual Science*, 45, 3203-3206.

Wamsley, S., Moster, M. R., Rai, S., Alvim, H. S., & Fontanarosa, J. (2004). Results of the use of the Ex-PRESS miniature glaucoma implant in technically challenging, advanced glaucoma cases: a clinical pilot study. *American Journal of Ophthalmology*, 138, 1049-1051.

Wang, W., Zhou, M., Huang, W., & Zhang, X. (2013). Ex-PRESS Implantation Versus Trabeculectomy in Uncontrolled Glaucoma: A Meta-Analysis. *PLoS One*, 8, e63591.

Watson, P. G. & Barnett, F. (1975). Effectiveness of Trabeculectomy in Glaucoma. *American Journal of Ophthalmology*, 79, 831-845.

Weinreb, R. N. & Khaw, P. T. (2004). Primary open-angle glaucoma. *Lancet*, 363, 1711-1720.

Weinreb, R. N. & Lindsey, J. D. (2005). The importance of models in glaucoma research. *Journal of Glaucoma*, 14, 302-304.

Wells, A. P., Bunce, C., & Khaw, P. T. (2004). Flap and suture manipulation after trabeculectomy with adjustable sutures: Titration of flow and intraocular pressure in guarded filtration surgery. *Journal of Glaucoma*, 13, 400-406.

Wells, A. P., Cordeiro, M. F., Bunce, C., & Khaw, P. T. (2003). Cystic bleb formation and related complications in limbus- versus fornix-based conjunctival flaps in pediatric and young adult trabeculectomy with mitomycin C. *Ophthalmology*, *110*, 2192-2197.

Wells, A. P., Marks, J., & Khaw, P. T. (2005). Spontaneous inferior subconjunctival haemorrhages in association with circumferential drainage blebs. *Eye*, *19*, 269-272.

Wilkins, M., Indar, A., & Wormald, R. (2005). Intra-operative mitomycin C for glaucoma surgery. *Cochrane Database of Systematic Reviews*, CD002897.

Wilson, M. R., Mendis, U., Smith, S. D., & Paliwal, A. (2000). Ahmed glaucoma valve implant vs trabeculectomy in the surgical treatment of glaucoma: a randomized clinical trial. *American Journal of Ophthalmology*, *130*, 267-273.

Wilson, R. P., Cantor, L., Katz, L. J., Schmidt, C. M., Steinmann, W. C., & Allee, S. (1992). Aqueous shunts. Molteno versus Schocket. *Ophthalmology*, *99*, 672-676.

Wise, J. B. (1993). Treatment of chronic postfiltration hypotony by intrableb injection of autologous blood. *Archives of Ophthalmology*, *111*, 827-830.

Wishart, P. K. (2009). Interpretation of the glaucoma "landmark studies". *British Journal of Ophthalmology*, *93*, 561-562.

Wolner, B., Liebmann, J. M., Sassani, J. W., Ritch, R., Speaker, M., & Marmor, M. (1991). Late bleb-related endophthalmitis after trabeculectomy with adjunctive 5-fluorouracil. *Ophthalmology*, *98*, 1053-1060.

Wong, M. H., Husain, R., Ang, B. C., Gazzard, G., Foster, P. J., Htoon, H. M. et al. (2013). The Singapore 5-Fluorouracil trial: Intraocular pressure outcomes at 8 years. *Ophthalmology*, *120*, 1127-1134.

Wong, T. T., Khaw, P. T., Aung, T., Foster, P. J., Htoon, H. M., Oen, F. T. S. et al. (2009). The Singapore 5-Fluorouracil Trabeculectomy Study: Effects on Intraocular Pressure Control and Disease Progression at 3 Years. *Ophthalmology*, *116*, 175-184.

World Health Organisation (2013). Priority eye diseases - Glaucoma. World Health Organisation [On-line]. Available:

<http://www.who.int/blindness/causes/priority/en/index7.html>

Xu, W., Yao, K., Wu, W., Li, Z., & Ye, P. (2010). Change in outflow pathway of porcine eyes in vitro by nonpenetrating filtering surgery. *Canadian Journal of Ophthalmology*, *45*, 632-636.

Young, B., Lowe, J. S., Stevens, A., & Heath, J. W. (2006). Blood. In *Wheater's Functional Histology: A Text and Colour Atlas* (5 ed., pp. 46-64). Philadelphia: Elsevier.

Zeimer, R. C., Gieser, D. K., Wilensky, J. T., Noth, J. M., Mori, M. M., & Odunukwe, E. E. (1983). A practical venomanometer. Measurement of episcleral venous pressure and assessment of the normal range. *Archives of Ophthalmology*, *101*, 1447-1449.

Zorab, A. (1912). The reduction of tension in chronic glaucoma. *Ophthalmoscope*, *10*, 258-261.

Appendix A

Fluid-structure characteristics of a rectangular elastic flap valve